

Faculty of Physics  
University of Warsaw

# **Spin-foam dynamics of Loop Quantum Gravity states**

Ph.D. thesis by Marcin Kisielowski

November 2014



Advisor:

prof. dr hab. Jerzy Lewandowski, *Uniwersytet Warszawski*

Referees:

prof. dr hab. Jerzy Jurkiewicz, *Uniwersytet Jagielloński*

prof. Carlo Rovelli, *Aix-Marseille Université*



*To my wife Zuzanna and my parents Helena and Stanisław.*



## Abstract

This thesis studies the dynamics of the Loop Quantum Gravity states defined by the spin-foam models of Euclidean 4D Quantum Gravity. A link between the 4D spin-foam theory and the kinematics of the (3+1) Loop Quantum Gravity (LQG) was proposed by J. Engle, R. Pereira, C. Rovelli and E. Livine [86]. Their model, called the EPRL spin-foam model, is a promising candidate for the spin-foam model of the dynamics of the Loop Quantum Gravity states. In the original formulation, the EPRL spin-foam model is defined for triangulations and is applicable to specific LQG states. A generalization of the model to all the LQG states was proposed in [123] by W. Kamiński, J. Lewandowski and myself. Some properties of the generalized model were studied in [123, 124, 125, 29]. In particular, in [29] a general framework for studying symmetries of spin-foam models was proposed. The heart of the generalization is the generalized EPRL vertex amplitude. E. Bianchi, D. Regoli and C. Rovelli proposed another spin-foam model of 4D Quantum Gravity with the generalized EPRL vertex amplitude [48]. E. Bianchi, C. Rovelli and F. Vidotto used the model [48] to construct the first model of Quantum Cosmology based on the spin-foam formalism [49]. They calculated a transition amplitude between coherent states peaked on homogeneous, isotropic geometries using certain approximations. The approximations were justified a posteriori by a correct semiclassical limit of the transition amplitude. One of them was a truncation of the transition amplitude to a contribution from a single foam with one internal vertex, four internal edges and a certain boundary, which we will call a BRV foam. F. Hellmann discussed contributions from other foams with these properties, which a priori cannot be discarded [115]. All the possible foams were listed in [130] by J. Lewandowski, J. Puchta and myself. The class of the foams considered was defined by graph diagrams, which we introduced in [129]. We expect that the contributions from the foams we have found can be neglected in the limit of large universe.

In chapter 1, I present the construction of the Loop Quantum Gravity states and introduce the spin-foam formalism. Since I do not take under consideration the matter couplings in this thesis, I consider the combinatorial Hilbert space [163] to be the Hilbert space of the Loop Quantum Gravity states.

In chapter 2, I briefly summarize the state of art of the research in the spin-foam models of 4D Quantum Gravity before my contribution and the key results of this thesis.

In chapter 3, I define and compare the two models generalizing the EPRL model. First, I present the generalized EPRL intertwiners and the generalized EPRL vertex amplitude that were constructed in [123] by W. Kamiński, J. Lewandowski and myself. After this, I present the two spin-foam models with the generalized EPRL vertex amplitude [123, 48] and compare them.

Each EPRL intertwiner is labelled with an  $SU(2)$  invariant tensor ( $SU(2)$  intertwiner). A map from a space of  $SU(2)$  intertwiners to a space of Spin(4) intertwiners that maps an  $SU(2)$  intertwiner into its corresponding EPRL intertwiner is linear. It will be called an EPRL map and its image will be called a space of EPRL intertwiners. In chapter 4, I show that an EPRL map is 1-1 if its co-domain is non-trivial. I also give an example of non-isometric EPRL map. The results were obtained by W. Kamiński, J. Lewandowski and myself and published in [86, 124, 125].

Since an EPRL map can be mapping an orthonormal basis into non-orthonormal one, there is an ambiguity in defining the sum over the intertwiners: in the model [48] the sum is over orthonormal basis of the  $SU(2)$  intertwiners and in the model [123] the sum is over a

basis of the EPRL intertwiners orthonormal in the scalar product inherited from the space of Spin(4) intertwiners. In chapter 5, I present an approach to spin foams where instead of labelling the internal edges with intertwiners and summing over them, one labels the internal edges with operators. This approach is called operator spin foams [29]. I study moves on the (operator) spin foams changing the orientations or refining the (operator) spin foams. The model [123] is symmetric with respect to the moves and the model [48] is not symmetric. This chapter is based on a paper by B. Bahr, F. Hellmann, W. Kamiński, J. Lewandowski and myself published in [29].

In chapter 1 the foams are defined as certain oriented piecewise linear 2-complexes. However, the complexes refer to auxiliary affine structures, which are not compatible with the diffeomorphism invariance of General Relativity. In chapter 6, I present another class of foams, introduced in [129] by J. Lewandowski, J. Puchta and myself, defined combinatorially by using certain diagrams, called graph diagrams. For each graph diagram I construct the corresponding foam and the boundary graph, which are oriented CW-complexes. I define operator spin-network diagrams as graph diagrams with suitable coloring. The coloring induces a coloring of the corresponding foam, making it an operator spin foam. I show that the construction of the operator spin foam corresponding to an operator spin-network diagram is not needed to calculate the spin-foam operator and thus to calculate the transition amplitudes. The spin-foam operator can be read directly from the operator spin-network diagram. As a result the formalism of operator spin-network diagrams can be used independently from the formalism of operator spin foams. I use this technical advantage in the following chapter.

In chapter 7, I construct all graph diagrams such that the corresponding foams have one internal vertex, four internal edges and the same boundary as the BRV foam. I discuss contributions to the transition amplitude from some of the graph diagrams. I show that in the limit of large volume of the universe they can be neglected in comparison to the contribution from the BRV foam. I expect that this property holds for every graph diagram constructed in this chapter. This chapter is based on a paper by J. Lewandowski, J. Puchta and myself published in [130].

## Streszczenie

Przedmiotem badań prezentowych w mojej rozprawie doktorskiej jest dynamika stanów pętlowej kwantowej grawitacji zdefiniowana przez pianowo-spinowe modele euklidesowej czterowymiarowej kwantowej grawitacji. Związek pomiędzy czterowymiarowymi teoriami pian spinowych a kinematyką pętlowej kwantowej grawitacji został zaproponowany przez J. Engle'a, R. Pereirę, C. Rovelliego i E. Livine'a [86]. Ich model, nazywany modelem EPRL, jest dobrze zapowiadającym się kandydatem na pianowo-spinowy model dynamiki stanów pętlowej kwantowej grawitacji. W pierwotnym sformułowaniu model EPRL jest zdefiniowany dla triangulacji czasoprzestrzeni i może być stosowany tylko dla pewnych stanów pętlowej kwantowej grawitacji. Uogólnienie modelu do wszystkich stanów zostało zaproponowane w [123] przez J. Lewandowskiego, W. Kamińskiego i przeze mnie. Pewne własności uogólnionego modelu zostały zbadane w [123, 124, 125, 29]. W szczególności w [29] została zaproponowana ogólna metoda badania symetrii modeli pian spinowych. Głównym elementem zaproponowanego uogólnienia jest uogólniona amplituda wierzchołka EPRL. E. Bianchi, D. Regoli i C. Rovelli zaproponowali inny pianowo-spinowy model czterowymiarowej kwantowej grawitacji z uogólnioną amplitudą wierzchołka EPRL [48]. E. Bianchi, C. Rovelli i F. Vidotto zastosowali model [48] w celu skonstruowania pierwszego modelu kwantowej kosmologii opartego na formalizmie pian spinowych [49]. Stosując pewne przybliżenia, obliczyli amplitudę przejścia pomiędzy stanami koherentnymi, skupionymi na jednorodnych, izotropowych geometriach. Zastosowane przybliżenia były uzasadnione a posteriori poprzez poprawną granicę semi-klasyczną amplitudy przejścia. Jednym z zastosowanych przybliżeń było obcięcie amplitudy przejścia do wkładu pochodzącego od jednej piany mającej jeden wierzchołek wewnętrzny, cztery wewnętrzne krawędzie i pewien brzeg, którą będziemy nazywać pianą BRV. F. Hellmann przedyskutował wkłady od innych pian, które nie mogą zostać odrzucone a priori [115]. Wszystkie możliwe piany z tymi własnościami zostały znalezione w [130] przez J. Lewandowskiego, J. Puchę i przeze mnie. Klasa rozważanych pian została zdefiniowana przez diagramy grafowe, które wprowadziliśmy w [129]. Spodziewamy się, że wkłady od znalezionych pian mogą zostać zaniedbane w granicy dużych rozmiarów wszechświata.

W rozdziale 1 prezentuję konstrukcję stanów pętlowej kwantowej grawitacji i wprowadzam formalizm pian spinowych. Nie rozważam w mojej rozprawie sprzężeń z materią, dlatego jako przestrzeń Hilberta stanów pętlowej kwantowej grawitacji przyjmuję kombinatoryczną przestrzeń Hilberta [163].

W rozdziale 2 krótko podsumowuję stan badań nad pianowo-spinowymi modelami czterowymiarowej kwantowej grawitacji przed rozpoczęciem moich badań oraz główne wyniki mojej rozprawy doktorskiej.

W rozdziale 3 definiuję i porównuję dwa modele uogólniające model EPRL. Najpierw prezentuję uogólnione splatacze EPRL i uogólnione amplitudy wierzchołków EPRL, które zostały skonstruowane w [123] przez W. Kamińskiego, J. Lewandowskiego i przeze mnie. Następnie prezentuję dwa wyżej wspomniane modele. Na końcu porównuję oba modele.

Splatacze EPRL są z definicji indeksowane tensorami niezmienniczymi ze względu na działanie grupy  $SU(2)$  (splataczami  $SU(2)$ ). Odwzorowanie z przestrzeni splataczy  $SU(2)$  w przestrzeń splataczy  $Spin(4)$  przyporządkowujące splataczowi  $SU(2)$  odpowiadający mu splatacz EPRL jest liniowe. Będzie nazywane odwzorowaniem EPRL, a obraz tego odwzorowania będzie nazywany przestrzenią splataczy EPRL. W rozdziale 4 pokazuję, że odwzorowanie EPRL jest injektywne, jeśli jego przeciwdziedzina jest nietrywialna. Prezen-

tuję również przykład odwzorowania EPRL, które nie jest izometrią. Prezentowane wyniki zostały uzyskane przez J. Lewandowskiego, W. Kamińskiego i przeze mnie. Zostały opublikowane w [123, 124, 125].

Odwzorowanie EPRL może przyporządkowywać bazie ortonormalnej bazę nieortonormalną. W rezultacie występuje pewna niejednoznaczność w definicji sumy po splataczach: w modelu [48] suma jest po ortonormalnej bazie splataczy  $SU(2)$ , natomiast w modelu [123] suma jest po bazie splataczy EPRL ortonormalnej w naturalnym iloczynie skalarnym w przestrzeni splataczy  $Spin(4)$ . W rozdziale 5 przedstawiam podejście do pian spinowych, w którym zamiast przypisywania splataczy krawędziom wewnętrzny piany i sumowania po nich, krawędziom wewnętrzny przypisuje się pewne operatory. Podejście to jest nazywane operatorowymi pianami spinowymi [29]. Badam ruchy na operatorowych pianach spinowych pozwalające na zmianę orientacji i zagęszczanie operatorowych pian spinowych. Model [123] jest symetryczny ze względu na te ruchy, natomiast model [48] nie jest symetryczny. Rozdział ten jest oparty na artykule napisanym przez B. Bahra, F. Hellmanną, W. Kamińskiego, J. Lewandowskiego i przeze mnie, opublikowanym w [29].

W rozdziale 1 piany są zdefiniowane jako pewne zorientowane kawałkami-liniowe dwukompleksy. Jednakże kompleksy te odwołują się do zbędnej struktury afinicznej, która jest niezgodna z dyfeomorficzną niezmienniczością ogólnej teorii względności. W rozdziale 6 przedstawiam inną klasę pian, wprowadzoną w [129] przez J. Lewandowskiego, J. Puchtę i przeze mnie, zdefiniowaną kombinatorycznie przy użyciu pewnych diagramów, które nazywamy diagramami grafowymi. Dla każdego diagramu grafowego konstruuję odpowiadającą mu pianę i graf brzegowy, które są zorientowanymi CW-kompleksami. Definiuję operatorowe sieciowo-spinowe diagramy jako diagramy grafowe z odpowiednim kolorowaniem. Każdemu operatorowemu sieciowo-spinowemu diagramowi odpowiada operatorowa piana spinowa. Pokazuję, że konstrukcja operatorowej piany spinowej, odpowiadającej operatorowemu sieciowo-spinowemu diagramowi, nie jest konieczna do obliczania pianowo-spinowego operatora, a zatem nie jest konieczna do obliczania amplitud przejścia. Pianowo-spinowy operator może być odczytany bezpośrednio z operatorowego sieciowo-spinowego diagramu. W rezultacie formalizm operatorowych sieciowo-spinowych diagramów może być stosowany niezależnie od formalizmu pian spinowych. Właśnie tę techniczną zaletę stosuję w następnym rozdziale.

W rozdziale 7 konstruuję wszystkie takie diagramy grafowe, że odpowiadające im piany mają jeden wierzchołek wewnętrzny, cztery wewnętrzne krawędzie i brzeg taki sam jak brzeg piany BRV. Omawiam wkłady do amplitudy przejścia, pochodzące od niektórych ze znalezionych diagramów grafowych. Pokazuję, że w granicy dużych rozmiarów wszechświata mogą być zaniedbane, w porównaniu do wkładu od piany BRV. Spodziewam się, że własność ta zachodzi dla każdego diagramu grafowego skonstruowanego w tym rozdziale. Rozdział ten jest oparty na pracy [130], którą napisałem wspólnie z J. Lewandowskim i J. Puchtą.

# Contents

<b>1. Loop Quantum Gravity states and spin foams</b>	<b>1</b>
1.1. Canonical analysis of General Relativity . . . . .	1
1.1.1. Holst-Palatini action . . . . .	1
1.1.2. 3+1 decomposition of space-time . . . . .	2
1.1.3. Hamiltonian theory . . . . .	4
1.2. The Hilbert space of the Loop Quantum Gravity states . . . . .	7
1.2.1. The cylindrical functions and the measure . . . . .	7
1.2.2. Abstract spin networks . . . . .	8
1.2.3. The spin-network cylindrical functions of connections . . . . .	13
1.2.4. Solutions to the Gauss constraint and the vector constraint . . . . .	14
1.2.5. Combinatorial Hilbert space . . . . .	15
1.3. Spin foams . . . . .	17
1.3.1. Spin foams as histories of spin networks . . . . .	17
1.3.2. Spin-foam models of quantum BF theory . . . . .	18
1.3.3. Spin foams . . . . .	22
1.3.4. Amplitude of a spin foam . . . . .	27
<b>2. The key results of the thesis</b>	<b>31</b>
2.1. The state of art before the author's contribution . . . . .	31
2.2. The key results of the thesis . . . . .	33
<b>3. Spin-foam models with the EPRL vertex amplitude</b>	<b>37</b>
3.1. General Relativity as constrained BF theory . . . . .	37
3.1.1. Continuous theory . . . . .	37
3.1.2. Discretized theory . . . . .	39
3.2. Quantum polyhedron . . . . .	40
3.2.1. Polyhedron in 3D . . . . .	40
3.2.2. Polyhedron in 4D . . . . .	41
3.2.3. Quantum polyhedron in 3D . . . . .	42
3.2.4. Quantum polyhedron in 4D . . . . .	43
3.3. The generalized EPRL vertex amplitude . . . . .	48
3.3.1. The EPRL intertwiners . . . . .	48
3.3.2. The EPRL map . . . . .	49
3.3.3. The EPRL spin networks . . . . .	50
3.3.4. The generalized EPRL vertex amplitude . . . . .	50
3.4. The spin-foam models with the EPRL vertex amplitude . . . . .	52
3.4.1. Spin(4) spin-foam model with the EPRL vertex . . . . .	52
3.4.2. SU(2) spin-foam model with the EPRL vertex . . . . .	52
3.4.3. Comparison of the models . . . . .	53

3.5. Other spin-foam models of 4D Quantum Gravity . . . . .	54
<b>4. Properties of the EPRL map</b>	<b>57</b>
4.1. Non-isometricity of the EPRL map . . . . .	57
4.2. Injectivity theorem . . . . .	58
4.3. Proof of the injectivity theorem in the case $\beta \geq 1$ . . . . .	60
4.4. Proof of the injectivity theorem in the case $0 \leq \beta < 1$ . . . . .	63
4.4.1. Proof of the theorem in simplified case . . . . .	65
4.4.2. Proof of the theorem . . . . .	71
<b>5. Operator spin foams</b>	<b>79</b>
5.1. Operator spin foam . . . . .	80
5.1.1. Definition . . . . .	80
5.1.2. The moves and the equivalence relation they define . . . . .	81
5.1.3. Glueing the operator spin foams . . . . .	87
5.2. Spin-foam operator . . . . .	89
5.2.1. Spin-foam operator . . . . .	89
5.2.2. Abstract index notation . . . . .	89
5.2.3. 2-edge contraction . . . . .	91
5.2.4. Symmetric spin-foam operator . . . . .	91
5.2.5. Relation with the spin foams . . . . .	93
5.2.6. Amplitude form of the spin-foam operator . . . . .	94
5.3. Operator spin-foam models . . . . .	95
5.3.1. Natural operator spin-foam models . . . . .	95
5.3.2. Symmetric operator spin-foam models . . . . .	96
5.3.3. Examples . . . . .	97
<b>6. Operator spin-network diagrams</b>	<b>103</b>
6.1. Graph diagrams . . . . .	103
6.1.1. Definition . . . . .	103
6.1.2. Face and edge relations . . . . .	105
6.1.3. A CW-complex corresponding to a graph diagram . . . . .	106
6.1.4. Boundary graph . . . . .	108
6.2. Operator spin-network diagrams . . . . .	109
6.2.1. Definition . . . . .	109
6.2.2. The operator spin foam corresponding to operator spin-network diagram . . . . .	110
6.2.3. The spin-network diagram operator . . . . .	111
6.2.4. Static operator spin-network diagrams . . . . .	113
6.3. The OSD models with the EPRL vertex amplitude . . . . .	114
6.3.1. The Spin(4) OSD model with the EPRL vertex . . . . .	115
6.3.2. The SU(2) OSD model with the EPRL vertex . . . . .	116
<b>7. Dipole Cosmology</b>	<b>117</b>
7.1. The Bianchi-Rovelli-Vidotto model . . . . .	117
7.2. The algorithm . . . . .	119
7.3. All the possible interaction graphs . . . . .	122

7.4. Possible operator spin-network diagrams . . . . .	127
7.4.1. Possible graph diagrams . . . . .	127
7.4.2. Possible colorings . . . . .	128
7.5. The transition amplitude . . . . .	129
7.5.1. Face amplitudes . . . . .	132
7.5.2. Vertex amplitudes . . . . .	133
<b>8. Discussion and outlook</b>	<b>139</b>
<b>A. The condition for non-triviality of SU(2) invariants</b>	<b>143</b>
<b>B. Notation</b>	<b>145</b>



# 1. Loop Quantum Gravity states and spin foams

We begin the thesis by introducing the main subjects underlying our study – the Loop Quantum Gravity and the spin foams. There is a number of books and publications reviewing the subjects. In this chapter we present the topics relevant for our study. We refer our reader to [17, 178, 162, 165, 164, 107, 19] for reviews of the Loop Quantum Gravity and to [165, 164, 20, 145, 146, 84, 19, 169] for reviews of the spin-foam formalism.

Our departing point is the canonical analysis of the General Relativity presented in section 1.1. The canonical theory is obtained from the Palatini action with the Holst term. A system of first class constraints is obtained: vector constraint generating the diffeomorphisms of space, Gauss constraint generating  $\text{SO}(3)$  gauge transformations and scalar constraint defining the dynamics.

In section 1.2.1 we present a (non-separable) Hilbert space for background independent quantum theories of (Poisson commuting) connections. In section 1.2.4 we impose the (quantum) vector and the (quantum) Gauss constraints and obtain a separable Hilbert space by using a procedure of averaging the solutions to the Gauss constraint (described by spin-network cylindrical functions) over certain group of extended diffeomorphisms [90]. The space depends on graphs and their linking and knotting. Since the dynamics of the pure (quantum) gravitational field seems not to depend on the linking and knotting [28, 179], as a Hilbert space of Loop Quantum Gravity we consider a subspace of this space (see section 1.2.5), called combinatorial Hilbert space [163].

The kinematics of the theory is well understood. A still open problem is to define the dynamics of the states. In section 1.3 we introduce the spin-foam formalism as a possible solution to the problem. It can be considered to be a path integral formulation of the dynamics. A particular example of a spin-foam model defining the dynamics of the Loop Quantum Gravity states is introduced in the next chapter.

## 1.1. Canonical analysis of General Relativity

We assume that the space-time manifold  $\mathcal{M}$  is an oriented product manifold  $\Sigma \times \mathbb{R}$ , where  $\Sigma$  is an oriented, compact 3-dimensional manifold without boundary. The space-time indices will be denoted by Greek letters  $\alpha, \beta, \mu, \nu$  and the space indices (indices in  $\Sigma$ ) will be denoted by small Latin letters  $a, b, c, d$ . We start with a Holst-Palatini formulation of General Relativity and then perform a canonical analysis of the theory. This will be a preparatory step for the quantization.

### 1.1.1. Holst-Palatini action

In the original formulation General Relativity is a theory of metrics. In the Palatini formulation the variables are connections and tetrads. A tetrad  $e_\mu^I$  is a 1-form with values

## 1. Loop Quantum Gravity states and spin foams

in  $V = \mathbb{R}^4$ . We use an index notation such that the capital letters  $I, J, K, L$  are the indices in the internal space  $V$ . The space  $V$  is equipped with a fixed metric  $\bar{\eta}_{IJ}$  of signature  $-,+,+,+.$  Our analysis also applies to the signature  $,+,+,+,+.$  We will denote by  $\text{SO}(\bar{\eta})$  the group of transformations of  $V$  leaving  $\bar{\eta}$  invariant and by  $\text{so}(\bar{\eta})$  we will denote its Lie algebra. For simplicity we assume that a connection is described by a global one-form  $\omega_\mu{}^I{}_J$  taking values in  $\text{so}(\bar{\eta})$  and that the tetrad is defined globally.

The theory is defined by an action

$$S_P[e, \omega] = \frac{1}{4k} \int_{\mathcal{M}} \epsilon_{IJKL} e^I \wedge e^J \wedge \mathcal{F}^{KL}, \quad (1.1)$$

where  $\epsilon_{IJKL}$  is an alternating tensor on  $V$  such that the orientation of  $\epsilon_{IJKL} e^I \wedge e^J \wedge e^K \wedge e^L$  agrees with the orientation of  $\mathcal{M}$ ,

$$\mathcal{F} = d\omega + \omega \wedge \omega$$

is the curvature of the connection  $\omega$  and  $k = 8\pi G$  where  $G$  is the Newton's constant.

The correspondence with the formulation in terms of metrics is the following. The metric is constructed from the tetrad:  $g_{\mu\nu} = \bar{\eta}_{IJ} e_\mu^I e_\nu^J$ . The variation of the action with respect to the connection leads to a field equation:

$$de + \omega \wedge e = 0. \quad (1.2)$$

Solving this equation for  $\omega$  and substituting the solution  $\omega(e)$  for the connection one-form  $\omega$  in the Palatini action gives the Einstein-Hilbert action:

$$S_P[e, \omega(e)] = \frac{1}{2k} \int_{\mathcal{M}} \sqrt{|\det(g)|} R,$$

where  $R$  is the scalar curvature of the metric  $g_{\mu\nu}$ .

Holst noticed that the field equations are not changed after adding a term [118] – the field equations resulting from the Palatini action (1.1) are the same as the field equations resulting from the following action:

$$S_H[e, \omega] = \frac{1}{4k} \int_{\mathcal{M}} \epsilon_{IJKL} e^I \wedge e^J \wedge \mathcal{F}^{KL} + \frac{\sigma}{2k\beta} \int_{\mathcal{M}} e^I \wedge e^J \wedge \mathcal{F}_{IJ}, \quad (1.3)$$

where the number  $\beta$  is called the Barbero-Immirzi parameter [34, 120] and  $\sigma$  is the sign of the determinant of the metric  $\bar{\eta}$ . Although the field equations resulting from the Holst action do not depend on the Barbero-Immirzi parameter  $\beta$ , the resulting quantum theories depend on this parameter.

### 1.1.2. 3+1 decomposition of space-time

In order to perform Legendre transform one introduces on  $\mathcal{M}$ :

- a smooth time function  $t$  such that  $dt$  is everywhere non-zero and each  $t = t$ ,  $t \in \mathbb{R}$  slice  $\Sigma_t$  is diffeomorphic to  $\Sigma$ ,
- a future directed vector field  $\mathbf{t} = t^\alpha \partial_\alpha$  such that  $t^\alpha \partial_\alpha t = 1$ .

### 1.1. Canonical analysis of General Relativity

Let  $n^\alpha$  be a unit time-like vector field normal to the slices  $\Sigma_t$ . Decompose  $t^\alpha$  as

$$t^\alpha = Nn^\alpha + N^\alpha, \quad N^\alpha n_\alpha = 0.$$

The function  $N$  is called the lapse and the vector field  $N^\alpha$  is called the shift. The vector field  $t^\alpha$  describes a "time flow" and can be used to identify  $\Sigma_t$  with  $\Sigma_0$  [182]. Each slice  $\Sigma_t$  is an embedded hypersurface and the embeddings  $\theta_t : \Sigma \rightarrow \mathcal{M}$  satisfy  $\frac{d}{dt} \theta_t^\alpha(q) = t^\alpha(\theta_t(q))$ .

Let us denote by  $T_p\mathcal{M}$  the tangent space to  $\mathcal{M}$  at point  $p$  and by  $T_p^*\mathcal{M}$  the cotangent space at point  $p$ . Let

$$T_s^r\mathcal{M} := \underbrace{T\mathcal{M} \otimes \dots \otimes T\mathcal{M}}_{r \text{ factors}} \otimes \underbrace{T^*\mathcal{M} \otimes \dots \otimes T^*\mathcal{M}}_{s \text{ factors}}$$

be the space of tensor fields of type  $(r, s)$ . Let us denote by  $H_p\mathcal{M}$  the subspace of  $T_p\mathcal{M}$  orthogonal to  $n^\alpha(p)$  and by  $H_p^*\mathcal{M}$  the subspace of  $T_p^*\mathcal{M}$  orthogonal to  $n_\alpha(p) := g_{\alpha\beta}(p)n^\beta(p)$ . The subspace of tensor fields orthogonal to  $n^\alpha$  (and  $n_\alpha$ ) at each point and in each of the indices will be denoted by  $H_s^r\mathcal{M}$ :

$$H_s^r\mathcal{M} := \underbrace{H\mathcal{M} \otimes \dots \otimes H\mathcal{M}}_{r \text{ factors}} \otimes \underbrace{H^*\mathcal{M} \otimes \dots \otimes H^*\mathcal{M}}_{s \text{ factors}}.$$

The restriction of  $T_s^r\mathcal{M}$  and  $H_s^r\mathcal{M}$  to tensor fields on  $\Sigma_t$  will be denoted by  $T_s^r\Sigma_t$  and  $H_s^r\Sigma_t$  respectively.

Let us note that the pullback map  $\theta_t^* : T_{\theta_t(q)}^*\Sigma_t \rightarrow T_q^*\Sigma$  annihilates forms in the direction of  $n_\alpha(\theta_t(q))$  and is 1-1 on the space  $H_{\theta_t(q)}^*\Sigma_t$ . The pushforward  $(\theta_t)_* : T_q\Sigma \rightarrow T_{\theta_t(q)}\Sigma_t$  is 1-1 and its image is  $H_{\theta_t(q)}\Sigma_t$ . For fixed  $t$  the map  $\theta_t$  induces two maps  $(\tilde{\theta}_t)_* : T_s^r\Sigma \rightarrow H_s^r\Sigma_t$  and  $\tilde{\theta}_t^* : H_s^r\Sigma_t \rightarrow T_s^r\Sigma$  defined as follows:

- We define

$$(\tilde{\theta}_t)_* : T_q^*\Sigma \rightarrow H_{\theta_t(q)}^*\Sigma_t$$

to be the inverse of  $\theta_t^*|_{H_{\theta_t(q)}^*\Sigma_t}$  and

$$(\tilde{\theta}_t)_* : T_q\Sigma \rightarrow H_{\theta_t(q)}\Sigma_t$$

to be the pushforward map  $(\theta_t)_* : T_q\Sigma \rightarrow H_{\theta_t(q)}\Sigma_t$ . The map can be naturally extended to arbitrary tensor fields in  $T_s^r\Sigma$ .

- We define

$$\tilde{\theta}_t^* : H_{\theta_t(q)}\Sigma_t \rightarrow T_q\Sigma$$

to be the inverse of the pushforward map  $(\theta_t)_*$  (where  $(\theta_t)_*$  is treated as a map  $(\theta_t)_* : T_q\Sigma \rightarrow H_{\theta_t(q)}\Sigma_t$ ) and

$$\tilde{\theta}_t^* : H_{\theta_t(q)}^*\Sigma_t \rightarrow T_q^*\Sigma$$

to be the map  $\theta_t^*|_{H_{\theta_t(q)}^*\Sigma_t}$ . The map  $\tilde{\theta}_t^*$  can be naturally extended to arbitrary tensor fields in  $H_s^r\Sigma_t$ .

## 1. Loop Quantum Gravity states and spin foams

Any tensor field  $T \in H_s^r \mathcal{M}$  induces a one-parameter family  $t \mapsto T_t \in T_s^r \Sigma$  of tensor fields on  $\Sigma$ :

$$T_t(q) := \tilde{\theta}_t^* T(\theta_t(q)).$$

On the other hand, a one-parameter family of tensor fields on  $\Sigma$  induces a tensor field on  $\mathcal{M}$ :

$$T(\theta_t(q)) = (\tilde{\theta}_t)_* T_t(q).$$

Consider the first fundamental form of  $\Sigma$  [113]:

$$h_t = \theta_t^* g.$$

The tensor field in  $T_2^0 \mathcal{M}$  corresponding to  $h_t$  is

$$h_{\alpha\beta} := ((\tilde{\theta}_t)_* h_t)_{\alpha\beta} = g_{\alpha\beta} - \sigma n_\alpha n_\beta.$$

The tensor  $h^\alpha_\beta := g^{\alpha\gamma} h_{\gamma\beta}$  considered as a map from  $T_{\theta_t(q)} \mathcal{M}$  to itself is a projector onto the subspace orthogonal to  $n^\alpha(\theta_t(q))$ , and considered as a map from  $T_{\theta_t(q)}^* \mathcal{M}$  to itself is a projector onto the subspace orthogonal to  $n_\alpha(\theta_t(q))$ . Therefore  $h^\alpha_\beta$  can be used to project tensor fields  $T_s^r \mathcal{M}$  onto  $H_s^r \mathcal{M}$ .

We define a time derivative of a one-parameter family of tensor fields on  $\Sigma$ :

$$\dot{T}_t^{a\dots b}_{c\dots d}(q) := \lim_{\Delta t \rightarrow 0} \frac{1}{\Delta t} \left( T_t^{a\dots b}_{c\dots d}(q) - T_{t-\Delta t}^{a\dots b}_{c\dots d}(q) \right).$$

Let  $T, \dot{T}$  be the tensor fields in  $H_s^r \mathcal{M}$  corresponding to  $T_t, \dot{T}_t$ . From the definition of the Lie derivative  $\mathcal{L}$  follows that:

$$\dot{T}^{\alpha\dots\beta}_{\mu\dots\nu} = \mathcal{L}_t T^{\alpha'\dots\beta'}_{\mu'\dots\nu'} h^\alpha_{\alpha'} \dots h^\beta_{\beta'} h^{\mu'}_{\mu} \dots h^{\nu'}_{\nu}.$$

### 1.1.3. Hamiltonian theory

#### Partial gauge fixing

In the passage to the canonical framework, one partially fixes the  $\text{SO}(\bar{\eta})$  internal gauge transformations: one fixes an internal vector field  $n^I$  such that  $n^I n_I = \sigma$  and restricts to tetrads such that  $e_\alpha^I n_I = n_\alpha$ , where  $n^\alpha$  is the unit normal to the hypersurfaces  $\Sigma_t$ . This reduces the  $\text{SO}(\bar{\eta})$  internal gauge group to its subgroup  $\text{SO}(\eta)$  leaving  $n^I$  invariant. The Lie algebra of  $\text{SO}(\eta)$  will be denoted by  $\text{so}(\eta)$ . Let  $\mathbf{q} : V \rightarrow V$  be a projector onto the space  $V_\perp$  orthogonal to  $n^I$ . The indices corresponding to  $V_\perp$  will be denoted by lowercase Latin letters  $i, j, k, l$ . In this notation  $\mathbf{q}_i^I$  is an orthonormal basis of  $V_\perp$ ,  $\mathbf{q}_I^i$  is the partial isometry from  $V$  to  $V_\perp$  such that  $\mathbf{q}_I^i n^I = 0$  and  $\mathbf{q}_J^i \mathbf{q}_J^I = \delta_J^i$ . The relation between  $\mathbf{q}_J^I$ ,  $\mathbf{q}_i^I$  and  $\mathbf{q}_I^i$  is the following  $\mathbf{q}_J^I = \mathbf{q}_i^I \mathbf{q}_J^i$ . The metric on  $V$  induces a metric on  $V_\perp$ :

$$\eta_{ij} = \mathbf{q}_i^I \mathbf{q}_j^J \bar{\eta}_{IJ}$$

and the alternating tensor  $\epsilon_{IJKL}$  on  $V$  induces an alternating tensor on  $V_\perp$ :

$$\epsilon_{ijk} = \mathbf{q}_i^I \mathbf{q}_j^K \mathbf{q}_k^L n^L \epsilon_{IJKL}.$$

### 1.1. Canonical analysis of General Relativity

The connection one-form  $\omega^{IJ}$  can be decomposed into "magnetic" and "electric" components with respect to  $n_I$ ,  $q_I^i$ :

$$\Gamma^i = \frac{1}{2} q_I^i n_J e^{IJ}_{\quad KL} \omega^{KL}, \quad K^i = q_I^i n_J \omega^{IJ}. \quad (1.4)$$

The induced one-forms on  $\Sigma$ :

$$\Gamma_t^i := \theta_t^* \Gamma^i, \quad K_t^i := \theta_t^* K^i$$

have a natural interpretation. Let us introduce a triad on  $\Sigma$ :

$$(e_t)_a^i := q_I^i (\theta_t^* e^I)_a.$$

The induced metric  $h$  on  $\Sigma$  coincides with the metric constructed from the triad:

$$h_{t ab} = \eta_{ij} (e_t)_a^i (e_t)_b^j.$$

If the connection  $\omega$  is compatible with the tetrad  $e$ , i.e. if equation (1.2) holds, then  $\Gamma^i$  is a so( $\eta$ ) connection on  $\Sigma$  compatible with  $(e_t)_a^i$ :

$$de_t^i + \epsilon_{jk}^i \Gamma_t^j \wedge e_t^k = 0$$

and  $K_t^i$  is the extrinsic curvature of  $\Sigma_t$ :

$$(K_t)_a^i = (e_t)_b^i (\tilde{\theta}_t^*)^\alpha_a (\tilde{\theta}_t^*)_\beta^b h^{\alpha'}_{\quad \alpha} h^{\beta}_{\quad \beta'} \nabla_{\alpha'} n^{\beta'},$$

where  $\nabla$  is the torsion-free derivative operator compatible with  $g_{\alpha\beta}$ .

#### Legendre transform and the constraints

In the following we omit the index  $t$  and denote a one-parameter family of tensor fields on  $\Sigma$  and the corresponding tensor field on  $\mathcal{M}$  by the same symbol. In order to pass to the canonical formulation, one performs Legendre transform of the Holst-Palatini action (1.3):

$$S = \int dt \int_\Sigma d^3x \left( P_i^a \dot{A}_a^i - h(A, P, N, N^a, \omega^i(\mathbf{t})) \right), \quad (1.5)$$

where

$$A_a^i := \Gamma_a^i + \beta K_a^i, \quad P_i^a := -\frac{\sigma}{2k\beta} e_b^j e_c^k \eta^{abc} \epsilon_{ijk},$$

$h$  is given by:

$$h(A, P, N, N^a, \omega^i(\mathbf{t})) = \omega^i(\mathbf{t}) G_i + N^a C_a + NC$$

with  $\omega^i(\mathbf{t}) = -\frac{1}{2} \epsilon^{ijk} \omega_{jk}(\mathbf{t})$ . By  $\eta^{abc}$  we denote the Levi-Civita tensor density (of weight 1) on  $\Sigma$ . Geometrically,  $A_a^i$  is a connection 1-form on  $\Sigma$  and  $P_i^a$  represents an orthonormal triad of density weight 1 on  $\Sigma$ :

$$P_i^a = \frac{1}{k\beta} \sqrt{|\det h|} e_i^a.$$

From the expression (1.5) follows that  $(A_a^i, P_i^a)$  is a canonical pair;  $\omega^i(\mathbf{t})$ ,  $N^a$ ,  $N$  are Lagrange multipliers. The dynamics of General Relativity is generated by a set of constraints:

## 1. Loop Quantum Gravity states and spin foams

- the Gauss constraint:

$$G_i = \mathcal{D}_a P_i^a := \partial_a P_i^a + \epsilon_{ij}^k A_a^j P_k^a = 0,$$

- the vector constraint:

$$C_a = P_i^b F_{ab}^i + \frac{\sigma - \beta^2}{\beta} K_a^i G_i = 0,$$

where  $F = dA + A \wedge A$  is the curvature of  $A$ ,

- the scalar constraint:

$$C = \frac{k\beta^2}{2\sqrt{|\det h|}} P_i^a P_j^b \left( \epsilon^{ij}_k F_{ab}^k + 2(\sigma - \beta^2) K_{[a}^i K_{b]}^j \right) + (\beta^2 - \sigma) k \partial_a \left( \frac{P_i^a}{\sqrt{|\det h|}} \right) G^i = 0.$$

The canonical phase space consists of set of pairs  $(A_i^a(x), P_b^j(y))$  that are canonically conjugate:

$$\{A_i^a(x), P_b^j(y)\} = \delta_i^j \delta_a^b \delta(x, y), \quad \{A_i^a(x), A_b^j(y)\} = 0, \quad \{P_i^a(x), P_b^j(y)\} = 0.$$

The evolution of the canonical pair is given by:

$$\dot{A}_i^a = \{A_i^a, H\}, \quad \dot{P}_a^i = \{P_a^i, H\},$$

where the Hamiltonian is  $H := \int_{\Sigma} d^3x h$ . Together with the three constraints, the evolution equations are equivalent to Einstein equations.

Let us consider functions on the phase space obtained by smearing:

- $G_i$  with any smooth function  $\Lambda^i$  on  $\Sigma$  with values in  $\text{so}(3)$ :

$$C_G(\Lambda) := \int_{\Sigma} d^3x \Lambda^i G_i,$$

- $C_a$  with any smooth vector field  $N^a$  on  $\Sigma$ :

$$C_{\text{Diff}}(\vec{N}) := \int_{\Sigma} d^3x N^a C_a,$$

- $C$  with any smooth function  $N$  on  $\Sigma$ :

$$C(N) := \int d^3x N C.$$

The function  $C_G(\Lambda)$  generates  $\text{SO}(3)$  gauge transformations in the direction of  $\Lambda^i$ :

$$\{A_a^i, C_G(\Lambda)\} = -\mathcal{D}_a \Lambda^i, \quad \{P_i^a, C_G(\Lambda)\} = \epsilon_{ij}^k \Lambda^j P_k^a.$$

The function  $C_{\text{Diff}}(\vec{N})$  generates diffeomorphisms along  $\vec{N}$ :

$$\{A_a^i, C_{\text{diff}}(\vec{N})\} = \mathcal{L}_{\vec{N}} A_a^i, \quad \{P_i^a, C_{\text{diff}}(\vec{N})\} = \mathcal{L}_{\vec{N}} P_i^a.$$

The function  $C(N)$  generates time evolution, "off"  $\Sigma$  [17].

## 1.2. The Hilbert space of the Loop Quantum Gravity states

### 1.2.1. The cylindrical functions and the measure

Let us consider a manifold  $\Sigma$ , a compact Lie group  $G$ , its Lie algebra  $\mathfrak{g}$ , and the set  $\mathfrak{A}(\Sigma)$  of the Lie algebra  $\mathfrak{g}$  valued differential one-forms (connection one-forms) on  $\Sigma$ .

A  $G$ -valued parallel transport function on  $\mathfrak{A}(\Sigma)$  is defined by each finite curve  $\ell$  in  $\Sigma$ , namely for every  $A \in \mathfrak{A}(\Sigma)$ ,

$$U_\ell(A) := \text{Pexp} \int_\ell -A. \quad (1.6)$$

The parallel transport functions are used to define the cylindrical functions  $\text{Cyl}(\mathfrak{A}(\Sigma))$ . A cylindrical function  $\Psi : \mathfrak{A}(\Sigma) \rightarrow \mathbb{C}$  is defined by an embedded graph  $\gamma$  and by a smooth complex-valued function  $\psi : G^N \rightarrow \mathbb{C}$ . An embedded graph  $\gamma$  [133, 17] is a finite set of compact 1-dimensional submanifolds of  $\Sigma$  called (embedded) links, such that:

- a link is an embedded interval with a boundary or an embedded circle with a marked point or an embedded circle;
- the intersection of two different links is either empty or is a finite set of points; each of the intersection points is either one of the endpoints of an embedded interval or a marked point of an embedded circle.

We will say that a function  $\Psi : \mathfrak{A}(\Sigma) \rightarrow \mathbb{C}$  is cylindrical if there is a graph  $\gamma$  such that

$$\Psi(A) := \psi(U_{\ell_1}(A), \dots, U_{\ell_N}(A)) \quad (1.7)$$

for a smooth complex-valued function  $\psi : G^N \rightarrow \mathbb{C}$ . We will say that  $\Psi$  is cylindrical with respect to graph  $\gamma$ . Let us note that a function cylindrical with respect to a graph  $\gamma$  is also cylindrical with respect to any larger graph.

On the space of cylindrical functions  $\text{Cyl}(\mathfrak{A}(\Sigma))$  there is a natural diffeomorphism invariant integral:

$$\text{Cyl}(\mathfrak{A}(\Sigma)) \ni \Psi \mapsto \int d\mu_0(A) \Psi(A) \quad (1.8)$$

defined as

$$\int d\mu_0(A) \Psi(A) := \int d\mu_H(g_1) \dots d\mu_H(g_N) \psi(g_1, \dots, g_N). \quad (1.9)$$

The graph  $\gamma$  is not uniquely defined but the right-hand side is independent of the choice of  $\gamma$ . The Hilbert space  $L^2(\mathfrak{A}(\Sigma), \mu_0)$  serves as the Hilbert space for background independent quantum theories of (Poisson commuting) connections, in particular as the Hilbert space in which Quantum Geometry of Loop Quantum Gravity is defined. In order to calculate a scalar product between two functions  $\Psi_1, \Psi_2 \in \text{Cyl}(\mathfrak{A}(\Sigma))$  cylindrical with respect to (in general different) graphs  $\gamma_1$  and  $\gamma_2$ , respectively, we introduce a third graph  $\gamma_3$  containing  $\gamma_1$  and  $\gamma_2$  (such graph exists if the differentiability class of the links is properly defined [132]). Clearly, the functions are cylindrical with respect to the graph  $\gamma_3$ :

$$\Psi_1(A) := \psi_1(U_{\ell_1}(A), \dots, U_{\ell_{N_3}}(A)), \quad \Psi_2(A) := \psi_2(U_{\ell_1}(A), \dots, U_{\ell_{N_3}}(A)).$$

## 1. Loop Quantum Gravity states and spin foams

The scalar product is:

$$\langle \Psi_1 | \Psi_2 \rangle = \int d\mu_H(g_1) \dots d\mu_H(g_{N_3}) \overline{\psi_1(g_1, \dots, g_{N_3})} \psi_2(g_1, \dots, g_{N_3}).$$

The gauge invariant cylindrical functions can be easily identified as the functions given by closed loops. The subspace  $\mathcal{H}_\Sigma \subset L^2(\mathfrak{A}(\Sigma), \mu_0)$  of the gauge invariant functions is defined by the functions of the form

$$\Psi(A) = \psi(U_{\alpha_1(A)}, \dots, U_{\alpha_m(A)}), \quad (1.10)$$

where  $\alpha_1, \dots, \alpha_m$  are free generators of the first homotopy group of an embedded graph  $\gamma$ . An orthonormal basis of  $\mathcal{H}_\Sigma$  can be constructed by endowing the embedded graphs with spin-network structures (see section 1.2.2).

In the Hilbert space  $L^2(\mathfrak{A}(\Sigma), \mu_0)$  one defines a quantum representation for the classical variables  $(A, P)$ , where the Poisson bracket is

$$\{f, h\} = \int_\Sigma \frac{\delta}{\delta A_a^i} f \frac{\delta}{\delta P_i^a} h - \int_\Sigma \frac{\delta}{\delta A_a^i} h \frac{\delta}{\delta P_i^a} f. \quad (1.11)$$

In particular, one defines the quantum flux operators

$$\hat{P}(S) = \frac{1}{i} \int_S \frac{\delta}{\delta A_a^i},$$

across a 2-surface  $S \subset \Sigma$ .

### 1.2.2. Abstract spin networks

#### Definition

Given a compact group  $G$ , a  $G$ -spin network is a triple  $(\gamma, \rho, \iota)$  (see figure 1.1):

- $\gamma$  is an oriented abstract graph. An oriented abstract graph is a finite set of nodes  $\gamma^{(0)}$ , a finite set of links  $\gamma^{(1)}$  and functions  $s : \gamma^{(1)} \rightarrow \gamma^{(0)}$ ,  $t : \gamma^{(1)} \rightarrow \gamma^{(0)}$  [22]. We say that the node  $s(\ell)$  is the source of the link  $\ell$ , or equivalently that the link  $\ell$  is outgoing from the node  $s(\ell)$ . We say that the node  $t(\ell)$  is the target of the link  $\ell$ , or equivalently that the link  $\ell$  is incoming to the node  $t(\ell)$ .
- $\rho$  is a coloring of the links of the graph  $\gamma$ . It maps the set  $\gamma^{(1)}$  into the set  $\text{Irr}(G)$  of the unitary irreducible representations of  $G$ . That is, to every link  $\ell$  we assign an irreducible representation  $\rho_\ell$  defined on a Hilbert space  $\mathcal{H}_\ell$ ,

$$\ell \mapsto \rho_\ell. \quad (1.12)$$

- $\iota$  is a coloring of the nodes of the graph  $\gamma$ . It maps each node  $n \in \gamma^{(0)}$  into the space

$$\mathcal{H}_n := \text{Inv} \left( \bigotimes_{\ell \text{ incoming to } n} \mathcal{H}_\ell^* \otimes \bigotimes_{\ell' \text{ outgoing from } n} \mathcal{H}_{\ell'} \right) \quad (1.13)$$

## 1.2. The Hilbert space of the Loop Quantum Gravity states

of invariant tensors (intertwiners) in

$$\bigotimes_{\ell \text{ incoming to } n} \mathcal{H}_\ell^* \otimes \bigotimes_{\ell' \text{ outgoing from } n} \mathcal{H}_{\ell'}, \quad (1.14)$$

where each  $\mathcal{H}_\ell^*$  denotes the dual vector space to  $\mathcal{H}_\ell$ . The map will be denoted by

$$n \mapsto \iota_n. \quad (1.15)$$

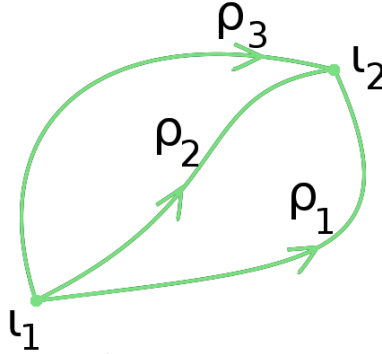


Figure 1.1.: A spin network.

We introduce an equivalence class on the set of oriented abstract graphs: two graphs are equivalent if and only if one differs from the other only by orientations of some of its links. The equivalence classes of this relation will be called unoriented abstract graphs and denoted by  $|\gamma|$ .

### Operations on spin networks

Following Baez [22] we introduce operations on the spin networks such as flipping orientation of a link, splitting a link, adding a link and adding a node. We supplement the operations with operations of taking complex conjugate of a spin network and Hilbert conjugate of a spin network.

*Flipping orientation* is the first operation we consider. Being given a spin network  $s = (\gamma, \rho, \iota)$ , let a graph  $\gamma'$  be obtained by flipping the orientation of one of the links, say  $\ell_0 \in \gamma^{(1)}$ . The flipped orientation link is denoted by  $\ell_0^{-1}$ . On  $\gamma'$  we define a spin network  $\text{flip}_{\ell_0}(s) := (\gamma', \rho', \iota')$ , where:

$$\iota' := \iota \quad (1.16)$$

$$\rho'_\ell := \begin{cases} (\rho_{\ell_0})^*, & \text{if } \ell = \ell_0^{-1}, \\ \rho_\ell, & \text{otherwise.} \end{cases} \quad (1.17)$$

*Splitting a link* of a spin network  $s = (\gamma, \rho, \iota)$  consists of considering the graph  $\gamma'$  obtained from  $\gamma$  by splitting one of its links, say  $\ell_0$ , into

$$\ell_0 = \ell'_2 \circ \ell'_1,$$

## 1. Loop Quantum Gravity states and spin foams

where we use a convention, that first we run through  $\ell'_1$  and then through  $\ell'_2$ . The links  $\ell'_1, \ell'_2$  are oriented in the agreement with  $\ell$ . We label each of the links  $\ell'_1, \ell'_2$  with the representation  $\rho_{\ell_0}$  and the new node  $n_{12}$  connecting the links  $\ell'_1$  and  $\ell'_2$  with the identity operator

$$\text{id} : \mathcal{H}_{\ell_0} \rightarrow \mathcal{H}_{\ell_0}$$

considered as an element of  $\text{Inv}(\mathcal{H}_{\ell'_1}^* \otimes \mathcal{H}_{\ell'_2}) = \text{Inv}(\mathcal{H}_{\ell_0}^* \otimes \mathcal{H}_{\ell_0})$ . In summary, we define a spin network  $\text{split}_{\ell_0}(s) := (\gamma', \rho', \iota')$ , where

$$\rho'_{\ell} := \begin{cases} \rho_{\ell_0}, & \text{if } \ell = \ell'_1, \ell'_2, \\ \rho_{\ell}, & \text{otherwise,} \end{cases} \quad (1.18)$$

$$\iota'_{n'} := \begin{cases} \text{id}, & \text{if } n' = n_{12}, \\ \iota_{n'}, & \text{if } n' \in \gamma^{(0)}. \end{cases} \quad (1.19)$$

*Adding a link* to a spin network  $s = (\gamma, \rho, \iota)$  is an operation that maps the spin network  $s$  to a spin network  $\text{add}_{n_0, n_1}(s) = (\gamma', \rho', \iota')$ , such that  $\gamma'$  is obtained from  $\gamma$  by adding a new link, say  $\ell_0$ , connecting (not necessarily different) nodes  $n_0, n_1$  of the graph  $\gamma$  oriented such that  $n_0$  is the source of the link  $\ell_0$  and  $n_1$  is a target of the link; we insert the trivial representation **1** on the new link  $\ell_0$ , and use the canonical isomorphism

$$\text{Inv} \left( \bigotimes_{\ell \text{ outgoing}} \mathcal{H}_{\rho_{\ell}} \otimes \bigotimes_{\ell \text{ incoming}} \mathcal{H}_{\rho_{\ell'}} \right) \rightarrow \text{Inv} \left( \mathbb{C} \otimes \bigotimes_{\ell \text{ outgoing}} \mathcal{H}_{\rho_{\ell}} \otimes \bigotimes_{\ell \text{ incoming}} \mathcal{H}_{\rho_{\ell'}} \right)$$

to map the intertwiners  $\iota_{n_0}, \iota_{n_1}$  on  $\gamma$  to intertwiners  $\tilde{\iota}_{n_0}, \tilde{\iota}_{n_1}$  on  $\gamma'$ . In detail,

$$\rho'_{\ell} := \begin{cases} \mathbf{1}, & \text{if } \ell = \ell_0, \\ \rho_{\ell}, & \text{if } \ell \in \gamma^{(1)}, \end{cases} \quad (1.20)$$

$$\iota'_{n} := \begin{cases} \tilde{\iota}_n, & \text{if } n = n_0 \text{ or } n = n_1, \\ \iota_n & \text{otherwise.} \end{cases} \quad (1.21)$$

*Adding a node* to a spin network  $s = (\gamma, \rho, \iota)$  is an operation that maps the spin network  $s$  to a spin network  $\text{add}_{n_0}(s) = (\gamma', \rho', \iota')$ , such that  $\gamma'$  is a disjoint union of  $\gamma$  and  $n_0$ ,  $\iota_{n_0} = 1 \in \mathbb{C}$ . In detail,

$$\rho'_{\ell} := \rho_{\ell} \quad (1.22)$$

$$\iota'_{\ell} := \begin{cases} 1 \in \mathbb{C}, & \text{if } n = n_0, \\ \iota_n & \text{otherwise.} \end{cases} \quad (1.23)$$

*The complex conjugate spin network*  $(\gamma, \bar{\rho}, \bar{\iota})$  to a given spin network  $(\gamma, \rho, \iota)$  is defined by using the conjugation map of any vector space

$$V \ni v \mapsto \bar{v} \in \bar{V}.$$

The conjugate vector space  $\bar{V}$  is defined as the same set  $V$  with a new multiplication  $\bar{\cdot}$  defined to be

$$a^- v := \bar{a}v,$$

## 1.2. The Hilbert space of the Loop Quantum Gravity states

the same adding operation  $\bar{+} = +$ , and the conjugation map being the identity. Clearly,

$$\bar{\iota}_n := \overline{\iota_n}, \quad \bar{\rho}_\ell := \overline{\rho_\ell}. \quad (1.24)$$

The Hilbert conjugate spin network  $(\gamma^\dagger, \rho^\dagger, \iota^\dagger)$  to a spin network  $(\gamma, \rho, \iota)$  is a spin network defined on the graph  $\gamma^\dagger$  obtained by flipping the orientation of each of the links of  $\gamma$ , and

$$\rho_{\ell^{-1}}^\dagger := \rho_\ell, \quad (1.25)$$

$$\iota_n^\dagger := (\iota_n)^\dagger, \quad (1.26)$$

where being given the Hilbert space  $\mathcal{H}$ , we denote by

$$\mathcal{H} \ni v \mapsto v^\dagger \in \mathcal{H}^*$$

the antilinear map defined by the Hilbert product (that is “ $|v\rangle^\dagger = \langle v|$ ”). It is not hard to check, that each spin network  $(\gamma^\dagger, \rho^\dagger, \iota^\dagger)$  can be obtained from the complex conjugate spin network  $(\gamma, \bar{\rho}, \bar{\iota})$  by the operations of flipping orientation of each of the links of  $\gamma$ .

### Spin-network functions

With a spin network  $s = (\gamma, \rho, \iota)$  we associate a function<sup>1</sup>

$$\psi_s : G^{\gamma^{(1)}} \rightarrow \mathbb{C}. \quad (1.27)$$

Let us denote elements of  $G^{\gamma^{(1)}}$  by

$$g : \gamma^{(1)} \rightarrow G, \quad \ell \mapsto g_\ell.$$

For every  $g \in G^{\gamma^{(1)}}$  there is a unique contraction

$$\psi_s(g) := \left( \bigotimes_{\ell \in \gamma^{(1)}} \rho_\ell(g_\ell) \right) \lrcorner \left( \bigotimes_{n \in \gamma^{(0)}} \iota_n \right). \quad (1.28)$$

In the abstract index notation, the contraction is defined as follows. We denote by  $A, B, C, D$  the indices in the representation spaces. For every link  $\ell \in \gamma^{(1)}$  we have  $\rho_B^A(g_\ell)$  in (1.28). At the start point  $n$  of  $\ell$ , there is an invariant  $\iota_{n \dots A \dots} \dots$  in (1.28) (the dots stand for the remaining indices) and at the end point  $n'$  of  $\ell$ , there is an invariant  $\iota_{n' \dots} \dots^B \dots$ . The corresponding part of (1.28) reads

$$\dots \iota_{n \dots A \dots} \dots \rho_B^A(g_\ell) \iota_{n' \dots} \dots^B \dots \dots$$

Given a graph  $\gamma$ , the spin-network functions form naturally a basis of the Hilbert space  $\mathcal{H}_\gamma \subset L^2(G^{\gamma^{(1)}}, \mu_H)$ , where  $\mu_H$  is the Haar measure. The subspace  $\mathcal{H}_\gamma$  coincides with the subspace of gauge invariant elements of  $L^2(G^{\gamma^{(1)}}, \mu_H)$ , where the gauge transformations

---

<sup>1</sup>Given two sets  $X$  and  $Y$ , by  $Y^X$  we denote the set of maps  $X \rightarrow Y$ . If  $X$  has  $N$  elements then  $Y^X \sim Y^N$ . This notation lets us avoid choosing an ordering in  $X$ .

## 1. Loop Quantum Gravity states and spin foams

are defined as follows: given a node  $n \in \gamma^{(0)}$  the gauge transformation defined by  $h \in G$  in  $G^{\gamma^{(1)}}$  is

$$(h, n)g_\ell = \begin{cases} g_\ell h, & \text{if } \ell \text{ begins at } n \text{ and ends elsewhere,} \\ h^{-1}g_\ell, & \text{if } \ell \text{ ends at } n \text{ and begins elsewhere,} \\ h^{-1}g_\ell h, & \text{if } \ell \text{ begins and ends at } n, \\ g_\ell, & \text{otherwise.} \end{cases} \quad (1.29)$$

The general gauge transformation is defined by a sequence of elements of  $G$  labelled by nodes.

Next, we define operations on the spin-network functions such as flipping orientation of a link, splitting a link, adding a link and adding a node (compare [22, 32]). They correspond to the operations on spin networks defined in the previous section.

If a graph  $\gamma'$  is obtained by *flipping the orientation* in one of the links, say  $\ell_0$ , of  $\gamma$ , then we define a map

$$\text{flip}_{\ell_0} : G^{\gamma'^{(1)}} \rightarrow G^{\gamma^{(1)}}, \quad (1.30)$$

$$(\text{flip}_{\ell_0}(g))_\ell = \begin{cases} g_{\ell_0}^{-1}, & \text{if } \ell = \ell_0, \\ g_\ell, & \text{otherwise.} \end{cases} \quad (1.31)$$

The map  $\text{flip}_{\ell_0}$  induces an isometric map  $\text{flip}_{\ell_0} : \mathcal{H}_\gamma \rightarrow \mathcal{H}_{\gamma'}$  defined by

$$(\text{flip}_{\ell_0} \psi)(g) := \psi(\text{flip}_{\ell_0}(g)).$$

In particular, the operation is related to the operation of flipping orientation of a link of a spin network (see section 1.2.2) by  $\text{flip}_{\ell_0} \psi_s = \psi_{\text{flip}_{\ell_0}(s)}$ .

In the case when  $\gamma'$  is obtained by *splitting one of the links*, say  $\ell_0$ , of  $\gamma$  into  $\ell_0 = \ell'_2 \circ \ell'_1$ , the corresponding map is

$$\text{split}_{\ell_0} : G^{\gamma'^{(1)}} \rightarrow G^{\gamma^{(1)}}, \quad (1.32)$$

$$\text{split}_{\ell_0}(g)_\ell = \begin{cases} g_{\ell'_2}g_{\ell'_1}, & \text{if } \ell = \ell_0, \\ g_\ell, & \text{otherwise.} \end{cases} \quad (1.33)$$

The map induces an isometric map  $\text{split}_{\ell_0} : \mathcal{H}_\gamma \rightarrow \mathcal{H}_{\gamma'}$  defined by

$$(\text{split}_{\ell_0} \psi)(g) := \psi(\text{split}_{\ell_0}(g)).$$

In particular  $\text{split}_{\ell_0} \psi_s = \psi_{\text{split}_{\ell_0}(s)}$ .

If a graph  $\gamma'$  is obtained by *adding a link*, i.e. connecting two nodes of  $\gamma$ , say  $n_0$  and  $n_1$ , with a new link, say  $\ell_0$ , the corresponding map is:

$$\text{add}_{n_0, n_1} : G^{\gamma'^{(1)}} \rightarrow G^{\gamma^{(1)}}, \quad (1.34)$$

$$(\text{add}_{n_0, n_1}(g))_\ell = g_\ell \text{ for } \ell \in \gamma^{(1)}. \quad (1.35)$$

Let us emphasize that  $\ell$  runs through the links of  $\gamma^{(1)}$ , and the link  $\ell_0$  is simply omitted. The map  $\text{add}_{n_0, n_1}$  induces an isometric map  $\text{add}_{n_0, n_1} : \mathcal{H}_\gamma \rightarrow \mathcal{H}_{\gamma'}$  defined by

$$(\text{add}_{n_0, n_1} \psi)(g) := \psi(\text{add}_{n_0, n_1}(g)).$$

## 1.2. The Hilbert space of the Loop Quantum Gravity states

In particular  $\text{add}_{n_0, n_1} \psi_s = \psi_{\text{add}_{n_0, n_1}(s)}$ .

Since *adding a node*, say  $n_0$ , does not change the set of links of the graph, the corresponding map  $\text{add}_{n_0} : G^{\gamma'^{(1)}} \rightarrow G^{\gamma^{(1)}}$  acts trivially on  $g$ :

$$\text{add}_{n_0}(g) = g.$$

The maps  $\text{add}_{n_0}$  induces an isometric map  $\text{add}_{n_0} : \mathcal{H}_\gamma \rightarrow \mathcal{H}_{\gamma'}$ :

$$(\text{add}_{n_0} \psi)(g) := \psi(g).$$

Again,  $\text{add}_{n_0} \psi_s = \psi_{\text{add}_{n_0}(s)}$ .

Not surprisingly the *complex conjugation* of a spin network has the following interpretation in terms of the spin-network functions

$$\psi_{\bar{s}} = \overline{\psi_s}. \quad (1.36)$$

### Equivalence relation

Any inclusion of a graph  $\gamma$  into a finer graph  $\gamma'$  can be represented as a sequence of operations of flipping the orientations of links, splitting links, adding links and adding nodes. As a result, the inclusion induces an isometric map from  $\mathcal{H}_\gamma$  to  $\mathcal{H}_{\gamma'}$ . We can therefore identify  $\mathcal{H}_\gamma$  with a subspace of  $\mathcal{H}_{\gamma'}$ . This identification induces an equivalence relation in the space of spin networks, namely two spin networks are equivalent if and only if one can be mapped into the other by a sequence of operations of splitting links and/or reorienting links and/or adding links and/or adding nodes. This equivalence allows us to treat a spin network defined on a graph  $\gamma$  as a spin network defined on arbitrary finer graph  $\gamma'$ .

### Evaluation of a spin network

Evaluation of a spin network  $s = (\gamma, \rho, \iota)$  is the number

$$s \mapsto \psi_s(I), \quad (1.37)$$

where  $I \in G^\gamma$  is the identity element.

### 1.2.3. The spin-network cylindrical functions of connections

Finally, we are in a position to explain the application of the spin networks in the Hilbert space of the cylindrical functions introduced in the previous section. Let us consider the graphs *embedded* in  $\Sigma$ , and embedded spin networks defined on them. Given an embedded spin network  $s = (\gamma, \rho, \iota)$ , we use the corresponding spin-network function  $\psi_s$ , to define a spin-network cylindrical function  $\Psi_s : \mathfrak{A}(\Sigma) \rightarrow \mathbb{C}$ . First, a connection  $A \in \mathfrak{A}(\Sigma)$  defines an element  $U_\gamma(A) \in G^{\gamma^{(1)}}$ ,

$$U_\gamma(A) : \ell \mapsto U_\ell(A) \in G. \quad (1.38)$$

Next, we use the spin-network function  $\psi_s$ ,

$$\Psi_s(A) := \psi_s(U_\gamma(A)). \quad (1.39)$$

## 1. Loop Quantum Gravity states and spin foams

In order to define an embedded spin-network on an embedded graph containing circles, we introduce a marked point on each circle. The spin-network cylindrical function does not depend on the location of the marked point on the circle.

If we put a restriction on embeddings to be piecewise analytic then the spin-network cylindrical functions span a dense subset of the Hilbert space  $\mathcal{H}_\Sigma$  and it is easy to construct from them an orthonormal basis. This assumption allow us to overcome some degenerated behaviour of the smooth category (see [27] for analogous construction in the smooth category). In the following we will assume that the embeddings are piecewise analytic.

The cylindrical functions lead to a natural equivalence relation between embedded spin networks: two embedded spin-network states are equivalent if and only if the corresponding spin-network states are equal.

### 1.2.4. Solutions to the Gauss constraint and the vector constraint

The Hilbert space of the theory of connections is  $L^2(\mathfrak{A}(\Sigma), \mu_0)$ . In Loop Quantum Gravity the gauge group  $G$  is the  $SU(2)$  group. The Gauss constraint generates  $SU(2)$  gauge transformations and the solutions to this constraint form a subspace  $\mathcal{H}_\Sigma \subset L^2(\mathfrak{A}(\Sigma), \mu_0)$  formed by the gauge invariant functions. This space can be written as a direct sum of Hilbert spaces  $\mathcal{H}'_{\Sigma, \gamma}$  spanned by  $SU(2)$  spin-network cylindrical functions  $\Psi_{(\gamma, \rho, \iota)}$  such that each representation  $\rho_\ell$  is non-trivial. Let us note, that a Hilbert space  $\mathcal{H}'_{\Sigma, \gamma}$  is non-trivial only if  $\gamma$  is closed, i.e. has no 1-valent nodes. The decomposition is

$$\mathcal{H}_\Sigma = \bigoplus_{\gamma \in \mathfrak{G}} \mathcal{H}'_{\Sigma, \gamma},$$

where  $\mathfrak{G}$  is a set of oriented embedded closed graphs  $\gamma$  such that:

- $\gamma$  has no spurious nodes, i.e. it cannot be obtained from another graph by a sequence of operations of splitting links or adding marked points to circles,
- any two different graphs in  $\mathfrak{G}$  cannot be related by the operations of flipping orientations of some links,
- any graph can be obtained from one of the graphs in  $\mathfrak{G}$  by a sequence of operations of flipping orientations of some links, splitting links, adding links.

We include a null graph  $K_0$ , i.e. graph having no nodes – in this case  $\mathcal{H}'_{\Sigma, K_0} = \mathbb{C}$ .

The vector constraint generates an action of the group of diffeomorphisms on the space  $\mathcal{H}_\Sigma$ . The constraint is solved by using averaging procedure. The action of a diffeomorphism  $\phi : \Sigma \rightarrow \Sigma$  on a cylindrical function  $\Psi$  is defined by [17]:

$$(\mathcal{U}_\phi \Psi)(A) := \Psi(\phi^* A).$$

In particular, the action of a diffeomorphism  $\phi : \Sigma \rightarrow \Sigma$  on an embedded spin-network is of the following form [178, 179]:

$$(\mathcal{U}_\phi \Psi_s)(A) = \psi_{\phi \cdot s}(U_{\phi(\gamma)}(A)),$$

where  $s = (\gamma, \rho, \iota)$ ,  $\phi \cdot s = (\phi(\gamma), \rho', \iota')$ ,  $\rho'_{\phi(\ell)} = \rho_\ell$ ,  $\iota'_{\phi(n)} = \iota_n$ . Let  $\text{Diff}_\gamma$  be a subgroup of the group of diffeomorphism which maps  $\gamma$  to itself and let  $\text{TDiff}_\gamma$  be its subgroup which preserves every link of  $\gamma$  and its orientation. The quotient

$$\text{GS}_\gamma = \text{Diff}_\gamma / \text{TDiff}_\gamma$$

## 1.2. The Hilbert space of the Loop Quantum Gravity states

is a finite group – it is the group of symmetries of  $\gamma$ .

The averaging procedure is the following [17]:

1. First, one defines a projection operator  $P_{\text{diff},\gamma} : \mathcal{H}'_{\Sigma,\gamma} \rightarrow \mathcal{H}'_{\Sigma,\gamma}$  by averaging each state  $\Psi \in \mathcal{H}'_{\Sigma,\gamma}$  over the group of symmetries of  $\gamma$

$$P_{\text{diff},\gamma}\Psi = \frac{1}{|\text{GS}_\gamma|} \sum_{\phi \in \text{GS}_\gamma} \mathcal{U}_\phi \Psi,$$

where  $|\text{GS}_\gamma|$  is the order of the group  $\text{GS}_\gamma$ .

2. Second, one averages over the diffeomorphisms that move the graph  $\gamma$ . The result of the averaging is an element of an algebraic dual of  $\text{Cyl}(\mathfrak{A}(\Sigma)) \cap \mathcal{H}_\Sigma$ ,  $(\eta(\Psi)| \in (\text{Cyl}(\mathfrak{A}(\Sigma)) \cap \mathcal{H}_\Sigma)^*$ , defined by its action on any state  $|\Phi\rangle \in \text{Cyl}(\mathfrak{A}(\Sigma)) \cap \mathcal{H}_\Sigma$ :

$$(\eta(\Psi)| \Phi\rangle = \sum_{\phi \in \text{Diff}/\text{Diff}_\gamma} \langle \mathcal{U}_\phi P_{\text{diff},\gamma} \Psi | \Phi \rangle,$$

where the bracket on the right-hand site denotes the scalar product in  $\mathcal{H}_\Sigma$ .

From the invariance of the scalar product in  $\mathcal{H}_\Sigma$  follows that  $(\eta(\Psi)|$  is invariant under the action of the group of diffeomorphisms:

$$(\eta(\Psi)| \mathcal{U}_\phi \Phi\rangle = (\eta(\Psi)| \Phi\rangle$$

for any diffeomorphisms  $\phi$ . The assignment  $\mathcal{H}'_{\Sigma,\gamma} \ni \Psi \mapsto (\eta(\Psi)| \in (\text{Cyl}(\mathfrak{A}(\Sigma)) \cap \mathcal{H}_\Sigma)^*$  extends to an anti-linear map  $\eta : \mathcal{H}_\Sigma \rightarrow (\text{Cyl}(\mathfrak{A}(\Sigma)) \cap \mathcal{H}_\Sigma)^*$ . The states  $(\eta(\Psi)|$  span a linear subspace of  $(\text{Cyl}(\mathfrak{A}(\Sigma)) \cap \mathcal{H}_\Sigma)^*$ , which can be equipped with a scalar product, defined by:

$$(\eta(\Psi)| \eta(\Phi)\rangle := (\eta(\Psi)| \Phi\rangle$$

and Cauchy completed. The resulting Hilbert space is the Hilbert space of solutions to the Gauss and the vector constraint. The Hilbert space obtained this way is non-separable. However, if instead of the group of diffeomorphisms we average over certain group of extended diffeomorphisms, we obtain a separable Hilbert space [90]. The group of extended diffeomorphisms is formed by invertible maps  $\phi : \Sigma \rightarrow \Sigma$  such that  $\phi$  and  $\phi^{-1}$  are continuous and infinitely differentiable everywhere except possibly at finite number of points. The resulting separable Hilbert space is spanned by elements  $(\eta(\Psi_{(\gamma,\rho,l)})|$  labelled by graphs  $\gamma$  representing the orbits of the action of the diffeomorphisms on the space of embedded graphs. In other words: one introduces an equivalence relation  $\gamma \sim \gamma'$  if and only if there is an extended diffeomorphism  $\phi$  such that  $\phi(\gamma) = \gamma'$ , and labels the states by representants of the equivalence classes of this relation. It was shown in [90] that these equivalence classes are equivalent to the singular knots. Since the knotting classes are countable, the space is separable.

### 1.2.5. Combinatorial Hilbert space

The quantum scalar constraint (see section 1.3.1) in the absence of matter does not change the linking and knotting. Neither is the spin-foam dynamics of the vacuum gravity sensitive to linking and knotting [28]. Therefore as the Hilbert space of the Loop Quantum Gravity

## 1. Loop Quantum Gravity states and spin foams

states we choose a subspace of the separable Hilbert space of solutions of the Gauss and the vector constraint from [90], spanned by elements obtained from  $(\eta(\Psi_{(\gamma,\rho,\iota)}))$  by averaging over possible knotting classes. In other words, we use the combinatorial Hilbert space [163]. We define the combinatorial Hilbert space in the following way:

- Let  $\gamma$  be an abstract graph. Let us consider the space  $\mathcal{H}_\gamma$  of gauge invariant elements in  $L^2(SU(2)^{\gamma^{(1)}}, \mu_H)$  introduced in section 1.2.2. Let us denote by  $\mathcal{H}'_\gamma$  the subspace spanned by (abstract) spin-network states  $\psi_{(\gamma,\rho,\iota)}$  such that each representation  $\rho_\ell$  is non-trivial.
- Let  $\phi \in \text{Aut}_\gamma$  be an automorphism of the graph  $\gamma$ , i.e. a pair of bijections  $\phi_0 : \gamma^{(0)} \rightarrow \gamma^{(0)}$  and  $\phi_1 : \gamma^{(1)} \rightarrow \gamma^{(1)}$  that preserve the source and the target relations [163]. Its action on  $SU(2)^{\gamma^{(1)}}$  is the following:

$$\mathbf{aut}_\phi(g)_\ell = g_{\phi_1(\ell)}.$$

It induces an action of the group  $\text{Aut}_\gamma$  on  $\mathcal{H}'_\gamma$

$$(\mathbf{aut}_\phi\psi)(g) = \psi(\mathbf{aut}_\phi(g)).$$

We define a projection operator onto the states invariant under the action of the group  $\text{Aut}_\gamma$ :

$$P_\gamma\psi = \frac{1}{|\text{Aut}_\gamma|} \sum_{\phi \in \text{Aut}_\gamma} \mathbf{aut}_\phi\psi.$$

We denote by  $\tilde{\mathcal{H}}_\gamma$  the range of the projection operator  $P_\gamma : \mathcal{H}'_\gamma \rightarrow \mathcal{H}'_\gamma$ .

- The combinatorial Hilbert space is a direct sum:

$$\mathcal{H}_{\text{comb}} = \bigoplus_{\gamma \in \mathfrak{G}} \tilde{\mathcal{H}}_\gamma,$$

where  $\mathfrak{G}$  is a set of oriented graphs  $\gamma$  such that:

- each node of  $\gamma$  either is at least 3-valent or is 2-valent and there is a link in  $\gamma^{(1)}$  starting and ending at the node,
- any two different graphs in  $\mathfrak{G}$  cannot be related by the operations of flipping orientations of some links,
- any graph can be obtained from one of the graphs in  $\mathfrak{G}$  by a sequence of operations flipping orientations of some links, splitting links, adding links and adding nodes.

We include a null graph  $K_0$ , which is a graph having 0 nodes – in this case  $\tilde{\mathcal{H}}_{K_0} = \mathbb{C}$ .

Let  $s = (\gamma, \rho, \iota)$  be a spin network. We define an action of the group of automorphisms on  $s$  by

$$\mathbf{aut}_\phi(s) := (\gamma, \rho', \iota'),$$

where  $\rho'_{\phi_1(\ell)} = \rho_\ell$ ,  $\iota'_{\phi_0(n)} = \iota_n$ . We define an equivalence relation in the space of spin networks: two spin networks  $s_1$  and  $s_2$  are equivalent if and only if there exists a third spin network  $s = (\gamma, \rho, \iota)$  such that  $s_1$  and  $s_2$  can be obtained from  $s$  by (in general

different and possibly empty) sequences of operations:  $\text{aut}_\phi$  (for some automorphisms  $\phi$  of the graph  $\gamma$ ) followed by splitting links, reorienting links, adding links, adding nodes. The equivalence classes of this relation, denoted by  $[s]$ , label the states spanning the combinatorial Hilbert space. The corresponding spin-network functions are:

$$\psi_{[s]} = 0 \oplus \dots \oplus 0 \oplus P_\gamma \psi_{(\gamma, \rho, \iota)} \oplus 0 \dots \in \mathcal{H}_{\text{comb}},$$

where  $\gamma \in \mathfrak{G}$ . It is always possible to choose  $\gamma \in \mathfrak{G}$ , because any graph is obtained from one of the graphs  $\gamma \in \mathfrak{G}$  by a sequence of operations splitting links, reorienting links, adding links and adding nodes.

## 1.3. Spin foams

### 1.3.1. Spin foams as histories of spin networks

In the previous section we constructed a Hilbert space of solutions of the Gauss constraint and the vector constraint. The transformations generated by these constraints will be called kinematical because they operate on a 'fixed time' surface. Finding the dynamics amounts to imposing the scalar constraint, which is still an open problem in Loop Quantum Gravity. The problem could be solved by quantizing the scalar constraint and solving the quantum constraint. Different quantizations of the constraint have been proposed [172, 100, 70, 71, 6]. In the approaches [172, 100, 70, 71] the quantum operator acts on spin network's nodes and modifies the spin networks by creating new links according to figure 1.2a [146]. In [6] the scalar constraint operator modifies the spin network by creating new links according to figure 1.2b.

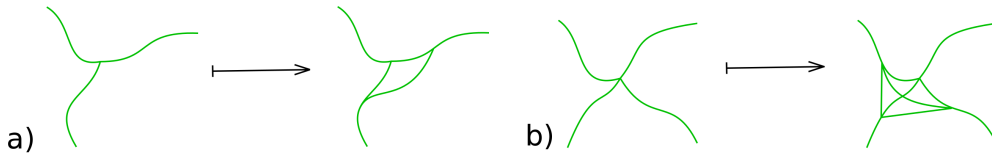


Figure 1.2.: The scalar constraint operator is changing the graph: a) the scalar constraint operator studied in [172, 100, 70, 71], b) the scalar constraint operator studied in [6].

Some simple solutions to the quantum constraint [172] are known. However, general solution is still missing. One of the reasons is complicated structure of the constraint operator. This can be attributed to the 3+1 splitting of space-time breaking the 4-dimensional diffeomorphism symmetry [146]. The spin-foam approach to LQG aims at finding the solutions by formulating the dynamics covariantly and developing an analog of the Feynman path integral. The idea of Rovelli and Reisenberger [155, 158] is that the paths should be suitably defined histories of the spin-network states called spin foams. Since the spin networks are graphs with a suitable coloring, the spin foams are 2-complexes (histories of graphs) with suitable colorings.

In standard formulation of quantum mechanics the path integrals define matrix elements of the evolution operator. In Quantum Gravity the path integrals provide a scalar product

## 1. Loop Quantum Gravity states and spin foams

between solutions to the constraints. The scalar product is interpreted as a transition amplitude between quantum geometry encoded in the initial state and the final state [111].

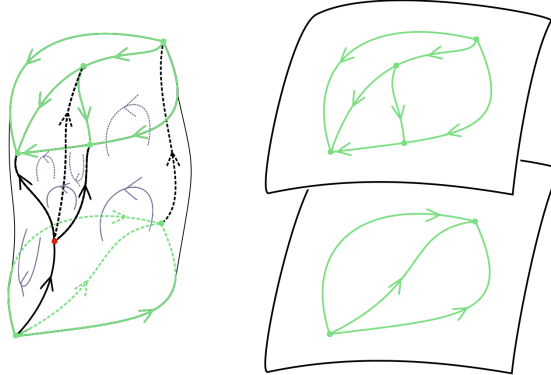
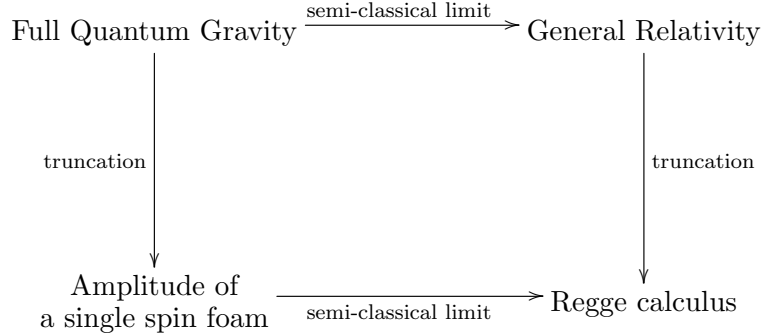


Figure 1.3.: a) A history of a spin network. b) The initial and, respectively, final spin network.

The advantage of using the spin-foam approach to define the dynamics of Loop Quantum Gravity is two-fold. First, it defines the solutions of the constraints. Second, it allows to define the dynamics in a covariant way without constructing the quantum constraints operators explicitly. The idea is to consider an amplitude assigned to a single spin foam as a truncation of the full transition amplitude. The corresponding truncation in the classical theory is defined by Regge calculus. The correspondence is a semiclassical limit. In summary (compare [165]):



The transition amplitude of the full theory of Quantum Gravity is either a sum of amplitudes of different spin foams or a refinement limit. In fact, in [166] the authors argue that the two definitions coincide.

A motivating example is the Ponzano-Regge model [150] (see also [42, 20]), which is a special case of a spin-foam model of quantum BF theory. We will discuss the model in the next subsection, starting with a general construction of the spin-foam models of quantum BF theory.

### 1.3.2. Spin-foam models of quantum BF theory

Let  $G$  be a compact group,  $\mathfrak{g}$  be its Lie algebra and  $M$  be a  $d$ -dimensional manifold. Let us denote by  $\langle , \rangle$  an invariant scalar product on  $\mathfrak{g}$ . In the BF theory the variables are:

- a  $\mathfrak{g}$  valued (d-2)-form  $B$  on  $M$ ,
- a connection one-form  $\omega$  on  $M$ .

The BF theory is defined on general principal fibre bundle [20]. For simplicity we restrict ourselves to trivial bundle ( $\omega$  and  $B$  are globally defined forms).

By  $\mathcal{F}$  we denote the curvature two-form of the connection one-form  $\omega$ . The BF theory is defined by action functional:

$$S[B, \omega] = \int_M \text{Tr}(B \wedge \mathcal{F}),$$

where  $\text{Tr}(B \wedge \mathcal{F}) = \langle \tau_p, \tau_q \rangle B^p \wedge \mathcal{F}^q$ ,  $\tau_p$  is a basis of  $\mathfrak{g}$ .

For simplicity, let us assume that the manifold  $M$  does not have boundary. In this case the object of interest is the partition function:

$$Z(M) = \int \mathfrak{D}[B] \mathfrak{D}[\omega] e^{i \int_M \text{Tr}(B \wedge \mathcal{F})}.$$

Formally, the integral over the  $B$  fields can be performed giving:

$$Z(M) = \int \mathfrak{D}[\omega] \delta(\mathcal{F}). \quad (1.40)$$

In order to construct a spin-foam model one introduces a triangulation of the manifold  $M$  and constructs a 2-skeleton of a complex dual to the triangulation (for definition of a triangulation see [119, 179] and for definition of a complex dual to a given complex see [119, 180, 179]). This 2-skeleton equipped with an orientation will be called a (simplicial) foam. The foam has one vertex in the center of each n-simplex, one edge intersecting each (n-1)-simplex, and one face intersecting each (n-2)-simplex. For example, if  $M$  is 3-dimensional, the relation between the elements of the triangulation and the foam is given in table 1.1. If  $M$  is 4-dimensional, the relation is given in table 1.2.

Triangulation	point	segment	triangle	tetrahedron
Foam ( $\kappa$ )		face ( $f$ )	edge ( $e$ )	vertex ( $v$ )

Table 1.1.: Relation between elements of a triangulation of 3-dimensional manifold and elements of the corresponding foam.

Triangulation	point	segment	triangle	tetrahedron	4-simplex
Foam ( $\kappa$ )			face ( $f$ )	edge ( $e$ )	vertex ( $v$ )

Table 1.2.: Relation between elements of a triangulation of 4-dimensional manifold and elements of the corresponding foam.

The connection is discretized by assigning one group element  $g_e$  to each oriented edge  $e$  of the foam. If an orientation of an edge, say  $e_0$ , is changed, the labelling is changed according to the rule (compare (1.31)):

$$g_e \mapsto \begin{cases} (g_{e_0^{-1}})^{-1}, & \text{if } e = e_0, \\ g_e, & \text{otherwise.} \end{cases}$$

## 1. Loop Quantum Gravity states and spin foams

The discrete connection is called flat if the holonomy around each (oriented) face is trivial:

$$g_{e_1 f} \cdots g_{e_{N_f} f} = I,$$

where

$$g_{ef} = \begin{cases} g_e, & \text{if the orientation of } e \text{ agrees with the orientation of } f, \\ (g_e)^{-1}, & \text{otherwise.} \end{cases}$$

The discrete analog of the partition function (1.40) is:

$$Z[\kappa] = \int \prod_{e \in \kappa^{(1)}} d\mu_H(g_e) \prod_{f \in \kappa^{(2)}} \delta(g_{e_1 f} \cdots g_{e_{N_f} f}),$$

where  $\kappa^{(1)}$  denotes the set of edges of the foam  $\kappa$ ,  $\kappa^{(2)}$  denotes the set of faces of the foam  $\kappa$ ,  $\mu_H$  denotes the Haar measure. Using Peter-Weyl theorem the  $\delta$  distribution can be expressed as a weighted sum of the characters of the group  $G$ :

$$\delta(g) = \sum_{\rho \in \text{Irr}(G)} \dim \mathcal{H}_\rho \text{Tr}(\rho(g)),$$

where the sum is over unitary irreducible representations of  $G$ ;  $\mathcal{H}_\rho$  is the representation space of the representation  $\rho$ . Using this formula, the expression for the partition function becomes:

$$Z[\kappa] = \sum_{\rho_f \in \text{Irr}(G)} \int \prod_{e \in \kappa^{(1)}} d\mu_H(g_e) \prod_{f \in \kappa^{(2)}} \dim \mathcal{H}_f \text{Tr}(\rho_f(g_{e_1 f} \cdots g_{e_{N_f} f})), \quad (1.41)$$

where we use a shorthand notation  $\mathcal{H}_f := \mathcal{H}_{\rho_f}$ . Let us split the faces containing an edge  $e$  into the faces which orientation agrees with the orientation of  $e$  and the faces which orientation is opposite. In order to calculate the integral over  $g_e$  in the expression above, we need to find a formula for

$$P_e = \int d\mu_H(g_e) \bigotimes_{f \text{ same orientation as } e} \rho_f(g_e) \otimes \bigotimes_{f \text{ opposite orientation to } e} \rho_f(g_e^{-1}).$$

Let us denote by  $\mathcal{H}_e$  the following Hilbert space:

$$\mathcal{H}_e = \bigotimes_{f \text{ same orientation as } e} \mathcal{H}_f \otimes \bigotimes_{f' \text{ opposite orientation to } e} \mathcal{H}_{f'}^*.$$

The integral over  $g_e$  is performed by noting that  $P$  considered as an operator

$$P_e : \mathcal{H}_e \rightarrow \mathcal{H}_e$$

is orthogonal projection onto the space  $\text{Inv}(\mathcal{H}_e) \subset \mathcal{H}_e$  of invariants of the representation:

$$\bigotimes_{f \text{ same orientation as } e} \rho_f \otimes \bigotimes_{f' \text{ opposite orientation to } e} \rho_{f'}^*.$$

The operator  $P_e$  can be written in the following way:

$$P_e = \sum_{\iota_e} \iota_e \otimes \iota_e^\dagger, \quad (1.42)$$

where the sum is over the orthonormal basis in  $\text{Inv}(\mathcal{H}_e) \subset \mathcal{H}_e$ .

In (1.41) the indices of the matrices  $\rho_f(g_{ef})$  are contracted. In order to study the contraction pattern of the indices of the invariants  $\iota_e^\dagger / \iota_{e'}$  let us first note that to each vertex  $v$  there corresponds a tensor (figure 1.4a):

$$\bigotimes_{\text{outgoing } e} \iota_e^\dagger \otimes \bigotimes_{\text{incoming } e'} \iota_{e'}. \quad (1.43)$$

For every face  $f$  intersecting  $v$ , there are exactly two edges at  $v$ , say  $e_1$  and  $e_2$ , contained in  $f$  (figure 1.4b). Let us take the corresponding invariants present in (1.43). One of them has exactly one index corresponding to the representation  $\rho_f$ . Then, the other one has exactly one index in the representation  $\rho_f^*$ . Let us contract those indices and repeat the procedure for every face intersecting  $v$ . The result can be symbolically denoted by,

$$\text{Tr}_v \left( \bigotimes_{\text{outgoing } e} \iota_e^\dagger \otimes \bigotimes_{\text{incoming } e'} \iota_{e'} \right). \quad (1.44)$$

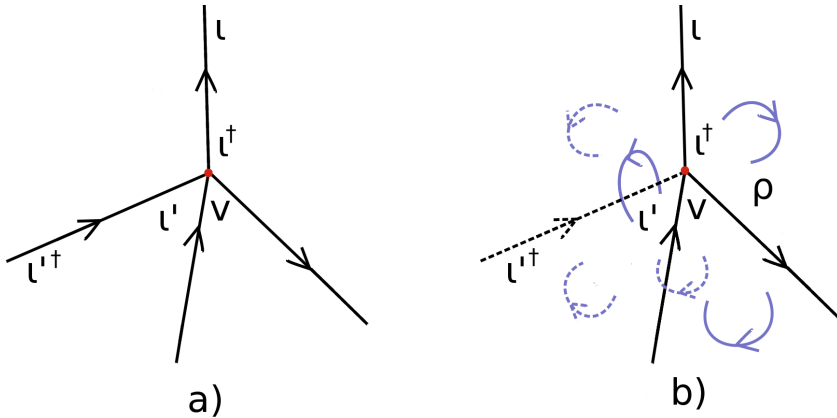


Figure 1.4.: a) Edges meet at vertices. Every edge contributes an invariant or hermitian conjugate invariant. b) Every face meeting  $v$  contains exactly two of the edges.

Applying this considerations to formula (1.41) we obtain

$$Z[\kappa] = \sum_{\rho} \sum_{\iota} \prod_{f \in \kappa^{(2)}} \dim \mathcal{H}_f \prod_{v \in \kappa_{\text{int}}^{(0)}} \text{Tr}_v \left( \bigotimes_{\text{outgoing } e} \iota_e^\dagger \otimes \bigotimes_{\text{incoming } e'} \iota_{e'} \right).$$

The numbers  $\dim \mathcal{H}_f$  and  $\text{Tr}_v \left( \bigotimes_{\text{outgoing } e} \iota_e^\dagger \otimes \bigotimes_{\text{incoming } e'} \iota_{e'} \right)$  are called face and vertex amplitudes, respectively. In general, the expression may also involve amplitudes assigned

## 1. Loop Quantum Gravity states and spin foams

to edges of the foam called edge amplitudes. Let us note that we considered manifolds without boundaries and as a result the foam  $\kappa$  does not have boundary. In the next section 1.3.3 we will introduce a general definition of a spin foam valid also for foams with boundary.

### The Ponzano-Regge model

An example of a spin-foam model of quantum BF theory is the Ponzano-Regge model [150, 42, 20]. In this model the structure group  $G$  is  $SU(2)$  and the manifold  $M$  is 3-dimensional. Remarkably in this case, the BF theory coincides with a 3-dimensional version of Euclidean General Relativity (see for example [146]). Since the unitary irreducible representations of the  $SU(2)$  group are labelled with spins  $j \in \frac{1}{2}\mathbb{N}$ , to each face  $f$  of a foam  $\kappa$  there corresponds a spin  $j_f$ . Since each face of the foam is dual to a segment of the triangulation, the labelling of  $\kappa$  induces a labelling of the segments of triangulation with spins. Ponzano and Regge interpret the spins as the lengths of the segments – strictly speaking a length  $l_f$  of a segment  $f$  is taken to be  $l_f = j_f + \frac{1}{2}$ . The lengths determine the geometry, in particular they define dihedral angles  $\Theta_f^v$ , which are the angles between the outward pointing normals to the two triangles of a tetrahedron  $v$  that are intersecting  $f$ . Using Regge calculus [154] it can be shown that the action:

$$S = \sum_v S_v, \text{ where } S_v = \sum_{f \subset v} l_f \Theta_f^v$$

approximates the Einstein-Hilbert action. Ponzano and Regge showed that the vertex amplitude

$$\text{Tr}_v \left( \bigotimes_{\text{outgoing } e} \iota_e^\dagger \otimes \bigotimes_{\text{incoming } e'} \iota_{e'} \right)$$

in the limit of large spins is asymptotic to:

$$\sqrt{\frac{2}{3\pi V}} \cos \left( S_v + \frac{\pi}{4} \right), \quad (1.45)$$

where  $V$  is the volume of the tetrahedron. One could expect to get the usual Feynman's weight  $e^{iS_v}$  but gets a cosine instead because the lengths determine the edges of the tetrahedron up to rotation and reflection. The phase shift  $\frac{\pi}{4}$  is the result of stationary phase approximation [20]. In the Ponzano-Regge model the semiclassical limit is the limit of large spins (see [165] for the tentative explanation why these limits may coincide). The limit corresponds to the lower arrow in the diagram in the previous subsection.

### 1.3.3. Spin foams

Motivated by the example of the model of quantum BF theory from the previous section we introduce now the definition of a spin foam.

### Foams

By a foam we mean in chapters 1, 3, 4, 5 an oriented piecewise linear 2-cell complex with (possibly empty) boundary. In chapter 6 we will introduce another class of 2-complexes defined diagrammatically.

A piecewise linear cell complex is defined in the following way [20, 160]. A cell is a convex hull of a finite number of points in  $\mathbb{R}^n$ . The dimension of the smallest affine space containing a cell is called the dimension of the cell. Let  $X$  be a cell and  $x \in X$ ; let  $\langle x, X \rangle$  denote a sum of lines  $L$  in  $\mathbb{R}^n$  such that  $L \cap X$  is a line segment and  $x$  is in its interior. If there are no such lines, then  $\langle x, X \rangle$  is defined to be  $\{x\}$ . The cell  $\langle x, X \rangle \cap X$  is called a face of  $X$ . If  $Y$  is a face of  $X$  we write  $Y \prec X$ . A piecewise linear complex  $K$  is a collection of cells such that:

- if  $X \in K$  and  $Y \prec X$  then  $Y \in K$ ,
- if  $X, Y \in K$  then  $X \cap Y$  is a face of both  $X$  and  $Y$ .

We say that a complex is  $k$ -dimensional if it has cells of dimension  $k$  but not higher. A complex is called oriented if the cells are equipped with orientations; it is assumed that 0-cells have positive orientation.

A foam  $\kappa$  is a piecewise linear oriented 2-complex such that each edge is contained in several (at least one) faces, each vertex is contained in several (at least one) edges and that the number of faces is finite. It consists of 2-cells called faces (n.b. this is a standard nomenclature; it should not be confused with the face of a cell in the definition of a cell complex given in the previous paragraph), 1-cells called edges, and 0-cells called vertices. We denote by  $\kappa^{(2)}$  the set of faces of  $\kappa$ ,  $\kappa^{(1)}$  the set of edges of  $\kappa$  and  $\kappa^{(0)}$  the set of vertices of  $\kappa$ .

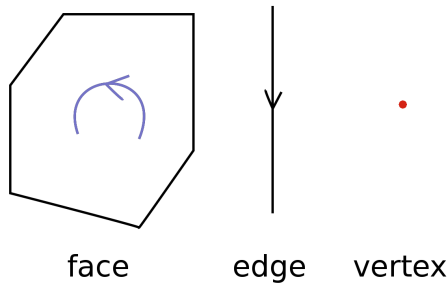


Figure 1.5.: Cells of the complex.

The boundary  $\partial\kappa$  is a 1-cell subcomplex (graph) of  $\kappa$  such that there exists a one-to-one affine map  $c : \partial\kappa \times [0, 1] \rightarrow \kappa$  which maps each cell of  $\partial\kappa \times [0, 1]$  onto the unique cell of  $\kappa$  and the set  $\partial\kappa \times [0, 1]$  onto an open subset of  $\kappa$  (see appendix of [20] for details). An edge of  $\kappa$  is called a boundary link if and only if it is contained in  $\partial\kappa$ . Otherwise, it is called an internal edge. An important technical subtlety of the definition of a boundary is that a vertex of  $\kappa$  is a vertex of  $\partial\kappa$  if and only if it is contained in exactly one internal edge of  $\kappa$ . Such vertex is called a boundary node. Each vertex which is not a boundary node is called an internal vertex of  $\kappa$ . We denote by  $\kappa_{\text{int}}^{(1)}$  the set of internal edges, by  $\kappa_{\text{int}}^{(0)}$  the set of internal vertices, by  $\partial\kappa^{(1)}$  the set of boundary links and by  $\partial\kappa^{(0)}$  the set of boundary nodes of  $\kappa$ .

### Coloring

Given a foam  $\kappa$ , a spin foam is defined by introducing three colorings (see figure 1.8):

## 1. Loop Quantum Gravity states and spin foams

- $\rho$  colors the faces of  $\kappa$  with unitary irreducible representations of the group  $G$ ,

$$\rho : \kappa^{(2)} \rightarrow \text{Irr}(G), \quad (1.46)$$

$$f \mapsto \rho_f. \quad (1.47)$$

We consider representation  $\rho_f$  as acting on a given Hilbert space  $\mathcal{H}_f$ .

- $\iota$  colors the internal edges of  $\kappa$  with invariants of suitable tensor product of the representations given by the coloring  $\rho$ . Let  $e \in \kappa_{\text{int}}^{(1)}$ . To define the space of invariants  $\text{Inv}(\mathcal{H}_e)$  we split the set of faces containing  $e$ , into faces which orientation coincides with that of  $e$  and respectively, with the opposite orientation (see figure 1.6),

$$\text{Inv}(\mathcal{H}_e) \subset \mathcal{H}_e := \bigotimes_{f \text{ same orientation as } e} \mathcal{H}_f \otimes \bigotimes_{f' \text{ opposite orientation to } e} \mathcal{H}_{f'}^*, \quad (1.48)$$

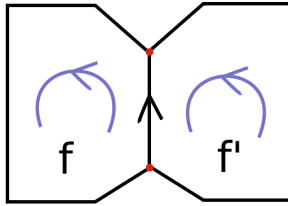
where the subset consists of the invariants of the representation

$$\bigotimes_{f \text{ same orientation}} \rho_f \otimes \bigotimes_{f' \text{ opposite orientation}} \rho_{f'}^*. \quad (1.49)$$

The coloring  $\iota$  is a map

$$e \mapsto \iota_e \in \text{Inv}(\mathcal{H}_e). \quad (1.50)$$

In fact, it is often convenient to think of  $\iota_e^\dagger$  as assigned to the edge  $e$  at the start point whereas at the end point we assign  $\iota_e$ . We will often consider  $\iota_e$  to be an element of  $\mathcal{H}_e$  by using the canonical embedding  $\text{Inv}(\mathcal{H}_e) \subset \mathcal{H}_e$ .



$$\mathcal{H}_e = \mathcal{H}_f \otimes \dots \otimes \mathcal{H}_{f'}^* \otimes \dots$$

Figure 1.6.: The edge Hilbert space  $\mathcal{H}_e$ .

- $\mathcal{A}$  colors the internal vertices of  $\kappa$  with linear functionals of suitable tensor product of the spaces  $\text{Inv}(\mathcal{H}_e)$ . Let  $v \in \kappa_{\text{int}}^{(0)}$ . We introduce (see figure 1.7):

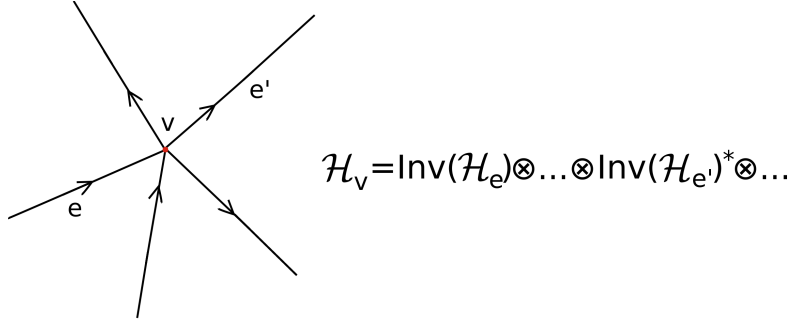
$$\mathcal{H}_v = \bigotimes_{e \text{ incoming at } v} \text{Inv}(\mathcal{H}_e) \otimes \bigotimes_{e \text{ outgoing at } v} \text{Inv}(\mathcal{H}_e)^*. \quad (1.51)$$

The coloring  $\mathcal{A}$  is a map

$$v \mapsto \mathcal{A}_v \in (\mathcal{H}_v)^*. \quad (1.51)$$

It is sometimes convenient to define the coloring in a bigger space

$$\widetilde{\mathcal{H}}_v = \bigotimes_{e \text{ incoming at } v} \mathcal{H}_e \otimes \bigotimes_{e \text{ outgoing at } v} \mathcal{H}_e^*,$$


 Figure 1.7.: The vertex Hilbert space  $\mathcal{H}_v$ .

A coloring of internal vertices with linear functionals

$$\kappa_{\text{int}}^{(0)} \ni v \mapsto \tilde{\mathcal{A}}_v \in (\widetilde{\mathcal{H}}_v)^*,$$

uniquely defines a coloring (1.51) by restricting  $\tilde{\mathcal{A}}_v$  to  $\mathcal{H}_v$ :

$$\mathcal{A}_v = \tilde{\mathcal{A}}_v|_{\mathcal{H}_v}.$$

An important example is the vertex trace  $\text{Tr}_v$  (compare (1.44)). It can be defined by a functional on  $\widetilde{\mathcal{H}}_v \simeq \bigotimes_{f:v \subset f} \mathcal{H}_f \otimes \mathcal{H}_f^*$  by taking

$$\widetilde{\text{Tr}}_v := \bigotimes_{f:v \subset f} \text{Tr}_{v,f},$$

where  $\text{Tr}_{v,f} : \mathcal{H}_f \otimes \mathcal{H}_f^* \rightarrow \mathbb{C}$  is the trace functional. On the other hand, any functional  $\mathcal{A}_v : \mathcal{H}_v \rightarrow \mathbb{C}$  can be extended to a functional  $\tilde{\mathcal{A}}_v$  on  $\widetilde{\mathcal{H}}_v$  by defining  $\tilde{\mathcal{A}}_v$  to be equal to  $\mathcal{A}_v$  on  $\mathcal{H}_v \subset \widetilde{\mathcal{H}}_v$  and to be zero on any element in orthogonal complement of  $\mathcal{H}_v$  in  $\widetilde{\mathcal{H}}_v$ . In this thesis we will omit the tilde and denote by  $\mathcal{A}_v$  the linear functional on  $\mathcal{H}_v$  as well as on  $\widetilde{\mathcal{H}}_v$ .

Let us note that the spin-foam structure has been defined in the interior of a foam.

### Induced boundary spin-network

Given a spin foam  $(\kappa, \rho, \iota, \mathcal{A})$ , the colorings  $\rho$  and  $\iota$  induce on the boundary  $\partial\kappa$  a spin-network structure  $(\partial\kappa, \partial\rho, \partial\iota)$ . For every link  $\ell$  of  $\partial\kappa$  let  $f_\ell$  denote the unique face of  $\kappa$  that contains  $\ell$ , and

$$\partial\rho_\ell := \begin{cases} \rho_{f_\ell}, & \text{if the orientations of } f_\ell \text{ and } \ell \text{ coincide,} \\ \rho_{f_\ell}^*, & \text{if they are opposite.} \end{cases} \quad (1.52)$$

For every node  $n$  of  $\partial\kappa$ , let  $e_n$  be the unique internal edge of  $\kappa$  that contains  $n$ , and

$$\partial\iota_n := \begin{cases} \iota_{e_n}^\dagger, & \text{if } n \text{ is the beginning of } e_n, \\ \iota_{e_n}, & \text{if } n \text{ is the end of } e_n. \end{cases} \quad (1.53)$$

## 1. Loop Quantum Gravity states and spin foams

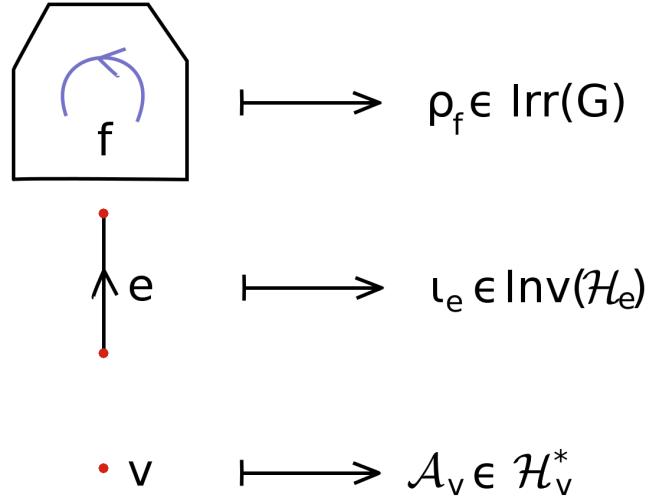


Figure 1.8.: a) Faces are colored with unitary irreducible representations of  $G$ . b) Internal edges are colored with invariants. c) Internal vertices are colored with contractors.

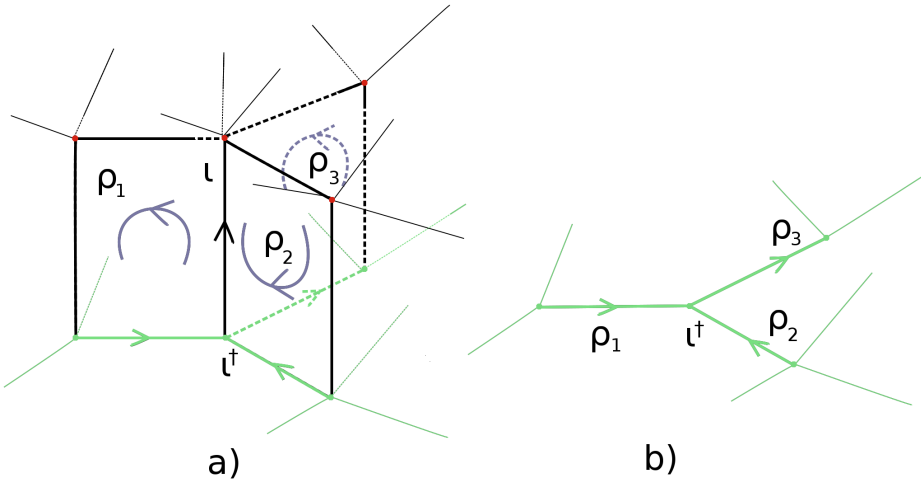


Figure 1.9.: a) A spin foam with boundary (in the bottom). b) Induced spin network on the boundary.

### The vertex spin network

Let us consider a spin foam  $(\kappa, \rho, \iota, \mathcal{A})$ . Given an internal vertex  $v$  and the intersecting faces, on each of the faces we consider a suitable neighbourhood of  $v$ . The neighbourhood is bounded by the segments of the sites of the face meeting at  $v$ , and a new extra edge connecting the segments (marked by a thinner curve on figure 1.10 a)). The union of the resulting neighbourhoods of  $v$  in each intersecting face is a foam neighbourhood of the vertex  $v$ . The foam neighbourhood of  $v$  is a spin foam with boundary itself. The boundary is formed by the thinner edges on figure 1.10 a)). Let us denote the spin network induced

on the boundary (figure 1.10 b)) by  $s_v = (\gamma_v, \rho, \iota)$ , and the corresponding spin-network function by  $\psi_{s_v}$ . We will call  $s_v$  a vertex spin network.

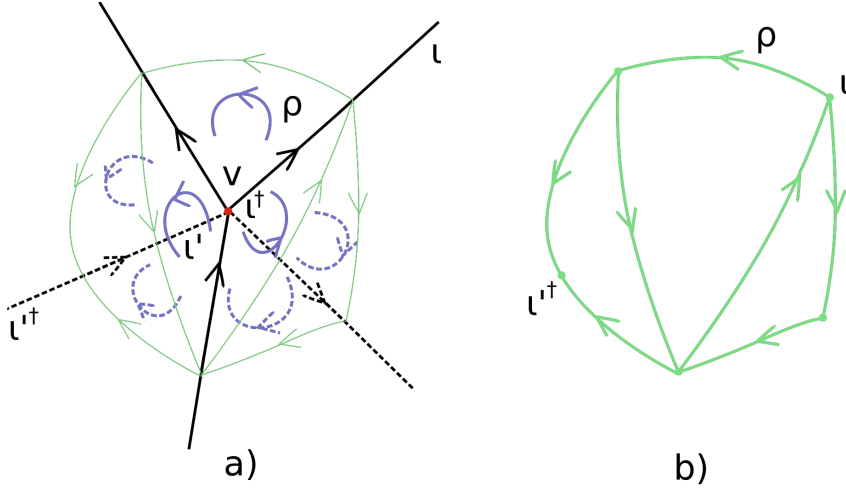


Figure 1.10.: a) A foam neighbourhood of the vertex  $v$  bounded by new, thinner edges. b) The spin network induced on the boundary of the neighbourhood. We will call it the vertex spin network and denote it by  $s_v$ .

### Vertex amplitude

A contractor  $\mathcal{A}_v$  defines a map

$$s_v^\dagger \mapsto \mathcal{A}_v(s_v^\dagger) := \mathcal{A}_v\left(\bigotimes_{n \in \gamma_v^{(0)}} \iota_n^\dagger\right). \quad (1.54)$$

The number  $\mathcal{A}_v(s_v^\dagger)$  is called the vertex amplitude.

Let us note that the vertex amplitude defined by the vertex trace (1.44) equals the evaluation of the conjugate spin network

$$\text{Tr}_v(s_v^\dagger) = \overline{\psi_{s_v}(I)} \quad (1.55)$$

The conjugate spin network itself is the spin network induced on the boundary of the spin foam obtained from  $(\kappa, \rho, \iota, \mathcal{A})$  by removing the neighbourhood of the vertex  $v$ .

In the case when the 2-complex is defined by a triangulation of 4-dimensional space-time, a vertex is dual to a 4-simplex (see table 1.2) and a vertex amplitude is called also a 4-simplex amplitude.

#### 1.3.4. Amplitude of a spin foam

A spin-foam model specifies a group  $G$ , a class of spin foams (a class of foams and possible colorings) and defines functions:  $A_{\text{face}} : \text{Irr}(G) \rightarrow \mathbb{C}$  and  $A_{\text{link}} : \text{Irr}(G) \rightarrow \mathbb{C}$  such that

$$A_{\text{face}}(\rho_1) = A_{\text{face}}(\rho_2), \quad A_{\text{link}}(\rho_1) = A_{\text{link}}(\rho_2)$$

## 1. Loop Quantum Gravity states and spin foams

if the representations  $\rho_1$  and  $\rho_2$  are equivalent. Let  $(\kappa, \rho, \iota, \mathcal{A})$  be a spin foam. The number  $A_{\text{face}}(\rho_f)$ , where  $f \in \kappa^{(2)}$ , is called a face amplitude. The number  $A_{\text{link}}(\partial\rho_\ell)$  is called a boundary link amplitude.

A spin-foam model assigns to each spin foam  $(\kappa, \rho, \iota, \mathcal{A})$  (in the class) a complex number:

$$Z(\kappa, \rho, \iota, \mathcal{A}) = \prod_{\ell \in (\partial\kappa)^{(1)}} A_{\text{link}}(\partial\rho_\ell) \prod_{f \in \kappa^{(2)}} A_{\text{face}}(\rho_f) \prod_{v \in \kappa_{\text{int}}^{(0)}} \mathcal{A}_v(s_v^\dagger).$$

$Z(\kappa, \rho, \iota, \mathcal{A})$  is called a spin-foam amplitude. In general, this expression could involve boundary node amplitudes and internal edge amplitudes. The amplitudes can be incorporated by redefining the boundary link amplitudes and the contractors [48].

It is easiest to understand the meaning of the amplitude of a spin foam by studying the causal approach [136, 20, 145, 146]. In this approach a spin foam  $(\kappa, \rho, \iota, \mathcal{A})$  is a history of an initial spin network  $s_{\text{in}}$  evolving into a final spin network  $s_{\text{out}}$ . The histories are defined by foams  $\kappa$  such that  $\partial\kappa = \gamma_{\text{out}} \cup \bar{\gamma}_{\text{in}}$ . The spin network  $s_{\text{in}}$  is the hermitian adjoint (= the complex conjugate) of the spin network induced on  $\gamma_{\text{in}}$  whereas  $s_{\text{out}}$  is the spin network induced on  $\gamma_{\text{out}}$ . A formal sum of the spin-foam amplitudes over all possible histories of an initial spin network  $s_{\text{in}}$  evolving into a final spin network  $s_{\text{out}}$ :

$$\sum_{(\kappa, \rho, \iota, \mathcal{A}): (\partial\kappa, \partial\rho, \partial\iota) = s_{\text{out}} \otimes s_{\text{in}}^\dagger} Z(\kappa, \rho, \iota, \mathcal{A}) \quad (1.56)$$

is called a transition amplitude. It can be interpreted as a scalar product between the solutions to all the (quantum) constraints. The solutions to vector and scalar constraint after averaging over the knotting classes are states in the combinatorial Hilbert space. The remaining problem is to solve the scalar constraint. If zero is in the continuous part of the spectrum of the (quantum) scalar constraint [146], the solutions will be distributional (as in the case of vector constraint) – tentatively they will be elements of the algebraic dual  $\mathcal{D}^*$  to some dense domain  $\mathcal{D} \subset \mathcal{H}_{\text{comb}}$  [179]. Let us denote by  $\hat{C}$  a quantum operator corresponding to the scalar constraint function  $C$ . The solutions to the constraint are expected to be given by an antilinear map  $\eta_{\text{scalar}} : \mathcal{D} \rightarrow \mathcal{D}^*$ , such that:

$$\hat{C}(\eta_{\text{scalar}}(\psi)) = 0$$

for all  $\psi \in \mathcal{D}$ . In other words, the map  $\eta_{\text{scalar}}$  is such that

$$\langle \eta_{\text{scalar}}(\psi) | \hat{C}\psi' \rangle = 0,$$

for any  $\psi, \psi' \in \mathcal{D}$ . The space of solutions to the scalar constraint  $\mathcal{D}_{\text{phys}}^*$  has a natural hermitian inner product:

$$\langle \eta_{\text{scalar}}(\psi) | \eta_{\text{scalar}}(\psi') \rangle := (\eta_{\text{scalar}}(\psi) | \psi') .$$

It defines a hermitian inner product on  $\mathcal{D}_{\text{phys}} := \mathcal{D} / \ker \eta_{\text{phys}}$ :

$$\langle \psi | \psi' \rangle_{\text{phys}} := \langle \eta_{\text{scalar}}(\psi) | \eta_{\text{scalar}}(\psi') \rangle ,$$

called the physical scalar product. The Cauchy completion of  $\mathcal{D}_{\text{phys}}$  in the physical scalar product is called the physical Hilbert space  $\mathcal{H}_{\text{phys}}$ .

The transition amplitude (1.56) is expected to define the physical scalar product <sup>2</sup>

$$\langle \psi_{[s_{\text{out}}]} | \psi_{[s_{\text{in}}]} \rangle_{\text{phys}} = " \sum_{(\kappa, \rho, \iota, \mathcal{A}): (\partial \kappa, \partial \rho, \partial \iota) = s_{\text{out}} \otimes s_{\text{in}}^\dagger} Z(\kappa, \rho, \iota, \mathcal{A}) ".$$

The modulus square of the transition amplitude is interpreted as a probability of a transition from the state  $\psi_{[s_{\text{in}}]}$  to the state  $\psi_{[s_{\text{out}}]}$ . It has a form of a sum of spin-foam amplitudes. Therefore spin foams can be thought of as a sum-over-histories approach (path-integral approach) to defining dynamics of the loop quantum gravity states. In chapter 5 we will define operator spin foams, which are obtained from spin foams by summing over the intertwiners. In the chapters 6, 7 we will use the operator spin foams instead of spin foams.

In general, the boundary does not have to be a disjoint union of two graphs. The expression

$$" \sum_{(\kappa, \rho, \iota, \mathcal{A}): (\partial \kappa, \partial \rho, \partial \iota) = s} Z(\kappa, \rho, \iota, \mathcal{A}) "$$

is interpreted as an action of a so-called boundary functional  $W$  on a boundary state  $\psi_{[s^\dagger]}$  and denoted by  $W(\psi_{[s^\dagger]})$ . The modulus square  $|W(\psi_{[s^\dagger]})|^2$  is a probability of a process defined by the boundary state  $\psi_{[s^\dagger]}$  [139, 141, 162, 165, 44].

---

<sup>2</sup>The spin-foam formalism provides a scalar product between solutions to all the constraints. Moreover, the spin-foam dynamics of vacuum gravity is insensitive to linking and knotting [28]. Therefore it seems reasonable to expect that the transition amplitude (1.56) is the same for any spin networks  $s_{\text{in}}$  and  $s_{\text{out}}$  in the equivalence classes  $[s_{\text{in}}]$  and  $[s_{\text{out}}]$ , respectively.



## 2. The key results of the thesis

This thesis presents the results from [123, 124, 125, 29, 130, 129]. The key results are briefly summarized in the section 2.2. We start this chapter with a short summary of the state of art of the research in the spin-foam models of 4D Quantum Gravity before the author's contribution.

### 2.1. The state of art before the author's contribution

The spin foams were defined in an attempt to solve the problem of the dynamics of the Loop Quantum Gravity states [21, 121, 155, 158, 136, 23]. The idea is to express the transition amplitude between spin-network states as a sum over histories of spin networks, called spin foams (see section 1.3.1). This idea was successfully realized in 3D Quantum Gravity, where the correspondence between the kinematics of 2+1 Loop Quantum Gravity and the 3D spin-foam dynamics was settled [138]. The spin-foam model of 3D Quantum Gravity is the Ponzano-Regge model [150]. It can be derived by formulating 3D General Relativity as a BF theory (see section 1.3.2).

The starting point for the derivation of the spin-foam models of 4D Quantum Gravity is a formulation of 4D General Relativity as a constrained BF theory [149, 95, 156, 67] (see section 3.1). Since the spin-foam model of quantum BF theory is well known (see section 1.3.2) the remaining problem is to impose the constraints in the quantum theory. For many years the proposal that attracted most of the attention was the Barrett-Crane model [38, 39] (BC model). The strategy of Barrett and Crane was to discretize the 4D General Relativity on a triangulation of the space-time and quantize the resulting theory. The Barrett-Crane spin-foam model is obtained from the BF spin-foam model by restricting the class of possible histories (spin foams) – the constraints restrict the representations labelling the faces and the intertwiners labelling the internal edges. In the Euclidean signature the Barrett-Crane spin foam is: a foam defined by a triangulation of the space-time; a labelling of the faces with certain  $\text{Spin}(4)$  (double cover of  $\text{SO}(4)$ ) representations, called balanced representations; and a labelling of the internal edges with certain  $\text{Spin}(4)$  intertwiners, called Barrett-Crane intertwiners (BC intertwiners). For a given internal edge and a labelling of the faces intersecting this edge with the balanced representations, the Barrett-Crane intertwiners form a vector space  $\text{Inv}_{\text{BC}}(\mathcal{H}_e) \subset \text{Inv}(\mathcal{H}_e)$  called the space of the Barrett-Crane intertwiners. Barrett and Crane provided a canonical element in this space, which is non-zero if  $\text{Inv}(\mathcal{H}_e)$  is non-trivial (see [123] for the proof). Later, Reisenberger proved that the intertwiner solving the Barrett-Crane constraints is unique up to a scale – in other words he proved that the space  $\text{Inv}_{\text{BC}}(\mathcal{H}_e)$  is one-dimensional if  $\text{Inv}(\mathcal{H}_e)$  is non-trivial [157]. The Barrett-Crane spin foams are histories of certain spin networks, called relativistic spin networks. The relativistic spin networks are  $\text{Spin}(4)$  spin networks with links labelled by the balanced representations and nodes labelled by the Barrett-Crane intertwiners.

## 2. The key results of the thesis

Barrett and Crane defined the 4-simplex amplitude as the evaluation of the (relativistic) vertex spin network (see also section 1.3.3). However, they did not specify the face amplitude and the normalization of the BC intertwiner. Without these the model was not complete<sup>1</sup>. In [157] Reisenberger argued that if the spin foam model is to be a restriction of the BF spin foam model to histories satisfying the constraints, the face amplitude must be the dimension of the representation assigned to a face and the internal edges must be labelled by the BC intertwiners normalized in the natural scalar product inherited from the edge Hilbert space. De Pietri, Freidel, Krasnov and Rovelli [68] proposed a certain quantum field theory which Feynman diagrams correspond to the spin foams appearing in the Barrett-Crane model and obtained precisely the same face amplitude and normalization of the BC intertwiner as those suggested by Reisenberger. To improve the convergence of the transition amplitudes also other choices of the face amplitude and normalization of the BC intertwiners were discussed [147, 26].

In the original derivation the relativistic spin networks are defined for graphs determined by triangulations of the space manifold and the Barrett-Crane spin foams are histories of such spin networks. In this formulation the Barrett-Crane model is a quantization of discretized Gravity. In order to become a model of Quantum Gravity with all its local degrees of freedom it should be generalized to histories of spin networks defined for arbitrary graphs. In [183] the n-valent Barrett-Crane intertwiner was constructed (see also [37] and [157]). Thanks to this generalization the relativistic spin network could be defined for arbitrary graphs and the Barrett-Crane vertex amplitude could be generalized to arbitrary vertex graphs. Using the n-valent BC intertwiners Reisenberger generalized the Barrett-Crane spin-foam model to a model including histories of arbitrary relativistic spin networks [157]. He interpreted the generalized model as a restriction of (generalized) BF spin-foam model to histories where left-handed and right-handed geometries match [157, 156].

It turned out that the Barrett-Crane model does not have enough degrees of freedom to give a proper classical limit. A calculation of the graviton propagator in the large-scale limit based on the dynamics defined by the Barrett-Crane vertex amplitude did not reproduce the correct tensorial structure of the propagator [47, 4, 1]. This result triggered a search for new spin-foam models of 4D Quantum Gravity [134, 88, 89, 5, 135]. Finally, two teams have proposed new spin-foam models called after the names of the authors the Engle-Pereira-Rovelli-Livine model [86] (EPRL model) and Freidel-Krasnov model [96] (FK model). The Barrett-Crane model was defined for the Palatini action. The new models are defined for the Holst-Palatini action with real Barbero-Immirzi parameter  $\beta > 0$ . In the Euclidean signature it is additionally assumed that the parameter is rational and different from 1 (see also section 4.2). In the Euclidean case when  $0 < \beta < 1$  the EPRL model and the FK model coincide and when  $\beta > 1$  the models are different. Short after the models were defined, the formula for the semiclassical limit of the EPRL 4-simplex amplitude was derived [40, 41]. It relates the EPRL 4-simplex amplitude to the Regge action of 4D General Relativity very much like the asymptotic formula in section 1.3.2 relates the Ponzano-Regge vertex amplitude to the Ponzano-Regge action. It was also shown that the EPRL 4-simplex amplitude reproduces the correct tensorial structure of the graviton propagator in the large-scale limit [3].

---

<sup>1</sup>One should also specify the boundary link amplitude. A natural choice is to take  $A_{\text{link}}(\partial\rho_\ell) = \frac{1}{\sqrt{A_{\text{face}}(\partial\rho_\ell)}}$  – see chapter 5.

## 2.2. The key results of the thesis

In this thesis we focus on the dynamics of the Loop Quantum Gravity states defined by the Euclidean EPRL spin-foam model.

### Generalization of the EPRL intertwiners and the EPRL vertex amplitude

In the original formulation [86] the EPRL model is defined only for triangulations of space-time. As a result the EPRL intertwiners are 4-valent and the EPRL vertex amplitude is defined only for the vertex graph that is the 1-skeleton of the 4-simplex, i.e. the complete graph on five nodes. We generalize the 4-valent EPRL intertwiners to n-valent EPRL intertwiners. Our n-valent EPRL intertwiners become the n-valent BC intertwiners in the limit  $\beta \rightarrow \infty$ . This is compatible with the fact that the Holst-Palatini action becomes the Palatini action in this limit. We use the generalized EPRL intertwiners to define the EPRL vertex amplitude for arbitrary vertex graphs and we generalize EPRL spin foams to a broader class of foams. Thanks to this generalization the EPRL spin-foam model can be used to define the dynamics of all Loop Quantum Gravity states, not only those defined for the graphs that are determined by the triangulations of the space manifold.

### Theorem concerning injectivity of an EPRL map

In our generalized EPRL spin foams the faces are labelled with  $\text{Spin}(4)$  representations satisfying certain constraints and the internal edges are labelled with the generalized EPRL intertwiners. To a given internal edge and a labelling of the faces intersecting this edge with the representations satisfying the constraints there correspond a vector space of the EPRL intertwiners  $\text{Inv}_{\text{EPRL}}(\mathcal{H}_e) \subset \text{Inv}(\mathcal{H}_e)$  and a vector space of  $\text{SU}(2)$  intertwiners. There is a linear map from the space of  $\text{SU}(2)$  intertwiners to the space of the EPRL intertwiners, called an EPRL map. The main technical result of this thesis is the proof that an EPRL map is 1-1 unless its co-domain is trivial and its domain is non-trivial. As a result the vector spaces of the EPRL intertwiners and the corresponding vector spaces of the  $\text{SU}(2)$  intertwiners are isomorphic unless the former is trivial and the latter is non-trivial. It is natural to ask if they are also isomorphic as Hilbert spaces (equipped with the natural scalar products inherited from the spaces of the  $\text{Spin}(4)$  intertwiners and, respectively, the  $\text{SU}(2)$  intertwiners). It turns out that this is not the case – we present an example of non-isometric EPRL map.

### Definition of the sum over the intertwiners

Since a space of EPRL intertwiners is usually more than 1-dimensional, a proper definition of the sum over the intertwiners is needed. In the Barrett-Crane model (as well as in the Ponzano-Regge model) the problem was simpler, because the only ambiguity was the scale factor. We define the sums by introducing operator spin foams, i.e. foams which faces are labelled with unitary irreducible representations, internal edges are labelled with certain operators and vertices are labelled with certain linear functionals.

Since an EPRL map in general is not an isometry, there is an ambiguity in defining the sum: one could either define it as a sum over orthonormal basis of the  $\text{SU}(2)$  intertwiners or over a basis of the EPRL intertwiners orthonormal in the scalar product inherited from the space of  $\text{Spin}(4)$  intertwiners. Our proposal is to use the latter sum – this

## 2. The key results of the thesis

choice corresponds to a coloring of each internal edge with the orthogonal projection from the space of  $\text{Spin}(4)$  intertwiners  $\text{Inv}(\mathcal{H}_e)$  onto its subspace of the EPRL intertwiners  $\text{InVEPRL}(\mathcal{H}_e)$ . In the limit  $\beta \rightarrow \infty$  our proposal coincides with the Reisenberger's choice of the BC intertwiner normalized in the natural scalar product in  $\text{Inv}(\mathcal{H}_e)$ . Let us mention that in the literature there is also a model that uses the former sum [48]. It will be also discussed in this thesis.

### **Moves on the operator spin foams and fixing the face and boundary link amplitudes**

We introduce moves on operator spin foams similar to the Baez's moves on spin networks (see section 1.2.2). The moves allow to split an edge, split a face, flip the orientation of an edge, flip the orientation of a face, add a face. Thanks to the choice of the coloring of the internal edges with orthogonal projections onto the space of the EPRL intertwiners, our operator spin-foam model is invariant under the move of splitting an internal edge. The remaining degrees of freedom are the face amplitude and the boundary link amplitude. We fix them by requiring our model to be symmetric with respect to all of the moves and to have a certain glueing property.

### **Definition of a class of foams**

A natural question is what is the optimal class of foams compatible with our generalization of the EPRL vertex amplitude and allowing histories of arbitrary spin networks. In [129] we defined such class combinatorially using certain diagrams called graph diagrams. We constructed an oriented CW complex (a foam) corresponding to a graph diagram. In [129] the foam corresponding to a graph diagram was constructed by using certain glueing procedure. In this thesis we present a construction of the foam that does not use this procedure. The class of foams defined by graph diagrams admits full variety of boundary graphs. We construct the boundary graph directly from the graph diagram – without needing to reconstruct the foam corresponding to the graph diagram. In [129] the boundary graph was constructed by using certain procedure of merging graphs. In this thesis it is constructed without reference to this procedure.

### **Independence of the operator spin-network diagram framework from the operator spin foam framework**

We define a coloring of a graph diagram turning it into an operator spin-network diagram. To each operator spin-network diagram there corresponds an operator spin foam. We show that the construction of the operator spin foam corresponding to an operator spin-network diagram is not needed to calculate the spin-foam operator – the spin-foam operator can be read directly from the operator spin-network diagram. As a result the operator spin-network diagrams can be used independently from the operator spin foams. We use this technical advantage in an application of graph diagrams to Dipole Cosmology.

### **Application of operator spin-network diagrams to Dipole Cosmology**

Our generalization of the EPRL vertex amplitude was used by Bianchi, Rovelli and Vidotto to introduce the first model of Quantum Cosmology based on the spin-foam formalism [49].

They calculated a transition amplitude between coherent states peaked on homogeneous and isotropic geometries using certain approximations and showed that the model recovers the Friedmann dynamics in the classical limit. One of the approximations was a truncation of the transition amplitude to a contribution from a single foam with one internal vertex, four internal edges and a certain boundary. *A priori* there is no good reason to restrict to only one such foam. In fact, the choice of this foam was judged *a posteriori* by correct classical limit. In [115] Frank Hellmann has discussed contributions from other foams with these properties. Our class defined by graph diagrams includes all the foams from [115] but it also includes many other foams with these properties. We find all of them: in particular we construct all possible vertex graphs. We discuss contributions from some of the foams we found and show that they can be neglected in the limit of large volume of the Universe.

### **Some improvements, reformulations**

The definition of a spin foam and operator spin foam we use is more general from the standard one [21, 29], because we introduce a coloring of the internal vertices with linear functionals called contractors. In particular, in this thesis the moves on the operator spin foams transform also the contractors.

The presentation of the EPRL intertwiners is original and based on the quantum polyhedral geometry introduced in [73]. It is similar to the interpretation of the Barrett-Crane intertwiners in terms of the quantum tetrahedra [24] (an extension of the interpretation to polyhedra was suggested in [157]).

The definition of a graph diagram is different from (but equivalent to) the definition from [129] – in place of a family of link relations we use a certain bijective map.



## 3. Spin-foam models with the EPRL vertex amplitude

In chapter 1 we presented a general definition of a spin-foam model. In this chapter we will present two spin-foam models of 4D Quantum Gravity basing on the so-called Engle-Pereira-Rovelli-Livine vertex amplitude: a model which we introduced in [123] and a model introduced by Bianchi, Regoli and Rovelli [48]. We call the models: the Spin(4) and, respectively, the SU(2) spin-foam model with the EPRL vertex. Although the model [48] is defined in the Euclidean as well as in the (physical) Lorentzian signature, we present only the Euclidean versions of both models. The Euclidean version is simpler as the structure group is compact. Due to non-compactness of the Lorentz group, the Lorentzian version requires regularization [87, 25, 39, 66] thanks to which the vertex amplitude is finite if the vertex graph is 3-edge connected [122].

The EPRL model was originally defined for triangulations of space-time [86] and the EPRL intertwiners were 4-valent. As a result, the boundary graphs were defined by triangulations of space and the model was not applicable to all the Loop Quantum Gravity states. In [123] we introduced n-valent EPRL intertwiners and generalized the EPRL vertex amplitude to arbitrary vertex graphs. We extended the original definition of the EPRL model to piecewise linear 2-complexes allowing full variety of boundary states. Another model generalizing the original EPRL model using the n-valent EPRL intertwiners and the generalized EPRL vertex amplitude was proposed in [48]. The (generalized) models are promising candidates for the spin-foam dynamics of the Loop Quantum Gravity states.

The spin-foam models of 4D Quantum Gravity are based on an interpretation of General Relativity as constrained BF theory (see section 3.1.1). The theory is discretized (see section 3.1.2) and the discrete theory is quantized. In sections 3.2.1 and 3.2.2 we will present an interpretation of the discrete constraints in terms of polyhedra that was proposed in [73]. Next, basing on the ideas from [73] and from [24], we will quantize the geometries of the polyhedra and define quantum polyhedra. By averaging over the vectors normal to the quantum polyhedra we will obtain (n-valent) EPRL intertwiners which are basic building blocks of the (generalized) EPRL vertex amplitude (see section 3.3). In section 3.4 we will present and compare the two models with the EPRL vertex amplitude. Other models of 4D Quantum Gravity will be shortly discussed in section 3.5.

### 3.1. General Relativity as constrained BF theory

#### 3.1.1. Continuous theory

In the previous chapter we constructed a spin-foam model of quantum BF theory. The construction of the spin-foam models of Quantum Gravity is based on a formulation of the General Relativity as a BF theory with constraints, which was introduced by Plebański

### 3. Spin-foam models with the EPRL vertex amplitude

[149]. The gravity theory can be interpreted as given by the action

$$S(B, \omega) = \frac{1}{2k} \int_{\mathcal{M}} B^{IJ} \wedge \mathcal{F}_{IJ} \quad (3.1)$$

with additional simplicity constraint

$$B^{IJ} = \frac{1}{2} \epsilon^{IJ}{}_{KL} e^K \wedge e^L \quad (3.2)$$

in the Palatini case, and

$$B^{IJ} = \frac{1}{2} \epsilon^{IJ}{}_{KL} e^K \wedge e^L + \frac{\sigma}{\beta} e^I \wedge e^J \quad (3.3)$$

in the Holst action case.

An alternative form of the constraints is based on the following observation. It can be shown [67] that if  $E^{IJ}$  satisfies

$$\eta^{\alpha\beta\mu\nu} E_{\alpha\beta}^{IJ} E_{\mu\nu}^{KL} = e \epsilon^{IJKL}, \quad (3.4)$$

where  $e = \frac{1}{4!} \epsilon_{IJKL} E_{\alpha\beta}^{IJ} E_{\mu\nu}^{KL} \eta^{\alpha\beta\mu\nu}$ ,  $\eta^{\alpha\beta\mu\nu}$  is the Levi-Civita tensor density on  $\mathcal{M}$  which orientation agrees with that of  $\mathcal{M}$ , then  $E^{IJ}$  is in one of the following five disjoint sectors:

$$(I\pm) \quad E^{IJ} = \pm e^I \wedge e^J,$$

$$(II\pm) \quad E^{IJ} = \pm \frac{1}{2} \epsilon^{IJ}{}_{KL} e^K \wedge e^L,$$

$$(\text{deg}) \quad e = 0.$$

The sectors are called Plebański sectors [67, 57, 81]. If the two-form  $E^{IJ}$  is in the sector (II+) then  $B^{IJ} = E^{IJ}$  in the Palatini case, and

$$B^{IJ} = E^{IJ} + \frac{1}{2\beta} \epsilon^{IJ}{}_{KL} E^{KL} \quad (3.5)$$

in the Holst case. For  $\beta \neq \pm i$  in the Lorentzian case and  $\beta \neq \pm 1$  in the Euclidean case, the relation (3.5) can be inverted:

$$E^{IJ} = \frac{\beta^2}{\beta^2 - \sigma} \left( B^{IJ} - \frac{1}{2\beta} \epsilon^{IJ}{}_{KL} B^{KL} \right). \quad (3.6)$$

By making the substitution (3.6) in (3.4) we obtain constraints on  $B^{IJ}$ . The solutions of the resulting equations are in one of the following sectors:

$$(I\pm) \quad B^{IJ} = \pm e^I \wedge e^J \pm \frac{1}{2\beta} \epsilon^{IJ}{}_{KL} e^K \wedge e^L,$$

$$(II\pm) \quad B^{IJ} = \pm \frac{1}{2} \epsilon^{IJ}{}_{KL} e^K \wedge e^L \pm \frac{\sigma}{\beta} e^I \wedge e^J,$$

$$(\text{deg}) \quad \epsilon_{IJKL} B_{\alpha\beta}^{IJ} B_{\mu\nu}^{KL} \eta^{\alpha\beta\mu\nu} = 0.$$

In fact, the constraints we use in the following section select the (II±) and (deg) sectors. However, no further constraints will be used to select the II+ sector. As a result the resulting spin-foam model mixes the (II±) and (deg) sectors. This issue is discussed in details in [81], and in [83, 82] a spin-foam model is proposed which is restricted to the (II+) sector. However, the model is defined for triangulations but a generalization to a broader class of foams is still an open problem.

### 3.1.2. Discretized theory

In order to pass to the spin-foam framework one approximates General Relativity by using Regge calculus [89]. In this approximation the space-time is approximated by piecewise flat manifold formed from flat oriented simplices glued such that the geometries of their boundaries match. Let us focus on a single oriented 4-simplex. The boundary of the 4-simplex consists of five tetrahedra. We number them by  $a = 0, 1, 2, 3, 4$ . Since each pair of tetrahedra shares a single triangle, this triangle is uniquely labelled by an unordered pair of indices  $\{a, b\}$  and the oriented triangle is uniquely labelled by an ordered pair  $ab$ . The connection  $\omega$  is discretized by assigning to each pair of neighbouring 4-simplices an  $SO(4)$  group element. The two-forms  $E^{IJ}$  are discretized by assigning to each triangle an element in the  $so(\bar{\eta})$  lie algebra,  $ab \mapsto E_{ab} \in so(\bar{\eta})$ , such that [81]

$$E_{ab} = -E_{ba}.$$

If  $e \neq 0$  then the constraints (3.4) are equivalent to the following ones [67]:

$$\epsilon_{IJKL} E_{\alpha\beta}^{IJ} E_{\mu\nu}^{KL} = e \eta_{\alpha\beta\mu\nu}.$$

In the discrete theory the constraints take the following form [67, 145]:

- $\forall_{a,b,c} \epsilon_{IJKL} E_{ab}^{IJ} E_{ac}^{KL} = 0 \quad (3.7)$
- for any permutation  $\pi : \{0, 1, 2, 3, 4\} \rightarrow \{0, 1, 2, 3, 4\}$

$$\epsilon_{IJKL} E_{\pi(1)\pi(2)}^{IJ} E_{\pi(3)\pi(4)}^{KL} = \text{sgn } \pi \epsilon_{IJKL} E_{12}^{IJ} E_{34}^{KL}. \quad (3.8)$$

It can be shown that if  $E_{ab}$  satisfy the following constraints:

- (closure)

$$\forall_a \sum_{b \neq a} E_{ab}^{IJ} = 0, \quad (3.9)$$

- (linear simplicity)

$$\forall_a \exists_{n_a \in \mathbb{R}^4} : \epsilon_{IJKL} n_a^J E_{ab}^{KL} = 0 \quad (3.10)$$

(in the Lorentzian case we assume that  $n_a$  is time-like, for other choices see [64, 62]),

then  $E_{ab}$  satisfy the constraints (3.7) and (3.8). In fact the closure and linear simplicity constraints restrict  $E_{ab}$  to the Plebański sectors  $(II\pm)$  or  $(deg)$  [81].

Since a variable in the action is  $B$ , not  $E$ , we need to express the constraints in terms of  $B_{ab}^{IJ}$ , where according to (3.5)  $B_{ab}^{IJ} = E_{ab}^{IJ} + \frac{1}{2\beta} \epsilon^{IJ}_{KL} E_{ab}^{KL}$ . Let  $q_a : V \rightarrow V$  be the orthogonal projection onto the space  $V_{a\perp}$  of vectors orthogonal to  $n_a^I$  (let us recall that  $V = \mathbb{R}^4$ ). Given  $n_a^I$ ,  $(q_a)_I^i$  we decompose each  $B_{ab}^{IJ}$  into "magnetic" and "electric" parts:

$$L_{ab}^i (n_a^I, (q_a)_I^i) = \frac{1}{2} (q_a)_I^i n_{aJ} \epsilon^{IJ}_{KL} B_{ab}^{KL}, \quad K_{ab}^i (n_a^I, (q_a)_I^i) = (q_a)_I^i n_{aJ} B_{ab}^{IJ}. \quad (3.11)$$

Note that although  $B_{ab}^{IJ}$  is antisymmetric in the indices  $ab$ ,  $L_{ab}^i$  and  $K_{ab}^i$  do not have this property. Using  $L_{ab}^i$  and  $K_{ab}^i$  from (3.11), we write the linear simplicity constraint in the following form:

$$L_{ab}^i - \frac{\sigma}{\beta} K_{ab}^i = 0.$$

### 3. Spin-foam models with the EPRL vertex amplitude

Therefore the constraints on  $B_{ab}^{IJ}$  become the following: for every tetrahedron "a" there exists a normalized vector  $n_a \in V$  such that  $L_{ab}^i$  and  $K_{ab}^i$  defined in equations (3.11) satisfy:

- (reduced closure)

$$\sum_{b \neq a} L_{ab}^i = 0, \quad (3.12)$$

- (linear simplicity)

$$L_{ab}^i - \frac{\sigma}{\beta} K_{ab}^i = 0. \quad (3.13)$$

Note that the equations do not depend on the choice of the basis in  $V_{a\perp}$ , i.e. on the choice of  $(q_a)_I^i$ . Note also that the reduced closure constraint (3.12) is equivalent to the closure constraint (3.9) if the linear simplicity constraint (3.13) is satisfied.

Classically the linear simplicity constraint is equivalent to the following one:

$$\sum_i \left( L_{ab}^i - \frac{\sigma}{\beta} K_{ab}^i \right)^2 = 0. \quad (3.14)$$

However, in the quantum theory, the expressions are not equivalent – in the quantum theory the formula (3.14) will be used. We introduce self-dual and anti-selfdual part of  $B_{ab}^{IJ}$ :

$$B_{ab}^{\pm i} = (B_{ab} \pm *B_{ab})^{IJ} (q_a)_I^i n_{aJ},$$

where the duality operator  $*$  is given by  $(*B_{ab})^{IJ} = \frac{1}{2} \epsilon^{IJ}_{KL} B_{ab}^{KL}$ . The relation between  $B_{ab}^{\pm i}$  and  $L_{ab}^i$ ,  $K_{ab}^i$  is the following:

$$B_{ab}^{\pm i} = K_{ab}^i \pm L_{ab}^i.$$

In the quantum theory we will use the equation (3.14) written in the following form:

$$\left(1 - \frac{1}{\beta^2}\right) (L_{ab}^i)^2 + \frac{1}{2\beta^2} \left( (B_{ab}^{+i})^2 + (B_{ab}^{-i})^2 \right) - \frac{\sigma}{2\beta} \left( (B_{ab}^{+i})^2 - (B_{ab}^{-i})^2 \right) = 0. \quad (3.15)$$

## 3.2. Quantum polyhedron

In this section we give a geometric interpretation to the closure and the linear simplicity constraints in terms of closed convex polyhedra in  $\mathbb{R}^4$ . By a closed convex polyhedron in  $\mathbb{R}^d$  ( $d \geq 3$ ) we mean a convex hull of a finite number of vectors in  $\mathbb{R}^d$  spanning a 3-dimensional subspace. Basing on the ideas from [73] and from [24] we quantize the geometries of the polyhedra and obtain quantum polyhedra. By averaging a 3D quantum polyhedron over possible embeddings into 4D we obtain an EPRL intertwiner – a basic building block of the models studied in this chapter.

### 3.2.1. Polyhedron in 3D

In  $\mathbb{R}^3$  the geometry of a polyhedron is given by unit vectors normal to the faces and areas of these faces. In fact, these data determine the polyhedron up to translations. The existence of a closed convex polyhedron with prescribed areas of the faces and vectors normal to these faces was proved by Minkowski [137, 8]:

**Theorem 1** (Minkowski). *If  $\vec{n}_1, \dots, \vec{n}_N$  are distinct non-coplanar unit vectors and  $A_1, \dots, A_N$  are positive numbers such that*

$$A_1\vec{n}_1 + \dots + A_N\vec{n}_N = 0,$$

*then there exists a closed convex polyhedron which faces have outwards normals  $\vec{n}_l$  and areas  $A_l$ .*

He also showed that the polyhedron is unique up to translations [8].

Instead of using unit normals and areas of the faces, one can use (non-zero) vectors  $\vec{L}_l$  normal to the faces but not necessarily normalized. They are related to the areas and the unit normals by the following equations

$$\|\vec{L}_l\| = A_l, \quad \vec{n}_l = \frac{1}{\|\vec{L}_l\|} \vec{L}_l.$$

The conditions on the areas and vectors normal to the faces are transformed into the following conditions on the vectors  $\vec{L}_l$ :

- the vectors are not coplanar and each pair of vectors is linearly independent,
  -
- $$\vec{L}_1 + \dots + \vec{L}_N = 0. \tag{3.16}$$

### 3.2.2. Polyhedron in 4D

In  $\mathbb{R}^4$  the geometry of a polyhedron is given by bivectors orthogonal to the faces. Given two orthogonal unit vectors  $v_1^I, v_2^J$  normal to a face, the corresponding bivector is:

$$E^{IJ} = 2Av_1^I v_2^J,$$

where  $A$  is the area of the face. The norm of the bivector is related to the area by  $E^{IJ} E_{IJ} = 2A^2$ .

Instead of using bivectors we describe the geometry in terms of antisymmetric matrices. By looking at the condition (3.16) in 3 dimensions one could anticipate that the matrices should satisfy the closure constraint. In 4 dimensions one needs additionally the linear simplicity constraint, because not every antisymmetric matrix is a bivector. We use the following geometric interpretation of the closure and the linear simplicity constraint (compare Theorem III.1. in [73]):

**Theorem 2.** *If  $N$  non-coplanar antisymmetric matrices  $E_1^{IJ}, \dots, E_N^{IJ}$  satisfy the conditions:*

- *each pair of matrices is linearly independent<sup>1</sup>,*
- *(closure constraint)*

$$E_1^{IJ} + \dots + E_N^{IJ} = 0,$$

- *(linear simplicity constraint)*

$$\exists n^I : n_I \epsilon^{IJ}{}_{KL} E_l^{KL} = 0 \text{ for all } l \in \{1, \dots, N\},$$

---

<sup>1</sup>Clearly, the space of antisymmetric matrices is a vector space.

### 3. Spin-foam models with the EPRL vertex amplitude

then there exists a closed convex polyhedron in  $\mathbb{R}^4$  such that  $E_{\mathbf{l}}^{IJ}$  are bivectors normal to its faces and  $E_{\mathbf{l}}^{IJ}E_{\mathbf{l}IJ} = 2A_{\mathbf{l}}^2$ , where  $A_{\mathbf{l}}$  is the area of the face  $\mathbf{l}$ .

*Proof.* Given  $n^I, \mathbf{q}_I^i$ , we decompose each  $E_{\mathbf{l}}^{KL}$  into "magnetic" and "electric" parts (compare (1.4)):

$$L_{\mathbf{l}}^i(n^I, \mathbf{q}_I^i) = \frac{1}{2}\mathbf{q}_I^i n_J \epsilon^{IJ}_{\phantom{IJ}KL} E_{\mathbf{l}}^{KL}, \quad K_{\mathbf{l}}^i(n^I, \mathbf{q}_I^i) = \mathbf{q}_I^i n_J E_{\mathbf{l}}^{IJ}.$$

The decomposition is an isomorphism between the space of  $4 \times 4$  antisymmetric matrices and  $\mathbb{R}^6$ . Indeed: if  $E^{IJ} = 2v^{[I}n^{J]}$  then  $L^i = 0$ ,  $K^i = \mathbf{q}_J^i v^J$ , and if  $E^{IJ} = \epsilon^{IJ}_{\phantom{IJ}KL} v^K n^L$  then  $L_{\mathbf{l}}^i = \mathbf{q}_J^i v^J$ ,  $K_{\mathbf{l}}^i = 0$ . This shows that the image of the map is the whole space  $\mathbb{R}^6$ . Therefore the map is an isomorphism.

It is easy to see that the linear simplicity constraint is equivalent to vanishing of the magnetic part of each matrix  $E_{\mathbf{l}}^{IJ}$ :  $L_{\mathbf{l}}^i = 0$  is equivalent to  $n_I \epsilon^{IJ}_{\phantom{IJ}KL} E_{\mathbf{l}}^{KL} = \lambda n^J$  for some  $\lambda \in \mathbb{R}$ ; however  $n_I \epsilon^{IJ}_{\phantom{IJ}KL} E_{\mathbf{l}}^{KL}$  is orthogonal to  $n^J$  and thus  $\lambda = 0$ . The vectors  $K_{\mathbf{l}}^i$  are  $N$  distinct vectors in  $\mathbb{R}^3$ . Since the matrices are non-coplanar, the vectors are also non-coplanar and since the matrices satisfy the closure constraint, the vectors satisfy:

$$K_1^i + K_2^i + K_3^i + K_4^i = 0.$$

From Minkowski theorem follows that there exists a closed convex polyhedron (in  $\mathbb{R}^3$ ) which faces have outward normals  $\vec{n}_{\mathbf{l}} = \frac{1}{\|\vec{K}_{\mathbf{l}}\|} \vec{K}_{\mathbf{l}}$  and areas  $A_{\mathbf{l}} = \|\vec{K}_{\mathbf{l}}\|$ .

Let us consider the isometric embedding  $\mathbf{q}_i^I : \mathbb{R}^3 \rightarrow \mathbb{R}^4$  such that  $\mathbf{q}_i^I n_I = 0$ ,  $\mathbf{q}_i^i \mathbf{q}_j^I = \delta_j^i$ . This embedding maps the tetrahedron in  $\mathbb{R}^3$  to a tetrahedron in  $\mathbb{R}^4$  preserving its geometry. Note that:

$$E_{\mathbf{l}}^{IJ} = 2K_{\mathbf{l}}^{[I} n^{J]},$$

where  $K_{\mathbf{l}}^I := \mathbf{q}_i^I K_{\mathbf{l}}^i$ . Indeed, it is the unique matrix which "electric" part is equal  $K_{\mathbf{l}}^i$  and "magnetic" part is equal 0. Clearly, the bivectors  $E_{\mathbf{l}}^{IJ}$  are normal to the faces and  $E_{\mathbf{l}}^{IJ} E_{\mathbf{l}IJ} = 2A_{\mathbf{l}}^2$ .  $\square$

If the closure constraint and the simplicity constraints are satisfied, but the matrices are coplanar or two matrices are colinear then the configuration is called degenerate. The degenerate configurations correspond to degenerate polyhedra obtained as a limit of (regular) polyhedra.

#### 3.2.3. Quantum polyhedron in 3D

We now switch to the quantum theory. Let  $\tau^i = i\sigma^i$ , where  $\sigma^i$  are the Pauli matrices. The matrices  $\tau_i$  form a basis of  $\text{su}(2)$  – the Lie algebra of the  $\text{SU}(2)$  group. Let us denote by  $\rho_k : \text{SU}(2) \rightarrow \text{U}(\mathcal{H}_k)$  a unitary irreducible representation of the  $\text{SU}(2)$  group with spin  $k$ , and by  $\rho'_k$  the corresponding representation of its Lie algebra. The quantum operators corresponding to the vectors  $L_{\mathbf{l}}^i$  from section 3.2.1 act in the Hilbert space

$$\mathcal{H}_{k_1} \otimes \dots \otimes \mathcal{H}_{k_N}$$

and are defined by

$$\hat{L}_{\mathbf{l}}^i = \text{id} \otimes \dots \otimes \rho'_{k_{\mathbf{l}}}(\tau^i) \otimes \dots \otimes \text{id}.$$

A tensor  $\mathcal{I} \in \mathcal{H}_{k_1} \otimes \dots \otimes \mathcal{H}_{k_N}$  will be called a quantum polyhedron in 3D if it satisfies the following quantum constraint:

$$\left( \hat{L}_1^i + \dots + \hat{L}_N^i \right) \mathcal{I} = 0. \quad (3.17)$$

This is quantum version of the classical constraint (3.16). Let us note that the operator

$$\hat{L}_1^i + \dots + \hat{L}_N^i$$

is a generator of a diagonal action of the  $SU(2)$  group on  $\mathcal{H}_{k_1} \otimes \dots \otimes \mathcal{H}_{k_N}$ :

$$u \cdot \mathcal{I} = \rho_{k_1}(u) \otimes \dots \otimes \rho_{k_N}(u) \mathcal{I}.$$

The solutions of the equation (3.17) are the invariant tensors  $\text{Inv}(\mathcal{H}_{k_1} \otimes \dots \otimes \mathcal{H}_{k_N})$ . The space  $\text{Inv}(\mathcal{H}_{k_1} \otimes \dots \otimes \mathcal{H}_{k_N})$  will be called the space of quantum polyhedra in 3D and any element of the space will be called a quantum polyhedron in 3D. If  $N = 4$  this definition reduces to the definition of quantum tetrahedron in 3D from [24, 36, 35].

### 3.2.4. Quantum polyhedron in 4D

#### In quantum theory the $SO(4)$ group is replaced with the $Spin(4)$ group

The Holst-Palatini formulation as well as the Plebański formulation allow to consider General Relativity as an example of a (diffeomorphism invariant)  $SO(1,3)$  gauge theory in the Lorentzian signature or  $SO(4)$  gauge theory in the Euclidean signature. In the quantum theory these groups will be replaced by their universal coverings [86]. In particular, the  $SO(4)$  group is replaced with  $Spin(4)$  group, which is isomorphic with the  $Spin(4) = SU(2) \times SU(2)$  group. The group homomorphism from the  $SU(2) \times SU(2)$  group to the  $SO(4)$  is defined in the following way (see for example [96]). Every element of  $\mathbb{R}^4 = \mathbb{C}^2$  can be identified with a  $2 \times 2$  complex matrix

$$x = \begin{pmatrix} z_1 & z_2 \\ -\bar{z}_2 & \bar{z}_1 \end{pmatrix}.$$

The action of an  $SU(2) \times SU(2)$  group element  $g = (g^+, g^-) \in Spin(4)$  on  $x$  is

$$g \cdot x = g^+ x (g^-)^{-1}.$$

Clearly, this action preserves the determinant  $|z_1|^2 + |z_2|^2$  and therefore is an orthogonal transformation of  $\mathbb{R}^4$ . In fact, it is an  $SO(4)$  transformation, because the group  $SU(2) \times SU(2)$  is connected, and the transformation corresponding to identity element in  $Spin(4)$  is the identity transformation of  $\mathbb{R}^4$ . Let us note that the diagonal subgroup  $(h, h)$  is the subgroup leaving

$$\mathring{\mathbf{n}} = \begin{pmatrix} 1 & 0 \\ 0 & 1 \end{pmatrix}$$

invariant (this matrix corresponds to the vector  $\mathring{\mathbf{n}}^I = \delta_0^I$ ). We will denote by  $[g]^I_J$  the  $SO(4)$  matrix corresponding to  $g$ .

### 3. Spin-foam models with the EPRL vertex amplitude

The unitary irreducible representations of the  $\text{Spin}(4)=\text{SU}(2)\times\text{SU}(2)$  group are defined by a pair of  $\text{SU}(2)$  unitary irreducible representations  $\rho_{j^+}, \rho_{j^-}$ . We denote by  $\rho_{j^+ j^-}$ ,  $j^+, j^- \in \frac{1}{2}\mathbb{N}$ , the representation :

$$\rho_{j^+ j^-}(g^+, g^-) = \rho_{j^+}(g^+) \otimes \rho_{j^-}(g^-)$$

acting in the tensor product  $\mathcal{H}_{j^+} \otimes \mathcal{H}_{j^-} =: \mathcal{H}_{j^+ j^-}$ . By  $\rho'_{j^+ j^-}$  we denote the corresponding representation of  $\text{spin}(4)$  (the Lie algebra of  $\text{Spin}(4)$ ).

Let  $\tau^{IJ}$  be a basis of  $\text{so}(4)$ ,  $\tau^{IJ} \in \text{End}(\mathbb{R}^4)$ , such that  $(\tau^{IJ})_{KL} = i(\delta_K^I \delta_L^J - \delta_L^K \delta_K^J)$ . The  $\text{spin}(4)$  Lie algebra and the  $\text{so}(4)$  Lie algebra are isomorphic. The isomorphism  $\text{spin}(4) \rightarrow \text{so}(4)$  is given by:

$$(\tau^i, 0) \mapsto \tau_+^i := \tau^{i0} + \frac{1}{2} \epsilon^{i0}{}_{jk} \tau^{jk}, \quad (0, \tau^i) \mapsto \tau_-^i := \tau^{i0} - \frac{1}{2} \epsilon^{i0}{}_{jk} \tau^{jk}.$$

It is easy to invert this isomorphism:

$$\tau^{i0} \mapsto (\frac{1}{2} \tau_i, \frac{1}{2} \tau_i), \quad \tau^{jk} \mapsto (-\frac{1}{2} \epsilon^{jk}{}_i \tau^i, \frac{1}{2} \epsilon^{jk}{}_i \tau^i).$$

The representation  $\rho'_{j^+ j^-}$  of the basis elements  $\tau^{IJ}$  is:

$$\rho'_{j^+ j^-}(\tau^{i0}) = \frac{1}{2} \rho'_{j^+}(\tau_i) \oplus \rho'_{j^-}(\tau_i), \quad \rho'_{j^+ j^-}(\tau^{jk}) = \frac{1}{2} \epsilon^{jk}{}_i \rho'_{j^+}(-\tau_i) \oplus \rho'_{j^-}(\tau_i).$$

#### Quantum polyhedron in 4D orthogonal to $n^I$

The quantum operators corresponding to  $B_{\mathbf{l}}^{IJ}$  act in the Hilbert space

$$\mathcal{H}_{j_1^+ j_1^-} \otimes \dots \otimes \mathcal{H}_{j_N^+ j_N^-}$$

and are defined by

$$\hat{B}_{\mathbf{l}}^{IJ} = \text{id} \otimes \dots \otimes \rho'_{j_l^+ j_l^-}(\tau^{IJ}) \otimes \dots \otimes \text{id}.$$

This choice of quantum operators is justified by the Poisson bracket structure of the discrete theory [73]. We decompose the operators into "electric" and "magnetic" parts:

$$\hat{\mathsf{L}}_{\mathbf{l}}^i = \frac{1}{2} n_I \mathsf{q}_J^i \epsilon^{IJ}{}_{KL} \hat{B}_{\mathbf{l}}^{KL}, \quad \hat{\mathsf{K}}_{\mathbf{l}}^i = n_I \mathsf{q}_J^i \hat{B}_{\mathbf{l}}^{IJ}.$$

and introduce the operators corresponding to the self-dual and anti-selfdual components  $B_{\mathbf{l}}^{i\pm}$ :

$$\hat{B}_{\mathbf{l}}^{i\pm} = \hat{\mathsf{K}}_{\mathbf{l}}^i \pm \hat{\mathsf{L}}_{\mathbf{l}}^i.$$

Let us note that the operators  $\hat{\mathsf{L}}_{\mathbf{l}}^i, \hat{\mathsf{K}}_{\mathbf{l}}^i$  as well as  $\hat{B}_{\mathbf{l}}^{i\pm}$  depend on the choice of basis in  $V_\perp$  (and thus on  $\mathsf{q}_I^i$ ). The quantum constraints do not depend on the choice of the basis and neither does the quantum polyhedron.

Let us quantize the reduced closure and the linear simplicity constraints (3.12), (3.15). Let  $\mathcal{H}_{\text{poly}}^{\mathbf{n}, \mathsf{q}_I^i}$  be a Hilbert space of solutions to the following equations ( $\iota \in \mathcal{H}_{j_1^+ j_1^-} \otimes \dots \otimes \mathcal{H}_{j_N^+ j_N^-}$ ):

- (quantum reduced closure)  $\sum_{\mathbf{l}=1}^N \hat{\mathsf{L}}_{\mathbf{l}}^i \iota = 0$ ,

- (quantum linear simplicity)

$$\left( \left( 1 - \frac{1}{\beta^2} \right) \widehat{(\mathcal{L}_I^i)^2} + \frac{1}{2\beta^2} \left( (\widehat{(B_I^{+i})^2} + (\widehat{(B_I^{-i})^2}) - \frac{1}{2\beta} \left( (\widehat{(B_I^{+i})^2} - (\widehat{(B_I^{-i})^2}) \right) \right) \iota = 0,$$

where

$$\begin{aligned} \widehat{(\mathcal{L}_I^i)^2} &= (\hat{\mathcal{L}}_I^i)^2 - \sqrt{(\hat{\mathcal{L}}_I^i)^2 + \frac{1}{4}\text{id}} + \frac{1}{2}\text{id}, \\ \widehat{(B_I^{\pm i})^2} &= (\hat{B}_I^{\pm i})^2 - \sqrt{(\hat{B}_I^{\pm i})^2 + \frac{1}{4}\text{id}} + \frac{1}{2}\text{id}. \end{aligned}$$

The choice of the operators  $\widehat{(\mathcal{L}_I^i)^2}$  and  $\widehat{(B_I^{\pm i})^2}$  seems to be very enigmatic and far from the expected operators  $(\hat{\mathcal{L}}_I^i)^2$  and  $(\hat{B}_I^{\pm i})^2$ . The choice becomes clear after inspecting the spectra of the operators: the spectrum of the operator  $(\hat{\mathcal{L}}_I^i)^2$  is  $k(k+1)$  while the spectrum of the operator  $\widehat{(\mathcal{L}_I^i)^2}$  is  $k^2$  and similarly for  $(\hat{B}_I^{\pm i})^2$  and  $\widehat{(B_I^{\pm i})^2}$ . When the spins are large, i.e. in the classical limit, the operators coincide – therefore the choice of  $\widehat{(\mathcal{L}_I^i)^2}$  instead of  $(\hat{\mathcal{L}}_I^i)^2$  can be interpreted as a quantization ambiguity. This choice of quantization is motivated by the fact that the solutions of the quantum linear simplicity constraint exist and in fact take a simple form.

The quantum constraints are matrix equations. Remarkably, the matrices commute and therefore there is a common basis diagonalizing them. The subspace of solutions is the subspace corresponding to zero eigenvalue of all the matrices. From the invariance of these equations under the choice of basis in  $V_\perp$  follows that the Hilbert spaces  $\mathcal{H}_{\text{poly}}^{\mathbf{n}, q_I^i}$  do not depend on the choice of  $q_I^i$ . Therefore we will write  $\mathcal{H}_{\text{poly}}^{\mathbf{n}} = \mathcal{H}_{\text{poly}}^{\mathbf{n}, q_I^i}$  and call  $\mathcal{H}_{\text{poly}}^{\mathbf{n}}$  the Hilbert space of quantum polyhedra in 4D orthogonal to  $n^I$ . The vectors in  $\mathcal{H}_{\text{poly}}^{\mathbf{n}}$  will be called quantum polyhedra in 4D orthogonal to  $n^I$  and denoted by  $\iota_{\text{poly}}^{\mathbf{n}}$ .

Let us construct the quantum polyhedra orthogonal to  $n^I$ . First, note that from the transformation property:

$$\rho_{j^+ j^-}(g) \rho'_{j^+ j^-}(\tau^{IJ}) \rho_{j^+ j^-}(g^{-1}) = [g^{-1}]^I_K [g^{-1}]^J_L \rho'_{j^+ j^-}(\tau^{KL}).$$

follows that, if  $\iota_{\text{poly}}^{\mathbf{n}}$  is a quantum polyhedron orthogonal to  $n^I$  then

$$\bigotimes_{I=1}^N \rho_{j_I^+ j_I^-}(g) \iota_{\text{poly}}^{\mathbf{n}}$$

is a quantum polyhedron orthogonal to  $(g \cdot \mathbf{n})^I = [g]^I_J n^J$ . As a result, the natural action of the Spin(4) group on  $\mathcal{H}_{j_1^+ j_1^-} \otimes \dots \otimes \mathcal{H}_{j_N^+ j_N^-}$ ,

$$\iota \mapsto g \cdot \iota := \bigotimes_{I=1}^N \rho_{j_I^+ j_I^-}(g) \iota \tag{3.18}$$

defines an isomorphism of the Hilbert spaces  $\mathcal{H}_{\text{poly}}^{\mathbf{n}}$  and  $\mathcal{H}_{\text{poly}}^{g \cdot \mathbf{n}}$ . In particular, from the invariance of the quantum constraints under the choice of basis in  $V_\perp$  follows that the space

### 3. Spin-foam models with the EPRL vertex amplitude

$\mathcal{H}_{\text{poly}}^{\mathbf{n}}$  is invariant under the action of  $SU_{\mathbf{n}}(2)$  – the  $SU(2)$  subgroup of  $\text{Spin}(4)$  leaving  $n^I$  invariant. We find the solutions to the quantum equations in the case  $\mathring{n}^I = \delta_0^I$ ,  $\mathring{q}_J^i = \delta_J^i$ , i.e. the Hilbert space  $\mathcal{H}_{\text{poly}}^{\mathring{\mathbf{n}}}$ . The Hilbert spaces  $\mathcal{H}_{\text{poly}}^{\mathbf{n}}$  are obtained by using the isomorphisms (3.18).

The reduced closure constraint has the following solutions. The operator  $\sum_{l=1}^N \hat{L}_l^i$  is an infinitesimal generator of the action of  $SU_{\mathbf{n}}(2)$  on  $\mathcal{H}_{\text{poly}}^{\mathbf{n}}$ :

$$u \cdot \iota = \bigotimes_{l=1}^N \rho_{j_l^+ j_l^-}(u) \iota, \quad u \in SU_{\mathbf{n}}(2)$$

and the solutions to this constraint are tensors invariant under the action. As a result, not only the Hilbert space  $\mathcal{H}_{\text{poly}}^{\mathbf{n}}$  is invariant under the action of the  $SU_{\mathbf{n}}(2)$  group but also each element of the space is invariant under this action. In the case  $\mathring{n}^I = \delta_0^I$  the  $SU(2)$  subgroup leaving  $n^I$  invariant is the diagonal subgroup  $SU_{\mathbf{n}}(2) = \{(h, h) : h \in SU(2)\}$  and the space of solutions of this constraint is spanned by elements of the following form:

$$\iota(\mathcal{I})^{A_1^+ A_1^- \dots A_N^+ A_N^-} = C_{A_1}^{A_1^+ A_1^-} \dots C_{A_N}^{A_N^+ A_N^-} \mathcal{I}^{A_1 \dots A_N},$$

where  $C_{k_l}^{j_l^+ j_l^-} \in \text{Inv}(\mathcal{H}_{j_l^+} \otimes \mathcal{H}_{j_l^-} \otimes \mathcal{H}_{k_l}^*)$ ,  $|j_l^+ - j_l^-| \leq k_l \leq j_l^+ + j_l^-$ ,  $k_l + j_l^+ + j_l^- \in \mathbb{N}$ ,  $\mathcal{I} \in \text{Inv}(\mathcal{H}_{\rho_{k_1}} \otimes \dots \otimes \mathcal{H}_{\rho_{k_N}})$ . We choose the normalization of  $C_{k_l}^{j_l^+ j_l^-}$  such that  $C_{k_l}^{j_l^+ j_l^-} : \mathcal{H}_{k_l} \rightarrow \mathcal{H}_{j_l^+} \otimes \mathcal{H}_{j_l^-}$  is an isometric embedding. By  $C_{j_l^+ j_l^-}^{k_l}$  we denote the adjoint operator. In the index notation we omit  $j_l^+, j_l^-, k_l$ , e.g.

$$C_{A_l}^{A_l^+ A_l^-} := (C_{k_l}^{j_l^+ j_l^-})_{A_l}^{A_l^+ A_l^-},$$

$A_l \in \{1, \dots, 2k_l + 1\}$  corresponds to the space  $\mathcal{H}_{k_l}$ ,  $A_l^+ \in \{1, \dots, 2j_l^+ + 1\}$  corresponds to the space  $\mathcal{H}_{j_l^+}^*$  and  $A_l^- \in \{1, \dots, 2j_l^- + 1\}$  corresponds to the space  $\mathcal{H}_{j_l^-}^*$ .

We impose now the quantum linear simplicity constraint. The vectors  $\iota(\mathcal{I})$  are eigenvectors of the operators  $(\hat{L}_l^i)^2$  and  $(\hat{B}_l^{\pm i})^2$ :

$$(\hat{L}_l^i)^2 \iota(\mathcal{I}) = k_l(k_l + 1) \iota(\mathcal{I}), \quad (\hat{B}_l^{\pm i})^2 \iota(\mathcal{I}) = j_l^{\pm}(j_l^{\pm} + 1) \iota(\mathcal{I}),$$

as well as of the operators  $\widehat{(\hat{L}_l^i)^2}$  and  $\widehat{(\hat{B}_l^{\pm i})^2}$ :

$$\widehat{(\hat{L}_l^i)^2} \iota(\mathcal{I}) = k_l^2 \iota(\mathcal{I}), \quad \widehat{(\hat{B}_l^{\pm i})^2} \iota(\mathcal{I}) = (j_l^{\pm})^2 \iota(\mathcal{I}).$$

The linear simplicity constraint becomes a constraint on the spins  $k_l, j_l^+, j_l^-$ :

$$\left(1 - \frac{1}{\beta^2}\right) k_l^2 + \frac{1}{2\beta^2} ((j_l^+)^2 + (j_l^-)^2) - \frac{1}{2\beta} ((j_l^+)^2 - (j_l^-)^2) = 0.$$

Using the fact that  $|j_l^+ - j_l^-| \leq k_l \leq j_l^+ + j_l^-$  it can be shown that this equation has the following solution [81]:

$$j_l^{\pm} = \frac{|1 \pm \beta|}{2} k_l,$$

provided that  $\frac{|1 \pm \beta|}{2} k_l \in \frac{1}{2}\mathbb{N}$ . As a result, if  $\beta$  and  $k_1, \dots, k_N$  are such that

$$\frac{|1 \pm \beta|}{2} k_l \in \frac{1}{2}\mathbb{N},$$

then for each  $\mathcal{I} \in \text{Inv}(\mathcal{H}_{k_1} \otimes \dots \otimes \mathcal{H}_{k_N})$  there is a quantum polyhedron

$$\mathring{\iota}_{\text{poly}}(\mathcal{I}) \in \text{Inv}(\mathcal{H}_{j_1^+ j_1^-} \otimes \dots \otimes \mathcal{H}_{j_N^+ j_N^-}), \quad j_l^\pm = \frac{|1 \pm \beta|}{2} k_l,$$

defined by

$$\mathring{\iota}_{\text{poly}}(\mathcal{I})^{A_1^+ A_1^- \dots A_N^+ A_N^-} = C_{A_1}^{A_1^+ A_1^-} \dots C_{A_N}^{A_N^+ A_N^-} \mathcal{I}^{A_1 \dots A_N}. \quad (3.19)$$

Using the isomorphism (3.18) we obtain that any element of  $\mathcal{H}_{\text{poly}}^n$  is of the following form:

$$\iota_{\text{poly}}(n^I, \mathcal{I}) = \bigotimes_{l=1}^N \rho_{j_l^+ j_l^-}(g) \mathring{\iota}_{\text{poly}}(\mathcal{I}), \quad (3.20)$$

for some  $g \in \text{Spin}(4)$  such that  $n^I = [g]_0^I$  and  $\mathcal{I} \in \text{Inv}(\mathcal{H}_{k_1} \otimes \dots \otimes \mathcal{H}_{k_N})$ . The map  $\text{Inv}(\mathcal{H}_{k_1} \otimes \dots \otimes \mathcal{H}_{k_N}) \rightarrow \mathcal{H}_{\text{poly}}^n$ ,  $\mathcal{I} \mapsto \iota_{\text{poly}}(n^I, \mathcal{I})$  is an isomorphism of Hilbert spaces. It maps a quantum polyhedron in 3 dimensions to a quantum polyhedron in 4 dimensions orthogonal to  $n^I$ .

### Quantum polyhedron in 4D

The linear simplicity constraint requires that there exists a unit vector  $n^I$  such that the condition (3.15) is satisfied. In order to meet this condition, we define the set of embedded quantum polyhedra to be

$$\bigcup_{\mathbf{n}} \mathcal{H}_{\text{poly}}^n \subset \mathcal{H}_{j_1^+ j_1^-} \otimes \dots \otimes \mathcal{H}_{j_N^+ j_N^-}$$

This is however not a Hilbert space. In order to obtain a Hilbert space we consider two embedded quantum polyhedra in 4D to be congruent if one can be obtained from the other by a  $\text{Spin}(4)$  transformation (the analogous congruence condition in 3D is trivially satisfied). As a result, we define

$$\mathcal{H}_{\text{poly}} := \left( \bigcup_{\mathbf{n}} \mathcal{H}_{\text{poly}}^n \right) / \text{Spin}(4),$$

i.e. the space of orbits of the action of the  $\text{Spin}(4)$  group on the set  $\bigcup_{\mathbf{n}} \mathcal{H}_{\text{poly}}^n$ . The elements of this space will be called quantum polyhedra in 4D. The space  $\mathcal{H}_{\text{poly}}$  has a natural vector space structure:

$$\lambda [\iota_{\text{poly}}(n^I, \mathcal{I})] + \lambda' [\iota_{\text{poly}}(n'^I, \mathcal{I}')] := [\lambda \iota_{\text{poly}}(n^I, \mathcal{I}) + \lambda' \iota_{\text{poly}}(n'^I, \mathcal{I}')],$$

and a natural scalar product:

$$\langle [\iota_{\text{poly}}(n^I, \mathcal{I})] | [\iota_{\text{poly}}(n'^I, \mathcal{I}')] \rangle := \langle \iota_{\text{poly}}(n^I, \mathcal{I}) | \iota_{\text{poly}}(n'^I, \mathcal{I}') \rangle.$$

As a result  $\mathcal{H}_{\text{poly}}$  is a Hilbert space. It will be called the Hilbert space of quantum polyhedra in 4D. Remarkably,  $\mathcal{H}_{\text{poly}}$  is isomorphic with the Hilbert space of quantum polyhedra in 3D. The states of  $\mathcal{H}_{\text{poly}}$  are obviously invariant under the action of the  $\text{Spin}(4)$  group – this can be interpreted as an implementation of the (full) closure constraint (3.9).

### 3. Spin-foam models with the EPRL vertex amplitude

#### The EPRL intertwiners

The EPRL intertwiner is obtained by averaging an embedded quantum polyhedron in 4D  $\iota_{\text{poly}}(n^I, \mathcal{I}) \in \mathcal{H}_{\text{poly}}^{\mathbf{n}}$  over the group of Spin(4) transformations (rotations of the embedded quantum polyhedron):

$$\iota_{\text{EPRL}}(\mathcal{I}) = \int_{\text{Spin}(4)} dg \bigotimes_{l=1}^N \rho_{j_1^+ j_1^-}(g) \iota_{\text{poly}}(n^I, \mathcal{I}).$$

Let us note that this integral does not depend on  $n^I$ . From the invariance of the embedded quantum polyhedron in 4D under the group or SU(2) transformations leaving  $n^I$  invariant, follows that one can equivalently write the integral as an average over the unit normals  $n^I$  (compare eq. (3.50) in [179]):

$$\iota_{\text{EPRL}}(\mathcal{I}) = \int_{\mathbb{S}^3} d\mathbf{n} \iota_{\text{poly}}(n^I, \mathcal{I}). \quad (3.21)$$

### 3.3. The generalized EPRL vertex amplitude

#### 3.3.1. The EPRL intertwiners

Here we summarize the construction of the EPRL intertwiners. In a given intertwiner space  $\text{Inv}(\mathcal{H}_{j_1^+ j_1^-} \otimes \dots \otimes \mathcal{H}_{j_N^+ j_N^-})$  a necessary condition for the existence of an EPRL intertwiner is

$$j_l^+ = \frac{|\beta + 1|}{|\beta - 1|} j_l^-, \quad l = 1, \dots, N, \quad (3.22)$$

where we assume that  $\beta \in \mathbb{R}, \beta \neq 0, \pm 1$  (in fact the condition can be satisfied only for  $\beta \in \mathbb{Q}$ ). An ingredient of the EPRL intertwiner is an SU(2) invariant

$$\mathcal{I} \in \text{Inv}(\mathcal{H}_{k_1} \otimes \dots \otimes \mathcal{H}_{k_N}), \quad (3.23)$$

where the spins  $k_l$  are adjusted as follows

$$k_l := \begin{cases} j_l^+ + j_l^-, & \text{if } -1 < \beta < 1 \\ |j_l^+ - j_l^-|, & \text{if } \beta < -1 \text{ or } 1 < \beta. \end{cases} \quad (3.24)$$

Given  $\mathcal{I}$ , an EPRL intertwiner  $\iota_{\text{EPRL}}(\mathcal{I})$  is defined using the invariants

$$C_{k_l}^{j_l^+ j_l^-} \in \text{Inv}(\mathcal{H}_{j_l^+} \otimes \mathcal{H}_{j_l^-} \otimes \mathcal{H}_{k_l}^*), \quad l = 1, \dots, N. \quad (3.25)$$

First, let us construct a tensor

$$C_{k_1}^{j_1^+ j_1^-} \otimes \dots \otimes C_{k_N}^{j_N^+ j_N^-} \lrcorner \mathcal{I} \in \mathcal{H}_{j_1^+} \otimes \dots \otimes \mathcal{H}_{j_n^+} \otimes \mathcal{H}_{j_1^-} \otimes \dots \otimes \mathcal{H}_{j_N^-}. \quad (3.26)$$

In the index notation

$$C_{B_1}^{A_1^+ A_1^-} \dots C_{B_N}^{A_N^+ A_N^-} \mathcal{I}^{B_1 \dots B_N}. \quad (3.27)$$

Next, let us project this tensor orthogonally onto the subspace of invariant tensors. The resulting tensor is the EPRL intertwiner:

$$\iota_{\text{EPRL}}(\mathcal{I}) := P C_{k_1}^{j_1^+ j_1^-} \otimes \dots \otimes C_{k_N}^{j_N^+ j_N^-} \lrcorner \mathcal{I}, \quad (3.28)$$

### 3.3. The generalized EPRL vertex amplitude

where

$$P : \mathcal{H}_{j_1^+ j_1^-} \otimes \dots \otimes \mathcal{H}_{j_N^+ j_N^-} \rightarrow \mathcal{H}_{j_1^+ j_1^-} \otimes \dots \otimes \mathcal{H}_{j_N^+ j_N^-}$$

is the orthogonal projection onto  $\text{Inv}(\mathcal{H}_{j_1^+ j_1^-} \otimes \dots \otimes \mathcal{H}_{j_N^+ j_N^-})$ . Since

$$\begin{aligned} \text{Inv}(\mathcal{H}_{j_1^+ j_2^-} \otimes \dots \otimes \mathcal{H}_{j_N^+ j_N^-}) &= \text{Inv}(\mathcal{H}_{j_1^+} \otimes \dots \otimes \mathcal{H}_{j_N^+}) \otimes \text{Inv}(\mathcal{H}_{j_1^-} \otimes \dots \otimes \mathcal{H}_{j_N^-}) \\ &\subset \mathcal{H}_{j_1^+} \otimes \dots \otimes \mathcal{H}_{j_N^+} \otimes \mathcal{H}_{j_1^-} \otimes \dots \otimes \mathcal{H}_{j_N^-}, \end{aligned} \quad (3.29)$$

the projection  $P$  is of the form:

$$P = P^+ \otimes P^-,$$

where

$$P^\pm : \mathcal{H}_{j_1^\pm} \otimes \dots \otimes \mathcal{H}_{j_N^\pm} \rightarrow \mathcal{H}_{j_1^\pm} \otimes \dots \otimes \mathcal{H}_{j_N^\pm}$$

are the orthogonal projections onto  $\text{Inv}(\mathcal{H}_{j_1^\pm} \otimes \dots \otimes \mathcal{H}_{j_N^\pm})$ . In the index notation the equation (3.28) takes the following form:

$$\iota_{\text{EPRL}}(\mathcal{I})^{A_1^+ \dots A_N^+ A_1^- \dots A_N^-} = P^{+A_1^+ \dots A_N^+}_{D_1^+ \dots D_N^+} P^{+A_1^- \dots A_N^-}_{D_1^- \dots D_N^-} C_{B_1}^{D_1^+ D_1^-} \dots C_{B_N}^{D_N^+ D_N^-} \mathcal{I}^{B_1 \dots B_N}. \quad (3.30)$$

The formula (3.28) can be written in a simpler way by skipping one of the projections, namely

$$\iota_{\text{EPRL}}(\mathcal{I}) = (P^+ \otimes 1) C_{k_1}^{j_1^+ j_1^-} \otimes \dots \otimes C_{k_N}^{j_N^+ j_N^-} \lrcorner \mathcal{I} = (1 \otimes P^-) C_{k_1}^{j_1^+ j_1^-} \otimes \dots \otimes C_{k_N}^{j_N^+ j_N^-} \lrcorner \mathcal{I}, \quad (3.31)$$

and in the index notation

$$\iota_{\text{EPRL}}(\mathcal{I})^{A_1^+ \dots A_N^+ A_1^- \dots A_N^-} = P^{+A_1^+ \dots A_N^+}_{D_1^+ \dots D_N^+} C_{B_1}^{D_1^+ A_1^-} \dots C_{B_N}^{D_N^+ A_N^-} \mathcal{I}^{B_1 \dots B_N} \quad (3.32)$$

The EPRL intertwiners form a subspace in  $\text{Inv}(\mathcal{H}_{j_1^+ j_1^-} \otimes \dots \otimes \mathcal{H}_{j_N^+ j_N^-})$ . This subspace will be called the space of EPRL intertwiners and denoted by

$$\text{Inv}_{\text{EPRL}}(\mathcal{H}_{j_1^+ j_1^-} \otimes \dots \otimes \mathcal{H}_{j_N^+ j_N^-}).$$

#### 3.3.2. The EPRL map

Given  $\beta \in \mathbb{Q}$  and  $k_l \in \frac{1}{2}\mathbb{N}$ ,  $l \in \{1, \dots, N\}$  such that  $\forall_l \ j_l^\pm := \frac{|1 \pm \beta|}{2} k_l \in \frac{1}{2}\mathbb{N}$ , the map

$$\iota_{\text{EPRL}} : \text{Inv}(\mathcal{H}_{k_1} \otimes \dots \otimes \mathcal{H}_{k_N}) \rightarrow \text{Inv}(\mathcal{H}_{j_1^+} \otimes \dots \otimes \mathcal{H}_{j_N^+}) \otimes \text{Inv}(\mathcal{H}_{j_1^-} \otimes \dots \otimes \mathcal{H}_{j_N^-}) \quad (3.33)$$

defined as follows:

$$\iota_{\text{EPRL}}(\mathcal{I})^{A_1^+ \dots A_N^+ A_1^- \dots A_N^-} := P^{+A_1^+ \dots A_N^+}_{D_1^+ \dots D_N^+} P^{+A_1^- \dots A_N^-}_{D_1^- \dots D_N^-} C_{B_1}^{D_1^+ D_1^-} \dots C_{B_N}^{D_N^+ D_N^-} \mathcal{I}^{B_1 \dots B_N}$$

will be called the Engle-Pereira-Rovelli-Livine map (EPRL map in short) and denoted by  $\iota_{\text{EPRL}}$  [123]. Let us note that although the EPRL intertwiner is defined for  $\beta \in \mathbb{Q}, \beta \neq$

### 3. Spin-foam models with the EPRL vertex amplitude

$0, \pm 1$ , we define the EPRL map for  $\beta \in \mathbb{Q}$  (see [123] for a discussion of the limits of the EPRL intertwiner and the EPRL spin-foam model as  $\beta \rightarrow 0, \pm 1$ ).

Let us note that the EPRL map can be also viewed as a map from a Hilbert space of quantum polyhedra in 4D into a space of  $\text{Spin}(4)$  invariant tensors assigning to a quantum polyhedron in 4D [ $\iota_{\text{poly}}(n^I, \mathcal{I})$ ] an EPRL intertwiner

$$\int_{\text{Spin}(4)} dg \bigotimes_{l=1}^N \rho_{j_l^+ j_l^-}(g) \iota_{\text{poly}}(n^I, \mathcal{I}).$$

Clearly, the EPRL intertwiner does not depend on the choice of the representant of the equivalence class [ $\iota_{\text{poly}}(n^I, \mathcal{I})$ ] and thus the map is well defined.

#### 3.3.3. The EPRL spin networks

An EPRL spin network is a  $\text{Spin}(4)$  spin network  $(\gamma, \rho^{\text{EPRL}}, \iota^{\text{EPRL}})$  such that:

- $\rho_\ell^{\text{EPRL}} = \rho_{j_\ell^+ j_\ell^-}$ , where  $j_f^\pm = \frac{|\beta+1|}{|\beta-1|} j_f^-$ ,
- $\iota_n^{\text{EPRL}}$  is an EPRL intertwiner:

$$\iota_n^{\text{EPRL}} \in \text{Inv}_{\text{EPRL}} \left( \bigotimes_{\ell \text{ incoming to } n} \mathcal{H}_\ell^* \otimes \bigotimes_{\ell' \text{ outgoing from } n} \mathcal{H}_{\ell'} \right) \subset \mathcal{H}_n.$$

To each  $\text{SU}(2)$  spin network  $s = (\gamma, \rho_k, \mathcal{I})$  such that  $\forall_{\ell \in \gamma^{(1)}} \frac{|1 \pm \beta|}{2} k_\ell \in \frac{1}{2}\mathbb{N}$  there corresponds an EPRL spin network  $\iota_{\text{EPRL}}(s) = (\gamma, \rho^{\text{EPRL}}, \iota^{\text{EPRL}})$  defined by the following conditions:

- $\rho_\ell^{\text{EPRL}} = \rho_{j_\ell^+ j_\ell^-}$ , where  $j_\ell^\pm = \frac{|1 \pm \beta|}{2} k_\ell$ ,
- $\iota_n^{\text{EPRL}} = \iota_{\text{EPRL}}(\mathcal{I}_n)$ .

#### 3.3.4. The generalized EPRL vertex amplitude

In the spin-foam model of quantum  $\text{Spin}(4)$  BF theory the vertices are colored with the vertex traces

$$\text{Tr}_v : \bigotimes_{e \text{ incoming at } v} \text{Inv}(\mathcal{H}_e) \otimes \bigotimes_{e \text{ outgoing at } v} \text{Inv}(\mathcal{H}_e)^* \rightarrow \mathbb{C}.$$

We define a pullback of the vertex trace  $\text{Tr}_v$  with the EPRL map:

$$\begin{aligned} \iota_{\text{EPRL}}^*(\text{Tr}_v) & \left( \bigotimes_{\text{outgoing } e} \mathcal{I}_e^\dagger \otimes \bigotimes_{\text{incoming } e'} \mathcal{I}_{e'} \right) := \\ & = \text{Tr}_v \left( \bigotimes_{\text{outgoing } e} \iota_{\text{EPRL}}(\mathcal{I}_e^\dagger) \otimes \bigotimes_{\text{incoming } e'} \iota_{\text{EPRL}}(\mathcal{I}_{e'}) \right). \end{aligned}$$

The contractor  $\iota_{\text{EPRL}}^*(\text{Tr}_v)$  will be called an EPRL contractor and denoted by  $\mathcal{A}_v^{\text{EPRL}}$ :

$$\mathcal{A}_v^{\text{EPRL}} := \iota_{\text{EPRL}}^*(\text{Tr}_v).$$

### 3.3. The generalized EPRL vertex amplitude

Since the EPRL map can be also viewed as a map from a Hilbert space of quantum polyhedra in 4D to a space of Spin(4) invariant tensors, the EPRL contractor could be also viewed as a linear functional on a tensor product of Hilbert spaces of quantum polyhedra in 4D.

The vertex amplitude corresponding to the EPRL contractor is called the EPRL vertex amplitude:

$$\mathcal{A}_v^{\text{EPRL}}(s_v^\dagger) := \mathcal{A}_v^{\text{EPRL}} \left( \bigotimes_{n \in \gamma_v^{(0)}} \mathcal{I}_n \right).$$

The EPRL vertex amplitude is the evaluation of the EPRL spin network corresponding to the SU(2) vertex spin network  $s_v^\dagger$ :

$$\mathcal{A}_v^{\text{EPRL}}(s_v^\dagger) = \overline{\psi_{\iota_{\text{EPRL}}(s_v)}(I)}.$$

We interpret the EPRL vertex amplitude in the following way. The quantum polyhedra in 3D  $\mathcal{I}_e^\dagger/\mathcal{I}_{e'}$  corresponding to a single internal vertex  $v$  are embedded into 4D and glued together to form a boundary of a 4-dimensional bulk. Then one integrates over the vectors  $n^I$  orthogonal to the quantum polyhedra in each bulk separately. A quantum polyhedron in 3D  $\mathcal{I}_e$  corresponding to an internal edge  $e$  is embedded to 4D twice, because it appears in the boundaries of the two adjacent bulks corresponding to the two internal vertices on the endpoints of  $e$ . The degrees of freedom corresponding to the connection are encoded in the Spin(4) transformation relating the two embeddings. The degrees of freedom corresponding to the  $B$  field are encoded in the intertwiners  $\mathcal{I}$ , the spins and partially in the vectors  $n^I$ . The integral over the vectors normal to the polyhedra (3.21) is a part of the functional integral – the degrees of freedom corresponding to the connection and some degrees of freedom corresponding to the  $B$  field are integrated out. Let us note that the geometries of the boundaries of the polyhedra in 3D that are embedded to 4D and glued together do not have to match. As a result the corresponding classical geometries do not have to be the Regge geometries but could be more general geometries [102] called twisted geometries [98, 99, 80, 171].

If the foam is defined by triangulation of space-time, the polyhedra are tetrahedra and the tetrahedra corresponding to a single internal vertex  $v$  are glued together to form a boundary of a 4-simplex. In this case the EPRL vertex amplitude is also called the EPRL 4-simplex amplitude. The semi-classical limit of the EPRL 4-simplex amplitude was studied in [40] for the Euclidean signature and in [41] for the Lorentzian signature. The asymptotic formula relates the EPRL 4-simplex amplitude to the Regge action of four-dimensional General Relativity very much like the asymptotic formula in section 1.3.2 relates the Ponzano-Regge vertex amplitude to the Ponzano-Regge action. This makes the models studied in the section 3.4 very promising. However, in [81] an issue with the semi-classical limit of the 4-simplex amplitude was raised. The author argues that the EPRL 4-simplex amplitude mixes the  $(II^\pm)$  and  $(\text{deg})$  Plebański sectors (see section 3.1). In [83, 82] the author proposes a new vertex amplitude in the Euclidean case. The model is however limited to foams defined by triangulations.

### 3.4. The spin-foam models with the EPRL vertex amplitude

In this section we compare the two models with the (generalized) EPRL vertex amplitude: the model we introduced in [123], which we will call Spin(4) spin-foam model with the EPRL vertex, and the model from [48], which we will call SU(2) spin-foam model with the EPRL vertex. The models depend on the Barbero-Immirzi parameter  $\beta$ , which we assume to be rational and different from  $0, \pm 1$ .

#### 3.4.1. Spin(4) spin-foam model with the EPRL vertex

In this subsection we present a model where the spin foams are histories of the EPRL spin networks. We introduced this model in [123] and studied it in [123, 124, 29].

- The Spin(4) EPRL spin foam  $(\kappa, \rho, \iota, \mathcal{A})$  is a foam  $\kappa$  with a coloring such that
  - $\rho_f = \rho_{j_f^+ j_f^-}$ , where  $j_f^+ = \frac{|\beta+1|}{|\beta-1|} j_f^-$ .
  - $\iota_e$  is an EPRL intertwiner,  $\iota_e \in \text{Inv}_{\text{EPRL}}(\mathcal{H}_e) \subset \text{Inv}(\mathcal{H}_e)$ ,
  - $\mathcal{A}_v$  is the vertex trace  $\mathcal{A}_v = \text{Tr}_v \in \mathcal{H}_v^*$  familiar from the BF theory (see section 1.3.2).
- The amplitude of each spin foam  $(\kappa, \rho, \iota, \mathcal{A})$  is defined by the formula:

$$Z(\kappa, \rho, \iota, \mathcal{A}) = \prod_{\ell \in (\partial\kappa)^{(1)}} \frac{1}{\sqrt{d_{f_\ell}}} \prod_{f \in \kappa^{(2)}} d_f \prod_{v \in \kappa_{\text{int}}^{(0)}} \text{Tr}_v(s_v^\dagger),$$

where  $d_f = \dim \mathcal{H}_f$ . In this model  $d_f = (2j_f^+ + 1)(2j_f^- + 1)$ .

- To sum with respect to the spin-network histories with the amplitude as a weight, one fixes an orthonormal basis in each space

$$\text{Inv}_{\text{EPRL}} \left( \mathcal{H}_{j_1^+ j_1^-} \otimes \dots \otimes \mathcal{H}_{j_M^+ j_M^-} \otimes \mathcal{H}_{j_{M+1}^+ j_{M+1}^-}^* \otimes \dots \otimes \mathcal{H}_{j_N^+ j_N^-}^* \right)$$

of the EPRL intertwiners. In the (suitably defined) sums the intertwiners run through the fixed basis, for each choice of the representations at each edge.

Let us note that the structure of the spin-foam amplitudes is that of the BF theory. It has the following interpretation: the amplitudes are calculated using Spin(4) spin-foam model of quantum BF theory, the Quantum Gravity is obtained by restricting to histories satisfying the constraints, i.e. restricting the possible coloring of faces and edges.

#### 3.4.2. SU(2) spin-foam model with the EPRL vertex

An alternative spin-foam model with the EPRL vertex amplitude was proposed in [48]. In this model the spin foams are histories of the SU(2) spin networks. The model is a modification of quantum SU(2) BF theory obtained by assigning to vertices the EPRL contractors. In this approach a boundary of a spin foam is an SU(2) spin network and therefore the model is naturally compatible with the standard SU(2) formulation of Loop Quantum Gravity.

### 3.4. The spin-foam models with the EPRL vertex amplitude

- The SU(2) EPRL spin foam  $(\kappa, \rho, \iota, \mathcal{A})$  is a foam  $\kappa$  with a coloring such that
  - $\rho_f = \rho_{k_f}$  is an SU(2) representation such that  $\frac{|1 \pm \beta|}{2} k_f \in \frac{1}{2} \mathbb{N}$ ,
  - $\iota_e$  is any invariant tensor in  $\text{Inv}(\mathcal{H}_e)$ ,
  - $\mathcal{A}_v$  is the EPRL contractor  $\mathcal{A}_v^{\text{EPRL}}$ .
- The amplitude of each spin foam  $(\kappa, \rho, \iota, \mathcal{A})$  is defined by the formula:

$$Z(\kappa, \rho, \iota, \mathcal{A}) = \prod_{\ell \in (\partial\kappa)^{(1)}} \frac{1}{\sqrt{d_{f_\ell}}} \prod_{f \in \kappa^{(2)}} d_f \prod_{v \in \kappa_{\text{int}}^{(0)}} \mathcal{A}_v^{\text{EPRL}}(s_v^\dagger),$$

where  $d_f = \dim \mathcal{H}_f = 2k_f + 1$ .

- To sum with respect to the spin-network histories with the amplitude as a weight, one fixes an orthonormal basis in each space

$$\text{Inv} \left( \mathcal{H}_{k_1} \otimes \dots \otimes \mathcal{H}_{k_M} \otimes \mathcal{H}_{k_{M+1}}^* \otimes \dots \otimes \mathcal{H}_{k_N}^* \right)$$

of the SU(2) intertwiners.

This model was successfully extended to the  $\text{SL}(2, \mathbb{C})$  theory [48, 163, 165].

#### 3.4.3. Comparison of the models

Since the SU(2) invariants parametrize the space of the EPRL intertwiners, one could also use SU(2) coloring from the SU(2) spin-foam model with the EPRL vertex in the Spin(4) spin-foam model with the EPRL vertex. The resulting model is defined in the following way:

- The spin foams  $(\kappa, \rho, \iota, \mathcal{A})$  are the SU(2) spin foams from section 3.4.2, i.e. they are foams  $\kappa$  with colorings such that
  - $\rho_f = \rho_{k_f}$  is an SU(2) representation such that  $\frac{|1 \pm \beta|}{2} k_f \in \frac{1}{2} \mathbb{N}$ ,
  - $\iota_e$  is any invariant tensor in  $\text{Inv}(\mathcal{H}_e)$ ,
  - $\mathcal{A}_v$  is the EPRL contractor  $\mathcal{A}_v^{\text{EPRL}}$ .
- The amplitude of each spin foam  $(\kappa, \rho, \iota, \mathcal{A})$  is defined by the formula:

$$Z(\kappa, \rho, \iota, \mathcal{A}) = \prod_{\ell \in (\partial\kappa)^{(1)}} A_{\text{link}}(\partial\rho_\ell) \prod_{f \in \kappa^{(2)}} A_{\text{face}}(\rho_f) \prod_{v \in \kappa_{\text{int}}^{(0)}} \mathcal{A}_v^{\text{EPRL}}(s_v^\dagger),$$

where  $A_{\text{face}}(\rho_k) = (|\beta + 1|k + 1)(|\beta - 1|k + 1)$ ,  $A_{\text{link}}(\rho_k) = \frac{1}{\sqrt{(|\beta+1|k+1)(|\beta-1|k+1)}}$ .

- To sum with respect to the spin-network histories with the amplitude as a weight, one fixes a basis in each  $\text{Inv} \left( \mathcal{H}_{k_1} \otimes \dots \otimes \mathcal{H}_{k_M} \otimes \mathcal{H}_{k_{M+1}}^* \otimes \dots \otimes \mathcal{H}_{k_N}^* \right)$  that is mapped with the EPRL map to an orthonormal basis in

$$\text{InvePRL} \left( \mathcal{H}_{j_1^+ j_1^-} \otimes \dots \otimes \mathcal{H}_{j_M^+ j_M^-} \otimes \mathcal{H}_{j_{M+1}^+ j_{M+1}^-}^* \otimes \dots \otimes \mathcal{H}_{j_N^+ j_N^-}^* \right).$$

### 3. Spin-foam models with the EPRL vertex amplitude

The correspondence with the model from section 3.4.1 is the following. A spin  $k_f$  uniquely determines a pair of spins  $j_f^+(k_f) = \frac{|1+\beta|}{2}k_f, j_f^-(k_f) = \frac{|1-\beta|}{2}k_f$  and therefore the coloring  $\rho_{k_f}$  is equivalent to the coloring  $\rho_{j_f^+ j_f^-}$  from section 3.4.1. As we will see in the next chapter, an EPRL map is 1-1 unless its domain is non-trivial but its co-domain is trivial. If the co-domain is trivial, the spin-foam amplitudes in the model presented in this section as well as in the model from section 3.4.1 are zero. Therefore these degenerate configurations do not contribute in neither of the models. If the co-domain is non-trivial, the EPRL map maps a basis of  $SU(2)$  intertwiners to a basis of the EPRL intertwiners. Therefore the coloring of intertwiners is equivalent to the coloring from section 3.4.1 and the correspondence is given by the EPRL map. Clearly, the sums over the intertwiners are also equivalent. Since the EPRL contractor is just a pullback of the vertex trace (see section 3.3.4), an amplitude of an  $SU(2)$  spin foam defined in this section is the same as the amplitude of the corresponding  $Spin(4)$  EPRL spin foam from section 3.4.1.

It is now easy to compare the  $Spin(4)$  spin-foam model with the EPRL vertex and the  $SU(2)$  spin-foam model with the EPRL vertex. The result of the comparison is summarized in table 3.1.

	Spin(4) spin-foam model with the EPRL vertex	$SU(2)$ spin-foam model with the EPRL vertex
face amplitude	$( \beta + 1 k_f + 1)( \beta - 1 k_f + 1)$	$2k_f + 1$
boundary link amplitude	$\frac{1}{\sqrt{( \beta+1 k_{f_\ell}+1)( \beta-1 k_{f_\ell}+1)}}$	$\frac{1}{\sqrt{2k_{f_\ell}+1}}$
vertex amplitude	EPRL vertex amplitude	
sum over intertwiners	sum over orthonormal basis in $Inv_{EPRL} \left( \bigotimes_f \mathcal{H}_{j_f^+ j_f^-} \otimes \bigotimes_{f'} \mathcal{H}_{j_{f'}^+ j_{f'}^-}^* \right)$	

Table 3.1.: Comparison of the  $SU(2)$  spin-foam model corresponding to the  $Spin(4)$  spin-foam model with the EPRL vertex and the  $SU(2)$  spin-foam model with the EPRL vertex.

## 3.5. Other spin-foam models of 4D Quantum Gravity

There are three main proposals for the spin-foam models of 4D Quantum Gravity:

1. The Barrett-Crane (BC) model corresponding to the Palatini action [38, 39].
2. The Engle-Pereira-Rovelli-Livine (EPRL) model corresponding to the Holst-Palatini action with real, positive value of the Barbero-Immirzi parameter  $\beta$ . In the Euclidean case it is additionally assumed that  $\beta$  is rational and different from 1 [86]<sup>2</sup>.

---

<sup>2</sup>Although in the original paper [86] the authors restrict to positive values of the Barbero-Immirzi parameter, the derivation of the Euclidean EPRL model works also for negative values. In this thesis we assume that in the Euclidean case  $\beta \in \mathbb{Q}, \beta \neq 0, \pm 1$ . The Barbero-Immirzi parameter  $\beta$  needs to be rational because the constraint  $j_l^\pm = \frac{|1 \pm \beta|}{2} k_l$  can be solved only for  $\beta$  rational (see section 4.2 for more detailed discussion).

### 3.5. Other spin-foam models of 4D Quantum Gravity

3. The Freidel-Krasnov (FK) model also corresponding to the Holst-Palatini action with real, positive value of the Barbero-Immirzi parameter  $\beta$ . In the Euclidean case it is additionally assumed that  $\beta$  is rational and different from 1 [96].

The Euclidean BC model is based on BC intertwiners. The BC intertwiners were derived by passing to the quantum level some symmetry between the self-dual and anti-self dual 2-forms [38, 183, 37, 157, 140]. In [4] it was noticed, that the BC states are insufficient to define physical semi-classical states of Quantum Gravity. That observation produced a new activity and led to the EPRL theory. The EPRL approach uses the Holst-Palatini action and the BC approach uses the Palatini action. In the limit  $\beta \rightarrow \pm\infty$  the conditions (3.22,3.23,3.24,3.25,3.32) defining the EPRL intertwiners go to (see section 3.3.1)

$$j_l^+ = j_l^- =: j_l, \quad k_l = 0, \quad C_{k_l}^{j_l^+ j_l^-} = e^{j_l^+ j_l^-}, \quad \mathcal{I} = 1, \quad (3.34)$$

$$\iota_{\text{EPRL}}(1)^{A_1^+ \dots A_n^+ A_1^- \dots A_n^-} = P_{D_1^+ \dots D_n^+}^{A_1^+ \dots A_n^+} \epsilon^{D_1^+ A_1^- \dots \epsilon^{D_N^+ A_N^-}}, \quad (3.35)$$

where  $e^{j_l^+ j_l^-} \in \text{Inv}(\mathcal{H}_{j_l^+} \otimes \mathcal{H}_{j_l^-})$  are invariants unique up to scaling (the normalization and reality condition reduce the scaling ambiguity to  $\pm 1$ ). The EPRL intertwiner becomes the BC intertwiner. This is consistent with the fact that the classical Holst-Palatini action becomes the Palatini action in the limit  $\beta \rightarrow \pm\infty$ .

The FK model also uses the Holst-Palatini action. The quantum simplicity constraint is encoded in a construction of suitable kinematical semiclassical states. Remarkably, in the Euclidean case the result coincides with the EPRL model as long as  $0 < \beta < 1$ , whereas the result is different for  $\beta > 1$ . In particular  $\beta \rightarrow \infty$  is no longer the BC model. We do not study the FK model in the case  $\beta > 1$  in the thesis.



## 4. Properties of the EPRL map

In this chapter we will show that the kernel of an EPRL map (see section 3.3.2) is trivial unless the co-domain of the map is trivial and the domain is non-trivial. We also give an example of non-isometric EPRL map.

The LQG states defined by spin networks such that each spin network has at least one node labelled with an intertwiner that is not in the domain of or happens to be annihilated by an EPRL map are not given any chance to play a role in the physical Hilbert space. In this sense they are degenerate. In section 4.2 we will formulate the theorem concerning injectivity of the EPRL map. We will also discuss the states which are not in the domain of the EPRL map. We will prove the injectivity theorem in the case  $|\beta| \geq 1$  in section 4.3 and in the case  $|\beta| < 1$  in section 4.4. The proof is technical and therefore we will begin the chapter with an example of a non-isometric EPRL map (section 4.1).

The importance of the non-isometricity of the EPRL map was already emphasized in the previous chapter (section 3.4). Given an orthonormal basis  $\mathcal{I}_1, \dots, \mathcal{I}_N$  of the Hilbert space

$$\text{Inv} \left( \mathcal{H}_{k_1} \otimes \dots \otimes \mathcal{H}_{k_M} \otimes \mathcal{H}_{k_{M+1}}^* \otimes \dots \otimes \mathcal{H}_{k_N}^* \right)$$

we have a basis  $\iota_{\text{EPRL}}(\mathcal{I}_1), \dots, \iota_{\text{EPRL}}(\mathcal{I}_N)$  of the corresponding Hilbert space<sup>1</sup>

$$\text{Inv}_{\text{EPRL}} \left( \mathcal{H}_{j_1^+ j_1^-} \otimes \dots \otimes \mathcal{H}_{j_M^+ j_M^-} \otimes \mathcal{H}_{j_{M+1}^+ j_{M+1}^-}^* \otimes \dots \otimes \mathcal{H}_{j_N^+ j_N^-}^* \right).$$

The question is, whether or not the latter basis is also orthonormal. In section 4.1 we will present an example, where this is not the case. As a result, in the example the Hilbert space of SU(2) spin networks and the Hilbert space of Spin(4) EPRL spin networks are not isomorphic. This leads to the ambiguity in the definition of the spin-foam model with the EPRL vertex amplitude: either one considers the spin foams as histories of the SU(2) spin networks and sums over orthonormal basis in the space of SU(2) intertwiners (see section 3.4.2), or one considers the spin foams as histories of the Spin(4) EPRL spin networks and sums over an orthonormal basis in the space of EPRL intertwiners (see section 3.4.1).

### 4.1. Non-isometricity of the EPRL map

In this section we give an example of a non-isometric EPRL map. Consider an SU(2) intertwiner  $\mathcal{I} \in \text{Inv}(\mathcal{H}_{k_1} \otimes \mathcal{H}_{k_2} \otimes \mathcal{H}_{k_3} \otimes \mathcal{H}_{k_4})$ . We choose a basis  $|k_l m_l\rangle$  (the eigenvector of the third component of angular momentum operator with eigenvalue  $m_l$ ) in each space  $\mathcal{H}_{k_l}$ ,  $l \in \{1, \dots, 4\}$ . We choose a real basis of the space  $\text{Inv}(\mathcal{H}_{k_1} \otimes \mathcal{H}_{k_2} \otimes \mathcal{H}_{k_3} \otimes \mathcal{H}_{k_4})$  in

---

<sup>1</sup>Unless all the intertwiners  $\iota_{\text{EPRL}}(\mathcal{I}_l)$  are trivial.

#### 4. Properties of the EPRL map

the following form [2]:

$$(\mathcal{I}_a)_{k_1 m_1 k_2 m_2 k_3 m_3 k_4 m_4} = \sqrt{2a+1} \sum_{m=-k}^k \sum_{m'=-a}^a (-1)^{a+m} \begin{pmatrix} k_1 & k_2 & a \\ m_1 & m_2 & m \end{pmatrix} \cdot \delta_{m,-m'} \begin{pmatrix} k_3 & k_4 & a \\ m_3 & m_4 & m' \end{pmatrix},$$

where  $\begin{pmatrix} k_1 & k_2 & k_3 \\ m_1 & m_2 & m_3 \end{pmatrix}$  is the Wigner 3j-Symbol,  $\delta_{m,m'}$  is the Kronecker Delta.

Let  $\iota_{j+} \otimes \iota_{j-}$  be the basis of the space  $\text{Inv}(\mathcal{H}_{j_1^+} \otimes \dots \otimes \mathcal{H}_{j_4^+}) \otimes \text{Inv}(\mathcal{H}_{j_1^-} \otimes \dots \otimes \mathcal{H}_{j_4^-})$ . The intertwiner  $\iota_{\text{EPRL}}(\mathcal{I}_a)$  expressed in this basis takes the following form:

$$\iota_{\text{EPRL}}(\mathcal{I}_a) = f_a^{a+a^-} \iota_{a^+} \otimes \iota_{a^-},$$

where  $f_a^{a+a^-}$  are real and are known as fusion coefficients [86]. We define a tensor  $h_{\bar{a}b}$ :

$$h_{\bar{a}b} := (\iota_{\text{EPRL}}(\mathcal{I}_a) | \iota_{\text{EPRL}}(\mathcal{I}_b)) = \sum_{a^+ a^-} f_a^{a+a^-} f_b^{a+a^-}.$$

As an example we give the result of the calculation of the  $h_{\bar{a}b}$  matrix for  $\beta = \frac{1}{2}, j_1 = 2, j_2 = 4, j_3 = 4, j_4 = 2; a, b \in \{2, \dots, 6\}$ :

$$\left( \begin{array}{ccccc} \frac{53723}{175616} & -\frac{2265\sqrt{\frac{5}{7}}}{50176} & \frac{5093\sqrt{5}}{1053696} & -\frac{3\sqrt{55}}{25088} & 0 \\ -\frac{2265\sqrt{\frac{5}{7}}}{50176} & \frac{117853}{501760} & -\frac{12805}{301056\sqrt{7}} & \frac{45\sqrt{\frac{11}{7}}}{7168} & -\frac{3\sqrt{\frac{13}{7}}}{8960} \\ \frac{5093\sqrt{5}}{1053696} & -\frac{12805}{301056\sqrt{7}} & \frac{741949}{3512320} & -\frac{781\sqrt{11}}{752640} & \frac{5\sqrt{13}}{5376} \\ -\frac{3\sqrt{55}}{25088} & \frac{45\sqrt{\frac{11}{7}}}{7168} & -\frac{781\sqrt{11}}{752640} & \frac{583}{2560} & 0 \\ 0 & -\frac{3\sqrt{\frac{13}{7}}}{8960} & \frac{5\sqrt{13}}{5376} & 0 & \frac{13}{40} \end{array} \right).$$

We used the analytic expression for the fusion coefficient presented in [2]. Clearly this matrix is non-diagonal. It shows that the EPRL map is not isometric.

#### 4.2. Injectivity theorem

##### The missed states

Given a value of the Barbero-Immirzi parameter  $\beta$ , an EPRL map is defined on an invariant space  $\text{Inv}(\mathcal{H}_{k_1} \otimes \dots \otimes \mathcal{H}_{k_N})$ , only if the spins  $k_1, \dots, k_N \in \frac{1}{2}\mathbb{N}$  are such that also each  $\frac{|1 \pm \beta|}{2}k_1, \dots, \frac{|1 \pm \beta|}{2}k_N \in \frac{1}{2}\mathbb{N}$ . That is why we assume that  $\beta$  is rational,

$$\beta = \frac{p}{q},$$

where  $p, q \in \mathbb{Z}, q > 0$  and they are relatively prime (the fraction can not be further reduced). If we need an explicit formula for  $k \in \frac{1}{2}\mathbb{N}$  such that  $\frac{|1 \pm \beta|}{2}k \in \frac{1}{2}\mathbb{N}$ , we find two possible cases of  $\beta$  and the corresponding formulas for  $k$ :

- (i) both  $p$  and  $q$  odd  $\Rightarrow k = qs$  where  $s \in \frac{1}{2}\mathbb{N}$ ,
- (ii) ( $p$  even and  $q$  odd) or ( $p$  odd and  $q$  even)  $\Rightarrow k = 2qs$  where  $s \in \frac{1}{2}\mathbb{N}$ .

Invariants involving even one value of spin  $k_l$  which is not that of (i), or respectively (ii) depending on  $\beta$ , are not in the domain of any EPRL map, hence they are missed by the EPRL maps.

### The annihilated states

We assume that there is given a space of invariants  $\text{Inv}(\mathcal{H}_{k_1} \otimes \dots \otimes \mathcal{H}_{k_N})$  such that each  $k_1, \dots, k_N$  satisfies (i) or, respectively, (ii) above. We assume also that the space is non-trivial. Recall, that for every  $N$ -tuple  $k_1, \dots, k_N$  of spins, the space  $\text{Inv}(\mathcal{H}_{k_1} \otimes \dots \otimes \mathcal{H}_{k_N})$  contains a non-zero element if and only if the spins satisfy the following conditions:

$$k_l \leq \sum_{j \neq l} k_j, \quad l = 1, \dots, N, \quad (4.1)$$

$$\sum_l k_l \in \mathbb{N}. \quad (4.2)$$

The proof is presented in appendix A. An  $N$ -tuple  $k_1, k_2, \dots, k_N$ ,  $k_l \in \frac{1}{2}\mathbb{N}$  satisfying conditions (4.1) and (4.2) will be called **admissible**.

The target space of the EPRL map

$$\text{Inv}(\mathcal{H}_{k_1} \otimes \dots \otimes \mathcal{H}_{k_N}) \rightarrow \text{Inv}(\mathcal{H}_{j_1^+} \otimes \dots \otimes \mathcal{H}_{j_N^+}) \otimes \text{Inv}(\mathcal{H}_{j_1^-} \otimes \dots \otimes \mathcal{H}_{j_N^-})$$

is nontrivial, if and only if

$$j_l^\pm \leq \sum_{j \neq l} j_j^\pm, \quad l = 1, \dots, N, \quad (4.3)$$

$$\sum_l j_l^\pm \in \mathbb{N}. \quad (4.4)$$

Whereas (4.1) does imply (4.3), the second condition

$$\sum_l j_l^\pm = \frac{|1 \pm \beta|}{2} \sum_l k_l \in \mathbb{N} \quad (4.5)$$

is not automatically satisfied for arbitrary  $\beta$ .

For example, let

$$\beta = \frac{1}{4}, \quad k_1, k_2, k_3 = 4.$$

Certainly the space  $\text{Inv}(\mathcal{H}_4 \otimes \mathcal{H}_4 \otimes \mathcal{H}_4)$  is non-empty. However,

$$j_1^-, j_2^-, j_3^- = \frac{3}{2}, \quad j_1^+, j_2^+, j_3^+ = \frac{5}{2}$$

and

$$\text{Inv}(\mathcal{H}_{\frac{3}{2}} \otimes \mathcal{H}_{\frac{3}{2}} \otimes \mathcal{H}_{\frac{3}{2}}) \otimes \text{Inv}(\mathcal{H}_{\frac{5}{2}} \otimes \mathcal{H}_{\frac{5}{2}} \otimes \mathcal{H}_{\frac{5}{2}}) = \{0\} \otimes \{0\}.$$

#### 4. Properties of the EPRL map

In other words, if  $\beta$  is 0.25, then the EPRL map annihilates the  $SU(2)$  invariant corresponding to the spins  $k_1 = k_2 = k_3 = 4$ .

For  $\beta$  and  $k_1, \dots, k_N$  satisfying condition (i) in the previous subsection, the equation (4.2) implies (4.4). If  $\beta$  and  $k_1, \dots, k_N$  satisfy (ii), there is a set of non-trivial subspaces  $\text{Inv}(\mathcal{H}_{k_1} \otimes \dots \otimes \mathcal{H}_{k_N})$  which are annihilated by the EPRL map, because the target  $\text{Inv}(\mathcal{H}_{j_1^+} \otimes \dots \otimes \mathcal{H}_{j_N^+}) \otimes \text{Inv}(\mathcal{H}_{j_1^-} \otimes \dots \otimes \mathcal{H}_{j_N^-})$  is just the trivial space.

The theorem formulated below states exactly, that the EPRL map does not annihilate more states than those characterized above.

#### The injectivity theorem

**Theorem 3.** Assume  $\beta \in \mathbb{Q}$ . For  $k_l \in \frac{1}{2}\mathbb{N}$ ,  $l \in \{1, \dots, N\}$  such that

- $\forall_l \ j_l^\pm := \frac{|1 \pm \beta|}{2} k_l \in \frac{1}{2}\mathbb{N}$ ,
- $\sum_{l=1}^N j_l^+ \in \mathbb{N}$

the EPRL map is injective.

Let us note that when  $\text{Inv}(\mathcal{H}_{k_1} \otimes \dots \otimes \mathcal{H}_{k_N})$  is trivial, injectivity trivially holds. Let us also note that injectivity of an EPRL map defined for  $\beta, k_l, j_l^\pm = \frac{|1 \pm \beta|}{2} k_l$  implies injectivity of an EPRL map defined for  $-\beta, k_l, j_l^\pm = \frac{|1 \mp \beta|}{2} k_l$ . It is therefore enough to prove the injectivity theorem for  $\beta \geq 0$ .

#### 4.3. Proof of the injectivity theorem in the case $\beta \geq 1$

We will show now that the EPRL map is injective in the case

$$k_I = j_I^+ - j_I^-,$$

provided  $j_1^- + \dots + j_N^- \in \mathbb{N}$ .

If we have found some  $\mathcal{I}_0$ , such that

$$\iota_{\text{EPRL}}(\mathcal{I}_0) = 0, \quad (4.6)$$

that is

$$P^{+A_1^+ \dots A_N^+}_{D_1^+ \dots D_N^+} C^{D_1^+ A_1^-}_{B_1^-} \dots C^{D_N^+ A_N^-}_{B_N^-} \mathcal{I}_0^{B_1 \dots B_N} = 0, \quad (4.7)$$

then any contraction of the left-hand side also vanishes, in particular

$$P^{+A_1^+ \dots A_N^+}_{D_1^+ \dots D_N^+} C^{D_1^+}_{A_1^- B_1} \dots C^{D_N^+}_{A_N^- B_N} \mathcal{I}_0^{B_1 \dots B_N} W^{A_1^- \dots A_N^-} = 0, \quad (4.8)$$

where we lowered the indices  $A_l^-$  with the  $\epsilon_{j_l^- j_l^-}$  bilinear forms and took any

$$0 \neq W \in \text{Inv}(\mathcal{H}_{j_1^-} \otimes \dots \otimes \mathcal{H}_{j_N^-}).$$

Such  $W$  exists if and only if  $j_1^- + \dots + j_N^- \in \mathbb{N}$ . We will show now that the last equality can not be true unless  $\mathcal{I}_0 = 0$  itself.

### 4.3. Proof of the injectivity theorem in the case $\beta \geq 1$

First, let us show a property of the spin composition map

$$C_{kj}^{k+j} : \mathcal{H}_k \otimes \mathcal{H}_j \rightarrow \mathcal{H}_{k+j}, \quad (4.9)$$

defined for any  $k, j \in \frac{1}{2}\mathbb{N}$ . In our notation the map is given by the intertwiners  $C_{BC}^A$ , namely

$$\mathcal{H}_k \otimes \mathcal{H}_j \ni K^{BC} \mapsto K^{BC} C_{BC}^A \in \mathcal{H}_{k+j}. \quad (4.10)$$

The key property is that the map can not annihilate a non-zero simple tensor  $K^{BC} = \mathcal{I}^B W^C$

$$\mathcal{I}^B W^C C_{BC}^A = 0 \Leftrightarrow \mathcal{I}^B W^C = 0. \quad (4.11)$$

To see that this is really true, view each of the Hilbert spaces  $\mathcal{H}_l$ ,  $l \in \frac{1}{2}\mathbb{N}$  as the symmetric part of the tensor product  $\mathcal{H}_{\frac{1}{2}} \otimes \dots \otimes \mathcal{H}_{\frac{1}{2}}$ , introduce an orthonormal basis  $|0\rangle, |1\rangle \in \mathcal{H}_{\frac{1}{2}}$  and define a basis  $v_0^{(l)}, \dots, v_{2l}^{(l)} \in \mathcal{H}_l$ ,

$$\begin{aligned} v_0^{(l)} &:= |0\rangle \otimes \dots \otimes |0\rangle, \\ v_1^{(l)} &:= \text{Sym}(|0\rangle \otimes \dots \otimes |0\rangle \otimes |1\rangle), \\ &\dots \\ v_{2l}^{(l)} &:= |1\rangle \otimes \dots \otimes |1\rangle, \end{aligned}$$

where

$$\text{Sym} : \mathcal{H}_{\frac{1}{2}} \otimes \dots \otimes \mathcal{H}_{\frac{1}{2}} \rightarrow \mathcal{H}_{\frac{1}{2}} \otimes \dots \otimes \mathcal{H}_{\frac{1}{2}}$$

denotes the projection onto the subspace of symmetric tensors. The spin composition map in this basis reads

$$C_{kj}^{k+j} : v_m^{(k)} \otimes v_{m'}^{(j)} \mapsto v_{m+m'}^{(k+j)}. \quad (4.12)$$

Hence, the product of two general elements is mapped in the following way

$$\sum_{m=m_1}^{2k} \mathcal{I}'^m v_m^{(k)} \otimes \sum_{m'=m'_1}^{2j} W'^{m'} v_{m'}^{(j)} \mapsto \mathcal{I}'^{m_1} W'^{m'_1} v_{m_1+m'_1}^{(k+j)} + \sum_{M>m_1+m'_1} \alpha^M v_M^{(k+j)} \neq 0, \quad (4.13)$$

where  $\mathcal{I}'^{m_1}$  and  $W'^{m'_1}$  are the first non-vanishing components. The result can not be zero, because the first term on the right-hand side is non-zero, and is linearly independent of the remaining terms.

Secondly, we generalize the statement (4.11) to the following one:

$$C_{A_1^- B_1}^{D_1^+} \dots C_{A_N^- B_N}^{D_N^+} \mathcal{I}^{B_1 \dots B_N} W^{A_1^- \dots A_N^-} = 0 \Leftrightarrow \mathcal{I}^{B_1 \dots B_N} W^{A_1^- \dots A_N^-} = 0, \quad (4.14)$$

for arbitrary  $\mathcal{I} \in \mathcal{H}_{k_1} \otimes \dots \otimes \mathcal{H}_{k_N}$  and  $W \in \mathcal{H}_{j_1^-} \otimes \dots \otimes \mathcal{H}_{j_N^-}$ . In the proof we will use a calculation similar to that of (4.13), with the difference that now the coefficients in (4.13) take values in the  $N - 1$  valent tensor products. Specifically, the left-hand side of the first equality in (4.14) is the result of the map

$$C_{k_1 j_1^-}^{k_1 + j_1^-} \otimes \dots \otimes C_{k_N j_N^-}^{k_N + j_N^-} : \mathcal{H}_{k_1} \otimes \dots \otimes \mathcal{H}_{k_N} \otimes \mathcal{H}_{j_1^-} \otimes \dots \otimes \mathcal{H}_{j_N^-} \rightarrow \mathcal{H}_{k_1 + j_1^-} \otimes \dots \otimes \mathcal{H}_{k_N + j_N^-}, \quad (4.15)$$

#### 4. Properties of the EPRL map

defined by (4.9), and applied to given  $\mathcal{I}'$  and  $W'$ . By analogy to (4.13), we can write

$$\mathcal{I} = \sum_{m=m_1}^{2k_1} v_m^{(k_1)} \otimes \mathcal{I}^m, \quad W = \sum_{m^-=m_1^-}^{2j_1^-} v_{m^-}^{(j_1^-)} \otimes W^{m^-}, \quad (4.16)$$

where  $\mathcal{I}^{m_1}$  is the first non-vanishing  $\mathcal{H}_{k_2} \otimes \dots \otimes \mathcal{H}_{k_N}$  valued component of  $\mathcal{I}$  and  $W^{m_1^-}$  is the first non-vanishing  $\mathcal{H}_{j_2^-} \otimes \dots \otimes \mathcal{H}_{j_N^-}$  valued component of  $W$ . Now we apply the map (4.15),

$$\begin{aligned} C_{k_1 j_1^-}^{k_1 + j_1^-} \otimes \dots \otimes C_{k_N j_N^-}^{k_N + j_N^-} & \left( \sum_{m=m_1}^{2k_1} v_m^{(k_1)} \otimes \mathcal{I}^m \otimes \sum_{m^-=m_1^-}^{2j_1^-} v_{m^-}^{(j_1^-)} \otimes W^{m^-} \right) \\ & = v_{m_1 + m_1^-}^{(k_1 + j_1^-)} \otimes \left( C_{k_2 j_2^-}^{k_2 + j_2^-} \otimes \dots \otimes C_{k_N j_N^-}^{k_N + j_N^-} (\mathcal{I}^{m_1} \otimes W^{m_1^-}) \right) + \\ & + \sum_{M > m_1 + m_1^-} v_M^{(k_1 + j_1^-)} \otimes \alpha^M. \end{aligned} \quad (4.17)$$

The first term on the right-hand side is linearly independent of the others, hence if it were nonzero so would be the right-hand side. But it is non-zero provided (4.14) holds for  $N$  replaced by  $N - 1$ . Since (4.14) is true for  $N = 1$ , the statement (4.14) follows by the mathematical induction.

Finally, we notice that if

$$\mathcal{I} = \mathcal{I}_0 \in \text{Inv}(\mathcal{H}_{k_1} \otimes \dots \otimes \mathcal{H}_{k_N})$$

and

$$W \in \text{Inv}(\mathcal{H}_{j_1^-} \otimes \dots \otimes \mathcal{H}_{j_N^-}),$$

then the tensor

$$C_{A_1^- B_1}^{D_1^+} \dots C_{A_N^- B_N}^{D_N^+} \mathcal{I}_0^{B_1 \dots B_N} W^{A_1^- \dots A_N^-} \quad (4.18)$$

defines an element of  $\text{Inv}(\mathcal{H}_{j_1^+} \otimes \dots \otimes \mathcal{H}_{j_N^+})$ , that is

$$C_{k_1 j_1^-}^{k_1 + j_1^-} \otimes \dots \otimes C_{k_N j_N^-}^{k_N + j_N^-} (\mathcal{I}_0 \otimes W) \in \text{Inv}(\mathcal{H}_{j_1^+} \otimes \dots \otimes \mathcal{H}_{j_N^+}). \quad (4.19)$$

Hence the projection  $P^+$  in (4.7) acts as the identity,

$$P^+ C_{k_1 j_1^-}^{k_1 + j_1^-} \otimes \dots \otimes C_{k_N j_N^-}^{k_N + j_N^-} (\mathcal{I}_0 \otimes W) = C_{k_1 j_1^-}^{k_1 + j_1^-} \otimes \dots \otimes C_{k_N j_N^-}^{k_N + j_N^-} (\mathcal{I}_0 \otimes W), \quad (4.20)$$

hence

$$P^+ C_{D_1^+ \dots D_N^+}^{A_1^+ \dots A_N^+} C_{A_1^- B_1}^{D_1^+} \dots C_{A_N^- B_N}^{D_N^+} \mathcal{I}_0^{B_1 \dots B_N} W^{A_1^- \dots A_N^-} = 0 \Leftrightarrow \mathcal{I}_0^{B_1 \dots B_N} W^{A_1^- \dots A_N^-} = 0, \quad (4.21)$$

but  $W$  is arbitrary in (4.7), hence

$$\mathcal{I}_0 = 0.$$

#### 4.4. Proof of the injectivity theorem in the case $0 \leq \beta < 1$

In this case the proof is more complicated. In order to make the presentation clear, we will divide it into sections. The main result is an inductive hypothesis stated below and proved in section 4.4.2. The injectivity of EPRL map follows from that result. In section 4.4.1 we present a proof of the theorem restricted to certain intertwiners which we call tree-irreducible. In the remaining (degenerate) cases the proof has the same scheme but details depend on a type of degeneracy and have to be taken care of case by case.

Under the conditions that we assume, for every intertwiner  $\mathcal{I} \in \text{Inv}(\mathcal{H}_{k_1} \otimes \cdots \otimes \mathcal{H}_{k_N})$  and its image  $\iota_{\text{EPRL}}(\mathcal{I})$  with respect to the EPRL map we construct an intertwiner  $\phi \in \text{Inv}(\mathcal{H}_{j_1^+} \otimes \cdots \otimes \mathcal{H}_{j_N^+}) \otimes \text{Inv}(\mathcal{H}_{j_1^-} \otimes \cdots \otimes \mathcal{H}_{j_N^-})$  such that the scalar product

$$\langle \phi, \iota_{\text{EPRL}}(\mathcal{I}) \rangle \neq 0.$$

It proves the triviality of the kernel of EPRL map (and thus injectivity of the map). The invariant will be such that the scalar product  $\langle \phi, \iota_{\text{EPRL}}(\mathcal{I}) \rangle$  factorizes (see figure 4.1), i.e. it has the form:

$$\langle \phi, \iota_{\text{EPRL}}(\mathcal{I}) \rangle = \chi_1 \cdots \chi_{N-2},$$

where each factor is given by a 9j-symbol (modulo non-zero factor) known not to vanish  $\chi_l \neq 0$ ,  $l \in \{1, \dots, N-2\}$ .

We construct such intertwiner  $\phi$  step by step and the proof takes the form of inductive procedure. In fact we prove inductively a more general theorem. We prove injectivity of a map  $\iota_{k_1 \dots k_N}$  analogous to EPRL map (compare (3.28)):

$$\iota_{k_1 \dots k_N}(\mathcal{I})^{A_1^+ \dots A_n^+ A_1^- \dots A_n^-} := P_{D_1^+ \dots D_n^+}^{A_1^+ \dots A_n^+} P_{D_1^- \dots D_n^-}^{-A_1^- \dots A_n^-} C_{B_1}^{D_1^+ D_1^-} \dots C_{B_N}^{D_N^+ D_N^-} \mathcal{I}^{B_1 \dots B_N}, \quad (4.22)$$

but defined under a bit more general conditions **Con N**.

**Con N:** Sequences  $(k_1, \dots, k_N)$  and  $(j_1^\pm, \dots, j_N^\pm)$ , where  $k_l, j_l^\pm \in \frac{1}{2}\mathbb{N}$ , are such that

- $(k_1, \dots, k_N)$  is admissible,
- $k_l \neq 0$  for all  $i > 1$ ,
- $j_1^+ + j_1^- = k_1$ ,
- $j_l^\pm = \frac{1 \pm \beta}{2} k_l$  for  $l \neq 1$  and

$$\frac{1+\beta}{2} k_1 - \frac{1}{2} \leq j_1^+ \leq \frac{1+\beta}{2} k_1 + \frac{1}{2}, \quad (4.23)$$

- $j_1^\pm + \dots + j_N^\pm \in \mathbb{N}$ ,
- (ordering)  $\exists l \geq 1$ :  $\begin{cases} j_J^+ \in \mathbb{N}, & J \leq l, \\ j_J^+ \in \mathbb{N} + \frac{1}{2}, & J > l. \end{cases}$

This generalization allows us to perform an inductive step. We base our proof on the following inductive hypothesis for  $N \geq 3$ ,  $N \in \mathbb{N}$ :

#### 4. Properties of the EPRL map

**Hyp N:** If  $(k_1, \dots, k_N), (j_1^\pm, \dots, j_N^\pm)$  satisfy condition **Con N** and

$$\mathcal{I} \in \text{Inv}(\mathcal{H}_{k_1} \otimes \dots \otimes \mathcal{H}_{k_N}),$$

then there exists

$$\phi \in \text{Inv}(\mathcal{H}_{j_1^+} \otimes \dots \otimes \mathcal{H}_{j_N^+}) \otimes \text{Inv}(\mathcal{H}_{j_1^-} \otimes \dots \otimes \mathcal{H}_{j_N^-})$$

such that  $\langle \phi, \iota_{k_1 \dots k_N}(\mathcal{I}) \rangle \neq 0$ .

As mentioned before, this proves injectivity of the EPRL map (theorem 3) for  $N \geq 3$ . Cases  $N = 1$  and  $N = 2$  are needed to be checked separately but this is straightforward.

Few remarks are worth mentioning:

- We would like to emphasize that although an EPRL map usually does not satisfy those conditions, it can be easily replaced by an equivalent map that satisfies **Con N**.

First of all, we can assume that  $k_l \neq 0$  for  $l \geq 1$ . Secondly, we can permute  $k_l$  in such a way that

$$\exists l: j_J^+ \in \mathbb{N}, \text{ for } J \leq l, \quad j_J^+ \in \mathbb{N} + \frac{1}{2}, \text{ for } J > l. \quad (4.24)$$

These are exactly conditions of **Con N**.

- From the definition above follows that  $j_l^+ + j_l^- = k_l$  for all  $l = 1, \dots, N$ .

- It follows also that

$$\frac{1-\beta}{2}k_1 - \frac{1}{2} \leq j_1^- \leq \frac{1-\beta}{2}k_1 + \frac{1}{2}.$$

- From conditions **Con N** follows that  $(j_1^\pm, \dots, j_N^\pm)$  satisfy admissibility conditions:

**Lemma 4.** Let  $(k_1, \dots, k_N)$  and  $(j_1^\pm, \dots, j_N^\pm)$  be elements of  $\frac{1}{2}\mathbb{N}$ , such that:  $(k_1, \dots, k_N)$  is admissible,  $j_l^\pm = \frac{1\pm\beta}{2}k_l$  for  $l \neq 1$ ,  $\frac{1+\beta}{2}k_1 + \frac{1}{2} \geq j_1^+ \geq \frac{1+\beta}{2}k_1 - \frac{1}{2}$ ,  $j_1^+ + j_1^- = k_1$ ,  $j_1^\pm + \dots + j_N^\pm \in \mathbb{N}$ , then  $(j_1^\pm, \dots, j_N^\pm)$  satisfy admissibility conditions.

*Proof.* From the definition of  $j_l^\pm$  and from the fact that  $(k_1, \dots, k_N)$  is admissible, we know that

$$j_1^\pm \leq \frac{1 \pm \beta}{2}k_1 + \frac{1}{2} \leq \frac{1 \pm \beta}{2}(k_2 + \dots + k_N) + \frac{1}{2} = j_2^\pm + \dots + j_N^\pm + \frac{1}{2}.$$

We have  $j_1^\pm + \dots + j_N^\pm \in \mathbb{N}$ , so  $j_1^\pm < j_2^\pm + \dots + j_N^\pm + \frac{1}{2}$ . As a result  $j_1^\pm \leq j_2^\pm + \dots + j_N^\pm$ . This is one of the desired inequalities.

Similarly for  $l \neq 1$  we have:

$$j_l^\pm = \frac{1 \pm \beta}{2}k_l \leq \frac{1 \pm \beta}{2}k_1 + \sum_{J>1, J \neq l} \frac{1 \pm \beta}{2}k_J \leq \sum_{J \neq l} j_J^\pm + \frac{1}{2}$$

As in the previous case  $j_1^\pm + \dots + j_N^\pm \in \mathbb{N}$  implies  $j_l^\pm < \sum_{J \neq l} j_J^\pm + \frac{1}{2}$  and finally  $j_l^\pm \leq \sum_{J \neq l} j_J^\pm$ . This finishes proof of this lemma.  $\square$

#### 4.4. Proof of the injectivity theorem in the case $0 \leq \beta < 1$

- Let us note that  $\langle \phi, \iota_{k_1 \dots k_N}(\mathcal{I}) \rangle = \langle \phi, \iota'_{k_1 \dots k_N}(\mathcal{I}) \rangle$ , where  $\iota'_{k_1 \dots k_N}$  is defined without projections onto invariants of  $\text{Spin}(4)$ , i.e.

$$\begin{aligned} \iota'_{k_1 \dots k_N} : \text{Inv}(\mathcal{H}_{k_1} \otimes \dots \otimes \mathcal{H}_{k_N}) &\rightarrow (\mathcal{H}_{j_1^+} \otimes \dots \otimes \mathcal{H}_{j_N^+}) \otimes (\mathcal{H}_{j_1^-} \otimes \dots \otimes \mathcal{H}_{j_N^-}) \\ \iota'_{k_1 \dots k_N}(\mathcal{I})^{A_1^+ \dots A_N^+ A_1^- \dots A_N^-} &= \mathcal{I}^{A_1 \dots A_N} C_{A_1}^{A_1^+ A_1^-} \dots C_{A_N}^{A_N^+ A_N^-} \end{aligned} \quad (4.25)$$

As a result, it is enough to find  $\phi$ , such that  $\langle \phi, \iota'_{k_1 \dots k_N}(\mathcal{I}) \rangle \neq 0$ .

##### 4.4.1. Proof of the theorem in simplified case

We will start the proof in a simpler case, called tree-irreducible case. To make the presentation more transparent, we will move some parts of it to the section entitled **The choice of  $j_\alpha^+$** .

We consider a restriction of the map  $\iota_{k_1 \dots k_N}$  to **tree irreducible intertwiners**, i.e. elements of the space

$$\left( \text{span} \left( \bigcup_{M=1}^{N-1} \text{Inv}(\mathcal{H}_{k_1} \otimes \dots \otimes \mathcal{H}_{k_M}) \otimes \text{Inv}(\mathcal{H}_{k_{M+1}} \otimes \dots \otimes \mathcal{H}_{k_N}) \right) \right)^\perp,$$

where the span denotes the linear span and  $\perp$  denotes orthogonal compliment in

$$\text{Inv}(\mathcal{H}_{k_1} \otimes \dots \otimes \mathcal{H}_{k_N}).$$

We denote the restricted map by  $\iota_{k_1 \dots k_N}^{\text{tree}}$ . We base the proof of injectivity of  $\iota_{k_1 \dots k_N}^{\text{tree}}$ , on the following inductive hypothesis ( $n \in \mathbb{N}_+, n \geq 3$ ):

**Hyp N:** If  $(k_1, \dots, k_N)$ ,  $(j_1^\pm, \dots, j_N^\pm)$  satisfy condition **Con N** and  $\mathcal{I} \in \text{Inv}(\mathcal{H}_{k_1} \otimes \dots \otimes \mathcal{H}_{k_N})$  is **tree-irreducible**, then there exists

$$\phi \in \text{Inv}(\mathcal{H}_{j_1^+} \otimes \dots \otimes \mathcal{H}_{j_N^+}) \otimes \text{Inv}(\mathcal{H}_{j_1^-} \otimes \dots \otimes \mathcal{H}_{j_N^-})$$

such that  $\langle \phi, \iota_{k_1 \dots k_N}(\mathcal{I}) \rangle \neq 0$ .

This in fact proves injectivity of  $\iota_{k_1 \dots k_N}^{\text{tree}}$ .

##### Proof of the tree-irreducible case of the inductive hypothesis

Let us assume that  $N > 3$  and that we have proved **Hyp N - 1**. Let  $(k_1, \dots, k_N)$  and  $(j_1^\pm, \dots, j_N^\pm)$  satisfy **Con N** and  $\mathcal{I} \in \text{Inv}(\mathcal{H}_{k_1} \otimes \dots \otimes \mathcal{H}_{k_N})$  be tree-irreducible. We may write the invariant in the following way:

$$\mathcal{I}^{A_1 A_2 \dots A_N} = \sum_{k_\alpha \in \mathfrak{J}} C_{A_\alpha}^{A_1 A_2} (\mathcal{I}^{k_\alpha})^{A_\alpha A_3 \dots A_N} \quad (4.26)$$

for the uniquely defined invariants  $\mathcal{I}^{k_\alpha} \in \text{Inv}(\mathcal{H}_{k_\alpha} \otimes \mathcal{H}_{k_3} \otimes \dots \otimes \mathcal{H}_{k_N})$ ,  $k_\alpha \in \frac{1}{2}\mathbb{N}$  and  $\mathfrak{J} := \{k_\alpha \in \frac{1}{2}\mathbb{N} : \mathcal{I}^{k_\alpha} \neq 0\}$ .

- Define  $k'_\alpha$  to be the minimal element in  $\mathfrak{J}$ . Note that if  $n > 2$ , then  $k'_\alpha \neq 0$ , because  $\mathcal{I}$  is tree-irreducible.

4. Properties of the EPRL map

2. Find  $j_\alpha^+$  (determined by  $k'_\alpha$ ) using the procedure defined in section entitled **The choice of  $j_\alpha^+$** . This procedure uses the fact that  $\mathcal{I}$  is tree-irreducible.

The  $j_\alpha^+ \in \frac{1}{2}\mathbb{N}$  is chosen by the following criteria:

$$\frac{1+\beta}{2}k'_\alpha - \frac{1}{2} \leq j_\alpha^+ \leq \frac{1+\beta}{2}k'_\alpha + \frac{1}{2},$$

$(j_\alpha^+, j_1^+, j_2^+)$  and  $(j_\alpha^-, j_1^-, j_2^-)$  are admissible ( $j_\alpha^- := k'_\alpha - j_\alpha^+$ ).

Note that  $j_\alpha^\pm + j_3^\pm + \dots + j_N^\pm \in \mathbb{N}$ . It follows from the fact that  $j_1^\pm, \dots, j_N^\pm \in \frac{1}{2}\mathbb{N}$  (i.e. from **Con N**) and the fact that  $j_\alpha^\pm + j_1^\pm + j_2^\pm \in \mathbb{N}$ .

Let us also note, that  $j_\alpha^+ \in \mathbb{N} + \frac{1}{2}$  only if exactly one of  $j_1^+$  or  $j_2^+$  belongs to  $\mathbb{N} + \frac{1}{2}$ . Then from the ordering condition only  $j_2^+ \in \mathbb{N} + \frac{1}{2}$  and so  $j_\alpha^+, j_3^+, \dots, j_N^+ \in \mathbb{N} + \frac{1}{2}$ . Ordering condition is thus satisfied also for  $(k_\alpha, k_3, \dots, k_N)$ .

Considerations above show that  $(k'_\alpha, k_3, \dots, k_N)$  and  $(j_\alpha^\pm, j_3^\pm, \dots, j_N^\pm)$  satisfy **Con N-1**. This justifies the choice of  $j_\alpha^+$ .

3. Notice that  $\mathcal{I}^{k'_\alpha}$  is tree-irreducible, because  $\mathcal{I}$  is.

From **Hyp N-1** follows that for  $\mathcal{I}^{k'_\alpha}$  there exists

$$\phi^{k'_\alpha} \in \text{Inv} \left( \mathcal{H}_{j_\alpha^+} \otimes \dots \otimes \mathcal{H}_{j_N^+} \right) \otimes \text{Inv} \left( \mathcal{H}_{j_\alpha^-} \otimes \dots \otimes \mathcal{H}_{j_N^-} \right)$$

such that  $\langle \phi^{k'_\alpha}, \iota'_{k'_\alpha k_3 \dots k_N}(\mathcal{I}^{k'_\alpha}) \rangle \neq 0$ .

4. Having defined  $\phi^{k'_\alpha}$ , we construct  $\phi$ :

$$\phi^{A_1^+ \dots A_N^+, A_1^- \dots A_N^-} := C_{A_\alpha^+}^{A_1^+ A_2^+} C_{A_\alpha^-}^{A_1^- A_2^-} (\phi^{k'_\alpha})^{A_\alpha A_3^+ \dots A_N^+, A_\alpha^- A_3^- \dots A_N^-}.$$

5. The  $\phi$  constructed in the previous point is the  $\phi$  we are looking for, i.e.

$$\langle \phi, \iota'_{k_1 \dots k_N}(\mathcal{I}) \rangle \neq 0.$$

In this point we will show it.

First, using equation (4.26) we write  $\langle \phi, \iota'_{k_1 \dots k_N}(\mathcal{I}) \rangle$  as a sum:

$$\langle \phi, \iota'_{k_1 \dots k_N}(\mathcal{I}) \rangle = \sum_{k_\alpha} \langle \phi, \iota'_{k_1 \dots k_N}(C_{k_\alpha}^{k_1 k_2} \circ \mathcal{I}^{k_\alpha}) \rangle, \quad (4.27)$$

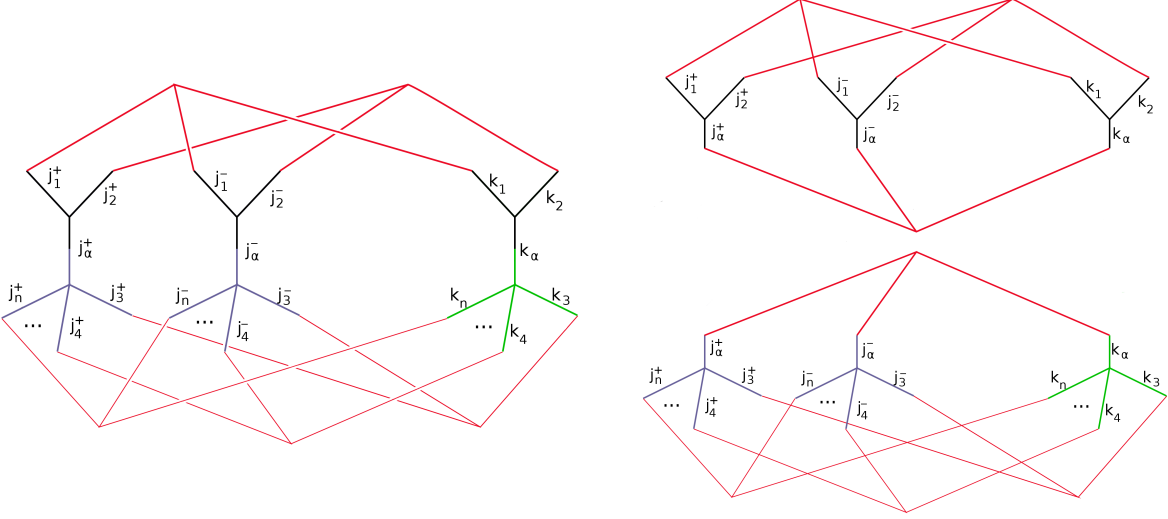
where  $(C_{k_\alpha}^{k_1 k_2} \circ \mathcal{I}^{k_\alpha})^{A_1 A_2 \dots A_N} := C_{A_\alpha}^{A_1 A_2} (\mathcal{I}^{k_\alpha})^{A_\alpha A_3 \dots A_N}$ .

From the definition of  $k'_\alpha$  in point 1 follows that the sum is actually over  $k_\alpha \geq k'_\alpha$ :

$$\langle \phi, \iota'_{k_1 \dots k_N}(\mathcal{I}) \rangle = \sum_{k_\alpha \geq k'_\alpha} \langle \phi, \iota'_{k_1 \dots k_N}(C_{k_\alpha}^{k_1 k_2} \circ \mathcal{I}^{k_\alpha}) \rangle. \quad (4.28)$$

Let us compute each term  $\langle \phi, \iota'_{k_1 \dots k_N}(C_{k_\alpha}^{k_1 k_2} \circ \mathcal{I}^{k_\alpha}) \rangle$  (such term is schematically illustrated on figure 4.1a):

#### 4.4. Proof of the injectivity theorem in the case $0 \leq \beta < 1$



$$(a) \langle \phi, \iota'_{k_1 \dots k_N} (C_{k_\alpha}^{k_1 k_2} \circ \mathcal{I}^{k_\alpha}) \rangle = \\ = \langle C_{j_\alpha^+}^{j_1^+ j_2^+} \otimes C_{j_\alpha^-}^{j_1^- j_2^-} \circ \phi^{k'_\alpha}, \iota'_{k_1 \dots k_N} (C_{k_\alpha}^{k_1 k_2} \circ \mathcal{I}^{k_\alpha}) \rangle$$

(b) The only non-trivial term in the sum (4.27) is  
 $\chi \langle \phi^{k'_\alpha}, \iota'_{k'_\alpha \dots k_N} (\mathcal{I}^{k'_\alpha}) \rangle.$

Figure 4.1.: The figure illustrates the structure of the contractions on the right-hand side of equation (4.29). The result is the evaluation of the spin network depicted on figure 4.1a. The figure 4.1b illustrates an algebraic identity: the evaluation of the spin network on the figure 4.1a equals the product of the evaluations of the spin networks on figure 4.1b. For  $k_\alpha = k'_\alpha$  the evaluation of the upper spin network is denoted by  $\chi$  in (4.30) and it is different than zero. This is proved in lemma 5. This refers to equation (4.31).

$$\begin{aligned} & \langle \phi, \iota'_{k_1 \dots k_N} (C_{k_\alpha}^{k_1 k_2} \circ \mathcal{I}^{k_\alpha}) \rangle = \\ & = (\phi^{k'_\alpha})^\dagger_{A_\alpha^+ A_3^+ \dots A_N^+ A_\alpha^- A_3^- \dots A_N^-} C_{A_1^+ A_2^+}^{A_\alpha^+} C_{A_1^- A_2^-}^{A_\alpha^-} C_{A_1}^{A_1^+ A_1^-} \dots C_{A_N}^{A_N^+ A_N^-} C_{A_\alpha}^{A_1 A_2} (\mathcal{I}^{k_\alpha})^{A_\alpha \dots A_N} = \\ & = C_{A_1^+ A_2^+}^{A_\alpha^+} C_{A_1^- A_2^-}^{A_\alpha^-} C_{A_1}^{A_1^+ A_1^-} C_{A_2}^{A_2^+ A_2^-} C_{A_\alpha}^{A_1 A_2} \\ & \quad \cdot (\phi^{k'_\alpha})^\dagger_{A_\alpha^+ A_3^+ \dots A_N^+ A_\alpha^- A_3^- \dots A_N^-} C_{A_3}^{A_3^+ A_3^-} \dots C_{A_N}^{A_N^+ A_N^-} (\mathcal{I}^{k_\alpha})^{A_\alpha A_3 \dots A_N}. \end{aligned} \quad (4.29)$$

We have

$$C_{A_1^+ A_2^+}^{A_\alpha^+} C_{A_1^- A_2^-}^{A_\alpha^-} C_{A_1}^{A_1^+ A_1^-} C_{A_2}^{A_2^+ A_2^-} C_{A_\alpha}^{A_1 A_2} = \begin{cases} 0, & k_\alpha > j_\alpha^+ + j_\alpha^-, \\ \chi C_{A_\alpha}^{A_\alpha^+ A_\alpha^-}, & k_\beta = j_\alpha^+ + j_\alpha^-. \end{cases} \quad (4.30)$$

The first equality is obvious because there exists no intertwiner if  $k_\alpha > j_\alpha^+ + j_\alpha^-$  (let us remind that  $j_\alpha^+ + j_\alpha^- = k'_\alpha$ ). The second equality is also obvious because for  $k_\alpha = j_\alpha^+ + j_\alpha^-$ , the space  $\text{Inv}(\mathcal{H}_{k_\alpha} \otimes \mathcal{H}_{k_2} \otimes \mathcal{H}_{k_3})$  is one-dimensional. The non-trivial statement is that  $\chi \neq 0$ . The non-triviality of  $\chi$  is assured by the following lemma.

**Lemma 5.** Let  $(j^+, k^+, l^+), (j^-, k^-, l^-)$  be admissible. Define  $j = j^+ + j^-$ ,  $k = k^+ + k^-$ ,  $l = l^+ + l^-$ . Take any non-zero  $\eta \in \text{Inv}(\mathcal{H}_j \otimes \mathcal{H}_k \otimes \mathcal{H}_l^*)$ ,

$\eta^+ \in \text{Inv}(\mathcal{H}_{j^+}^* \otimes \mathcal{H}_{k^+}^* \otimes \mathcal{H}_{l^+})$  and  $\eta^- \in \text{Inv}(\mathcal{H}_{j^-}^* \otimes \mathcal{H}_{k^-}^* \otimes \mathcal{H}_{l^-})$ . We have:

$$\eta^{+C^+}_{A^+ B^+} \eta^{-C^-}_{A^- B^-} C_A^{A^+ A^-} C_B^{B^+ B^-} \eta_C^{AB} = \chi C_C^{C^+ C^-}$$

#### 4. Properties of the EPRL map

for  $\chi \neq 0$ .

*Proof.* The fact that  $\chi \neq 0$  was first proved in [124]. Here we present an alternative proof from [125].

First notice that it is enough to show that under assumptions above,

$$\eta^{+C^+}_{A+B^+} \eta^{-C^-}_{A-B^-} C_A^{A+A^-} C_B^{B+B^-} \eta_C^{AB} C_{C+C^-}^C \neq 0$$

for some non-zero  $C_{l+l-}^l$ .

However the expression  $\eta^{+C^+}_{A+B^+} \eta^{-C^-}_{A-B^-} C_A^{A+A^-} C_B^{B+B^-} \eta_C^{AB} C_{C+C^-}^C$  is proportional with non-zero proportionality factor to 9j-symbol, i.e.:

$$\eta^{+C^+}_{A+B^+} \eta^{-C^-}_{A-B^-} C_A^{A+A^-} C_B^{B+B^-} \eta_C^{AB} C_{C+C^-}^C = \lambda \left\{ \begin{array}{ccc} j^- & l^- & k^- \\ j^+ & l^+ & k^+ \\ j & l & k \end{array} \right\},$$

where  $\lambda \neq 0$ . The appearance of this 9j-symbol here is strictly connected with the expansion of fusion coefficient into product of 9j-symbols done in four-valent case in the article [2]. From the properties of 9j-symbol and admissibility of  $(j^+, k^+, l^+)$ ,  $(j^-, k^-, l^-)$  follows that this 9j-symbol is proportional to a 3j-symbol (see e.g. equation (37) in [2]) with non-zero proportionality constant, i.e.:

$$\left\{ \begin{array}{ccc} j^- & l^- & k^- \\ j^+ & l^+ & k^+ \\ j & l & k \end{array} \right\} = \mu \left( \begin{array}{ccc} l^- & l^+ & l \\ j^- - k^- & j^+ - k^+ & -(j - k) \end{array} \right),$$

where  $\mu \neq 0$ .

Recall that  $l = l^+ + l^-$ , so

$$\left( \begin{array}{ccc} l^- & l^+ & l \\ j^- - k^- & j^+ - k^+ & -(j - k) \end{array} \right) = (-1)^{l^- - l^+ + j - k} \cdot \left[ \frac{(2l^-)!(2l^+)!}{(2l+1)!} \frac{(l+j-k)!(l-j+k)!}{(l^- + j^- - k^-)!(l^- - j^- + k^-)!(l^+ + j^+ - k^+)!(l^+ - j^+ + k^+)} \right]^{\frac{1}{2}}.$$

From admissibility of  $(j^+, k^+, l^+)$ ,  $(j^-, k^-, l^-)$  follows that

$$\left( \begin{array}{ccc} l^- & l^+ & l \\ j^- - k^- & j^+ - k^+ & -(j - k) \end{array} \right) \neq 0.$$

Finally:

$$\eta^{+C^+}_{A+B^+} \eta^{-C^-}_{A-B^-} C_A^{A+A^-} C_B^{B+B^-} \eta_C^{AB} C_{C+C^-}^C = \lambda \mu \left( \begin{array}{ccc} l^- & l^+ & l \\ j^- - k^- & j^+ - k^+ & -(j - k) \end{array} \right) \neq 0.$$

□

Summarizing, for some  $\chi \in \mathbb{C} \setminus \{0\}$ , we have:

$$\langle \phi, \iota'_{k_1 \dots k_N} (C_{k_\alpha}^{k_1 k_2} \circ \mathcal{I}^{k_\alpha}) \rangle = \begin{cases} 0, & k_\alpha > k'_\alpha, \\ \chi \langle \phi^{k'_\alpha}, \iota'_{k'_\alpha k_3 \dots k_N} (\mathcal{I}^{k'_\alpha}) \rangle, & k_\alpha = k'_\alpha, \\ *, & k_\alpha < k'_\alpha. \end{cases}$$

#### 4.4. Proof of the injectivity theorem in the case $0 \leq \beta < 1$

The star \* in the formula above is a number which value is irrelevant for the further considerations. As a result all but one term in the sum (4.28) are equal zero and:

$$\langle \phi, \iota'_{k_1 \dots k_N}(\mathcal{I}) \rangle = \chi \langle \phi^{k'_\alpha}, \iota'_{k'_\alpha k_3 \dots k_N}(\mathcal{I}^{k'_\alpha}) \rangle \neq 0. \quad (4.31)$$

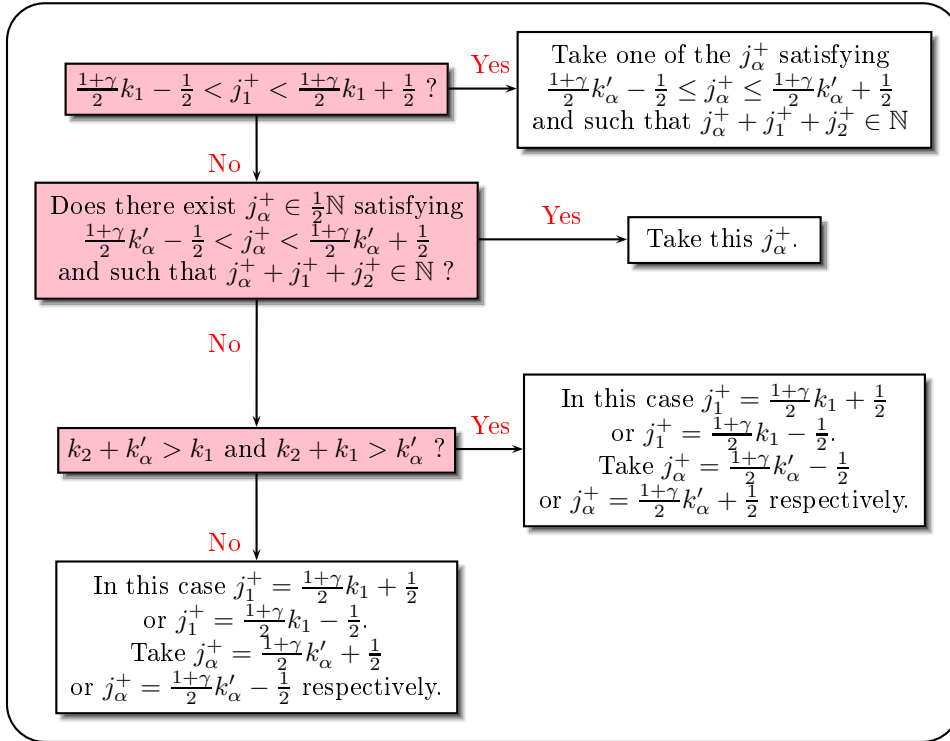
We recall that the non-vanishing of  $\langle \phi^{k'_\alpha}, \iota'_{k'_\alpha k_3 \dots k_N}(\mathcal{I}^{k'_\alpha}) \rangle$  follows from **Hyp**  $N - 1$ .

We obtained that for  $N > 3$ , **Hyp**  $N$  follows from **Hyp**  $N - 1$ . In order to finish the inductive proof, it remains to check that **Hyp** 3 is true. In this case sequences  $(k_1, k_2, k_3)$  and  $(j_1^\pm, j_2^\pm, j_3^\pm)$  are admissible and invariant spaces are one dimensional. **Hyp** 3 follows now from lemma 5.

This proof of first inductive step is valid in general case, because for  $N = 3$  all invariants are tree-irreducible.

#### The choice of $j_\alpha^+$

In this section we will present the procedure of choosing  $j_\alpha^+$ . It is depicted on the diagram below and it is justified by three lemmas 6, 7, 8. Note that  $k_1 \neq 0$  and  $k_\alpha \neq 0$  (on every step of inductive procedure), because  $\mathcal{I}$  is tree-irreducible. It is reflected in these lemmas by the condition, that  $j \neq 0$  and  $l \neq 0$ .



We define  $j_\alpha^- := k'_\alpha - j_\alpha^+$ . In each case in the diagram above lemmas 6, 7, 8 show that  $(j_\alpha^+, j_1^+, j_2^+)$  and  $(j_\alpha^-, j_1^-, j_2^-)$  are admissible. The first lemma is used in the first and second case depicted in the diagram (in those cases we use lemma 6 with  $j = k_1, k = k_2, l = k_\alpha, k^\pm = j_1^\pm, j^\pm = j_2^\pm, l^\pm = j_\alpha^\pm$  and  $j = k_\alpha, k = k_2, l = k_1, k^\pm = j_\alpha^\pm, j^\pm = j_2^\pm, l^\pm = j_1^\pm$  respectively). The second and third lemma are used in the last step. We prove now those lemmas.

#### 4. Properties of the EPRL map

**Lemma 6.** Let  $(j, k, l)$  be admissible and  $j \neq 0, l \neq 0$ . If  $j^+, k^+, l^+$  are elements of  $\frac{1}{2}\mathbb{N}$  satisfying:  $\frac{1+\beta}{2}j - \frac{1}{2} < j^+ < \frac{1+\beta}{2}j + \frac{1}{2}$ ,  $k^+ = \frac{1+\beta}{2}k$ ,  $\frac{1+\beta}{2}l - \frac{1}{2} \leq l^+ \leq \frac{1+\beta}{2}l + \frac{1}{2}$  and  $j^+ + k^+ + l^+ \in \mathbb{N}$ , then  $(j^+, k^+, l^+)$  and  $(j - j^+, k - k^+, l - l^+)$  are admissible.

*Proof.* We denote  $j^- := j - j^+, k^- := k - k^+, l^- := l - l^+$ .

1. Notice that  $j^-, k^-, l^-$  satisfy  $\frac{1-\beta}{2}j - \frac{1}{2} < j^- < \frac{1-\beta}{2}j + \frac{1}{2}$ ,  $k^- = \frac{1-\beta}{2}k$ ,  $\frac{1-\beta}{2}l - \frac{1}{2} \leq l^- \leq \frac{1-\beta}{2}l + \frac{1}{2}$  and  $j^- + k^- + l^- \in \mathbb{N}$ . It is a direct check. Inequalities  $\frac{1+\beta}{2}j - \frac{1}{2} < j^+ < \frac{1+\beta}{2}j + \frac{1}{2}$  imply, that

$$\frac{1+\beta}{2}j - \frac{1}{2} < j - j^- < \frac{1+\beta}{2}j + \frac{1}{2}.$$

As a result

$$\frac{-1+\beta}{2}j - \frac{1}{2} < -j^- < \frac{-1+\beta}{2}j + \frac{1}{2}$$

and

$$\frac{1-\beta}{2}j - \frac{1}{2} < j^- < \frac{1-\beta}{2}j + \frac{1}{2}.$$

The same with  $\frac{1-\beta}{2}l - \frac{1}{2} \leq l^- \leq \frac{1-\beta}{2}l + \frac{1}{2}$  and  $k^- = \frac{1-\beta}{2}k$  is obvious. Finally  $j^- + k^- + l^- \in \mathbb{N}$  follows from the fact that  $j^+ + k^+ + l^+ \in \mathbb{N}$  and  $j + k + l \in \mathbb{N}$ .

2. Note also that  $j^- \geq 0, k^- \geq 0, l^- \geq 0$ :  $\frac{1-\beta}{2}j - \frac{1}{2} < j^-$ , so  $-\frac{1}{2} < j^-$ ; similarly  $\frac{1-\beta}{2}l - \frac{1}{2} \leq l^-$  implies  $-\frac{1}{2} < l^-$ , because  $l \neq 0$  and  $|\beta| < 1$ ;  $k^\pm \geq 0$  is straightforward.
3. We check now triangle inequalities.

$$j^+ + k^+ > \frac{1+\beta}{2}j - \frac{1}{2} + \frac{1+\beta}{2}k = \frac{1+\beta}{2}(j+k) - \frac{1}{2} \geq \frac{1+\beta}{2}l - \frac{1}{2} \geq l^+ - 1.$$

It follows that

$$j^+ + k^+ - l^+ > -1.$$

However  $j^+ + k^+ + l^+ \in \mathbb{N}$ , so  $j^+ + k^+ - l^+ \in \mathbb{Z}$ . As a result

$$j^+ + k^+ - l^+ \geq 0.$$

Similarly,

$$k^+ + l^+ \geq \frac{1+\beta}{2}k + \frac{1+\beta}{2}l - \frac{1}{2} = \frac{1+\beta}{2}(k+l) - \frac{1}{2} \geq \frac{1+\beta}{2}j - \frac{1}{2} > j^+ - 1.$$

We obtain  $k^+ + l^+ - j^+ \geq 0$ .

We also have

$$l^+ + j^+ > \frac{1+\beta}{2}l + \frac{1+\beta}{2}j - 1 = \frac{1+\beta}{2}(j+l) - 1 \geq \frac{1+\beta}{2}k - 1 = k^+ - 1.$$

Finally  $l^+ + j^+ - k^+ \geq 0$ . This proves that  $(j^+, k^+, l^+)$  is admissible. The proof for  $(j^-, k^-, l^-)$  is the same.

#### 4.4. Proof of the injectivity theorem in the case $0 \leq \beta < 1$

□

**Lemma 7.** Let  $(j, k, l)$  be admissible and  $j \neq 0, l \neq 0$ . If  $j^+, k^+, l^+$  are elements of  $\frac{1}{2}\mathbb{N}$  satisfying:  $j^+ = \frac{1+\beta}{2}j \pm \frac{1}{2}$ ,  $k^+ = \frac{1+\beta}{2}k$ ,  $l^+ = \frac{1+\beta}{2}l \mp \frac{1}{2}$ ,  $j^+ + k^+ + l^+ \in \mathbb{N}$ ,  $k + l > j$  and  $j + k > l$ , then  $(j^+, k^+, l^+)$  and  $(j - j^+, k - k^+, l - l^+)$  are admissible.

*Proof.* As previously, we denote  $j^- := j - j^+$ ,  $k^- := k - k^+$ ,  $l^- := l - l^+$  (it is easy to check that they are non-negative).

Let us check triangle inequalities:

$$j^+ + k^+ = \frac{1+\beta}{2}j \pm \frac{1}{2} + \frac{1+\beta}{2}k = \frac{1+\beta}{2}(j+k) \pm \frac{1}{2} > \frac{1+\beta}{2}l \pm \frac{1}{2} = l^+ \mp 1.$$

By arguments used in the previous lemma, we obtain  $j^+ + k^+ - l^+ \geq 0$ .

Let us check another inequality:

$$k^+ + l^+ = \frac{1+\beta}{2}k + \frac{1+\beta}{2}l \mp \frac{1}{2} = \frac{1+\beta}{2}(k+l) \mp \frac{1}{2} > \frac{1+\beta}{2}j \mp \frac{1}{2} = j^+ \pm 1.$$

As a result  $k^+ + l^+ - j^+ \geq 0$ .

Finally

$$j^+ + l^+ = \frac{1+\beta}{2}j \pm \frac{1}{2} + \frac{1+\beta}{2}l \mp \frac{1}{2} = \frac{1+\beta}{2}(j+l) \geq \frac{1+\beta}{2}k = k^+.$$

This finishes the prove of triangle inequalities. Proof for  $j^-, k^-, l^-$  is the same. □

**Lemma 8.** Let  $(j, k, l)$  be admissible and  $j \neq 0, l \neq 0$ . If  $j^+, k^+, l^+$  are elements of  $\frac{1}{2}\mathbb{N}$  satisfying:  $j^+ = \frac{1+\beta}{2}j \pm \frac{1}{2}$ ,  $k^+ = \frac{1+\beta}{2}k$ ,  $l^+ = \frac{1+\beta}{2}l \pm \frac{1}{2}$ ,  $j^+ + k^+ + l^+ \in \mathbb{N}$ ,  $k + l = j$  or  $j + k = l$ , then  $(j^+, k^+, l^+)$  and  $(j - j^+, k - k^+, l - l^+)$  are admissible.

*Proof.* Let  $k + l = j$ . Then  $k^+ + l^+ = j^+$  which proves triangle inequalities. The proof is the same for  $j + k = l$ . One can check in the same way that  $(j - j^+, k - k^+, l - l^+)$  is admissible. □

#### 4.4.2. Proof of the theorem

Previously, we restricted ourselves to tree-irreducible intertwiners, because then the lowest spin  $k_\alpha$  in the decomposition (4.26) (we denote it by  $k'_\alpha$ ) as well as  $k_1$  are different than 0, if  $n > 3$ . In general  $k'_\alpha$  or  $k_1$  may be equal 0 for  $n > 3$  and then our procedure determining  $j_\alpha^+$  and  $j_\alpha^-$  may not be applied (lemmas 6, 7, 8 require  $k_\alpha \neq 0$ ,  $k_1 \neq 0$ ). Actually the case  $k'_\alpha = 0$  (so  $k_1 = k_2$ ) and  $j_1^+ = j_2^+$  is not problematic – we simply take  $j_\alpha^+ = 0$  and follow steps 3-5 in section 4.4.1. The case  $k_1 = 0$  is also simple, because  $j_1^+ + j_1^- = k_1 = 0$  implies  $j_1^\pm = 0$  and the inductive step is trivial. Problems appear when  $k'_\alpha = 0$  and  $j_1^+ = j_2^+ \pm \frac{1}{2}$ ,  $j_1^- = j_2^- \mp \frac{1}{2}$ . We treat this case separately.

We start the inductive step (as in simplified case in section 4.4.1) by expanding  $\mathcal{I}$  as in equation (4.26) and finding minimal  $k_\alpha$  which we call  $k'_\alpha$ . We may perform the procedure from section 4.4.1 unless we are in the problematic case. Note that in this case

$$j_l^+ \in \mathbb{N} + \frac{1}{2}, \quad l > 1, \tag{4.32}$$

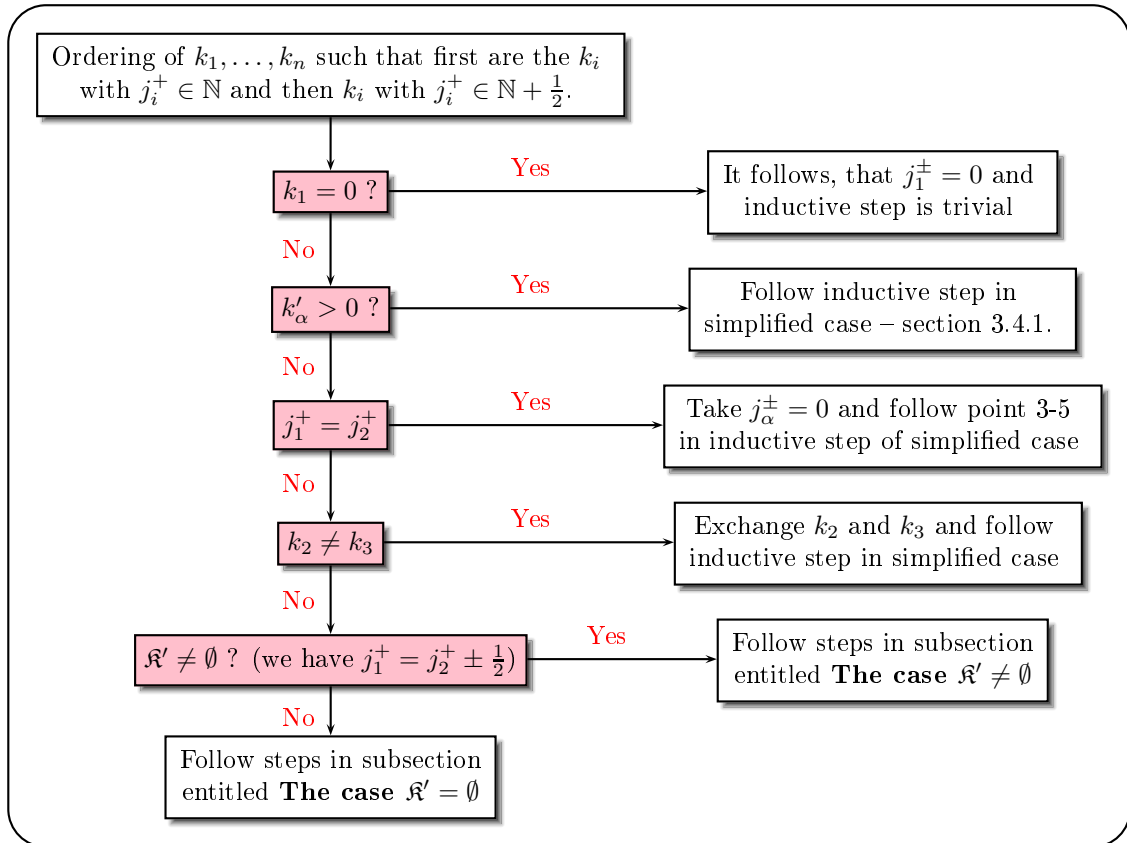
#### 4. Properties of the EPRL map

as  $j_1^+ = j_2^+ \pm \frac{1}{2}$  and sequences are ordered. If this is the case, we expand the intertwiner  $\mathcal{I}$  one level further, i.e. instead of formula (4.26) we use the following one:

$$\mathcal{I}^{A_1 A_2 \dots A_N} = \sum_{(k_\alpha, k_\beta) \in \mathfrak{K}} C_{A_\alpha}^{A_1 A_2} C_{A_\beta}^{A_\alpha A_3} (\mathcal{I}^{k_\alpha k_\beta})^{A_\beta A_4 \dots A_N}, \quad (4.33)$$

where  $\mathfrak{K} := \{(k_\alpha, k_\beta) \in \frac{1}{2}\mathbb{N} \times \frac{1}{2}\mathbb{N} : \mathcal{I}^{k_\alpha k_\beta} \neq 0\}$ . We define  $\mathfrak{K}' = \mathfrak{K} \cap \{(k_\alpha, k_\beta) : k_\beta < k_3\}$ . There are two cases  $\mathfrak{K}' = \emptyset$  and  $\mathfrak{K}' \neq \emptyset$  which we will describe in the next two sections. The procedure is summarized by the diagram below.

It is important to notice that in the case  $n = 4$ , we either obtain  $k'_\alpha > 0$  or  $k'_\alpha = 0$ ,  $j_1^+ = j_2^+$ . In this case notice that either  $j_1^+ \in \mathbb{N}$ ,  $j_2^+ \in \mathbb{N}$  or  $j_1^+ \in \mathbb{N} + \frac{1}{2}$ ,  $j_2^+ \in \mathbb{N} + \frac{1}{2}$  (this follows from the fact that  $j_1^+ + j_2^+ + j_3^+ + j_4^+ \in \mathbb{N}$  and from ordering of  $k_1$ ) – as a result if  $k'_\alpha = 0$  then  $j_1^+ = j_2^+$ . This means that when  $n = 4$ , the inductive step from simplified case may be used. As a result the check of initial conditions done in the proof of tree-irreducible case is sufficient in the general case presented here.



#### The case $\mathfrak{K}' \neq \emptyset$

- Find  $k''_\alpha$  and  $k'_\beta$ , such that:

$$k''_\alpha = \min\{k_\alpha : \exists k_\beta, (k_\alpha, k_\beta) \in \mathfrak{K}'\} \quad (4.34)$$

#### 4.4. Proof of the injectivity theorem in the case $0 \leq \beta < 1$

and

$$k'_\beta = \min\{k_\beta : (k'_\alpha, k_\beta) \in \mathfrak{K}'\}. \quad (4.35)$$

They exist, because  $\mathfrak{K}'$  is non-empty.

2. Notice that  $k''_\alpha > 0$  because  $(k_3, k''_\alpha, k'_\beta)$  is admissible and  $k'_\beta < k_3$ . We define  $j_\alpha^\pm$  using the procedure from section 4.4.1.

If  $k'_\beta > 0$ , we use the same procedure (but for triple  $(k''_\alpha, k_3, k'_\beta)$ ) to define  $j_\beta^\pm$  and if  $k_\beta = 0$ , we take  $j_\beta^\pm = 0$ . Let us check now if  $j_\alpha^\pm$  and  $j_\beta^\pm$  is a good choice.

- $(j_1^\pm, j_2^\pm, j_\alpha^\pm)$  are admissible – this is guaranteed by procedure from section 4.4.1.
- $(j_\alpha^\pm, j_3^\pm, j_\beta^\pm)$  are admissible:

If  $k'_\beta > 0$  then this is guaranteed by procedure from section 4.4.1.

If  $k'_\beta = 0$ , then  $k''_\alpha = k_3$ . As a result we have  $j_3^+ - \frac{1}{2} \leq j_\alpha^+ \leq j_3^+ + \frac{1}{2}$ . However  $j_\alpha^+ \in \mathbb{N} + \frac{1}{2}$  ( $j_1^+ = j_2^+ + \frac{1}{2}$  or  $j_1^+ = j_2^+ - \frac{1}{2}$ , so  $j_1^+ + j_2^+$  is not an integer). From the ordering  $j_3^+ \in \mathbb{N} + \frac{1}{2}$ . Finally we have  $j_\alpha^+ = j_3^+$  and  $j_\alpha^- = k''_\alpha - j_\alpha^+ = k_3 - j_3^+ = j_3^-$ . Obviously  $(j_\alpha^\pm, j_3^\pm, 0)$  are admissible.

- $j_\beta^\pm + j_4^\pm + \dots + j_N^\pm \in \mathbb{N}$ :

We know that  $j_1^+ \in \mathbb{N}$ ,  $j_2^+ \in \mathbb{N} + \frac{1}{2}$ ,  $j_3^+ \in \mathbb{N} + \frac{1}{2}$ , so  $j_\beta^+ \in \mathbb{N}$  and  $j_1^+ + j_2^+ + j_3^+ \in \mathbb{N}$ . Finally from  $j_1^+ + j_2^+ + j_3^+ + j_4^+ \dots + j_N^+ \in \mathbb{N}$ , follows that  $j_\beta^+ + j_4^+ \dots + j_N^+ \in \mathbb{N}$ .

Using the facts that  $j_\beta^- + j_4^- \dots + j_N^- = k'_\beta + k_4 \dots + k_N - (j_\beta^+ + j_4^+ \dots + j_N^+)$  and  $k'_\beta + k_4 \dots + k_N \in \mathbb{N}$ , we obtain  $j_\beta^- + j_4^- \dots + j_N^- \in \mathbb{N}$ .

- We see that  $\frac{1+\beta}{2}k'_\beta - \frac{1}{2} \leq j_\beta^+ \leq \frac{1+\beta}{2}k'_\beta + \frac{1}{2}$ . We also have  $j_4^+ \in \mathbb{N} + \frac{1}{2}$  and so the ordering property is satisfied.

Eventually, **Con N – 2** is fulfilled for  $(k'_\beta, k_4, \dots, k_N)$  and  $(j_\beta^\pm, j_4^\pm, \dots, j_N^\pm)$ .

3. From **Hyp N – 2** follows that for  $\mathcal{I}^{k''_\alpha k'_\beta}$  from (4.33) there exists

$$\phi^{k''_\alpha k'_\beta} \in \text{Inv} \left( \mathcal{H}_{j_\alpha^+} \otimes \mathcal{H}_{j_\beta^+} \otimes \dots \otimes \mathcal{H}_{j_N^+} \right) \otimes \text{Inv} \left( \mathcal{H}_{j_\alpha^-} \otimes \mathcal{H}_{j_\beta^-} \otimes \dots \otimes \mathcal{H}_{j_N^-} \right),$$

such that

$$\langle \phi^{k''_\alpha k'_\beta}, l'_{k'_\beta \dots k_N}(\mathcal{I}^{k''_\alpha k'_\beta}) \rangle \neq 0.$$

4. Having defined  $\phi^{k''_\alpha k'_\beta}$ , we construct  $\phi$ :

$$\phi^{A_1^+ \dots A_N^+, A_1^- \dots A_N^-} := C_{A_\alpha^+}^{A_1^+ A_2^+} C_{A_\beta^+}^{A_\alpha^+ A_3^+} C_{A_\alpha^-}^{A_1^- A_2^-} C_{A_\beta^-}^{A_\alpha^- A_3^-} (\phi^{k''_\alpha k'_\beta})^{A_\beta^+ A_4^+ \dots A_N^+, A_\beta^- A_4^- \dots A_N^-}$$

5. The  $\phi$  constructed in the previous point is the  $\phi$  we are looking for, i.e.

$$\langle \phi, l'_{k_1 \dots k_N}(\mathcal{I}) \rangle \neq 0.$$

We will now prove this statement.

#### 4. Properties of the EPRL map

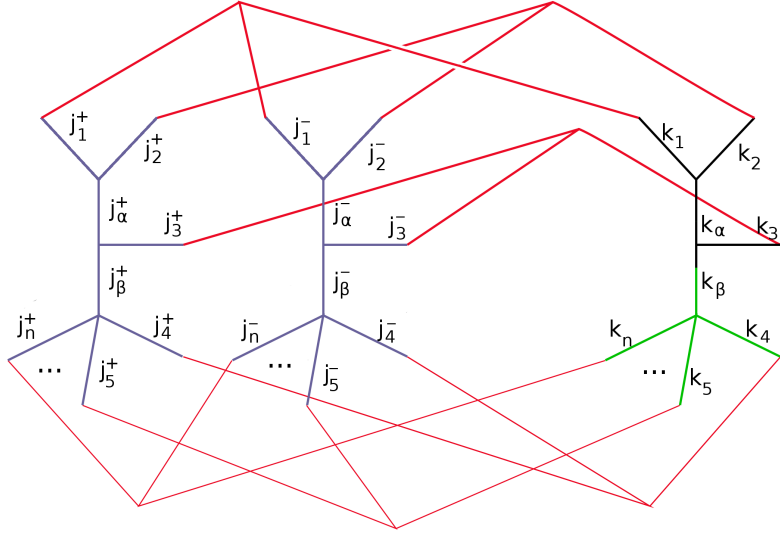


Figure 4.2.: Schematic picture of a term in the sum (4.36). The evaluation of the spin network depicted on this figure is equal to the term  $\langle \phi, \iota'_{k_1 \dots k_N} (C_{k_\alpha}^{k_1 k_2} \circ C_{k_\beta}^{k_\alpha k_3} \circ \mathcal{I}^{k_\alpha k_\beta}) \rangle$ .

a) First, using equation (4.33) write  $\langle \phi, \iota'_{k_1 \dots k_N} (\mathcal{I}) \rangle$  as a sum:

$$\langle \phi, \iota'_{k_1 \dots k_N} (\mathcal{I}) \rangle = \sum_{(k_\alpha, k_\beta) \in \mathbb{K}} \langle \phi, \iota'_{k_1 \dots k_N} (C_{k_\alpha}^{k_1 k_2} \circ C_{k_\beta}^{k_\alpha k_3} \circ \mathcal{I}^{k_\alpha k_\beta}) \rangle, \quad (4.36)$$

where  $(C_{k_\alpha}^{k_1 k_2} \circ C_{k_\beta}^{k_\alpha k_3} \circ \mathcal{I}^{k_\alpha k_\beta})^{A_1 A_2 \dots A_N} := C_{A_\alpha}^{A_1 A_2} C_{A_\beta}^{A_\alpha A_3} (\mathcal{I}^{k_\alpha k_\beta})^{A_\beta A_4 \dots A_N}$ .

b) Let us compute  $\langle \phi, \iota'_{k_1 \dots k_N} (C_{k_\alpha}^{k_1 k_2} \circ C_{k_\beta}^{k_\alpha k_3} \circ \mathcal{I}^{k_\alpha k_\beta}) \rangle$  (see fig. 4.2):

$$\begin{aligned} \langle \phi, \iota'_{k_1 \dots k_N} (C_{k_\alpha}^{k_1 k_2} \circ C_{k_\beta}^{k_\alpha k_3} \circ \mathcal{I}^{k_\alpha k_\beta}) \rangle &= (\phi^{k''_\alpha k'_\beta})^\dagger_{A_\beta^+ A_4^+ \dots A_N^+, A_\beta^- A_4^- \dots A_N^-} C_{A_1^+ A_2^+}^{A_\alpha^+} C_{A_\alpha^+ A_3^+}^{A_\beta^+} \\ &\quad C_{A_1^- A_2^-}^{A_\alpha^-} C_{A_\alpha^- A_3^-}^{A_\beta^-} C_{A_1}^{A_1^+ A_1^-} \dots C_{A_N}^{A_N^+ A_N^-} C_{A_\alpha}^{A_1 A_2} C_{A_\beta}^{A_\alpha A_3} (\mathcal{I}^{k_\alpha k_\beta})^{A_\beta A_4 \dots A_N} = \\ &= C_{A_1^+ A_2^+}^{A_\alpha^+} C_{A_1^- A_2^-}^{A_\alpha^-} C_{A_1}^{A_1^+ A_1^-} C_{A_2}^{A_2^+ A_2^-} C_{A_\alpha}^{A_1 A_2} C_{A_\alpha^+ A_3^+}^{A_\beta^+} C_{A_\alpha^- A_3^-}^{A_\beta^-} C_{A_3}^{A_3^+ A_3^-} C_{A_\beta}^{A_\alpha A_3} \\ &(\phi^{k''_\alpha k'_\beta})^\dagger_{A_\beta^+ A_4^+ \dots A_N^+, A_\beta^- A_4^- \dots A_N^-} C_{A_4}^{A_4^+ A_4^-} \dots C_{A_N}^{A_N^+ A_N^-} (\mathcal{I}^{k_\alpha k_\beta})^{A_\beta A_4 \dots A_N}. \end{aligned}$$

Using lemma 5 we can show that for some  $\chi_1 \neq 0$

$$C_{A_1^+ A_2^+}^{A_\alpha^+} C_{A_1^- A_2^-}^{A_\alpha^-} C_{A_1}^{A_1^+ A_1^-} C_{A_2}^{A_2^+ A_2^-} C_{A_\alpha}^{A_1 A_2} = \begin{cases} 0, & k_\alpha > j_\alpha^+ + j_\alpha^-, \\ \chi_1 C_{A_\alpha}^{A_\alpha^+ A_\alpha^-}, & k_\alpha = j_\alpha^+ + j_\alpha^-. \end{cases}$$

Applying this lemma again we can show that for some  $\chi_2 \neq 0$

$$C_{A_\alpha^+ A_3^+}^{A_\beta^+} C_{A_\alpha^- A_3^-}^{A_\beta^-} C_{A_\alpha}^{A_\alpha^+ A_\alpha^-} C_{A_3}^{A_3^+ A_3^-} C_{A_\beta}^{A_\alpha A_3} = \begin{cases} 0, & k_\beta > j_\beta^+ + j_\beta^-, \\ \chi_2 C_{A_\beta}^{A_\beta^+ A_\beta^-}, & k_\beta = j_\beta^+ + j_\beta^-. \end{cases}$$

#### 4.4. Proof of the injectivity theorem in the case $0 \leq \beta < 1$

Finally, for  $\chi := \chi_1 \chi_2 \neq 0$ :

$$\langle \phi, \iota'_{k_1 \dots k_N} (C_{k_\alpha}^{k_1 k_2} \circ C_{k_\beta}^{k_\alpha k_3} \circ \mathcal{I}^{k_\alpha k_\beta}) \rangle = \begin{cases} 0, & k_\alpha > k''_\alpha \text{ or } k_\beta > k'_\beta, \\ \chi \langle \phi^{k''_\alpha k'_\beta}, \iota'_{k'_\beta \dots k_N} (\mathcal{I}^{k''_\alpha k'_\beta}) \rangle, & k_\alpha = k'_\alpha \text{ and } k_\beta = k'_\beta, \\ *, & \text{otherwise.} \end{cases} \quad (4.37)$$

c) Now we use formula just obtained (4.37) to calculate the sum (4.36).

First notice that  $k'_\beta \leq k_3$ . As a result the elements in the sum (4.36) with  $k_\beta > k_3$  vanish and the sum is actually over the  $\mathfrak{K}'$ :

$$\langle \phi, \iota'_{k_1 \dots k_N} (\mathcal{I}) \rangle = \sum_{(k_\alpha, k_\beta) \in \mathfrak{K}'} \langle \phi, \iota'_{k_1 \dots k_N} (C_{k_\alpha}^{k_1 k_2} \circ C_{k_\beta}^{k_\alpha k_3} \circ \mathcal{I}^{k_\alpha k_\beta}) \rangle.$$

However from the definition of  $k''_\alpha$  and  $k'_\beta$  follows that

$$\langle \phi, \iota'_{k_1 \dots k_N} (\mathcal{I}) \rangle = \sum_{k_\alpha \geq k''_\alpha, k_\beta \geq k'_\beta} \langle \phi, \iota'_{k_1 \dots k_N} (C_{k_\alpha}^{k_1 k_2} \circ C_{k_\beta}^{k_\alpha k_3} \circ \mathcal{I}^{k_\alpha k_\beta}) \rangle.$$

Finally, using (4.37) we obtain:

$$\langle \phi, \iota'_{k_1 \dots k_N} (\mathcal{I}) \rangle = \chi \langle \phi^{k''_\alpha k'_\beta}, \iota'_{k'_\beta \dots k_N} (\mathcal{I}^{k''_\alpha k'_\beta}) \rangle$$

and

$$\langle \phi, \iota'_{k_1 \dots k_N} (\mathcal{I}) \rangle \neq 0.$$

#### The case $\mathfrak{K}' = \emptyset$

Let us change the basis used previously in the decomposition of  $\mathcal{I}$  (4.33):

$$\mathcal{I}^{A_1 A_2 \dots A_N} = \sum_{(k_{\tilde{\alpha}}, k_\beta) \in \mathfrak{L}} C_{A_{\tilde{\alpha}}}^{A_2 A_3} C_{A_\beta}^{A_1 A_{\tilde{\alpha}}} (\mathcal{I}^{k_{\tilde{\alpha}} k_\beta})^{A_\beta A_4 \dots A_N}, \quad (4.38)$$

where  $\mathfrak{L} := \{(k_{\tilde{\alpha}}, k_\beta) \in \frac{1}{2}\mathbb{N} \times \frac{1}{2}\mathbb{N} : \mathcal{I}^{k_{\tilde{\alpha}} k_\beta} \neq 0\}$ .

We define:

$$\mathfrak{L}' = \mathfrak{L} \cap \{(k_{\tilde{\alpha}}, k_\beta) : k_\beta = k_3\}.$$

This set is non-empty, because  $k_\beta = k_3$  was present in the decomposition (4.33). In fact  $(k_\alpha = 0, k_\beta = k_3) \in \mathfrak{K}$  and so  $k_\beta = k_3$  occurs also in the decomposition (4.38).

1. Find  $k'_{\tilde{\alpha}}$  such that:

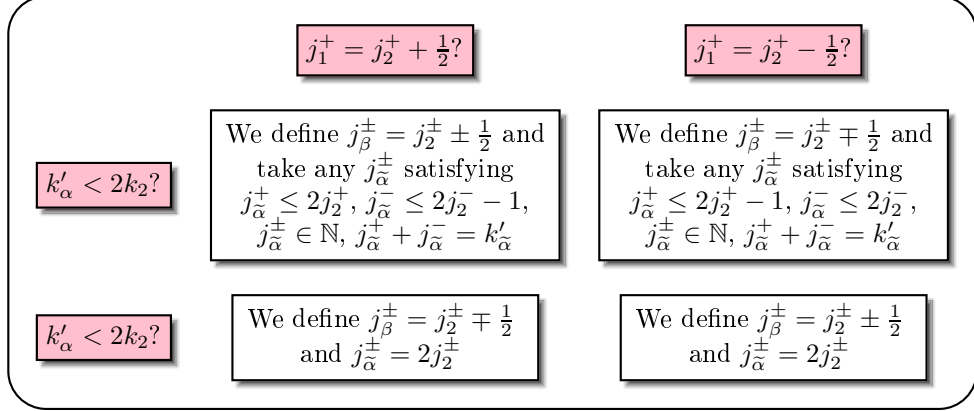
$$k'_{\tilde{\alpha}} = \min\{k_{\tilde{\alpha}} : \exists k_\beta, (k_{\tilde{\alpha}}, k_\beta) \in \mathfrak{L}'\}.$$

Note that  $k_\beta < k_3$  does not appear in this decomposition because they are absent in the decomposition (4.33). Note also that if we defined  $k'_\beta$  in analogous way to (4.35), i.e.  $k'_\beta = \min\{k_\beta : (k'_{\tilde{\alpha}}, k_\beta) \in \mathfrak{L}'\}$ , we would obtain trivially  $k'_\beta = k_3$ . In this section one may think that  $k'_\beta = k_3$ . However, we will not write this  $k'_\beta$  explicitly.

#### 4. Properties of the EPRL map

2. We now define  $j_{\alpha}^{\pm}$ ,  $j_{\beta}^{\pm}$ . Note that only  $j_{\beta}^{\pm}$  (but not  $j_{\alpha}^{\pm}$ ) has to be of special form to match **Con N - 2**. The requirements for  $j_{\alpha}^{\pm}$  may be limited to assure admissibility conditions and the condition that  $j_{\alpha}^{+} + j_{\alpha}^{-} = k_{\alpha}$ . We will use this freedom to define  $j_{\alpha}^{\pm}$ ,  $j_{\beta}^{\pm}$ .

Note that, in our case  $(j_2^{\pm}, j_3^{\pm}, j_{\alpha}^{\pm})$  are admissible iff  $j_{\alpha}^{\pm} \leq 2j_2^{\pm}$  and  $j_{\alpha}^{\pm} \in \mathbb{N}$  (because  $j_2^+ = j_3^+$ ). We also have  $j_1^+ = j_2^+ \pm \frac{1}{2}$ . The choices of  $j_{\alpha}^{\pm}$  and  $j_{\beta}^{\pm}$  in this case are given in the following diagram.



Let us justify this choice. Suppose that  $j_1^+ = j_2^+ + \frac{1}{2}$  (the case  $j_1^+ = j_2^+ - \frac{1}{2}$  is analogous).

- **Case of  $k_{\alpha}' < 2k_2$ .** Note that  $k_2 \neq 0$ . As a result  $j_2^- \geq \frac{1}{2}$  ( $|\beta| < 1$ ) and there exist  $j_{\alpha}^{\pm}$ , such that  $j_{\alpha}^+ \leq 2j_2^+$ ,  $j_{\alpha}^- \leq 2j_2^- - 1$ ,  $j_{\alpha}^{\pm} \in \mathbb{N}$ . It is possible to choose  $j_{\alpha}^{\pm}$  satisfying  $j_{\alpha}^+ + j_{\alpha}^- = k_{\alpha}'$ , because  $j_{\alpha}^+ + j_{\alpha}^- \leq 2(j_2^+ + j_2^-) - 1 \Rightarrow j_{\alpha}^+ + j_{\alpha}^- < 2k_2$  (and  $k_{\alpha}' < 2k_2$ ).

It is straightforward to check that  $(j_2^{\pm}, j_3^{\pm}, j_{\alpha}^{\pm})$ ,  $(j_1^{\pm}, j_{\alpha}^{\pm}, j_{\beta}^{\pm})$  are admissible:

$$0 = |j_2^{\pm} - j_3^{\pm}| \leq j_{\alpha}^{\pm} \leq j_2^{\pm} + j_3^{\pm} = 2j_2^{\pm}, \quad 0 = |j_1^{\pm} - j_{\beta}^{\pm}| \leq j_{\alpha}^{\pm} \leq j_1^{\pm} + j_{\beta}^{\pm} \quad (4.39)$$

but  $j_1^+ + j_{\beta}^+ = 2j_2^+$  and  $j_1^- + j_{\beta}^- = 2j_2^- - 1$ .

- **Case of  $k_{\alpha}' = 2k_2$ .**

As it was previously pointed out if  $k_2 \neq 0$ , then  $j_2^{\pm} \geq \frac{1}{2}$ . It follows that  $2j_2^{\pm} \geq 1$ . So  $j_{\alpha}^{\pm} \geq 1$  and  $j_{\alpha}^{\pm} \in \mathbb{N}$ ,  $j_{\alpha}^+ + j_{\alpha}^- = k_{\alpha}'$ .

It is straightforward to check that  $(j_2^{\pm}, j_3^{\pm}, j_{\alpha}^{\pm})$ ,  $(j_1^{\pm}, j_{\alpha}^{\pm}, j_{\beta}^{\pm})$  are admissible:

$$0 = |j_2^{\pm} - j_3^{\pm}| \leq j_{\alpha}^{\pm} \leq j_2^{\pm} + j_3^{\pm} = 2j_2^{\pm}, \quad 1 = |j_1^{\pm} - j_{\beta}^{\pm}| \leq j_{\alpha}^{\pm} \leq j_1^{\pm} + j_{\beta}^{\pm} = 2j_2^{\pm}. \quad (4.40)$$

3. Note that since  $j_1^+$  and  $j_{\alpha}^+$  are natural then also  $j_{\beta}^+ \in \mathbb{N}$ . Recall also that  $j_1^+ \in \mathbb{N}$ ,  $j_2^+, j_3^+ \in \mathbb{N} + \frac{1}{2}$  and  $j_1^+ + \dots + j_N^+ \in \mathbb{N}$ . As a result  $j_{\beta}^+ + j_4^+ + \dots + j_N^+ \in \mathbb{N}$  and

$$j_{\beta}^- + j_4^- + \dots + j_N^- = k_3 + k_4 + \dots + k_N - (j_{\beta}^+ + j_4^+ + \dots + j_N^+) \in \mathbb{N}.$$

We also have that  $\frac{1+\beta}{2}k_3 - \frac{1}{2} \leq j_{\beta}^+ \leq \frac{1+\beta}{2}k_3 + \frac{1}{2}$  and  $j_4^+ \in \mathbb{N} + \frac{1}{2}$ , so **Con N - 2** is fulfilled for  $(k_3, k_4, \dots, k_N)$  and  $(j_{\beta}^{\pm}, j_4^{\pm}, \dots, j_N^{\pm})$ .

#### 4.4. Proof of the injectivity theorem in the case $0 \leq \beta < 1$

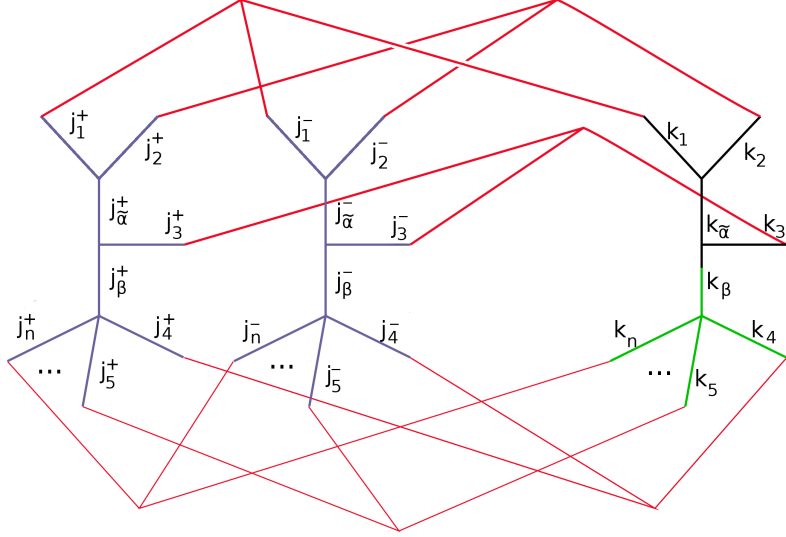


Figure 4.3.: Schematic picture of a term in the sum (4.41). The evaluation of the spin network depicted on this figure is equal to the term  $\langle \phi, \iota'_{k_1 \dots k_N} (C_{k_\alpha}^{k_2 k_3} \circ C_{k_\beta}^{k_\alpha k_1} \circ \mathcal{I}^{k_\alpha k_\beta}) \rangle$ .

4. From **Hyp N – 2** follows that for  $\mathcal{I}^{k_\alpha' k_3}$  from (4.38) there exists

$$\phi^{k_\alpha' k_3} \in \text{Inv} \left( \mathcal{H}_{j_\alpha^+} \otimes \mathcal{H}_{j_\beta^+} \otimes \dots \otimes \mathcal{H}_{j_N^+} \right) \otimes \text{Inv} \left( \mathcal{H}_{j_\alpha^-} \otimes \mathcal{H}_{j_\beta^-} \otimes \dots \otimes \mathcal{H}_{j_N^-} \right),$$

such that

$$\langle \phi^{k_\alpha' k_3}, \iota'_{k_3 \dots k_N} (\mathcal{I}^{k_\alpha' k_3}) \rangle \neq 0.$$

5. Having defined  $\phi^{k_\alpha' k_3}$ , we construct  $\phi$ :

$$\phi^{A_1^+ \dots A_N^+, A_1^- \dots A_N^-} := C_{A_\alpha^+}^{A_2^+ A_3^+} C_{A_\beta^+}^{A_\alpha^+ A_1^+} C_{A_\alpha^-}^{A_2^- A_3^-} C_{A_\beta^-}^{A_\alpha^- A_1^-} (\phi^{k_\alpha' k_3})^{A_\beta^+ A_4^+ \dots A_N^+, A_\beta^- A_4^- \dots A_N^-}.$$

6. The  $\phi$  constructed in the previous point is the  $\phi$  we are looking for, i.e.

$$\langle \phi, \iota'_{k_1 \dots k_N} (\mathcal{I}) \rangle \neq 0.$$

We will now prove this statement.

a) First, using equation (4.38) write  $\langle \phi, \iota'_{k_1 \dots k_N} (\mathcal{I}) \rangle$  as a sum:

$$\langle \phi, \iota'_{k_1 \dots k_N} (\mathcal{I}) \rangle = \sum_{(k_\alpha, k_\beta) \in \mathcal{L}} \langle \phi, \iota'_{k_1 \dots k_N} (C_{k_\alpha}^{k_2 k_3} \circ C_{k_\beta}^{k_1 k_\alpha} \circ \mathcal{I}^{k_\alpha k_\beta}) \rangle, \quad (4.41)$$

where  $(C_{k_\alpha}^{k_2 k_3} \circ C_{k_\beta}^{k_1 k_\alpha} \circ \mathcal{I}^{k_\alpha k_\beta})^{A_1 A_2 \dots A_N} := C_{A_\alpha}^{A_2 A_3} C_{A_\beta}^{A_1 A_\alpha} (\mathcal{I}^{k_\alpha k_\beta})^{A_\beta A_4 \dots A_N}$ .

b) Let us compute  $\langle \phi, \iota'_{k_1 \dots k_N} (C_{k_\alpha}^{k_2 k_3} \circ C_{k_\beta}^{k_1 k_\alpha} \circ \mathcal{I}^{k_\alpha k_\beta}) \rangle$  (see fig. 4.4.2):

#### 4. Properties of the EPRL map

$$\begin{aligned} \langle \phi, \iota'_{k_1 \dots k_N} (C_{k_\alpha}^{k_1 k_2} \circ C_{k_\beta}^{k_\alpha k_3} \circ \mathcal{I}^{k_\alpha k_\beta}) \rangle &= (\phi^{k'_\alpha k'_\beta})^\dagger_{A_\beta^+ A_4^+ \dots A_N^+, A_\beta^- A_4^- \dots A_N^-} C_{A_\alpha^+ A_1^+}^{A_\beta^+} C_{A_2^+ A_3^+}^{A_\alpha^+} \\ &C_{A_\alpha^- A_1^-}^{A_\beta^-} C_{A_2^- A_3^-}^{A_\alpha^-} C_{A_1}^{A_1^+ A_1^-} \dots C_{A_N}^{A_N^+ A_N^-} C_{A_\alpha}^{A_2 A_3} C_{A_\beta}^{A_\alpha A_1} (\mathcal{I}^{k_\alpha k_\beta})^{A_\beta A_4 \dots A_N} = \\ &= C_{A_2^+ A_3^+}^{A_\alpha^+} C_{A_2^- A_3^-}^{A_\alpha^-} C_{A_2}^{A_2^+ A_2^-} C_{A_3}^{A_3^+ A_3^-} C_{A_\alpha}^{A_2 A_3} C_{A_\alpha^+ A_1^+}^{A_\beta^+} C_{A_\alpha^- A_1^-}^{A_\beta^-} C_{A_1}^{A_1^+ A_1^-} C_{A_\beta}^{A_\alpha A_1} \\ &(\phi^{k'_\alpha k'_\beta})^\dagger_{A_\beta^+ A_4^+ \dots A_N^+, A_\beta^- A_4^- \dots A_N^-} C_{A_4}^{A_4^+ A_4^-} \dots C_{A_N}^{A_N^+ A_N^-} (\mathcal{I}^{k_\alpha k_\beta})^{A_\beta A_4 \dots A_N}. \end{aligned}$$

Using lemma 5 we can show that for some  $\chi_1 \neq 0$

$$C_{A_2^+ A_3^+}^{A_\alpha^+} C_{A_2^- A_3^-}^{A_\alpha^-} C_{A_2}^{A_2^+ A_2^-} C_{A_3}^{A_3^+ A_3^-} C_{A_\alpha}^{A_2 A_3} = \begin{cases} 0, & k_\alpha > j_\alpha^+ + j_\alpha^-, \\ \chi_1 C_{A_\alpha}^{A_\alpha^+ A_\alpha^-}, & k_\alpha = j_\alpha^+ + j_\alpha^-. \end{cases}$$

Applying this lemma again we can show that for some  $\chi_2 \neq 0$

$$C_{A_\alpha^+ A_1^+}^{A_\beta^+} C_{A_\alpha^- A_1^-}^{A_\beta^-} C_{A_\alpha}^{A_\alpha^+ A_\alpha^-} C_{A_1}^{A_1^+ A_1^-} C_{A_\beta}^{A_\alpha A_1} = \begin{cases} 0, & k_\beta > j_\beta^+ + j_\beta^-, \\ \chi_2 C_{A_\beta}^{A_\beta^+ A_\beta^-}, & k_\beta = j_\beta^+ + j_\beta^-. \end{cases}$$

Finally, for  $\chi = \chi_1 \chi_2 \neq 0$  :

$$\langle \phi, \iota'_{k_1 \dots k_N} (C_{k_\alpha}^{k_2 k_3} \circ C_{k_\beta}^{k_\alpha k_1} \mathcal{I}^{k_\alpha k_\beta}) \rangle = \begin{cases} 0, & k_\alpha > k'_\alpha \text{ or } k_\beta > k'_\beta, \\ \chi \langle \phi^{k'_\alpha k'_\beta}, \iota'_{k'_\beta \dots k_N} (\mathcal{I}^{k'_\alpha k'_\beta}) \rangle, & k_\alpha = k'_\alpha \text{ and } k_\beta = k'_\beta, \\ *, & \text{otherwise.} \end{cases} \quad (4.42)$$

c) Now we use the formula just obtained (4.42) to calculate the sum (4.41).

First notice that in this case  $k_\beta \geq k_3$ . Moreover, the elements in the sum (4.41) with  $k_\beta > k_3$  vanish (4.42) and the sum is actually over  $\mathfrak{L}'$ :

$$\langle \phi, \iota'_{k_1 \dots k_N} (\mathcal{I}) \rangle = \sum_{(k_\alpha, k_\beta) \in \mathfrak{L}'} \langle \phi, \iota'_{k_1 \dots k_N} (C_{k_\alpha}^{k_2 k_3} \circ C_{k_\beta}^{k_1 k_\alpha} \circ \mathcal{I}^{k_\alpha k_\beta}) \rangle.$$

However, from the definition of  $k'_\alpha$  follows that

$$\langle \phi, \iota'_{k_1 \dots k_N} (\mathcal{I}) \rangle = \sum_{k_\alpha \geq k'_\alpha} \langle \phi, \iota'_{k_1 \dots k_N} (C_{k_\alpha}^{k_2 k_3} \circ C_{k_3}^{k_1 k_\alpha} \circ \mathcal{I}^{k_\alpha k_3}) \rangle.$$

Finally, using (4.42) we obtain:

$$\langle \phi, \iota'_{k_1 \dots k_N} (\mathcal{I}) \rangle = \chi \langle \phi^{k'_\alpha k_3}, \iota'_{k_3 \dots k_N} (\mathcal{I}^{k'_\alpha k_3}) \rangle$$

and

$$\langle \phi, \iota'_{k_1 \dots k_N} (\mathcal{I}) \rangle \neq 0.$$

## 5. Operator spin foams

In the previous chapter we showed that the EPRL map is not isometric. As a result there are two inequivalent spin-foam models with the EPRL vertex amplitude: the  $SU(2)$  spin-foam model with the EPRL vertex [48] and the  $Spin(4)$  spin-foam model with the EPRL vertex [124]. In the second model one sums the spin-foam amplitudes over an orthonormal basis of the space of EPRL intertwiners. This can be done by mapping a basis  $\mathcal{I}_a$  of the space of  $SU(2)$  intertwiners to a basis  $\iota_{EPRL}(\mathcal{I}_a)$  of the space of the EPRL intertwiners<sup>1</sup> and orthonormalizing it. Another possibility is to go back to equation (1.42) and modify the definition of a spin foam. Instead of assigning an invariant tensor to each edge of a foam, one can assign to each edge an operator  $P_e : \mathcal{H}_e \rightarrow \mathcal{H}_e$ . Let us assume for simplicity that  $\partial\kappa = \emptyset$ ; a general case will be studied shortly. In the BF theory  $P_e$  is the orthogonal projection onto the subspace of invariant tensors  $\text{Inv}(\mathcal{H}_e)$ . The operator can be written in the following form:

$$P_e = \sum_{\iota_e} \iota_e \otimes \iota_e^\dagger,$$

where  $\iota_e$  runs through orthonormal basis of the space  $\text{Inv}(\mathcal{H}_e)$ . Since the tensor structure of the operator is the same as  $\iota_e \otimes \iota_e^\dagger$ , where  $\iota_e \in \text{Inv}(\mathcal{H}_e)$ , there is a natural contraction of the indices of the operators and the contractors  $\mathcal{A}_v$ . The partition function is defined by this contraction:

$$Z(\kappa, \rho, \iota, \mathcal{A}) = \prod_f \dim \mathcal{H}_f \bigotimes_v \text{Tr}_v \bigotimes_e P_e.$$

In the  $Spin(4)$  spin-foam model with the EPRL vertex we introduce a coloring of edges with orthogonal projection operators  $P_e^{\text{EPRL}} : \mathcal{H}_e \rightarrow \mathcal{H}_e$  onto a subspace of the solutions to the EPRL constraints  $\text{Inv}_{\text{EPRL}}(\mathcal{H}_e)$  [124]. This operator can be written in terms of an orthonormal basis of the space  $\text{Inv}_{\text{EPRL}}(\mathcal{H}_e)$ :

$$P_e^{\text{EPRL}} = \sum_{\iota_e^{\text{EPRL}}} \iota_e^{\text{EPRL}} \otimes (\iota_e^{\text{EPRL}})^\dagger,$$

where  $\iota_e^{\text{EPRL}}$  runs through an orthonormal basis of  $\text{Inv}_{\text{EPRL}}(\mathcal{H}_e)$ . It can also be written in terms of any basis of  $\text{Inv}_{\text{EPRL}}(\mathcal{H}_e)$ , in particular in terms of  $\iota_{EPRL}(\mathcal{I}_{e,a})$ :

$$P_e = \sum_{a,b} h_e^{ab} \iota_{EPRL}(\mathcal{I}_{e,a}) \otimes \iota_{EPRL}(\mathcal{I}_{e,b})^\dagger,$$

where  $h_e^{ab}$  is the inverse matrix to  $h_{e\bar{b}a} = \langle \iota_{EPRL}(\mathcal{I}_{e,b}) | \iota_{EPRL}(\mathcal{I}_{e,a}) \rangle$ ,  $\langle \cdot | \cdot \rangle$  is the scalar product in  $\mathcal{H}_e$ .

---

<sup>1</sup>According to the injectivity theorem from the previous chapter, either  $\iota_{EPRL}(\mathcal{I}_a)$  is a basis of the space of the EPRL intertwiners or all vectors  $\iota_{EPRL}(\mathcal{I}_a)$  are zero.

## 5. Operator spin foams

In section 5.1.1, we will define *operator spin foams* (see also [29]), which are foams labelled by group representations, operators and linear functionals, as our main tool. In section 5.1.2, we will introduce moves on operator spin foams analogous to the operations of splitting a link, flipping the orientation of a link, adding a link and adding a node to a spin network. A set of moves we introduce in the set of the operator spin foams allows (among other operations) splitting an edge of a foam, splitting a face, adding a face and changing the orientations. The moves are used to introduce an equivalence relation. One may, but does not have to, consider two equivalent operator spin foams as the same operator spin foam. In section 5.2, we will assign to each operator spin foam a *spin-foam operator*, by contracting the indices and multiplying the resulting contracted operator by the face and the boundary link amplitudes. Next in section 5.3, we will define *operator spin foam models* and consider a class of models assumed to be symmetric with respect to the moves from section 5.1.2. Our operator spin-foam framework can be translated into the language of spin foams and spin-foam amplitudes. Among our spin-foam models there are the BF spin-foam model, the BC model, and the models with the EPRL vertex amplitude [123, 48]. We will show that the Spin(4) (operator) spin-foam model with the EPRL vertex [123] is symmetric with respect to the moves we introduce and the SU(2) (operator) spin-foam model with the EPRL vertex [48] is not symmetric. Of course we do not mean to insist that the model of [123] is better than the one of [48]. We will simply find a set of natural properties that lead to the former model, the bottom line is that the latter model is inconsistent with some of the conditions we will spell out. Our operator spin-foam framework can be also used in more general spin-foam models that are not symmetric with respect to one or all of the moves we consider.

### 5.1. Operator spin foam

#### 5.1.1. Definition

An operator spin foam is a quadruple  $(\kappa, \rho, P, \mathcal{A})$ , where  $\rho, P$  and  $\mathcal{A}$  are colorings by representations and, respectively, operators and contractors defined below (see also figure 5.1).

- $\rho$  is a coloring of the faces with unitary irreducible representations of  $G$ :

$$\rho : \kappa^{(2)} \rightarrow \text{Irr}(G), \quad (5.1)$$

$$f \mapsto \rho_f. \quad (5.2)$$

- $P$  is a coloring of the internal edges with operators:

$$\kappa_{\text{int}}^{(1)} \ni e \mapsto P_e, \quad (5.3)$$

$$P_e : \text{Inv}(\mathcal{H}_e) \rightarrow \text{Inv}(\mathcal{H}_e). \quad (5.4)$$

The operator  $P_e$  is defined on  $\text{Inv}(\mathcal{H}_e)$ . However, it can be treated as an operator  $P_e : \mathcal{H}_e \rightarrow \mathcal{H}_e$ . The space  $\mathcal{H}_e$  is a direct sum  $\text{Inv}(\mathcal{H}_e) \oplus \text{Inv}(\mathcal{H}_e)^\perp$ , where  $\text{Inv}(\mathcal{H}_e)^\perp$  is the orthogonal complement of  $\text{Inv}(\mathcal{H}_e)$  in  $\mathcal{H}_e$ . To the operator  $P_e : \text{Inv}(\mathcal{H}_e) \rightarrow \text{Inv}(\mathcal{H}_e)$  there corresponds a unique operator  $\tilde{P}_e : \mathcal{H}_e \rightarrow \mathcal{H}_e$  defined by

$$\tilde{P}_e = \begin{bmatrix} P_e & 0 \\ 0 & 0 \end{bmatrix} : \begin{array}{c} \text{Inv}(\mathcal{H}_e) \\ \oplus \\ \text{Inv}(\mathcal{H}_e)^\perp \end{array} \rightarrow \begin{array}{c} \text{Inv}(\mathcal{H}_e) \\ \oplus \\ \text{Inv}(\mathcal{H}_e)^\perp \end{array}.$$

For example, let  $\text{id} : \text{Inv}(\mathcal{H}_e) \rightarrow \text{Inv}(\mathcal{H}_e)$  be the identity operator. Then

$$\tilde{\text{id}} : \mathcal{H}_e \rightarrow \mathcal{H}_e$$

is the orthogonal projection onto  $\text{Inv}(\mathcal{H}_e)$ . In this thesis we will omit the tilde in the notation and we will simply denote by  $P_e$  the operator on  $\mathcal{H}_e$  corresponding to  $P_e : \text{Inv}(\mathcal{H}_e) \rightarrow \text{Inv}(\mathcal{H}_e)$ .

- $\mathcal{A}$  is a coloring of the internal vertices with linear functionals (figure 5.1)

$$\kappa_{\text{int}}^{(0)} \ni v \mapsto \mathcal{A}_v \in \mathcal{H}_v^*.$$

It will be sometimes convenient to consider the function  $\mathcal{A}_v$  as a functional on a bigger space (see remarks in section 1.3.3)

$$\bigotimes_{e \text{ incoming to } v} \mathcal{H}_e \otimes \bigotimes_{e' \text{ outgoing from } v} \mathcal{H}_{e'}^*.$$

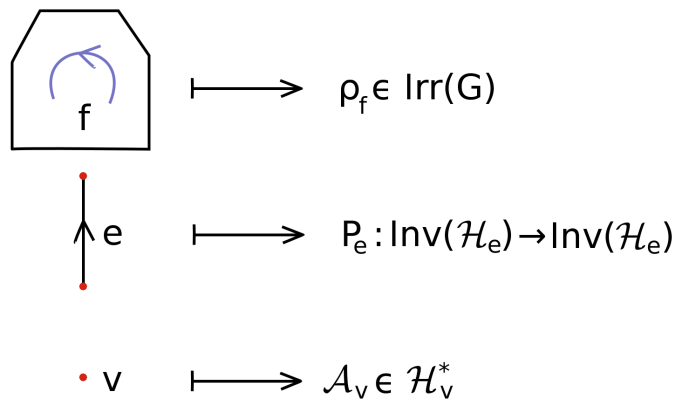


Figure 5.1.: a) Faces are colored by irreducible representations of  $G$ . b) Internal edges are colored with operators  $P_e : \text{Inv}(\mathcal{H}_e) \rightarrow \text{Inv}(\mathcal{H}_e)$ . c) Internal vertices are colored with contractors.

### 5.1.2. The moves and the equivalence relation they define

In the space of operator spin foams we consider a set of moves and an equivalence relation they define. The moves allow to subdivide edges and faces, change their orientation, use colorings with equivalent representations, add faces and edges. In the following paragraphs we describe that equivalence relation in detail. The moves are analogous to the moves in the space of the spin networks. Two equivalent operator spin foams are not literally identified in this paper. The equivalence relation is used as a symmetry of the structures we define in this chapter.

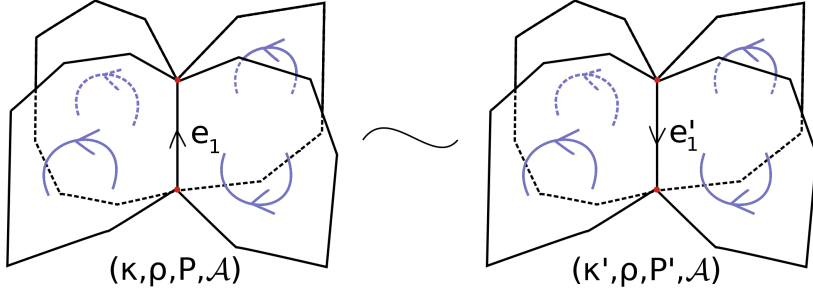


Figure 5.2.: Edge reorientation

### Edge reorientation

Being given an operator spin foam  $(\kappa, \rho, P, \mathcal{A})$ , let us flip the orientation of its edge  $e_1$ ,

$$e'_1 = e_1^{-1}, \quad (5.5)$$

and leave all the other orientations unchanged. Let us denote the resulting 2-complex by  $\kappa'$ . To define an operator spin foam  $(\kappa', \rho', P', \mathcal{A}')$  that is equivalent to  $(\kappa, \rho, P, \mathcal{A})$ , first let us suppose that the edge  $e_1$  is internal and

- leave the labelling  $\rho$ , namely

$$\rho' = \rho. \quad (5.6)$$

Now,  $\rho'$  determines the Hilbert space  $\mathcal{H}_{e'_1}$  to be

$$\mathcal{H}_{e'_1} = \mathcal{H}_{e_1}^*, \quad (5.7)$$

where  $*$  denotes the algebraic dualization. The natural choice for  $P'_{e'_1}$  is

- for the reoriented edge  $e'_1 = e_1^{-1}$ ,

$$P'_{e'_1} = P_{e_1}^*, \quad (5.8)$$

- whereas for the remaining edges of  $\kappa'$  we leave

$$P'_e = P_e. \quad (5.9)$$

Flipping the orientation of an edge does not change the Hilbert spaces  $\mathcal{H}_v$ . The natural choice for the contractors is:

$$\mathcal{A}'_v = \mathcal{A}_v.$$

The operator spin foams  $(\kappa, \rho, P, \mathcal{A})$  and  $(\kappa', \rho, P', \mathcal{A})$  are equivalent,

$$(\kappa, \rho, P, \mathcal{A}) \equiv (\kappa', \rho, P', \mathcal{A}). \quad (5.10)$$

The remaining case when the reoriented edge  $e_1$  is not internal is yet simpler: both labellings  $\rho$  and  $P$  are defined on the faces/edges unaffected by the reorientation of  $e_1$ ; we just leave them unchanged that is we set  $\rho' = \rho$ ,  $P' = P$  and  $\mathcal{A}' = \mathcal{A}$ .

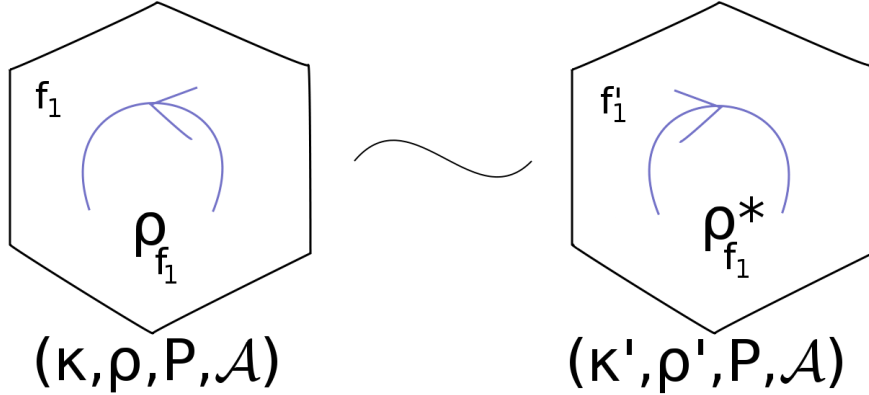


Figure 5.3.: Face reorientation

### Face reorientation

Being given an operator spin foam  $(\kappa, \rho, P, \mathcal{A})$ , let us switch the orientation of its face  $f_1$  and denote the reoriented face  $f'_1$ . Let us denote the resulting 2-complex by  $\kappa'$ . To define an operator spin foam  $(\kappa', \rho', P', \mathcal{A}')$  equivalent to  $(\kappa, \rho, P, \mathcal{A})$ , we modify the labelling  $\rho$  in the following way:

- for the reoriented face  $f'_1$  we take the dual representation,

$$\rho'_{f'_1} = \rho^*_{f_1}, \quad (5.11)$$

- for the remaining faces, the labelling  $\rho'$  coincides with  $\rho$ ,

$$\rho'_f = \rho_f, \text{ for } f \neq f'_1. \quad (5.12)$$

At each edge  $e$ , the labelling  $\rho'$  defines the same Hilbert space  $\mathcal{H}_e$  as  $\rho$  in  $(\kappa, \rho, P, \mathcal{A})$ . Therefore, the following definitions of  $P'$  and  $\mathcal{A}'$  are possible,

- For a labelling  $P'$  the choice is

$$P' = P. \quad (5.13)$$

- For a labelling  $\mathcal{A}'$  the choice is

$$\mathcal{A}' = \mathcal{A}.$$

Again, we will consider  $(\kappa', \rho', P, \mathcal{A})$  and  $(\kappa, \rho, P, \mathcal{A})$  equivalent,

$$(\kappa, \rho, P, \mathcal{A}) \equiv (\kappa', \rho', P, \mathcal{A}). \quad (5.14)$$

### Face splitting

Let us consider an operator spin foam  $(\kappa, \rho, P, \mathcal{A})$ . Split one of its faces, say  $f_0$ , into  $f'_1$  and  $f'_2$  such that a resulting new edge  $e'_0$  (oriented arbitrarily) contained in  $f'_1$  and in  $f'_2$  connects two vertices  $v_1, v_2$  belonging to  $\kappa^{(0)}$ . Choose an orientation of the new faces to be the one induced by  $f_0$ . The resulting new 2-complex  $\kappa'$  is obtained by replacing the face  $f_0$  by the pair of faces  $f'_1$  and  $f'_2$  and by adding the edge  $e'_0$ . Define a labelling  $\rho'$  on  $\kappa'$  in the following way

## 5. Operator spin foams

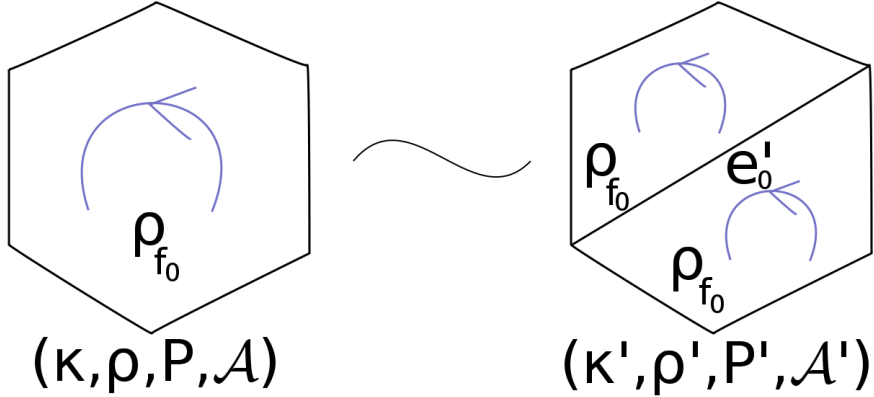


Figure 5.4.: Face subdivision

- $\rho'$  coincides with  $\rho$  on the unsplitted faces,

$$\rho'_{f'} = \rho_{f'}, \text{ if } f' \neq f'_1, f'_2 \quad (5.15)$$

- and  $\rho'$  agrees with  $\rho$  on the faces  $f'_1, f'_2$  resulting from the splitting

$$\rho'_{f'} = \rho_{f_0}, \text{ if } f' = f'_1, f'_2. \quad (5.16)$$

The Hilbert space  $\text{Inv}(\mathcal{H}_{e'_0}) = \text{Inv}(\mathcal{H}_{f_0} \otimes \mathcal{H}_{f_0}^*)$  is isomorphic to  $\mathbb{C}$ . Indeed, by Schur's Lemma every element of  $\text{Inv}(\mathcal{H}_{f_0} \otimes \mathcal{H}_{f_0}^*) \subset \mathcal{H}_{f_0} \otimes \mathcal{H}_{f_0}^*$  is proportional to identity map  $\text{id} : \mathcal{H}_{f_0} \rightarrow \mathcal{H}_{f_0}$ . We denote by  $\Lambda_{e'_0}$  the linear isomorphism

$$\Lambda_{e'_0} : \text{Inv}(\mathcal{H}_{e'_0}) = \text{Inv}(\mathcal{H}_{f_0} \otimes \mathcal{H}_{f_0}^*) \rightarrow \mathbb{C}$$

such that

$$\Lambda_{e'_0}(\text{id}) = 1.$$

Since  $\text{id}$  can be treated as an element of the space  $\text{Inv}(\mathcal{H}_{e'_0})$  or as an element of the space  $\text{Inv}(\mathcal{H}_{e'_0})^*$ ,  $\Lambda_{e'_0}$  can be treated as a functional  $\Lambda_{e'_0} : \text{Inv}(\mathcal{H}_{e'_0}) \rightarrow \mathbb{C}$  or as a functional  $\Lambda_{e'_0} : \text{Inv}(\mathcal{H}_{e'_0})^* \rightarrow \mathbb{C}$ .

Let us define a labelling  $P'$  of the internal edges of  $\kappa'$

- to be the identity on the new edge  $e'_0$  resulting from the splitting,

$$P'_{e'} = \text{id} : \text{Inv}(\mathcal{H}_{e'_0}) \rightarrow \text{Inv}(\mathcal{H}_{e'_0}), \text{ if } e' = e'_0 \quad (5.17)$$

- and to coincide with  $P$  on the old edges

$$P'_{e'} = P_{e'}, \text{ if } e' \neq e'_0. \quad (5.18)$$

Let us define a labelling  $\mathcal{A}'$  of the internal vertices of  $\kappa'$

- to be

$$\mathcal{A}'_{v_1} = \mathcal{A}_{v_1} \otimes \Lambda_{e'_0}, \quad \mathcal{A}'_{v_2} = \mathcal{A}_{v_2} \otimes \Lambda_{e'_0},$$

- and to coincide with  $\mathcal{A}$  on the old vertices

$$\mathcal{A}'_v = \mathcal{A}_v, \text{ if } v \neq v_1, v_2.$$

The resulting operator spin foam is equivalent to  $(\kappa, \rho, P, \mathcal{A})$ ,

$$(\kappa, \rho, P, \mathcal{A}) \equiv (\kappa', \rho', P', \mathcal{A}'). \quad (5.19)$$

### Edge splitting

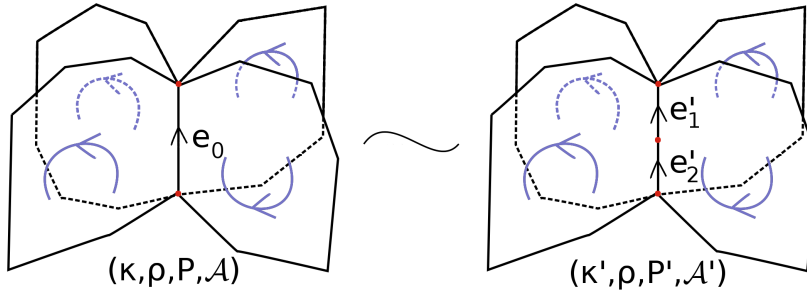


Figure 5.5.: Invariance under the edge subdivision

In an operator spin foam  $(\kappa, \rho, P, \mathcal{A})$  we split an edge  $e_0$  into  $e'_1$  and  $e'_2$

$$e_0 = e'_2 \circ e'_1 \quad (5.20)$$

which orientations are induced by  $e_0$ . The splitting adds new vertex  $v_0$  to the 2-complex  $\kappa$ . Denote the resulting 2-complex by  $\kappa'$ . Strictly speaking, the edge splitting move is not well defined in the class of piecewise linear cell complexes because  $\kappa'$  is not in the class. In order to stay in the class, this move should be always followed by splitting each face intersecting the edge such that the resulting new edge is connecting the new vertex with either another internal vertex intersecting the face or a vertex obtained after splitting another internal edge intersecting the face.

An operator spin foam  $(\kappa', \rho', P', \mathcal{A}')$  defined on  $\kappa'$  is equivalent to  $(\kappa, \rho, P, \mathcal{A})$ ,

$$(\kappa, \rho, P, \mathcal{A}) \equiv (\kappa', \rho', P', \mathcal{A}'), \quad (5.21)$$

whenever the following conditions are satisfied by  $\rho'$ ,  $P'$  and  $\mathcal{A}'$ :

- $\rho$  is unchanged,

$$\rho' = \rho, \quad (5.22)$$

- $\mathcal{A}'$  coincides with  $\mathcal{A}$  on the vertices  $v' \neq v_0$ ,

- $\mathcal{A}'_{v_0}$  is defined by the identity operator in  $\text{Inv}(\mathcal{H}_e)$ :

$$\mathcal{A}'_{v_0} = \text{id} \in \text{Inv}(\mathcal{H}_e) \otimes \text{Inv}(\mathcal{H}_e)^*,$$

## 5. Operator spin foams

- $P'$  coincides with  $P$  on the edges  $e' \neq e'_1, e'_2$ ,
- $P'_{e'_1}$  and  $P'_{e'_2}$  satisfy the following constraint

$$P'_{e'_2} \circ P'_{e'_1} = P_{e_0}, \quad (5.23)$$

provided the edge  $e_0$  is internal.

### Rescaling of the operators

Every operator spin foam  $(\kappa, \rho, P, \mathcal{A})$  is equivalent to any operator spin foam  $(\kappa, \rho, P', \mathcal{A}')$  defined by rescalings:

$$P'_e = a_e P_e, \quad e \in \kappa_{\text{int}}^{(1)}, a_e \in \mathbb{C}, \quad (5.24)$$

such that

$$\prod_{e \in \kappa_{\text{int}}^{(1)}} a_e = 1. \quad (5.25)$$

### Face relabelling with equivalent representations

Let us consider an operator spin foam  $(\kappa, \rho, P, \mathcal{A})$  and  $(\kappa, \rho', P', \mathcal{A}')$ , where

- $\rho_f = \rho'_f$  for all but one face  $f = f_0$ , and for  $f_0$  there exists an isomorphism

$$\zeta : \mathcal{H}_{f_0} \rightarrow \mathcal{H}'_{f_0}$$

which intertwines the representations, namely  $\zeta \circ \rho_{f_0} = \rho'_{f_0} \circ \zeta$ ;

- $P_e = P'_e$  for every internal edge  $e$  not contained in the face  $f_0$ ;

$$P'_e = \text{id} \otimes \dots \otimes \zeta \otimes \text{id} \otimes \dots \otimes \text{id} \circ P_e \circ \text{id} \otimes \dots \otimes \zeta^{-1} \otimes \text{id} \otimes \dots \otimes \text{id}, \quad (5.26)$$

if the face  $f_0$  is outgoing from the edge  $e$ ;

$$P'_e = \text{id} \otimes \dots \otimes \zeta^{*-1} \otimes \text{id} \otimes \dots \otimes \text{id} \circ P_e \circ \text{id} \otimes \dots \otimes \zeta^* \otimes \text{id} \otimes \dots \otimes \text{id}, \quad (5.27)$$

if the face  $f_0$  is incoming to the edge  $e$ .

- $\mathcal{A}'_v = \mathcal{A}_v$  for every internal vertex  $v$  not contained in the face  $f_0$ ;

$$\mathcal{A}'_v = \text{id} \otimes \text{id} \otimes \dots \otimes \mathcal{I} \otimes \zeta^{*-1} \otimes \dots \otimes \text{id} \otimes \text{id} (\mathcal{A}_v),$$

where  $\mathcal{A}_v$  is considered to be an element of the space  $\bigotimes_f \mathcal{H}_f \otimes \mathcal{H}_f^*$  with  $f$  running through the faces containing  $v$ .

The two spin foams are equivalent:

$$(\kappa, \rho, P, \mathcal{A}) \equiv (\kappa, \rho', P', \mathcal{A}'). \quad (5.28)$$

### Adding a face labelled by the trivial representation

Our definition of the operator spin foams does not exclude the trivial representation from the set of labels assigned to the faces. Every operator spin foam  $(\kappa, \rho, P, \mathcal{A})$  will be considered equivalent to an operator spin foam  $(\kappa', \rho', P', \mathcal{A}')$  obtained by adding a face  $f'_1$  and labelling it by the trivial representation **1**. That is,

$$\rho'_{f'} = \begin{cases} \rho_{f'}, & \text{if } f' \in \kappa^{(2)} \\ \mathbf{1}, & \text{if } f' = f'_1. \end{cases}$$

All the internal edges  $e$  and the corresponding Hilbert spaces  $\mathcal{H}_e$  coincide, and  $P'$  is defined to be,

$$P' = P.$$

Also all the internal vertices  $v$  and the corresponding Hilbert spaces  $\mathcal{H}_v$  coincide, and  $\mathcal{A}'$  is defined to be

$$\mathcal{A}' = \mathcal{A}.$$

#### 5.1.3. Glueing the operator spin foams

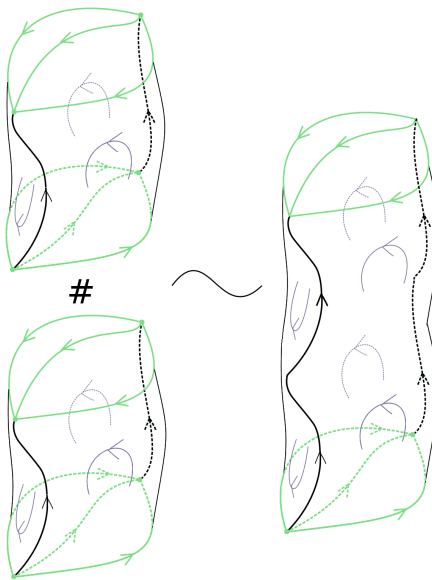


Figure 5.6.: Glueing of the operator spin foams

There is the natural operation of glueing foams (see figure 5.6). It admits a natural extension to an operation of glueing the operator spin foams, which we will describe in this section, for the sake of completeness. Two oriented piecewise linear 2-cell complexes  $\kappa$  and  $\kappa'$  can be glued along a connected component  $\gamma$  of the boundary  $\partial\kappa$  and a connected component  $\gamma'$  of  $\partial\kappa'$ , provided that  $\gamma$  and  $\gamma'$  are isomorphic closed 1-cell complexes (unoriented graphs) and the orientations of the glued faces and, respectively, their sites match. If  $\phi : \gamma \rightarrow \gamma'$  is an isomorphism, then the glueing amounts to glueing along each link  $\ell$  of  $\gamma$  a face  $f_\ell$  of  $\kappa$  containing  $\ell$ , with the face  $f'_{\phi(\ell)}$  of  $\kappa'$  containing the link  $\phi(\ell)$  of

## 5. Operator spin foams

$\gamma'$ . In what follows we will assume that the map

$$\gamma^{(1)} \ni \ell \mapsto f_\ell, \quad \gamma'^{(1)} \ni \ell' \mapsto f'_{\ell'} \quad (5.29)$$

is 1-1 (each  $\ell$  has its own  $f_\ell$ ). This can be always achieved by dividing the faces and edges. The resulting face  $f_\ell \# f'_{\phi(\ell)}$  can be oriented either according to the orientation of  $f_\ell$  or to the orientation of  $f'_{\phi(\ell)}$ ; coinciding of the two orientations is the matching relation we have mentioned above. A similar matching condition applies to the oriented sides of the faces  $f_\ell$  and  $f'_{\phi(\ell)}$ . Repeating this glueing for every link  $\ell$  of  $\gamma$ , we complete the glueing of  $\kappa$  and  $\kappa'$  along  $\gamma$ . The result can be denoted by  $\kappa \# \kappa'$  and it depends on the graphs  $\gamma$ ,  $\gamma'$  and the isomorphism  $\phi$ . If the 2-complexes above were endowed with the structures of the operator spin foams  $(\kappa, \rho, P, \mathcal{A})$ , and respectively,  $(\kappa', \rho', P', \mathcal{A}')$ , the operator spin foams can be glued into an operator spin foam  $(\kappa \# \kappa', \rho \# \rho', P \# P', \mathcal{A} \# \mathcal{A}')$  provided the representations agree on the boundary, and the glueing condition is

$$\rho'_{f'_{\phi(\ell)}} = \rho_{f_\ell} \quad (5.30)$$

for every pair  $\ell$  and  $\phi(\ell)$  of the identified edges.

- For each of the boundary links  $\ell$ , due to the glueing condition we can set

$$(\rho \# \rho')_{f_\ell \# f'_{\phi(\ell)}} = \rho_{f_\ell} = \rho'_{\phi(\ell)}. \quad (5.31)$$

- For the remaining faces we use either  $\rho$  or respectively,  $\rho'$

$$(\rho \# \rho')_{f''} = \begin{cases} \rho_{f''}, & \text{if } f'' \in \kappa^{(2)}, \\ \rho'_{f''}, & \text{if } f'' \in \kappa'^{(2)}. \end{cases} \quad (5.32)$$

For the operator part  $P \# P'$ , the glueing consists in

- taking the composition of the operators for every pair  $(\tilde{e}, \tilde{e}')$  of sides of the faces  $f_\ell$ , and respectively  $f'_{\phi(\ell)}$  that are glued into a side of the face  $f_\ell \# f'_{\phi(\ell)}$ , that is either

$$(P \# P')_{\tilde{e} \circ \tilde{e}'} = P_{\tilde{e}} \circ P_{\tilde{e}'} \quad (5.33)$$

or

$$(P \# P')_{\tilde{e}' \circ \tilde{e}} = P_{\tilde{e}'} \circ P_{\tilde{e}} \quad (5.34)$$

depending on the orientations.

- For each of the remaining internal edges of  $\kappa \# \kappa'$  we leave the corresponding operator of either  $\kappa$  or  $\kappa'$ ,

$$(P \# P')_{e''} = \begin{cases} P_{e''}, & \text{if } e'' \in \kappa_{\text{int}}^{(1)}, \\ P'_{e''}, & \text{if } e'' \in \kappa'_{\text{int}}^{(1)}. \end{cases} \quad (5.35)$$

The coloring  $\mathcal{A} \# \mathcal{A}'$  of the internal vertices is that of either  $\kappa$  or  $\kappa'$ :

$$(\mathcal{A} \# \mathcal{A}')_v = \begin{cases} \mathcal{A}_v, & \text{if } v \in \kappa_{\text{int}}^{(0)}, \\ \mathcal{A}'_v, & \text{if } v \in \kappa'_{\text{int}}^{(0)}. \end{cases}$$

## 5.2. Spin-foam operator

### 5.2.1. Spin-foam operator

There is a canonical contraction

$$\text{Tr}(\kappa, \rho, P, \mathcal{A}) := \bigotimes_{v \in \kappa_{\text{int}}^{(0)}} \mathcal{A}_v \lrcorner \bigotimes_{e \in \kappa_{\text{int}}^{(1)}} P_e \quad (5.36)$$

called *the contracted operator spin foam*. It is defined by contracting each  $\mathcal{A}_v$  with either:

- $\text{Inv}(\mathcal{H}_e)^*$  part of the operator  $P_e \in \text{Inv}(\mathcal{H}_e) \otimes \text{Inv}(\mathcal{H}_e)^*$  if the edge  $e$  is outgoing from  $v$ ,
- or  $\text{Inv}(\mathcal{H}_e)$  part of the operator  $P_e \in \text{Inv}(\mathcal{H}_e) \otimes \text{Inv}(\mathcal{H}_e)^*$  if the edge  $e$  is incoming to  $v$ .

The *spin-foam operator* of an operator spin foam  $(\kappa, \rho, P, \mathcal{A})$  is obtained by multiplying the contracted operator spin foam by the face and boundary link amplitudes:

$$\mathcal{Z}(\kappa, \rho, P, \mathcal{A}) = \prod_{\ell \in (\partial\kappa)^{(1)}} A_{\text{link}}(\partial\rho_\ell) \prod_{f \in \kappa^{(2)}} A_{\text{face}}(\rho_f) \text{Tr}(\kappa, \rho, P, \mathcal{A}). \quad (5.37)$$

The spin-foam operator  $\mathcal{Z}(\kappa, \rho, P, \mathcal{A})$  is indeed an operator. Identifying each operator  $P_e : \text{Inv}(\mathcal{H}_e) \rightarrow \text{Inv}(\mathcal{H}_e)$  with an element of  $\text{Inv}(\mathcal{H}_e) \otimes \text{Inv}(\mathcal{H}_e)^*$ , the spin-foam operator  $\mathcal{Z}(\kappa, \rho, P, \mathcal{A})$  is identified with an element of the Hilbert space

$$\mathcal{H}_{\partial\kappa} = \bigotimes_{e \text{ incoming to } \partial\kappa} \text{Inv}(\mathcal{H}_e) \otimes \bigotimes_{e' \text{ outgoing from } \partial\kappa} \text{Inv}(\mathcal{H}_{e'})^*. \quad (5.38)$$

Any splitting  $\mathcal{H}_{\partial\kappa} = \mathcal{H}_{\text{out}} \otimes \mathcal{H}_{\text{in}}^*$  makes the spin-foam operator  $\mathcal{Z}(\kappa, \rho, P, \mathcal{A})$  an operator  $\mathcal{H}_{\text{in}} \rightarrow \mathcal{H}_{\text{out}}$ .

### 5.2.2. Abstract index notation

In order to understand the contraction better, it is useful to introduce the (abstract) index notation. The given

$$w \in \text{Inv} \left( \bigotimes_{f \text{ opposite orientation to } e} \mathcal{H}_f^* \otimes \bigotimes_{f' \text{ same orientation as } e} \mathcal{H}_{f'} \right) \quad (5.39)$$

is denoted in the index notation as

$$w = w_{A\dots}{}^{A'\dots} \quad (5.40)$$

where the lower/upper indices correspond to the spaces  $\mathcal{H}_f^* / \mathcal{H}_{f'}$ . The action of the operator  $P_e$  reads

$$(P_e w)_{A\dots}{}^{A'\dots} = P_e{}^{A'\dots B\dots} w_{B\dots}{}^{B'\dots}. \quad (5.41)$$

Moreover, the vector  $w_{A\dots}{}^{A'\dots}$  is associated to the beginning of the given edge  $e$ , whereas the vector  $(P_e w)_{A\dots}{}^{A'\dots}$  lives at the end of  $e$ . In this sense, the indices  $B, B'$  of  $P_e{}^{A'\dots B\dots}$

## 5. Operator spin foams

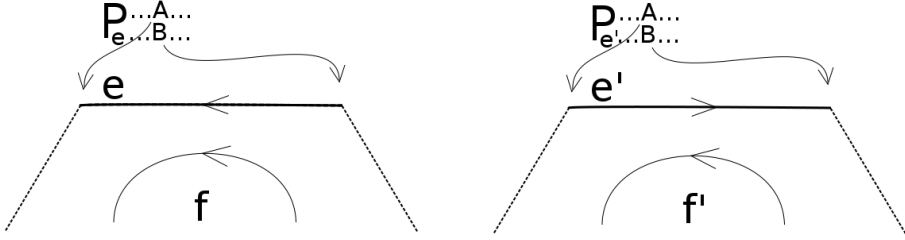


Figure 5.7.: The rule of assigning an index of  $P_e$  to a corner  $v$  of a face  $f$ . Being given an edge  $e$  contained in a face  $f$ , the indices of  $P_e$  corresponding to the Hilbert space  $\mathcal{H}_f$  are assigned to the two internal vertices intersecting  $e$ . If the orientation of  $e$  is the same as that of  $f$ , the lower / upper index is assigned to the beginning / ending point of  $e$ . If the orientation of  $e$  is opposite to that of  $f$ , the lower / upper index is assigned to the end / beginning point of  $e$ . The oriented arc marks the orientation of the polygonal face  $f$ .

are associated with the beginning point of  $e$ , whereas the indices  $A, A'$  of  $P_{eA...B...}^{A'...B'...}$  with the end point of  $e$ . Therefore, for every internal edge  $e$  and for each face  $f$  containing  $e$ , there are two indices in the operator  $P_e$ , an upper and a lower one corresponding to the Hilbert space  $\mathcal{H}_f$ . The indices are associated with the ends of the edge  $e$ , according to the rule introduced above and presented in figure 5.7.

There is a canonical contraction of the indices of the contractors and the indices of the edge operators (see figure 5.8). Whenever in the operator  $P_e$  there is an upper/lower index associated with an internal vertex  $v \prec e$ , there is a lower/upper index in the contractor  $\mathcal{A}_v$ . We contract the indices and obtain the contracted operator spin foam.

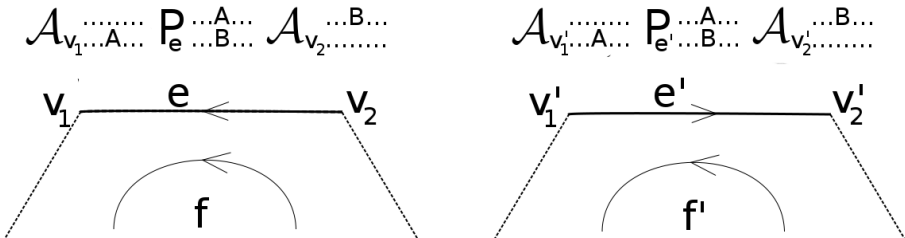


Figure 5.8.: The contraction of the indices. There is a canonical contraction of the indices of the contractors and the indices of the edge operators. The figure depicts situations when an edge is connecting two internal vertices. In this case, all indices of the corresponding edge operator are contracted with the indices of the contractors. If an edge connects an internal vertex and a boundary node, then half of the indices of the corresponding edge operator are contracted with the indices of the contractor corresponding to the internal vertex (and half of the indices is left uncontracted). If an edge connects two boundary nodes, then all the indices of the corresponding edge operator are left uncontracted.

### 5.2.3. 2-edge contraction

Wherever two internal edges of a spin foam  $(\kappa, \rho, P, \mathcal{A})$  meet, the geometry of a spin foam defines a natural contraction between the corresponding operators.

For every pair of edges  $e$  and  $e'$  which belong to the same face  $f$  and share a vertex  $v$ , if the index of  $P_e$  corresponding to  $f$  and  $v$  is upper / lower, then the index of  $P_{e'}$  corresponding to  $f$  and  $v$  is lower / upper, respectively. The indices can be contracted. In this way the natural contraction  $\text{Tr}_{v,f}$  at  $v$  (figure 5.9) is defined.

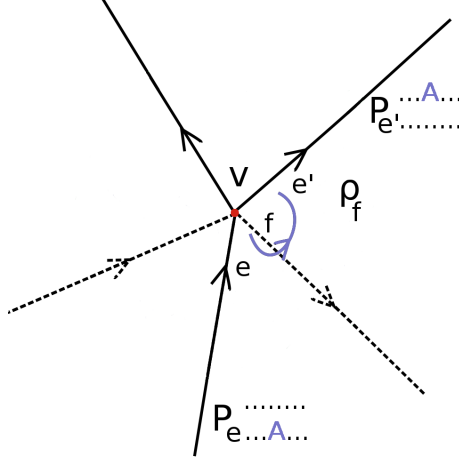


Figure 5.9.: 2-edge contraction of indices: The edges  $e$  and  $e'$  are connected by the face  $f$ . The blue indices  $A$  of  $P_e$  and respectively  $P_{e'}$  correspond to the Hilbert space  $\mathcal{H}_f$  and get contracted by  $\text{Tr}_{v,f}$ .

As a result there is a distinguished contractor:

$$\text{Tr}_v = \bigotimes_f \text{Tr}_{v,f},$$

where the product is over faces containing the vertex  $v$ . This is the vertex trace (1.44) used in the spin-foam model of quantum BF theory (section 1.3.2) and the Spin(4) spin-foam model with the EPRL vertex (section 3.4.1).

### 5.2.4. Symmetric spin-foam operator

#### Contraction and the equivalence moves

The expression (5.36) is not invariant with respect to the equivalence moves introduced in the previous subsection. Being given an operator spin foam  $(\kappa, \rho, P, \mathcal{A})$  let us suppose that an operator spin foam  $(\kappa', \rho', P', \mathcal{A}')$  is obtained from  $(\kappa, \rho, P, \mathcal{A})$  by one of the equivalence moves except for the face splitting move. Then

$$\text{Tr}(\kappa', \rho', P', \mathcal{A}') = \text{Tr}(\kappa, \rho, P, \mathcal{A}). \quad (5.42)$$

However, if an operator spin foam  $(\kappa', \rho', P', \mathcal{A}')$  is obtained from  $(\kappa, \rho, P, \mathcal{A})$  by the move of splitting a face  $f_0$  (see section 5.1.2), then

$$\text{Tr}(\kappa', \rho', P', \mathcal{A}') \neq \text{Tr}(\kappa, \rho, P, \mathcal{A}),$$

## 5. Operator spin foams

except for the case  $\dim \mathcal{H}_{f_0} = 1$ . The Hilbert space

$$\text{Inv}(\mathcal{H}_{f'_1} \otimes \mathcal{H}_{f'_2}^*) = \text{Inv}(\mathcal{H}_{f_0} \otimes \mathcal{H}_{f_0}^*)$$

is spanned by the identity operator  $\text{id} : \mathcal{H}_{f_0} \rightarrow \mathcal{H}_{f_0}$ . In the index notation,  $\text{id}_B^A = \delta_B^A$ ,  $(\Lambda_{e'_0})_B^A = \frac{1}{d_{f_0}} \delta_B^A$ ,

$$P'_{e'_0 B A'} = \frac{1}{d_{f_0}} \delta_B^A \delta_{A'}^{B'}, \quad (5.43)$$

where

$$d_{f_0} = \dim \mathcal{H}_{f_0}. \quad (5.44)$$

It is easy to verify that

$$\text{Tr}(\kappa', \rho', P', \mathcal{A}') = \frac{1}{d_{f_0}} \text{Tr}(\kappa, \rho, P, \mathcal{A}). \quad (5.45)$$

This shows that the move is not a symmetry indeed.

### Face amplitude restores the equivalence

Introducing suitable face amplitude makes the contraction  $\text{Tr}$  of operator spin foam exactly invariant with respect to all the moves. Let us consider a spin-foam operator defined by a formula (tilde will be removed when we establish the final form of the operator)

$$\tilde{\mathcal{Z}}(\kappa, \rho, P, \mathcal{A}) = \left( \prod_{f \in \kappa^{(2)}} A_f \right) \text{Tr}(\kappa, \rho, P, \mathcal{A}) \quad (5.46)$$

where

$$f \mapsto A_f$$

is an unknown function, a face amplitude. Then a unique solution for  $f \mapsto A_f$  such that for every operator spin foam  $(\kappa, \rho, P, \mathcal{A})$  and every equivalent operator spin foam  $(\kappa', \rho', P', \mathcal{A}')$

$$\tilde{\mathcal{Z}}_{(\kappa, \rho, P, \mathcal{A})} = \tilde{\mathcal{Z}}_{(\kappa', \rho', P', \mathcal{A}')}, \quad (5.47)$$

is

$$A_f = \dim \mathcal{H}_f. \quad (5.48)$$

### Boundary amplitude restores the compatibility with the glueing

The introduction of the face amplitude destroys the compatibility with the glueing of the operator spin foams. Consider two operator spin foams  $(\kappa, \rho, P, \mathcal{A})$  and  $(\kappa', \rho', P', \mathcal{A}')$ , and their composition  $(\kappa, \rho, P, \mathcal{A}) \# (\kappa', \rho', P', \mathcal{A}')$  glued along a graph  $\gamma$ . The operator spin foam contraction induces the contraction of the operators  $\tilde{\mathcal{Z}}(\kappa, \rho, P, \mathcal{A})$  and  $\tilde{\mathcal{Z}}(\kappa', \rho', P', \mathcal{A}')$  – let us denote it by  $\text{Tr}_\gamma$ . The result is

$$\text{Tr}_\gamma \left( \tilde{\mathcal{Z}}(\kappa, \rho, P, \mathcal{A}) \otimes \tilde{\mathcal{Z}}(\kappa', \rho', P', \mathcal{A}') \right) = \prod_{\ell \in \gamma^{(0)}} d_{f_\ell} \tilde{\mathcal{Z}}(\kappa \# \kappa', \rho \# \rho', P \# P', \mathcal{A} \# \mathcal{A}'). \quad (5.49)$$

To restore the compatibility of  $\tilde{\mathcal{Z}}$  with glueing the operator spin foams we multiply  $\tilde{\mathcal{Z}}$  by suitable boundary link amplitudes. Finally, we find that the symmetric spin-foam operator is of the form:

$$\mathcal{Z}(\kappa, \rho, P, \mathcal{A}) = \prod_{\ell \in (\partial\kappa)^{(1)}} \frac{1}{\sqrt{d_{f_\ell}}} \tilde{\mathcal{Z}}(\kappa, \rho, P, \mathcal{A}), \quad (5.50)$$

We assume that  $\ell \neq \ell' \Rightarrow f_\ell \neq f_{\ell'} -$  this can be always achieved by splitting faces and edges. Now we have

$$\text{Tr}_\gamma (\mathcal{Z}(\kappa, \rho, P, \mathcal{A}) \otimes \mathcal{Z}(\kappa', \rho', P', \mathcal{A}')) = \mathcal{Z}(\kappa \# \kappa', \rho \# \rho', P \# P', \mathcal{A} \# \mathcal{A}'). \quad (5.51)$$

### 5.2.5. Relation with the spin foams

The operator spin foam formalism seems to differ from the usual formulation of spin foams presented in section 1.3.3, because there are operators assigned to edges instead of intertwiners. However, if the operators  $P_e$  are orthogonal projections,

$$P_e P_e = P_e, \quad P_e^\dagger = P_e,$$

then the spin-foam operator can be interpreted as the result of summing the spin-foam amplitudes over the intertwiners. Since  $P_e$  is an orthogonal projection, it can be written in the following form:

$$P_e = \sum_{\iota_e} \iota_e \otimes \iota_e^\dagger, \quad (5.52)$$

where the sum is over an orthonormal basis in  $\text{ran } P_e$ . Using the decomposition (5.52), the tensor product  $\bigotimes_e P_e$  can be written as a linear combination of terms of the following form:

$$\bigotimes_{e \in \kappa_{\text{int}}^{(1)}} \iota_e \otimes \iota_e^\dagger.$$

As a result, it is sufficient to assign to each internal edge  $e$  an intertwiner  $\iota_e \in \text{ran } P_e$  and sum over an orthonormal basis of each space  $\text{ran } P_e$ . After applying the decomposition of  $\bigotimes_{e \in \kappa_{\text{int}}^{(1)}} P_e$  to the contracted operator spin foam (5.36), we obtain

$$\text{Tr}(\kappa, \rho, P, \mathcal{A}) = \bigotimes_{v \in \kappa_{\text{int}}^{(0)}} \mathcal{A}_v \lrcorner \bigotimes_{e \in \kappa_{\text{int}}^{(1)}} P_e = \sum_{\iota} \prod_{v \in \kappa_{\text{int}}^{(0)}} \mathcal{A}_v(s_v^\dagger) \bigotimes_{n \in \partial\kappa^{(0)}} \partial\iota_n.$$

Since a spin-foam operator is obtained from contracted operator spin foam by multiplying by face and boundary link amplitudes, we obtain

$$\mathcal{Z}(\kappa, \rho, P, \mathcal{A}) = \sum_{\iota} \prod_{\ell \in \partial\kappa^{(1)}} A_{\text{link}}(\partial\rho_\ell) \prod_{f \in \kappa_{\text{int}}^{(2)}} A_{\text{face}}(\rho_f) \prod_{v \in \kappa_{\text{int}}^{(0)}} \mathcal{A}_v(s_v^\dagger) \bigotimes_{n \in \partial\kappa^{(0)}} \partial\iota_n.$$

The relation between the spin-foam operator  $\mathcal{Z}$  and the spin-foam amplitude  $Z$  is the following:

$$\mathcal{Z}(\kappa, \rho, P, \mathcal{A}) = \sum_{\iota} Z(\kappa, \rho, \iota, \mathcal{A}) \bigotimes_{n \in \partial\kappa^{(0)}} \partial\iota_n.$$

In this sense the operator spin foams formalism is obtained from the standard spin-foam formalism by summing over the intertwiners.

## 5. Operator spin foams

### 5.2.6. Amplitude form of the spin-foam operator

In general, we decompose each  $P_e$ ,

$$P_e = \sum_{\iota_e \in \mathcal{B}_e} \sum_{\iota'_e \in \mathcal{B}_e^\dagger} A_e(\iota_e, \iota'_e) \iota_e \otimes \iota'_e \quad (5.53)$$

in any basis,

$$\mathcal{B}_e \subset \mathcal{H}_e, \quad (5.54)$$

and the conjugate basis

$$\mathcal{B}_e^\dagger = \{\iota_e^\dagger : \iota_e \in \mathcal{B}_e\} \subset \mathcal{H}_e^*, \quad (5.55)$$

where  $\mathcal{H} \ni v \mapsto v^\dagger \in \mathcal{H}^*$  is the canonical antilinear map (denoted by  $|v\rangle \mapsto \langle v|$  in the Dirac notation).

After the substitution of the right hand side of (5.53) for  $P_e$ , the tensor product  $\bigotimes_{e \in \kappa_{\text{int}}^{(1)}} P_e$  becomes a linear combination of the tensor products

$$\bigotimes_{e \in \kappa_{\text{int}}^{(1)}} \iota_e \otimes \iota'_e, \quad (5.56)$$

in which to each internal edge  $e$  there is assigned a (tensor product of a) pair of the intertwiners  $\iota_e \otimes \iota'_e$ , where  $\iota_e \in \mathcal{B}_e$  and  $\iota'_e \in \mathcal{B}_e^\dagger$  are independent of each other. In fact, from the point of view of the contractions we use,  $\iota'_e$  is assigned to the start point of  $e$  whereas  $\iota_e$  is assigned to the end point of  $e$ . That is the generalized case of a spin foam that was derived in [124] (see figure 5.10).

Being given a vertex  $v$ , the application of the contractor to the tensor product of intertwiners assigned to the vertex  $v$  produces a  $\mathbb{C}$  number factor

$$\mathcal{A}_v \left( \bigotimes_{e \text{ incoming to } v} \iota_e \otimes \bigotimes_{e' \text{ outgoing from } v} \iota'_{e'} \right). \quad (5.57)$$

It is natural to call the factor the vertex amplitude also in the generalized case.

Finally, the substitution of the right hand side of (5.53) into the spin foam operator  $\mathcal{Z}(\kappa, \rho, P, \mathcal{A})$  definition (5.37) gives the following sum with respect to all the labellings  $\iota$  and  $\iota'$ :

$$\mathcal{Z}(\kappa, \rho, P, \mathcal{A}) = \sum_{\iota, \iota'} Z(\kappa, \rho, \iota, \iota', \mathcal{A}) \bigotimes_{n \in (\partial\kappa)^{(0)}} \partial\iota_n, \quad (5.58)$$

where

$$\partial\iota_n = \begin{cases} \iota_{e_n} & \text{if } e_n \text{ is incoming to } n, \\ \iota'_{e_n} & \text{if } e_n \text{ is outgoing from } n, \end{cases}$$

$e_n$  is the unique internal edge containing the boundary node  $n$ ,

$$\begin{aligned} Z(\kappa, \rho, \iota, \iota', \mathcal{A}) = & \prod_{\ell \in (\partial\kappa)^{(1)}} A_{\text{link}}(\partial\rho_\ell) \prod_{f \in \kappa^{(2)}} A_{\text{face}}(\rho_f) \prod_{e \in \kappa_{\text{int}}^{(1)}} A_e(\iota_e, \iota'_e) \cdot \\ & \cdot \prod_{v \in \kappa_{\text{int}}^{(0)}} \mathcal{A}_v \left( \bigotimes_{e \text{ incoming to } v} \iota_e \otimes \bigotimes_{e' \text{ outgoing from } v} \iota'_{e'} \right) \end{aligned}$$

can be considered to be a (generalized) spin-foam amplitude.

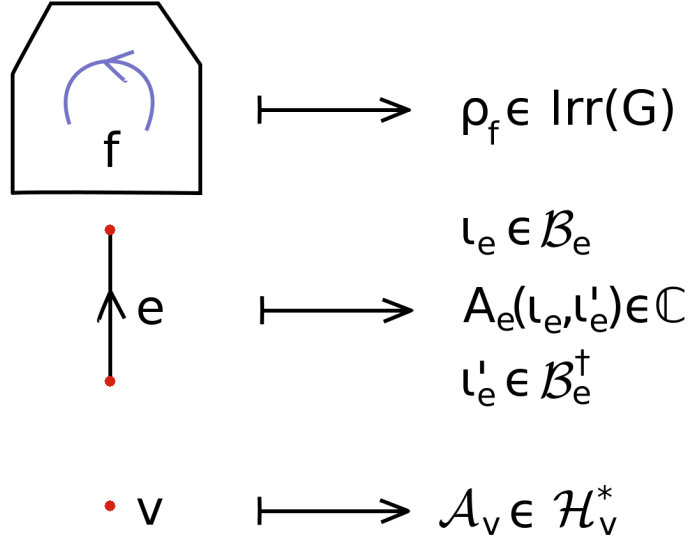


Figure 5.10.: The operator approach is equivalent to an approach in which we assign an irreducible representations of group  $G$  to each face of the 2-complex, a pair of intertwiners  $\iota_e \in \mathcal{B}_e$ ,  $\iota'_e \in \mathcal{B}_e^\dagger$  together with the complex number  $A_e(\iota_e, \iota'_e) \in \mathbb{C}$  to each internal edge and a contractor  $\mathcal{A}_v \in \mathcal{H}_v^*$  to each internal vertex.

### 5.3. Operator spin-foam models

A  $G$  operator spin-foam model defines

- a class of possible operator spin foams  $(\kappa, \rho, P, \mathcal{A})$  (a class of foams and possible colorings),
- a spin-foam operator  $\mathcal{Z}(\kappa, \rho, P, \mathcal{A})$  for each operator spin foam  $(\kappa, \rho, P, \mathcal{A})$  in the class.

Given  $(\kappa, \rho, P, \mathcal{A})$  the spin-foam operator  $\mathcal{Z}(\kappa, \rho, P, \mathcal{A})$  is defined uniquely up to the face and boundary link amplitudes (see section 5.2.1). The second point is therefore equivalent to saying that a spin-foam model defines the face and boundary link amplitudes.

#### 5.3.1. Natural operator spin-foam models

We will consider below a class of natural operator spin-foam models, that is models such that, briefly speaking,

- the assignment  $e \mapsto P_e$  depends only on an unordered sequence of labels  $\rho_f$  such that  $e \prec f$ ,
- the assignment  $v \mapsto \mathcal{A}_v$  depends only on the vertex graph and the labelling of the links of the graph induced by the labelling  $\rho$  (see section 1.3.3),

and are independent of the other parts of a given 2-complex  $\kappa$  - see below for a technical definition. We will also assume that each  $P_e$  is self-adjoint, that is

## 5. Operator spin foams

- for every internal edge  $e \in \kappa_{\text{int}}^{(1)}$

$$P_e^\dagger = P_e. \quad (5.59)$$

Technically, the first assumption means, that for every unordered sequence  $R$  of allowed unitary irreducible representations of the group  $G$ , we fix an operator

$$P_R : \text{Inv} \left( \bigotimes_{\rho \in R} \mathcal{H}_\rho \right) \rightarrow \text{Inv} \left( \bigotimes_{\rho \in R} \mathcal{H}_\rho \right). \quad (5.60)$$

The second assumption means, that for every pair  $(\gamma, \rho)$  of oriented graph  $\gamma$  and coloring  $\rho$  of its links with (allowed) unitary irreducible representations of the group  $G$ , we fix a linear functional

$$\mathcal{A}_{(\gamma, \rho)} : \bigotimes_{n \in \gamma^{(0)}} \mathcal{H}_n \rightarrow \mathbb{C},$$

such that

$$\mathcal{A}_{(\gamma', \rho')} = \mathcal{A}_{(\gamma, \rho)}, \quad (5.61)$$

if  $\gamma'$  is obtained from  $\gamma$  by flipping an orientation of a link, say  $\ell_0$ , and

$$\rho'_{\ell'} = \begin{cases} \rho_{\ell_0}^*, & \text{if } \ell' = \ell_0^{-1} \\ \rho_{\ell'}, & \text{otherwise.} \end{cases}$$

Next, being given any (allowed) pair  $(\kappa, \rho)$ :

- we can use the equivalence relation to reorient the faces  $f$  containing  $e$ , such that their orientations agree with that of  $e$ , and therefore an operator  $P_e$  should be a map

$$P_e : \bigotimes_{f: e \prec f} \mathcal{H}_f \rightarrow \bigotimes_{f: e \prec f} \mathcal{H}_f, \quad (5.62)$$

and set

$$P_e = P_{R_e} \quad (5.63)$$

with the unordered sequence  $R_e$  of the representations  $\rho_f$  where  $f$  ranges the set of faces containing  $e$ ;

- we set

$$\mathcal{A}_v = \mathcal{A}_{(\gamma_v, \rho_v)},$$

where  $\gamma_v$  is the vertex graph corresponding to the vertex  $v$  and  $\rho_v$  is the coloring of its links with unitary irreducible representations induced by the coloring of faces containing  $v$  (see section 1.3.3).

### 5.3.2. Symmetric operator spin-foam models

A symmetric model is a model such that all the equivalence moves of section 5.1.2 are symmetries of the model. That is, whenever  $(\kappa, \rho, P, \mathcal{A})$  is in the class of operator spin foams defined by the model, so does any  $(\kappa', \rho', P', \mathcal{A}')$  that can be obtained from  $(\kappa, \rho, P, \mathcal{A})$  by the equivalence moves.

### Symmetric natural operator spin-foam models

An important class of models is the subclass of symmetric models in the class of the natural operator spin-foam models. The set of conditions defining the models has a general solution. First, the assumed symmetry with respect to the face splitting move of section 5.1.2 implies that

- for every unordered sequence  $R$  given by the pair of elements  $\rho$  and  $\rho^*$

$$P_R = \text{id}, \quad (5.64)$$

- if  $\gamma'$  is obtained from  $\gamma$  by splitting one of its links, say  $\ell_0$ , into two links  $\ell_0 = \ell'_2 \circ \ell'_1$  by adding a node  $n'_0$ , then

$$\mathcal{A}_{(\gamma', \rho')} = \mathcal{A}_{(\gamma, \rho)} \otimes \Lambda_{n'_0}, \quad (5.65)$$

where

$$\rho'_{\ell'} = \begin{cases} \rho_{\ell_0}, & \text{if } \ell' = \ell'_1 \text{ or } \ell' = \ell'_2 \\ \rho_{\ell'}, & \text{if } \ell' \in \gamma^{(1)}. \end{cases}$$

Second, the consequence of the symmetry with respect to the edge splitting move of section 5.1.2 implies that

- for every unordered sequence  $R$  of unitary irreducible representations, the operator  $P_R$  (5.60) satisfies

$$P_R P_R = P_R, \quad (5.66)$$

- for any theta graph  $\Theta$ , i.e. a graph having two nodes  $n, n'$  and  $N$  links connecting the two different nodes outgoing from the node  $n$  and incoming to the node  $n'$ , the contractor is trivial:

$$\mathcal{A}_{(\Theta, \rho)} = \text{id} \in \mathcal{H}_n \otimes \mathcal{H}_{n'}^*. \quad (5.67)$$

A direct consequence of (5.66) and (5.59) is that each operator  $P_e$  is an orthogonal projection onto a subspace

$$\mathcal{H}_R^s \subset \mathcal{H}_R. \quad (5.68)$$

The subspaces  $\mathcal{H}_R^s$  are subject to the isomorphisms following from (5.26),(5.27). They give rise to subspaces  $\mathcal{H}_e^s$  assigned to the internal edges  $e$  of the 2-complexes.

#### 5.3.3. Examples

In the following, we will show how different choices of the operator labelling  $P$  and the labelling with contractors  $\mathcal{A}$  defining different operator spin-foam models, reproduce different spin-foam models. Three of the examples we will discuss below fall into the class of the symmetric natural operator spin-foam models, one is a natural operator spin-foam model but it is not symmetric and one is not natural but it is symmetric.

The symmetric natural operator spin-foam models presented here assign to each vertex the distinguished contractor

$$\mathcal{A}_v = \text{Tr}_v.$$

## 5. Operator spin foams

By construction each operator (5.3) is a projection. The remaining choice consists in fixing a subspace (5.68),

$$\mathcal{H}_R^s \subset \mathcal{H}_R = \text{Inv} \left( \bigotimes_{\rho \in R} \mathcal{H}_\rho \right) \quad (5.69)$$

for every unordered sequence  $R$  of the equivalence classes of unitary irreducible representations of  $G$  (see the conditions (5.26),(5.27)). Each of the models can be thought of as a quantization of G BF theory with constraints. For a given operator spin foam  $(\kappa, \rho, P, \mathcal{A})$  of a given model, elements of the Hilbert subspaces  $\mathcal{H}_e^s = \mathcal{H}_{R_e}^s$  assigned to the edges are quantum solutions to the constraints.

The next to last model reproduces the spin-foam model presented in section 3.4.2. As we will see, it is a natural spin-foam model but it is not symmetric. In this model each operator (5.3) is a projection, but the contractors  $\mathcal{A}_{(\gamma, \rho)}$  do not satisfy equations (5.65), (5.67). The last model is a modification of the preceding model that is symmetric but not natural operator spin-foam model.

### BF theory

The easiest nontrivial choice is the spin-foam model of quantum BF theory. For a given compact group  $G$  the BF operator spin foam  $(\kappa, P, \rho, \mathcal{A})$  is a foam  $\kappa$  with the coloring such that:

- $\rho_f$  is arbitrary unitary irreducible representations of  $G$ ,
- $P_e$  is the identity operator,  $P_e = \text{id} : \text{Inv}(\mathcal{H}_e) \rightarrow \text{Inv}(\mathcal{H}_e)$ ,
- $\mathcal{A}_v$  is the vertex trace (1.44),  $\mathcal{A}_v = \text{Tr}_v$ .

The spin-foam operator corresponding to an operator spin foam  $(\kappa, \rho, P, \mathcal{A})$  is:

$$\mathcal{Z}(\kappa, \rho, P, \mathcal{A}) = \prod_{\ell \in (\partial\kappa)^{(1)}} \frac{1}{\sqrt{d_{f_\ell}}} \prod_{f \in \kappa^{(2)}} d_f \text{Tr}(\kappa, \rho, P, \mathcal{A}).$$

Clearly, it is a symmetric operator spin-foam model with  $\mathcal{H}_e^s = \text{Inv}(\mathcal{H}_e)$ .

### The Barrett-Crane model

In terms of our framework the Barrett-Crane model [38] is a  $G = \text{Spin}(4)$  operator spin-foam model. The BC operator spin foam  $(\kappa, P, \rho, \mathcal{A})$  is a foam  $\kappa$  with the coloring such that:

- $\rho_f = \rho_{j_f^+ j_f^-}$ , where  $j_f^+ = j_f^- =: j_f$ ,
- $P_e$  is orthogonal projection onto the subspace  $\text{Inv}_{BC}(\mathcal{H}_e)$  spanned by invariants of the form  $\mathcal{I} \otimes \mathcal{I} \in \text{Inv}(\mathcal{H}_e)$ , where

$$\mathcal{I} \in \text{Inv} \left( \bigotimes_{f \text{ opposite orientation to } e} \mathcal{H}_{j_f}^* \otimes \bigotimes_{f' \text{ same orientation as } e} \mathcal{H}_{j_{f'}} \right)$$

- $\mathcal{A}_v$  is the vertex trace,  $\mathcal{A}_v = \text{Tr}_v$ .

The spin-foam operator corresponding to an operator spin foam  $(\kappa, \rho, P, \mathcal{A})$  is:

$$\mathcal{Z}(\kappa, \rho, P, \mathcal{A}) = \prod_{\ell \in (\partial\kappa)^{(1)}} \frac{1}{\sqrt{d_{f_\ell}}} \prod_{f \in \kappa^{(2)}} d_f \text{Tr}(\kappa, \rho, P, \mathcal{A}).$$

Clearly, it is a symmetric operator spin-foam model with  $\mathcal{H}_e^s = \text{Inv}_{\text{BC}}(\mathcal{H}_e)$ .

### The Spin(4) operator spin-foam model with the EPRL vertex

In this operator spin-foam model again  $G = \text{Spin}(4)$ . The EPRL model relies on the Barbero-Immirzi parameter  $\beta$  that needs to be a rational number  $\beta \neq 0, \pm 1$ . The Spin(4) operator spin foam with the EPRL vertex is a quadruple  $(\kappa, \rho, P, \mathcal{A})$  such that:

- $\rho_f = \rho_{j_f^+ j_f^-}$ , where  $j_f^+ = \frac{|\beta+1|}{|\beta-1|} j_f^-$ ,
- $P_e$  is orthogonal projection onto the subspace of the EPRL intertwiners  $\text{Inv}_{\text{EPRL}}(\mathcal{H}_e)$ ,
- $\mathcal{A}_v$  is the vertex trace,  $\mathcal{A}_v = \text{Tr}_v$ .

The spin-foam operator corresponding to an operator spin foam  $(\kappa, \rho, P, \mathcal{A})$  is:

$$\mathcal{Z}(\kappa, \rho, P, \mathcal{A}) = \prod_{\ell \in (\partial\kappa)^{(1)}} \frac{1}{\sqrt{d_{f_\ell}}} \prod_{f \in \kappa^{(2)}} d_f \text{Tr}(\kappa, \rho, P, \mathcal{A}).$$

Clearly, it is a symmetric operator spin-foam model with  $\mathcal{H}_e^s = \text{Inv}_{\text{EPRL}}(\mathcal{H}_e)$ .

The amplitude form of the operator spin-foam model is the following [124, 29]. Using the EPRL map, a (typically orthonormal) basis

$$\mathcal{B} \subset \text{Inv}(\mathcal{H}_{k_1} \otimes \dots \otimes \mathcal{H}_{k_N})$$

is mapped into a basis

$$\mathcal{B}^{\text{EPRL}} \subset \text{Inv}_{\text{EPRL}}\left(\mathcal{H}_{j_1^+ j_1^-} \otimes \dots \otimes \mathcal{H}_{j_N^+ j_N^-}\right)$$

(typically not orthonormal). We can expand the operator  $P_e$  in the basis  $\mathcal{B}_e^{\text{EPRL}}$ :

$$P_e = \sum_{\mathcal{I}_e \in \mathcal{B}_e, \mathcal{I}'_e \in \mathcal{B}_e^\dagger} A_e(\mathcal{I}_e, \mathcal{I}'_e) \iota_{\text{EPRL}}(\mathcal{I}_e) \otimes \iota_{\text{EPRL}}(\mathcal{I}'_e), \quad (5.70)$$

where the coefficients  $A_e(\mathcal{I}_e, \mathcal{I}'_e)$  are defined by the following conditions

$$\sum_{\mathcal{I} \in \mathcal{B}_e} A_e(\mathcal{I}_1, \mathcal{I}^\dagger) (\iota_{\text{EPRL}}(\mathcal{I}) | \iota_{\text{EPRL}}(\mathcal{I}_2)) = \begin{cases} 1 & \text{if } \mathcal{I}_1 = \mathcal{I}_2, \\ 0 & \text{if } \mathcal{I}_1 \neq \mathcal{I}_2, \end{cases} \quad (5.71)$$

$\mathcal{I}_1, \mathcal{I}_2 \in \mathcal{B}_e$ ,  $(\cdot | \cdot)$  is the Hilbert product in  $\mathcal{H}_e$ . As a result instead of assigning an operator  $P_e$  to each edge  $e$ , one considers a set of assignments of two  $SU(2)$  intertwiners  $\mathcal{I}_e, \mathcal{I}'_e$ , to the end and respectively, the start point of each edge  $e$  (figure 5.10). Following the

## 5. Operator spin foams

derivation of the amplitude form of the spin-foam operator done in section 5.2.6 we obtain:

$$\begin{aligned} \mathcal{Z}(\kappa, \rho, P, \mathcal{A}) = & \sum_{\mathcal{I}, \mathcal{I}'} \prod_{\ell \in (\partial\kappa)^{(1)}} \frac{1}{\sqrt{(2j_{f_\ell}^+ + 1)(2j_{f_\ell}^- + 1)}} \prod_{f \in \kappa^{(2)}} (2j_f^+ + 1)(2j_f^- + 1) \cdot \\ & \cdot \prod_{e \in \kappa_{\text{int}}^{(1)}} A_e(\mathcal{I}_e, \mathcal{I}'_e) \prod_{v \in \kappa_{\text{int}}^{(0)}} \mathcal{A}_v^{\text{EPRL}} \left( \bigotimes_{e_v} \mathcal{I}_{e_v} \otimes \bigotimes_{e'_v} \mathcal{I}'_{e'_v} \right) \bigotimes_{\tilde{e}} \iota_{\text{EPRL}}(\mathcal{I}_{\tilde{e}}) \otimes \bigotimes_{\tilde{e}'} \iota_{\text{EPRL}}(\mathcal{I}'_{\tilde{e}'}) \end{aligned} \quad (5.72)$$

where  $e_v/e'_v$  ranges the set of edges incoming/outgoing at the vertex  $v$ ,  $\tilde{e}/\tilde{e}'$  ranges the set of edges intersecting  $\partial\kappa$  at the end/start point.

Note that the edge amplitude  $A_e(\mathcal{I}_e, \mathcal{I}'_e)$  has to be included if  $P_e$  is supposed to be an orthogonal projection onto the space of the EPRL solutions to the constraints, since the EPRL map  $\iota_{\text{EPRL}}$  (typically) is not an isometry. The edge amplitude can be interpreted as a measure factor appearing when summing over intertwiners. If the  $A_e(\mathcal{I}_e, \mathcal{I}'_e)$  factors are not included in the spin-foam amplitude, then the EPRL intertwiners are summed over with a different measure, and lead to  $P_e$  not being an orthogonal projection – in particular, the operator  $\mathcal{Z}(\kappa, \rho, P, \mathcal{A})$  is no longer invariant under the edge splitting move.

### The SU(2) operator spin-foam model with the EPRL vertex

The SU(2) operator spin-foam model for the EPRL intertwiners is an operator spin foam with the coloring such that:

- $\rho_f = \rho_{k_f}$  is an SU(2) unitary irreducible representation such that  $\frac{|1 \pm \beta|}{2} k_f \in \frac{1}{2}\mathbb{N}$ ,
- $P_e$  is the identity operator  $\text{id} : \text{Inv}(\mathcal{H}_e) \rightarrow \text{Inv}(\mathcal{H}_e)$ ,
- $\mathcal{A}_v$  is the EPRL contractor,  $\mathcal{A}_v = \mathcal{A}_v^{\text{EPRL}}$ .

The spin-foam operator corresponding to an operator spin foam  $(\kappa, \rho, P, \mathcal{A})$  is:

$$\mathcal{Z}(\kappa, \rho, P, \mathcal{A}) = \prod_{\ell \in (\partial\kappa)^{(1)}} \frac{1}{\sqrt{d_{f_\ell}}} \prod_{f \in \kappa^{(2)}} d_f \text{Tr}(\kappa, \rho, P, \mathcal{A}).$$

Obviously, the operators  $P_e$  are orthogonal projections and therefore satisfy equations (5.66) as well as (5.64). However, the coloring with contractors does not satisfy equations (5.65) and (5.67), therefore the model is not symmetric.

### A modification of the SU(2) operator spin-foam model with the EPRL vertex

If we give up the requirement of naturalness we can modify the SU(2) operator spin-foam model with the EPRL vertex and restore the symmetry. First, we define the model according to the definition from the previous subsection for each 2-complex which cannot be obtained from another 2-complex by splitting an edge or splitting a face. Then we apply the operations of splitting edges and splitting faces to define the model for any 2-complex. When splitting an edge we choose the labelling of the new edges to be the identity operators (as in the model in the previous subsection). With this choice the

### 5.3. Operator spin-foam models

condition (5.23) is satisfied because  $P'_{e'}$  and  $P_e$  are orthogonal projections (for any  $e'$  and  $e$ ). Let us note, that in this model the coloring of edges is the same as in the model in the previous subsection; the models differ in the coloring of some of the internal vertices.



# 6. Operator spin-network diagrams

The piecewise linear foams refer to auxiliary affine structures, which are not compatible with the diffeomorphism invariance of General Relativity. In [129] we proposed to use another class of foams defined purely combinatorially (see also [152, 127]). The foams allow all possible closed graphs to be boundary graphs and all closed, connected graphs to be vertex graphs. The class is defined by certain diagrams that we call graph diagrams (see section 6.1.1). Graph diagrams are a generalization of the diagrams defined by Frank Hellmann [114] for the triangulations. To each graph diagram there corresponds an oriented CW-complex (a foam), which we construct in section 6.1.3. In the paper [129] the foam was obtained by glueing together elementary building blocks that are certain foams with one internal vertex. In this thesis the foam is constructed directly from the diagram, without reference to the glueing procedure. The foams have a clearly defined boundary, which we describe in section 6.1.4. In [129] the boundary is constructed by using a certain procedure of merging graphs. However, in this thesis the boundary graph is constructed without reference to this procedure. On the one hand there are some foams in the class that were not allowed in the class of piecewise linear foams – for example, in a piecewise linear 2-complex each face is bounded by at least three edges, which is clearly not the case in the foam depicted in figure 6.2b. On the other hand we impose a restriction demanding that a (non-empty) foam has at least one internal vertex. This complicates, for example, the definition of the static spin foam representing a trivial evolution of a spin network (see section 6.2.4).

In section 6.2.1 we will define operator spin-network diagrams (OSD) as suitably colored graph diagrams. For each graph diagram its coloring induces a coloring of the corresponding foam making it an operator spin foam (see section 6.2.2). The spin-foam operator can be calculated without constructing the corresponding operator spin foam explicitly (see section 6.2.3). We will use this technical advantage in the next chapter.

Importantly, the operator spin-network diagrams accommodate the two versions of the EPRL model[123, 48], as well as other possible spin-foam models. In section 6.3 we present the OSD models such that the corresponding operators spin-foam models are: the Spin(4) operator spin-foam model with the EPRL vertex described in section 5.3.3 and the SU(2) operator spin-foam model with the EPRL vertex described in section 5.3.3.

## 6.1. Graph diagrams

### 6.1.1. Definition

Beginning from this chapter by a graph we will mean an oriented abstract graph (see definition in section 1.2.2). We say that a graph is connected if there is an (undirected) path from every node to every other node. We say that a graph is closed if each of its nodes is at least 2-valent. Let us denote by

$$\gamma_n^{\text{in}} = \{\ell \in \gamma^{(1)} : t(\ell) = n\} = t^{-1}(n)$$

## 6. Operator spin-network diagrams

the set of links incoming to the node  $n$  and by

$$\gamma_n^{\text{out}} = \{\ell \in \gamma^{(1)} : s(\ell) = n\} = s^{-1}(n)$$

the set of links outgoing from the node  $n$ .

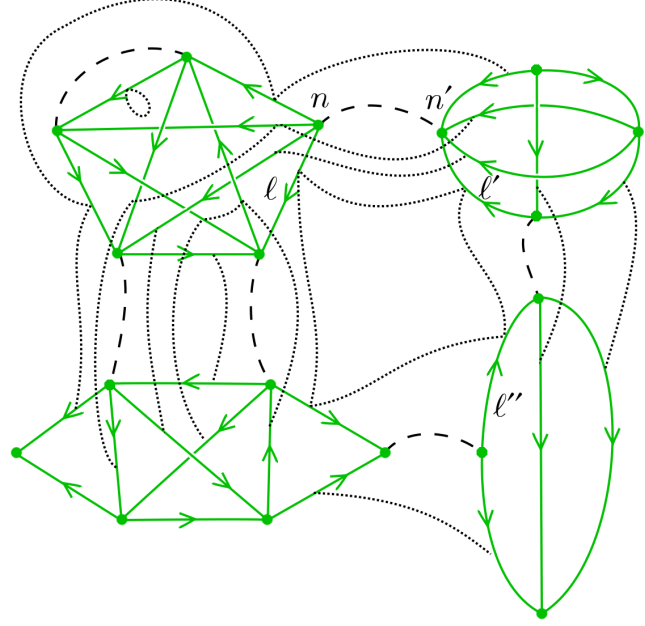


Figure 6.1.: A graph diagram. The thick dots represent the nodes of the graphs, the solid lines with arrows represent the oriented links of the graphs, the dashed lines illustrate the node relation  $\mathcal{R}_{\text{node}}$  and the dotted lines illustrate the glueing map. For example:  $(n, n') \in \mathcal{R}_{\text{node}}, \varphi(\ell) = \ell', \varphi(\ell') = \ell''$ .

A general graph diagram  $\mathcal{D} = (\mathcal{G}, \mathcal{R}_{\text{node}}, \varphi)$  consists of a finite set  $\mathcal{G}$  of connected, closed graphs  $\{\gamma_1, \dots, \gamma_N\}$ , a relation  $\mathcal{R}_{\text{node}}$  and a map  $\varphi$ :

- $\mathcal{R}_{\text{node}}$ : a symmetric relation on the set of nodes of the graphs, which we call the *node relation*, such that each node  $n$  is either in relation with precisely one  $n' \neq n$  or is unrelated. In the later case, it will be called a *boundary node*. A necessary condition for two different nodes  $n$  and  $n'$  to be in node relation is that

$$\#\gamma_n^{\text{in}} = \#\gamma_{n'}^{\text{out}}, \quad \#\gamma_n^{\text{out}} = \#\gamma_{n'}^{\text{in}}.$$

- $\varphi$ : a 1-1 map from the set  $\mathcal{G}^{\text{out}} := \bigcup_{(n, n') \in \mathcal{R}_{\text{node}}} \gamma_n^{\text{out}}$  to the set  $\mathcal{G}^{\text{in}} := \bigcup_{(n, n') \in \mathcal{R}_{\text{node}}} \gamma_n^{\text{in}}$  such that

$$\forall (n, n') \in \mathcal{R}_{\text{node}} \quad (\ell \in \gamma_n^{\text{out}} \implies \varphi(\ell) \in \gamma_{n'}^{\text{in}}).$$

We will call  $\varphi$  a *glueing map*.

Let us note that  $\varphi$  is in fact a bijection. We denote by  $\mathcal{G}^{(0)}$  the set of nodes of all graphs:

$$\mathcal{G}^{(0)} = \bigcup_I \gamma_I^{(0)}, I \in \{1, \dots, N\}$$

and by  $\mathcal{G}^{(1)}$  the set of links of all graphs:

$$\mathcal{G}^{(1)} = \bigcup_l \gamma_l^{(1)}, l \in \{1, \dots, N\}.$$

Let us note that if there are no boundary nodes, then  $\mathcal{G}^{\text{in}} = \mathcal{G}^{\text{out}} = \mathcal{G}^{(1)}$ . In this case a glueing map is a permutation of the links of all graphs.

In [129, 130] we used a family of symmetric relations, called link relations, in place of the glueing map. Two links  $\ell \in \gamma_n^{\text{out}}$ ,  $\ell' \in \gamma_{n'}^{\text{in}}$  identified with each other by a glueing map (i.e.  $\ell' = \varphi(\ell)$ ) were said to be in the link relation  $\mathcal{R}_{\text{link}}^{(n,n')}$  at the nodes  $n$  and  $n'$ . In this thesis we prefer to use the definition in terms of the glueing map and we do not use the notion of link relations.

### 6.1.2. Face and edge relations

The node relation  $\mathcal{R}_{\text{node}}$  and the glueing map  $\varphi$  introduced with the definition of graph diagram lead to equivalence relation in the set of all links of all graphs. We say that a link  $\ell$  is in face relation with a link  $\ell'$  if and only if there exists a sequence of links  $(\ell_1, \dots, \ell_M)$ ,  $M \geq 1$  such that

$$\ell_K \in \mathcal{G}^{(1)}, K \in \{1, \dots, M\}, \quad (6.1)$$

$$\ell_{K+1} = \varphi(\ell_K), K \in \{1, \dots, M-1\}, \quad (6.2)$$

$$\ell_1 = \ell, \ell_M = \ell' \text{ or } \ell_1 = \ell', \ell_M = \ell. \quad (6.3)$$

The equivalence classes of face relation will be denoted by  $[\ell]$  and the set of the equivalence classes will be denoted by  $\mathfrak{F}$ . To each equivalence class  $[\ell]$  there corresponds a sequence  $(\ell_1, \dots, \ell_M)$  such that each element of  $[\ell]$  appears precisely once in the sequence and the condition (6.2) is satisfied. If in addition  $(t(\ell_1), s(\ell_M)) \in \mathcal{R}_{\text{node}}$  then the equivalence class is called *closed*. Otherwise it is called open. The set of closed equivalence classes will be denoted by  $\mathfrak{F}_{\text{closed}}$  and the set of open equivalence classes will be denoted by  $\mathfrak{F}_{\text{open}}$ . Let us note that if  $[\ell]$  is closed, then

$$\ell_1 = \varphi(\ell_M).$$

If  $[\ell]$  is open, the sequence is unique. The face relation will be used in the construction of a CW-complex corresponding to a graph diagram (see section 6.1.3). It carries information about the faces of the CW-complex and allows to introduce face amplitude without explicit reference to the complex itself (see section 6.2.3).

For our convenience we will also introduce the *edge* relation  $\mathcal{R}_{\text{edge}}$ . The edge relation  $\mathcal{R}_{\text{edge}}$  is the unique equivalence relation on the set  $\mathcal{G}^{(0)}$  such that two different nodes are in the relation if and only if they are in node relation. There are two types of the equivalence classes:

1. Each node unrelated to any other node by  $\mathcal{R}_{\text{node}}$  sets a one-element equivalence class of  $\mathcal{R}_{\text{edge}}$ .
2. Each pair of nodes  $\{n, n'\}$  related by the  $\mathcal{R}_{\text{node}}$  sets a two-element equivalence class of  $\mathcal{R}_{\text{edge}}$ .

The equivalence classes of the edge relation will be denoted by  $[n]$ . The set of equivalence classes of the edge relation will be denoted by  $\mathfrak{E}$ .

## 6. Operator spin-network diagrams

### 6.1.3. A CW-complex corresponding to a graph diagram

In this section we construct a CW-complex corresponding to a given graph diagram. A general CW-complex is defined by the following procedure [112]:

1. Define  $X^0$  to be a discrete set – the points of  $X^0$  are called 0-cells,
2.  $X^d$  is constructed from  $X^{d-1}$  by attaching  $d$ -cells  $e_\alpha^d$  via continuous maps

$$\phi_\alpha^d : S^{d-1} \rightarrow X^{d-1}.$$

$X^d$  is the quotient space of a disjoint union

$$X^{d-1} \sqcup \bigsqcup_\alpha D_\alpha^d$$

of  $X^{d-1}$  with a collection of  $d$ -disks  $D_\alpha^d$  under the identifications  $x \sim \phi_\alpha^{d-1}(x)$  for  $x \in \partial D_\alpha^d$ . As a set  $X^d = X^{d-1} \sqcup \bigsqcup_\alpha e_\alpha^d$ , where each  $e_\alpha^d$  is an open disk.

The CW-complex corresponding to a graph diagram  $\mathcal{D} = (\{\gamma_1, \dots, \gamma_N\}, \mathcal{R}_{\text{node}}, \varphi)$ , is constructed in the following way.

1.  $X^0$  is a disjoint union of the boundary nodes and  $N$  points  $v_1, \dots, v_N$  corresponding to the graphs  $\gamma_1, \dots, \gamma_N$  in  $\mathcal{G}$ . The points  $v_1, \dots, v_N$  will be called the internal vertices. We denote by  $v_l$  the point corresponding to the graph  $\gamma_l$ , by  $v_\ell$  the point corresponding to the graph  $\gamma \in \mathcal{G}$  such that  $\ell \in \gamma^{(1)}$  and by  $v_n$  the point corresponding to the graph  $\gamma \in \mathcal{G}$  such that  $n \in \gamma^{(0)}$ .
2.  $X^1$  is constructed in the following way. The collection of 1-disks ( $[0, 1]$  segments) is labelled by the equivalence classes of the edge relation  $[n]$  and the open equivalence classes of the face relation  $[\ell]$ . We denote the cells corresponding to  $[n]$  by  $e_{[n]}$  and call them the internal edges. The attaching maps  $\phi_{[n]}^1$  map the endpoints  $\{0, 1\}$  of the segments  $D_{[n]}^1$  to the points of  $X^0$  such that
  - a)  $\phi_{[n]}^1(0) = v_n, \quad \phi_{[n]}^1(1) = v_{n'}$ ,  
where  $n$  and  $n'$  are the two different nodes in  $[n]$ .<sup>1</sup>
  - b)  $\phi_{[n]}^1(0) = v_n, \quad \phi_{[n]}^1(1) = n$ ,  
where  $n$  is a boundary node,
  - c)  $\phi_{[\ell]}^1(0) = s(\ell), \quad \phi_{[\ell]}^1(1) = t(\ell')$ ,  
where  $\ell$  is the link in  $[\ell]$  outgoing from a boundary node and  $\ell'$  is the link in  $[\ell]$  incoming to a boundary node.

---

<sup>1</sup>At the level of CW-complex it is irrelevant, if  $\phi_{[n]}^1(0) = v_n, \phi_{[n]}^1(1) = v_{n'}$  or  $\phi_{[n]}^1(1) = v_n, \phi_{[n]}^1(0) = v_{n'}$ .

The two different cases will correspond to different orientations of the internal edge  $e_{[n]}$  in the oriented CW-complex that we will introduce in this section. However, the operator spin foams constructed in the section 6.2.2, corresponding to the different cases will be equivalent.

3.  $X^2$  is constructed in the following way. The collection of 2-disks is labelled by the equivalence classes of the face relation  $[\ell]$ . The corresponding 2-cells will be denoted by  $f_{[\ell]}$  and will be called the faces. The definition of an attaching map  $\phi_{[\ell]}^2$  depends on whether the equivalence class  $[\ell]$  is closed or open.

- a) To each closed equivalence class there corresponds a sequence  $(\ell_1, \dots, \ell_M)$  such that each link in  $[\ell]$  appears precisely once in the sequence, (6.2) holds and  $t(\ell_1)$  is in the node relation with  $s(\ell_M)$  (see section 6.1.2). The attaching map  $\phi_{[\ell]}^2$  is the continuous map

$$\phi_{[\ell]}^2 : \mathbb{R}/M\mathbb{Z} \rightarrow X^1$$

such that  $\phi_{[\ell]}^2(K - 1) = v_{\ell_K}$ , and

$$\phi_{[\ell]}^2(t) = \begin{cases} t - K + 1 \in \text{int } D_{[s(\ell_K)]}^1, & \text{if } \phi_{[s(\ell_K)]}^1(0) = v_{\ell_K}, t \in ]K - 1, K[, \\ 1 - (t - K + 1) \in \text{int } D_{[s(\ell_K)]}^1, & \text{if } \phi_{[s(\ell_K)]}^1(1) = v_{\ell_K}, t \in ]K - 1, K[, \end{cases}$$

where  $K \in \{1, 2, \dots, M\}$ .

- b) To each open equivalence class there corresponds a unique sequence  $(\ell_1, \dots, \ell_M)$  such that each link in  $[\ell]$  appears precisely once in the sequence, (6.2) holds and  $t(\ell_1)$  is a boundary node (see section 6.1.2). The attaching map  $\phi_{[\ell]}^2$  is a map

$$\phi_{[\ell]}^2 : \mathbb{R}/(M + 2)\mathbb{Z} \rightarrow X^1$$

such that  $\phi_{[\ell]}^2(0) = t(\ell_1)$ ,  $\phi_{[\ell]}^2(K) = v_{\ell_K}$ ,  $\phi_{[\ell]}^2(M) = v_{\ell_M}$ ,  $\phi_{[\ell]}^2(M + 1) = s(\ell_M)$ , and

$$\phi_{[\ell]}^2(t) = \begin{cases} 1 - t \in \text{int } D_{[t(\ell_1)]}^1, & \text{if } t \in ]0, 1[, \\ t - K \in \text{int } D_{[s(\ell_K)]}^1, & \text{if } \phi_{[s(\ell_K)]}^1(0) = v_{\ell_K}, t \in ]K, K + 1[, \\ 1 - (t - K) \in \text{int } D_{[s(\ell_K)]}^1, & \text{if } \phi_{[s(\ell_K)]}^1(1) = v_{\ell_K}, t \in ]K, K + 1[, \\ t - M \in \text{int } D_{[s(\ell_M)]}^1, & \text{if } t \in ]M, M + 1[, \\ t - M - 1 \in \text{int } D_{[\ell]}^1, & \text{if } t \in ]M + 1, M + 2[, \end{cases}$$

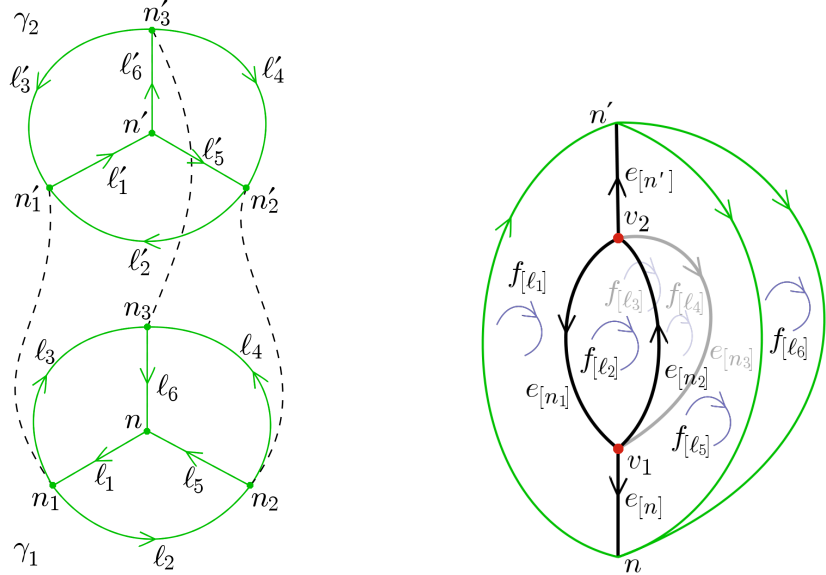
where  $K \in \{1, 2, \dots, M - 1\}$ .

The cells can be equipped with natural orientation: we assume that the boundary nodes and internal vertices have positive orientation, the orientation of each edge is the orientation inherited from the natural orientation of the segment  $[0, 1]$  and the orientation of the face is the orientation inherited from the natural orientation of  $\mathbb{R}/N\mathbb{Z}$ . The resulting oriented CW-complex will be called a *foam corresponding to a graph diagram  $\mathcal{D}$*  and denoted by  $\kappa_{\mathcal{D}}$ .

Let us note that a graph diagram does not contain any information about orientations of the internal edges of the corresponding CW-complex. We choose the orientations of the internal edges connecting two internal vertices arbitrarily and we fix the orientations of the edges connecting a boundary node and an internal vertex to be incoming to the boundary node. The operator spin foams constructed in the section 6.2.3, corresponding to different choices of orientations of the internal edges connecting two internal vertices, will be equivalent.

An example of a graph diagram and the corresponding foam is given on figure 6.2.

## 6. Operator spin-network diagrams



(a) A graph diagram. The dashed lines denote the node relation. The glueing map is the unique map  $\varphi : \mathcal{G}^{\text{out}} \rightarrow \mathcal{G}^{\text{in}}$  such that  $\ell'_J = \varphi(\ell_J) \vee \ell_J = \varphi(\ell'_J)$ ,  $J \in \{1, \dots, 6\}$ .

(b) The foam (oriented CW-complex) corresponding to the graph diagram (a). The orientations of the internal edges connecting two internal vertices can be chosen arbitrarily. We fix the orientations of the edges connecting an internal vertex with a boundary node such that the boundary node is the target of the edge.

Figure 6.2.: A graph diagram and the corresponding foam (oriented CW-complex). To each graph there corresponds an internal vertex. The equivalence classes of the edge relation are  $[n] = \{n\}$ ,  $[n'] = \{n'\}$ ,  $[n_K] = \{n_K, n'_K\}$ ,  $K = \{1, 2, 3\}$ . The nodes  $n$  and  $n'$  are boundary nodes,  $n_K$  and  $n'_K$  are in node relation. To each boundary node there corresponds a node on the boundary of the CW-complex, to each equivalence class of node relation there corresponds an internal edge. The equivalence classes of face relation are  $[\ell_J] = \{\ell_J, \ell'_J\}$ ,  $J \in \{1, \dots, 6\}$ . The equivalence classes  $[\ell_1], [\ell_5], [\ell_6]$  are open and the equivalence classes  $[\ell_2], [\ell_3], [\ell_4]$  are closed. To each equivalence class of face relation there corresponds a face. Additionally, to each open equivalence class of face relation there corresponds a boundary link.

### 6.1.4. Boundary graph

The boundary graph is a subcomplex of the complex  $\kappa$  constructed in the following way:

1.  $X^0$  is a disjoint union of the boundary nodes,
2.  $X^1$  is defined in the following way. The collection of 1-disks ( $[0,1]$  segments) is labelled by the open equivalence classes of the face relation. The attaching maps  $\phi_\alpha^1$  are mapping the endpoints  $\{0, 1\}$  of the segments  $D_\alpha^1$  to the points of  $X^0$ , such that

$$\phi_{[\ell]}^1(0) = s(\ell), \quad \phi_{[\ell]}^1(1) = t(\ell'),$$

where  $\ell$  is the link in  $[\ell]$  outgoing from a boundary node and  $\ell'$  is the link in  $[\ell]$  incoming to a boundary node.

An example of a graph diagram and the corresponding boundary graph is given on figure 6.3.

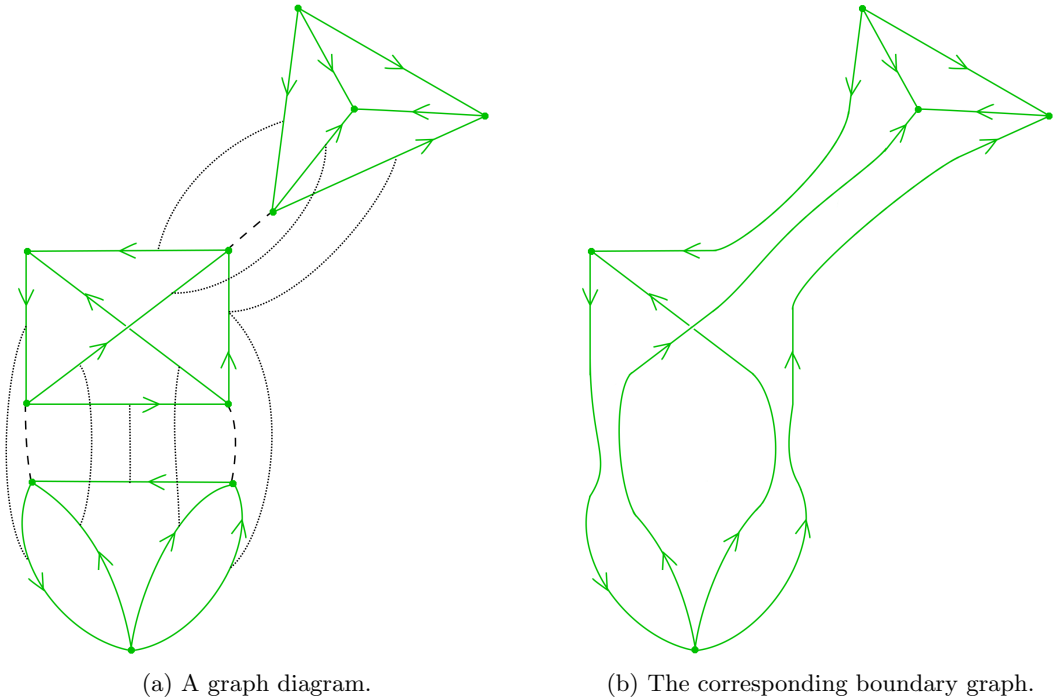


Figure 6.3.: A graph diagram and the corresponding boundary graph. The boundary graph is the boundary of the foam corresponding to the graph diagram.

## 6.2. Operator spin-network diagrams

### 6.2.1. Definition

An operator spin-network diagram  $(\mathcal{D}, \rho, P, \mathcal{A})$  is defined by coloring a graph diagram  $\mathcal{D} = (\mathcal{G}, \mathcal{R}_{\text{node}}, \varphi)$  as follows:

- The coloring  $\rho$  assigns to each link  $\ell \in \mathcal{G}^{(1)}$  a unitary irreducible representation of the group  $G$ :

$$\ell \mapsto \rho_\ell \in \text{Irr}(G). \quad (6.4)$$

It is assumed that

$$\forall \ell \in \mathcal{G}^{\text{out}} \quad \rho_\ell = \rho_{\varphi(\ell)}. \quad (6.5)$$

- The coloring  $P$  assigns to each node  $n \in \mathcal{G}^{(0)}$  an operator:

$$n \mapsto P_n \in \mathcal{H}_n \otimes \mathcal{H}_n^*, \quad (6.6)$$

## 6. Operator spin-network diagrams

where  $\mathcal{H}_n = \text{Inv} \left( \bigotimes_{\ell \text{ incoming to } n} \mathcal{H}_\ell^* \otimes \bigotimes_{\ell' \text{ outgoing from } n} \mathcal{H}_{\ell'} \right)$  is the node Hilbert space (see section 1.2.2).

Whenever two nodes  $n$  and  $n'$  are related by  $\mathcal{R}_{\text{node}}$ , then from (6.5) it follows that  $\mathcal{H}_n = \mathcal{H}_{n'}^*$  and it is assumed about  $P$  that

$$P_n = P_{n'}^*. \quad (6.7)$$

- The coloring  $\mathcal{A}$  assigns to each graph  $\gamma_I$  a contractor

$$\gamma_I \mapsto \mathcal{A}_I \in \left( \bigotimes_{n \in \gamma_I^{(0)}} \mathcal{H}_n \right)^*. \quad (6.8)$$

If a node  $n \in \mathcal{G}^{(0)}$  is related by  $\mathcal{R}_{\text{node}}$  with another node  $n' \in \mathcal{G}^{(0)}$  (and thus  $n$  and  $n'$  are in the same equivalence class of edge relation,  $[n] = [n']$ ), then  $P_n$  and  $P_{n'}$  are elements of the same Hilbert space  $\bigotimes_{\tilde{n} \in [n]} \mathcal{H}_{\tilde{n}}$ ; due to (6.7) they appear to be the same element

$$P_{[n]} \in \bigotimes_{\tilde{n} \in [n]} \mathcal{H}_{\tilde{n}}. \quad (6.9)$$

We extend this notation to any equivalence class of node relation by defining

$$P_{[n]} := P_n \quad (6.10)$$

for any boundary node  $n$ .

A natural example of a contractor exists due to the fact that the Hilbert space  $\bigotimes_n \mathcal{H}_n$  can be uniquely embedded into a space (see remarks in section 1.3.3 concerning the coloring with the contractors):

$$\bigotimes_{n \in \gamma_I^{(0)}} \mathcal{H}_n \hookrightarrow \bigotimes_{\ell \in \gamma_I^{(1)}} \mathcal{H}_\ell \otimes \mathcal{H}_\ell^*. \quad (6.11)$$

The distinguished element of  $(\bigotimes_n \mathcal{H}_n)^*$  is

$$\text{Tr}_I = \bigotimes_{\ell \in \gamma_I^{(1)}} \text{Tr}_\ell, \quad (6.12)$$

where  $\text{Tr}_\ell \in \mathcal{H}_\ell \otimes \mathcal{H}_\ell^*$  is the trace functional. If  $\gamma_I$  is the graph obtained from a vertex graph by flipping the orientation of each link and each  $\rho_\ell, \ell \in \gamma_I$  is the representation dual to the representation induced on the corresponding link of the vertex graph, the contractor  $\text{Tr}_I$  is the vertex trace (see section 1.3.2 and section 5.2.3).

### 6.2.2. The operator spin foam corresponding to operator spin-network diagram

In section 6.1.3 we constructed a foam corresponding to a graph diagram. In this section we construct an operator spin foam for each operator spin-network diagram  $(\mathcal{D}, \rho, P, \mathcal{A})$ :

1. The foam is the oriented CW-complex  $\kappa_{\mathcal{D}}$  constructed in section 6.1.3.

2. Let us recall, that the faces of  $\kappa_D$  are labelled with the equivalence classes of faces relation and are denoted by  $f_{[\ell]}$ . We define the coloring:

$$\rho : \kappa^{(2)} \rightarrow \text{Irr}(G),$$

to be

$$\rho_{f_{[\ell]}} = \rho_\ell.$$

3. Let us recall, that the internal edges of the foam  $\kappa_D$  are labelled by the equivalence classes of the edge relation and denoted by  $e_{[n]}$ .

- a) If  $\# [n] = 2$ , the relation between the edge Hilbert spaces and the node Hilbert spaces is:

$$\text{Inv}(\mathcal{H}_{e_{[n]}}) = \mathcal{H}_n,$$

where  $n$  is the node in  $[n]$  such that  $v_n$  is the source of the edge  $e_{[n]}$  (i.e.  $v_n = \phi_{[n]}^1(0)$ ). We define the edge operator to be:

$$P_{e_{[n]}} = P_n : \mathcal{H}_n \rightarrow \mathcal{H}_n.$$

- b) If  $\# [n] = 1$ , then

$$\text{Inv}(\mathcal{H}_{e_{[n]}}) = \mathcal{H}_n.$$

We define the edge operator to be:

$$P_{e_{[n]}} = P_n : \mathcal{H}_n \rightarrow \mathcal{H}_n.$$

4. Let us recall, that the internal vertices of the foam  $\kappa_D$  correspond to the graphs  $\gamma_l$  and are denoted by  $v_l$ . Note that the vertex Hilbert space is

$$\mathcal{H}_{v_l} = \bigotimes_{n \in \gamma_l^{(0)}} \mathcal{H}_n.$$

We define the coloring with contractors to be

$$\mathcal{A}_{v_l} = \mathcal{A}_{\gamma_l}.$$

An example of an operator spin-network diagram and the corresponding operator spin foam is depicted in figure 6.4.

### 6.2.3. The spin-network diagram operator

There is a canonical contraction, which we will call contracted operator spin-network diagram (compare section 5.2.1),

$$\text{Tr}(\mathcal{D}, \rho, P, \mathcal{A}) = \left( \bigotimes_l \mathcal{A}_l \right) \sqcup \left( \bigotimes_{[n] \in \mathfrak{E}} P_{[n]} \right) \quad (6.13)$$

## 6. Operator spin-network diagrams

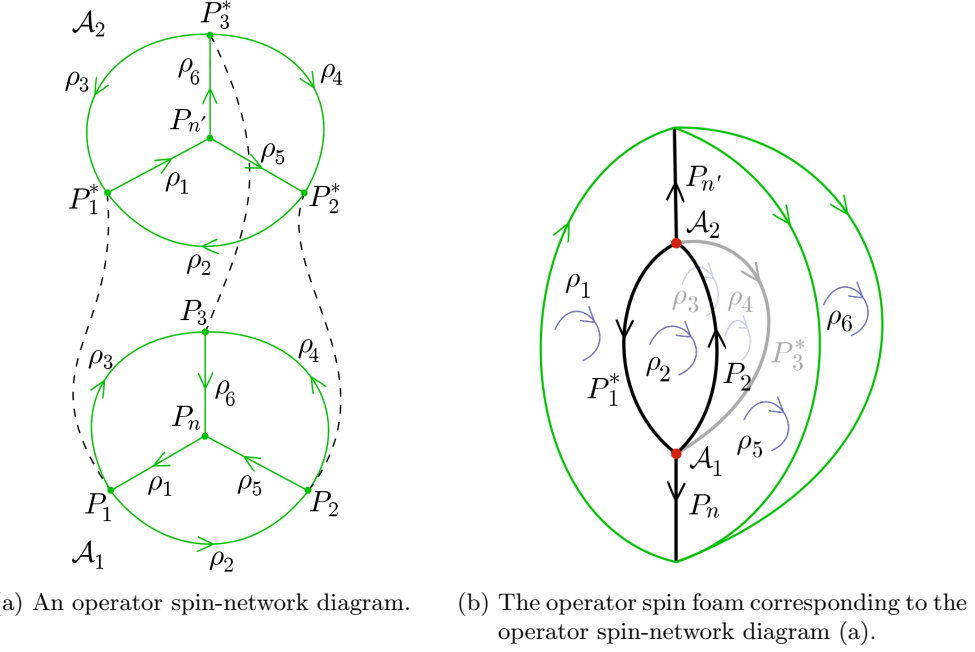


Figure 6.4.: An operator spin-network diagram and the corresponding operator spin foam. The orientations of the internal edges connecting two internal vertices can be chosen arbitrarily. For example, if we had chosen the orientation of the edge  $e_{[n_1]}$  (see figure 6.2b) to be opposite to the one indicated on figure (b), the operator corresponding to this link would be  $P_1$  (instead of  $P_1^*$ ). As a result, the corresponding operator spin foam would be equivalent to the operator spin foam on figure (b) (see section 5.1.2).

where  $\mathbb{I}$  labels the graphs in  $\mathcal{G}$ . It is defined by contracting each  $\mathcal{A}_\mathbb{I}$  with the  $\mathcal{H}_n$ -part of each operator  $P_{[n]}$ ,  $n \in \gamma_\mathbb{I}^{(0)}$  (see (6.9) and (6.10)). As a consequence, the  $\mathcal{H}_n^*$  part of each operator  $P_{[n]}$  assigned to a boundary node  $n$  remains uncontracted, and

$$\mathrm{Tr}(\mathcal{D}, \rho, P, \mathcal{A}) \in \bigotimes_{\text{boundary } n} \mathcal{H}_n^*. \quad (6.14)$$

We define the spin-network diagram operator to be

$$\mathcal{Z}(\mathcal{D}, \rho, P, \mathcal{A}) = \prod_{[\ell] \in \mathfrak{F}_{\text{open}}} \mathcal{A}_{\text{link}}(\rho_{[\ell]}) \prod_{[\ell] \in \mathfrak{F}} \mathcal{A}_{\text{face}}(\rho_{[\ell]}) \mathrm{Tr}(\mathcal{D}, \rho, P, \mathcal{A}), \quad (6.15)$$

where  $\rho_{[\ell]} := \rho_\ell$  for any  $\ell \in [\ell]$ .

A comparison of (6.13) with (5.36) and (6.15) with (5.37) shows that the spin-network diagram operator of an operator spin-network diagram and the spin-foam operator of the operator spin foam corresponding to the operator spin-network diagram coincide. As a result, the formalism of operator spin-network diagrams can be used independently from the formalism of operator spin foams.

### 6.2.4. Static operator spin-network diagrams

Given a pair  $(\gamma, \rho)$  of an oriented graph  $\gamma$  and a labelling of its links with representations, the *static operator spin foam* is:

- A 2-complex  $\kappa = \gamma \times [0, 1]$ . The boundary graph of  $\kappa$  is  $\gamma_{\text{in}} \cup \gamma_{\text{out}}$ , where  $\gamma_{\text{out}} = \gamma$  and  $\gamma_{\text{in}} = \bar{\gamma}$  is obtained from  $\gamma$  by flipping the orientations of all the links. For each link  $\ell$  of  $\gamma$ , the face  $f_\ell = \ell \times [0, 1]$  of  $\kappa$  is oriented in agreement with  $\ell$ .
- A coloring of faces of the foam  $\rho$  is such that

$$\rho_{f_\ell} = \rho_\ell.$$

- For each node  $n$  of  $\gamma_{\text{in}}$ , there corresponds an internal edge  $e_n = n \times [0, 1]$  of the foam. It is colored by the identity operator

$$P_{e_n} = \text{id} \in \text{Inv}(\mathcal{H}_{e_n}) \otimes \text{Inv}(\mathcal{H}_{e_n})^*. \quad (6.16)$$

- Since there are no internal vertices, no contractors are needed.

An example of a static foam  $\kappa = \gamma \times [0, 1]$  is shown on figure 6.5. The spin-foam operator corresponding to the static operator spin foam is:

$$\mathcal{Z}(\kappa, \rho, P) = \bigotimes_{n \in \gamma^{(0)}} P_{e_n} \in \left( \bigotimes_{n \in \gamma^{(0)}} \mathcal{H}_n \right) \otimes \left( \bigotimes_{n \in \gamma^{(0)}} \mathcal{H}_n \right)^* \quad (6.17)$$

and due to the choice of coloring (6.16) it is the identity operator. The static operator spin foam represents therefore a trivial evolution of a spin network.

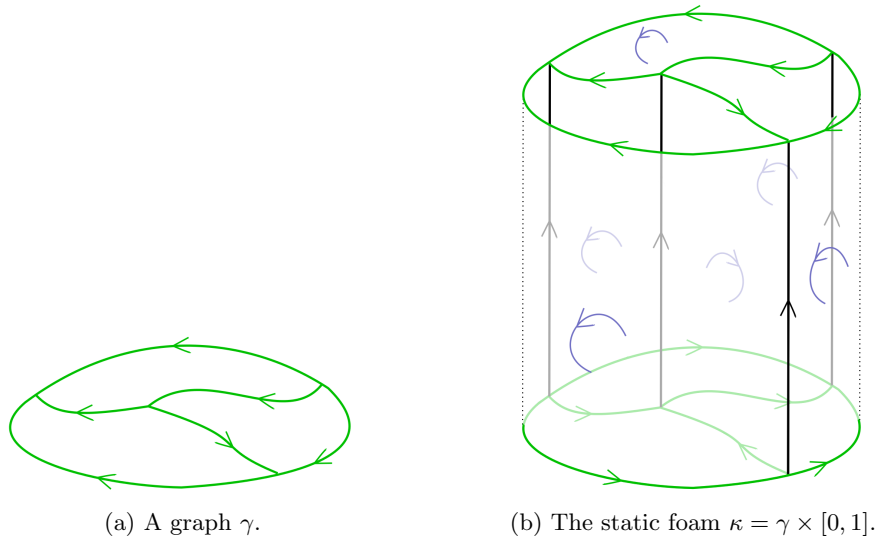


Figure 6.5.: Static foam corresponding to a graph  $\gamma$ .

In analogy to the static spin foam, we define a static operator spin-network diagram. The diagram will consist of the so called (generalized)  $\theta$ -graphs. A generalized theta graph is a graph  $\theta$  such that  $\#\theta^{(0)} = 2$ ,  $\#\theta^{(1)} \geq 2$  and  $\forall_{\ell \in \theta^{(1)}} s(\ell) \neq t(\ell)$ . The *static operator spin-network diagram* is  $(\mathcal{D}_\gamma, \rho, P, \mathcal{A})$  such that

## 6. Operator spin-network diagrams

- $\mathcal{G} = \{\tilde{\theta}_n : n \in \gamma^{(0)}\}$ , where  $\tilde{\theta}_n$  is defined in the following way (see also figure 6.6):
  1. The graph  $\theta_n$  is a generalized theta graph such that  $\theta_n^{(0)} = \{n^d, n^u\}$  and
 
$$\#s^{-1}(n^d) = \#t^{-1}(n), \quad \#t^{-1}(n^d) = \#s^{-1}(n),$$
 i.e. the number of incoming/outgoing links at the node  $n^d \in \theta_n^{(0)}$  is equal to the number of outgoing/incoming links at the node  $n \in \gamma^{(0)}$ .
  2. The graph  $\tilde{\theta}_n$  is obtained from  $\theta_n$  by splitting each link of the graph. We use the following notation:
 
$$\begin{aligned} \tilde{\theta}_n^{(0)} &= \{n^d, n^u\} \cup \{s_\ell : \ell \in \gamma_n^{\text{out}}\} \cup \{t_\ell : \ell \in \gamma_n^{\text{in}}\}, \\ \tilde{\theta}_n^{(1)} &= \{(n, n') : n = n^d \vee n = n^u, n' = s_\ell \vee n' = t_\ell\}, \\ s((n, n')) &= \begin{cases} n, & \text{if } (n, n') = (n^d, t_\ell) \text{ or } (n, n') = (n^u, s_\ell), \\ n', & \text{if } (n, n') = (n^d, s_\ell) \text{ or } (n, n') = (n^u, t_\ell), \end{cases} \\ t((n, n')) &= \begin{cases} n, & \text{if } (n, n') = (n^d, s_\ell) \text{ or } (n, n') = (n^u, t_\ell), \\ n', & \text{if } (n, n') = (n^d, t_\ell) \text{ or } (n, n') = (n^u, s_\ell). \end{cases} \end{aligned}$$

- $\mathcal{R}_{\text{node}} = \{(s_\ell, t_\ell) : \ell \in \gamma^{(1)}\} \cup \{(t_\ell, s_\ell) : \ell \in \gamma^{(1)}\}$  (see figure 6.6b). Since each node  $s_\ell, t_\ell$  is two-valent and there are one link incoming and one link outgoing from the node, there is only one possible glueing map.

- We set the following coloring:

1. The coloring  $\rho : \tilde{\theta}_n^{(1)} \rightarrow \text{Irr}(G)$  is the following:

$$\rho_{(n, s_\ell)} := \rho_\ell, \quad \rho_{(n, t_\ell)} := \rho_\ell,$$

where  $n \in \{n^d, n^u\}$ .

2. Each node  $n \in \mathcal{G}^{(0)}$  is colored by the identity operator, the canonical element of the corresponding space  $\mathcal{H}_n \otimes \mathcal{H}_n^*$ .
3. Each graph  $\tilde{\theta}_n$  in the diagram is colored by the natural contractor (6.12).

The figure 6.6b shows the graph diagram  $\mathcal{D}_\gamma$ . The operator spin foam corresponding to  $(\mathcal{D}_\gamma, \rho, P, \mathcal{A})$  is not the static operator spin foam (compare figure 6.5b and figure 6.7). However, it can be obtained from the static operator spin foam by the moves of splitting edges and faces from section 5.1.2. As a result the spin-network diagram operator corresponding to the trivial diagram is (equal to) the identity operator (6.17).

## 6.3. The OSD models with the EPRL vertex amplitude

In section 3.4 we presented two models with the EPRL vertex amplitude: the SU(2) spin-foam model with the EPRL vertex and the Spin(4) spin-foam model with the EPRL vertex and in section 5.3.3 we constructed the corresponding operator spin-foam models. In this section we present two OSD models such that the corresponding operator spin-foam models are the ones from section 5.3.3 and section 5.3.3.<sup>2</sup> The first one is a Spin(4) OSD model, whereas the second one is an SU(2) OSD model.

---

<sup>2</sup>Provided that the foam corresponding to a graph diagram can be equipped with a piecewise linear structure making it a piecewise linear 2-complex.

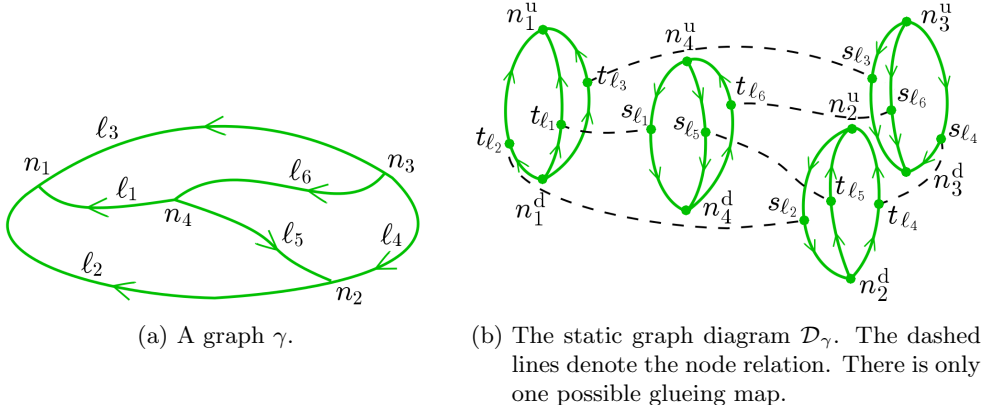
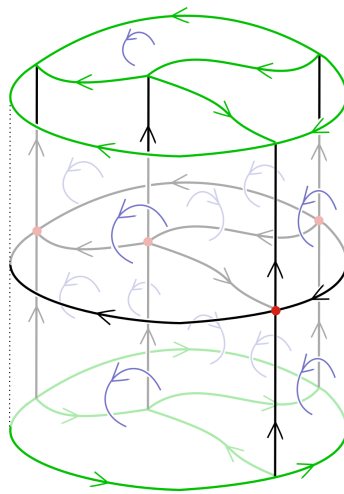

 Figure 6.6.: Static graph diagram corresponding to a graph  $\gamma$ .


Figure 6.7.: A foam corresponding to the static graph diagram from figure 6.6b. It can be related to the static foam from figure 6.5b by the moves of splitting the edges and the faces.

### 6.3.1. The Spin(4) OSD model with the EPRL vertex

Given a value of the Barbero-Immirzi parameter  $\beta \in \mathbb{Q}$ ,  $\beta \neq 0, \pm 1$ , the Spin(4) operator spin-network diagram with the EPRL vertex is a graph diagram  $\mathcal{D}$  with the following coloring.

- We color each link  $\ell$  with a unitary irreducible representation  $\rho_{j_\ell^+ j_\ell^-}$  of the Spin(4) group ( $j_\ell^\pm \in \frac{1}{2}\mathbb{N}$ ) such that  $j_\ell^+ = \frac{|\beta+1|}{|\beta-1|} j_\ell^-$ .
- We color each node  $n$  with an operator  $P_n$  that is the orthogonal projection onto the space of the EPRL intertwiners (see also section 5.3.3):

$$\text{Inv}_{\text{EPRL}} \left( \bigotimes_{\ell \text{ incoming to } n} \mathcal{H}_{j_\ell^+ j_\ell^-}^* \otimes \bigotimes_{\ell' \text{ outgoing from } n} \mathcal{H}_{j_{\ell'}^+ j_{\ell'}^-} \right) \subset \mathcal{H}_n. \quad (6.18)$$

## 6. Operator spin-network diagrams

- We color each graph  $\gamma_I$  with the natural trace contractor (6.12):

$$\mathcal{A}_I = \text{Tr}_I. \quad (6.19)$$

The spin-network diagram operator corresponding to  $(\mathcal{D}, \rho, P, \mathcal{A})$  is

$$\mathcal{Z}(\mathcal{D}, \rho, P, \mathcal{A}) = \prod_{[l] \in \mathfrak{F}_{\text{open}}} \frac{1}{\sqrt{d_{[l]}}} \prod_{[l] \in \mathfrak{F}} d_{[l]} \text{Tr}(\mathcal{D}, \rho, P, \mathcal{A}),$$

where  $d_{[l]} = \dim \rho_{j_\ell^+ j_\ell^-} = (2j_\ell^+ + 1)(2j_\ell^- + 1)$  for any link  $\ell \in [l]$ .

The corresponding operator spin foam model is the Spin(4) operator spin foam model with the EPRL vertex described in section 5.3.3.

### 6.3.2. The SU(2) OSD model with the EPRL vertex

Given a value  $\beta \in \mathbb{Q}$ ,  $\beta \neq 0, \pm 1$ , the SU(2) OSD with the EPRL vertex is a graph diagram  $\mathcal{D}$  with the following coloring.

- We color each link  $\ell$  with a unitary irreducible representation  $\rho_{k_\ell}$  of the SU(2) group ( $k_\ell \in \frac{1}{2}\mathbb{N}$ ) such that  $\frac{|1 \pm \beta|}{2} k_\ell \in \frac{1}{2}\mathbb{N}$ .
- We color each node  $n$  with the identity operator,

$$P_n = \text{id} \in \mathcal{H}_n \otimes \mathcal{H}_n^*.$$

- Let  $\text{Tr}_I \in \bigotimes_{\ell \in \gamma_I^{(1)}} \mathcal{H}_{j_\ell^+ j_\ell^-}$ , where  $j_\ell^\pm = \frac{|1 \pm \beta|}{2} k_\ell$ , be the natural trace contractor (6.12). We define a pull-back of  $\text{Tr}_I$  with the EPRL map (compare section 3.3.4):

$$\iota_{\text{EPRL}}^*(\text{Tr}_I) \left( \bigotimes_{n \in \gamma_I^{(0)}} \mathcal{I}_n \right) := \text{Tr}_I \left( \bigotimes_{n \in \gamma_I^{(0)}} \iota_{\text{EPRL}}(\mathcal{I}_n) \right),$$

for any  $\mathcal{I}_n \in \mathcal{H}_n$ . We color each graph  $\gamma_I$  with the contractor

$$\mathcal{A}_I = \iota_{\text{EPRL}}^*(\text{Tr}_I) \in \left( \bigotimes_n \mathcal{H}_n \right)^*. \quad (6.20)$$

It will be called the EPRL contractor and denoted by

$$\mathcal{A}_I^{\text{EPRL}} := \iota_{\text{EPRL}}^*(\text{Tr}_I).$$

The spin-network diagram operator corresponding to  $(\mathcal{D}, \rho, P, \mathcal{A})$  is

$$\mathcal{Z}(\mathcal{D}, \rho, P, \mathcal{A}) = \prod_{[l] \in \mathfrak{F}_{\text{open}}} \frac{1}{\sqrt{d_{[l]}}} \prod_{[l] \in \mathfrak{F}} d_{[l]} \text{Tr}(\mathcal{D}, \rho, P, \mathcal{A}),$$

where  $d_{[l]} = \dim \rho_{k_\ell} = 2k_\ell + 1$  for any link  $\ell \in [l]$ .

The corresponding operator spin foam model is the SU(2) operator spin foam model with the EPRL vertex described in section 5.3.3.<sup>2</sup>

## 7. Dipole Cosmology

Bianchi, Rovelli and Vidotto used the  $SU(2)$  spin-foam model with the EPRL vertex amplitude (see sections 3.4.2, 5.3.3, 6.3.2) to construct the first model of Quantum Cosmology based on the spin-foam formalism. They calculated a transition amplitude between coherent states peaked on homogeneous, isotropic geometries using certain approximations, and showed that the resulting amplitude recovers the vacuum Friedmann dynamics in a classical limit. The first approximation was a truncation of the LQG state space to the states associated with a generalized theta graph with 4 links, called a *dipole graph* (see figure 7.1a). The second one was a truncation of the transition amplitude to a contribution from a single foam (we will call it a BRV foam) with one internal vertex, four internal edges and a boundary formed by two disjoint dipole graphs (see figure 7.1b) — the first order of vertex expansion. The third one was that of large volume of the universe. The class of foams defined by OSD includes the BRV foam. However, it also includes a variety of other possible foams with one internal vertex, four internal edges and the given boundary, which *a priori* cannot be discarded. Contributions from some other foams having these properties were investigated in [115]. The class of foams we consider includes all the foams from [115] as well as many others. We found all of them [130] (see also [128]). In section 7.1 we will briefly summarize the Bianchi-Rovelli-Vidotto model. In the following sections 7.2, 7.3 and 7.4 we will describe the foams in the class defined by OSD that may contribute to the transition amplitude in the first order of the vertex expansion. In section 7.2 we will present the algorithm for constructing the diagrams. Different operator spin-network diagrams correspond to different choices of: orientations of the links of the two dipole graphs in the boundary; the graph corresponding to the internal vertex (which we call interaction graph); node relation; glueing map; coloring of the links of the graph diagram with unitary irreducible representations. In section 7.3 we will find all possible interaction graphs and in section 7.4 we discuss the remaining degrees of freedom.

At that point a question arises whether the transition amplitude including contributions from all the foams still has the correct classical limit. We expect that the transition amplitude in the limit of large universe is dominated by the BRV transition amplitude and therefore it indeed recovers the vacuum Friedmann dynamics in a classical limit. In section 7.5 we will present some arguments supporting this hypothesis.

### 7.1. The Bianchi-Rovelli-Vidotto model

The idea of the Bianchi-Rovelli-Vidotto model of spin-foam cosmology [49] is to calculate the transition amplitude of the  $SU(2)$  EPRL model with the EPRL vertex (see sections 3.4.2, 5.3.3, 6.3.2) between coherent states peaked on homogeneous, isotropic geometry. The amplitude is calculated under certain approximations and it is shown that in a classical limit the vacuum Friedmann dynamics is recovered. The following approximations are used:

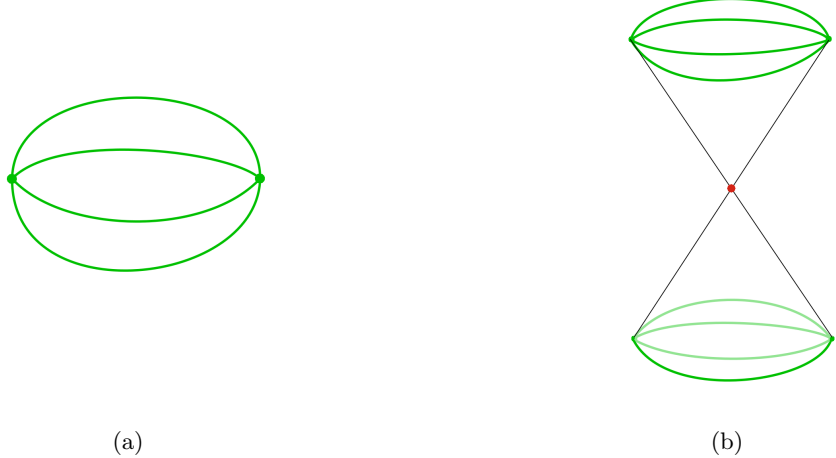


Figure 7.1.: (a) The dipole graph  $|\theta_4|$ , (b) The Bianchi-Rovelli-Vidotto 2-complex. It is a cone  $((|\theta_{\text{in}}| \sqcup |\theta_{\text{out}}|) \times [0, 1]) / ((|\theta_{\text{in}}| \sqcup |\theta_{\text{out}}|) \times \{0\})$ .

- 1. Graph expansion.** The Hilbert space is truncated to states supported on graphs contained in a generalized theta graph with four links  $\theta_4$  (see section 6.2.4), called a dipole graph [167, 49]:

$$\mathcal{H}_{\text{comb}}^{\theta_4} = \bigoplus_{\gamma \in \mathfrak{G}: \gamma \subseteq \theta_4} \tilde{\mathcal{H}}_\gamma$$

The corresponding truncation in the classical theory is defined by a triangulation of a three-sphere  $\mathbb{S}^3$  consisting of two tetrahedra which faces are identified. The tetrahedra correspond to the nodes of the graph (compare section 3.2.3). To each link of the dipole graph  $\theta_4$  there corresponds a triangle in the boundary of each tetrahedron – the triangles in the two different tetrahedra corresponding to the same link are identified. An approximation of the universe with two tetrahedra may seem to be crude. However, the Regge-type calculations show that even few tetrahedra may approximate the continuous FRW universe [61].

- 2. Vertex expansion.** The transition amplitude is truncated to a contribution from a single 2-complex with one internal vertex. The boundary of the 2-complex is formed by two disjoint unoriented dipole graphs  $|\theta_{\text{in}}| = |\theta_{\text{out}}| = |\theta_4|$  (see section 1.2.2 for the definition of an unoriented abstract graph). The 2-complex is a cone

$$C(|\theta_{\text{in}}| \sqcup |\theta_{\text{out}}|) = ((|\theta_{\text{in}}| \sqcup |\theta_{\text{out}}|) \times [0, 1]) / ((|\theta_{\text{in}}| \sqcup |\theta_{\text{out}}|) \times \{0\})$$

(see [112] and figure 7.1b). This approximation is analogous to first-order calculations in the perturbation approach to Quantum Field Theory [49, 165, 168].

- 3. Large volume expansion.** The transition amplitude is calculated in the limit in which the universe is large compared to the Planck scale.

The geometry is encoded in coherent states (in and out). Each state is of the heat-kernel type [49, 45, 46, 176, 173, 174, 175, 170, 177, 30, 31, 92, 93, 18]:

$$\Psi_{H_\ell}(U_\ell) = \int \prod_{n \in \theta_4^{(0)}} d\mu_H(g_n) \prod_{\ell \in \theta_4^{(1)}} K_t(g_{t(\ell)}^{-1} U_\ell g_{s(\ell)} H_\ell^{-1}), \quad (7.1)$$

where  $K_t$  is the analytic continuation to  $\text{SL}(2, \mathbb{C})$  of the heat kernel on  $\text{SU}(2)$ ,  $t$  is a spread of the heat kernel. The integration is over two copies of the  $\text{SU}(2)$  group and implements the projection onto gauge invariant states. The state is peaked at a classical geometry encoded in  $\text{SL}(2, \mathbb{C})$  matrices  $H_\ell$ . The homogeneity and isotropy of the geometry is reflected in a special form of the matrices:

$$H_\ell(u_\ell, z_\ell) = u_\ell e^{iz_\ell \frac{\sigma_3}{2}} u_\ell^{-1}, \quad (7.2)$$

where  $u_\ell \in SU(2)$ ,

$$z_\ell = \begin{cases} z_{\text{in}} \in \mathbb{C}, & \text{if } \ell \text{ is a link of the graph } |\theta_{\text{in}}|, \\ z_{\text{out}} \in \mathbb{C}, & \text{if } \ell \text{ is a link of the graph } |\theta_{\text{out}}|, \end{cases}$$

$\sigma_1, \sigma_2, \sigma_3$  are the Pauli matrices. Each matrix  $u_\ell$  gives rise to a normalized vector  $\vec{n}_\ell \in \mathbb{R}^3$  defined by  $\vec{n}_\ell \cdot \vec{\sigma} = u_\ell \sigma_3 u_\ell^{-1}$ . The vectors  $\vec{n}_\ell$  ( $-\vec{n}_\ell$ ) are interpreted as vectors normal to the corresponding triangles bounding the tetrahedron associated to the source (target) of the link  $\ell$ . It is assumed that the tetrahedra are regular [165], i.e.  $\vec{n}_\ell \cdot \vec{n}_{\ell'} = -\frac{1}{3}$  for any two different links  $\ell \neq \ell'$ . The real and imaginary parts of the complex numbers  $z_{\text{in/out}}$  are interpreted as the standard scale factor  $a$  of cosmology and its time derivative  $\dot{a}$ , i.e. the real part of  $z_{\text{in/out}}$  is proportional to  $\dot{a}_{\text{in/out}}$  and the imaginary part is proportional to  $a_{\text{in/out}}$ ,  $\Re(z_{\text{in/out}}) \sim \dot{a}_{\text{in/out}}$ ,  $\Im(z_{\text{in/out}}) \sim a_{\text{in/out}}$ . The transition amplitude is a function of two complex variables  $W(z_{\text{in}}, z_{\text{out}})$ . In the approximation of large universe it satisfies a quantum constraint:

$$\hat{H} W(z, z') = 0. \quad (7.3)$$

The corresponding classical constraint turns out to be the Friedmann hamiltonian constraint [49].

Our expectation is that the transition amplitude  $\widetilde{W}(z, z')$ , including contributions from the operator spin-network diagrams we find in this chapter, converges in a limit of large universe to  $W(z, z')$  and therefore the full transition amplitude in the approximation of large universe still satisfies the quantum constraint:  $\hat{H} \widetilde{W}(z, z') = 0$ .

## 7.2. The algorithm

We will present now an algorithm for constructing all the operator spin-network diagrams with boundary fixed (modulo orientations of the links) to be the graph  $|\gamma_{\text{dipole}}|$  that consists of two disjoint 4-valent theta graphs  $|\theta_{\text{in}}| = |\theta_{\text{out}}| = |\theta_4|$  (figure 7.2),

$$|\gamma_{\text{dipole}}| = |\theta_{\text{in}}| \sqcup |\theta_{\text{out}}|, \quad (7.4)$$

and such that the corresponding operator spin foams have one internal vertex and four internal edges. The spin foams contribute to the transition amplitude in the first order of vertex expansion. The algorithm is the following:

## 7. Dipole Cosmology

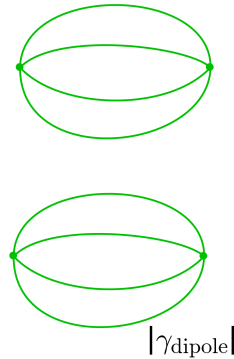


Figure 7.2.: The dipole boundary graph  $|\gamma_{\text{dipole}}| = |\theta_{\text{in}}| \sqcup |\theta_{\text{out}}|$ .

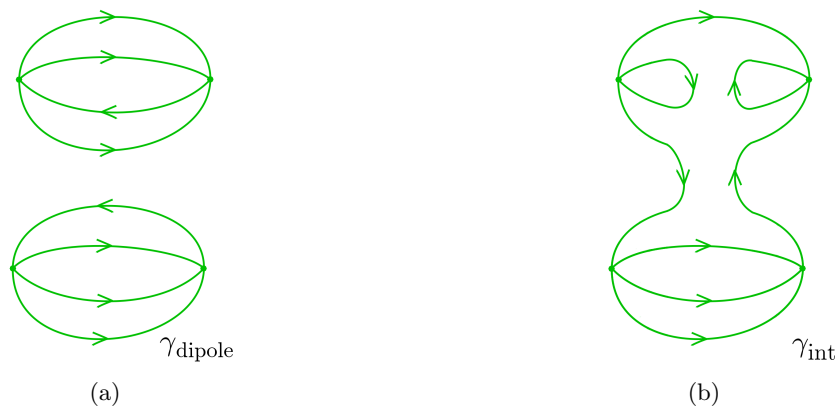


Figure 7.3.: Construction of the graph diagram. (a) Step 1 – choose an orientation of each link of the unoriented graph  $|\gamma_{\text{dipole}}|$ . (b) Step 2 – construct an interaction graph  $\gamma_{\text{int}}$ ; an example is depicted.

1.  $\gamma_{\text{dipole}}$ : choose an orientation of each link of the unoriented graph  $|\gamma_{\text{dipole}}|$  (figure 7.3a), i.e. choose a representant of the equivalence class  $|\gamma_{\text{dipole}}|$ .
  2.  $\gamma_{\text{int}}$ : Construct an interaction graph  $\gamma_{\text{int}}$ . It is any graph with the following properties:

$$\gamma_{\text{dipole}}^{(0)} = \gamma_{\text{int}}^{(0)}, \quad (7.5)$$

$$\forall n \in \gamma_{\text{dipole}}^{(0)} \quad \#(\gamma_{\text{int}})_n^{\text{in}} = \#(\gamma_{\text{dipole}})_n^{\text{in}} \quad \wedge \quad \#(\gamma_{\text{int}})_n^{\text{out}} = \#(\gamma_{\text{dipole}})_n^{\text{out}}. \quad (7.6)$$

We obtain each interaction graph  $\gamma_{\text{int}}$  by assigning an orientation to each link of an unoriented graph  $|\gamma_{\text{int}}|$  having the following two properties:

- each graph  $|\gamma_{\text{int}}|$  has exactly **4 nodes**,
  - each node of  $|\gamma_{\text{int}}|$  is precisely **four-valent**.

In the next subsection we will construct and list all the possible unoriented interaction graphs  $|\gamma_{\text{int}}|$  (they are depicted in figure 7.10).

3.  $\mathcal{D}_{\gamma_{\text{dipole}}} \# \gamma_{\text{int}}$ : Use the static graph diagram  $\mathcal{D}_{\gamma_{\text{dipole}}}$  of the graph  $\gamma_{\text{dipole}}$  (see section 6.2.4 and figure 7.4a) and the interaction graph  $\gamma_{\text{int}}$  to construct a diagram  $\mathcal{D}_{\gamma_{\text{dipole}}} \# \gamma_{\text{int}}$  (figure 7.4b). It is any graph diagram with the following properties:

- The set of graphs consists of the graphs  $\tilde{\theta}_n, n \in \gamma_{\text{dipole}}^{(0)}$  and the connected components of  $\gamma_{\text{int}}$ .
- The node relation is such that:  $s_\ell$  is in relation with  $t_\ell$  (see section 6.2.4), each node  $n^d$  is in relation with a node  $n' \in \gamma_{\text{int}}^{(0)}$ , each node  $n^u$  is a boundary node.
- The glueing map is arbitrary.

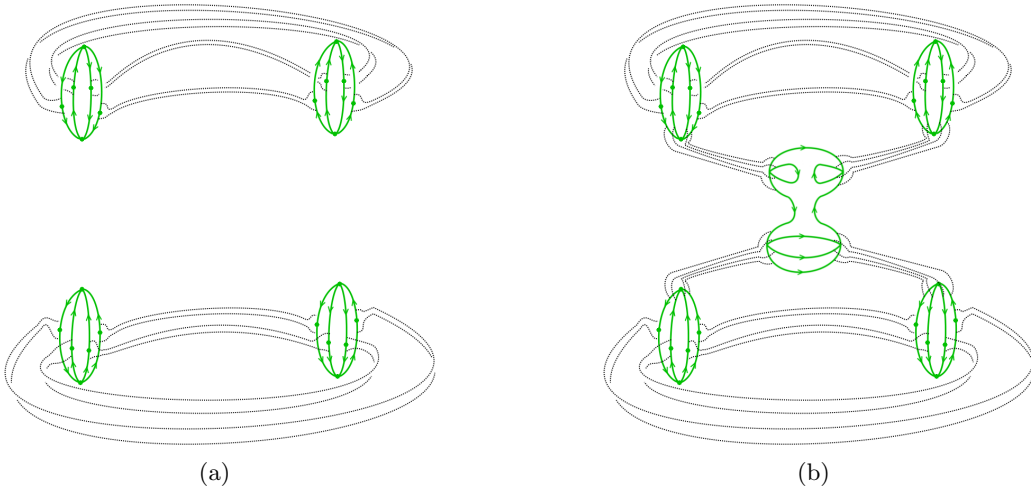


Figure 7.4.: Step 3 – construction of the graph diagram  $\mathcal{D}_{\gamma_{\text{dipole}}} \# \gamma_{\text{int}}$ : (a) the static graph diagram  $\mathcal{D}_{\gamma_{\text{dipole}}}$ , (b) the graph diagram  $\mathcal{D}_{\gamma_{\text{dipole}}} \# \gamma_{\text{int}}$ . The dotted lines denote the glueing map.

4. Define the following colorings:

- a coloring  $\rho_k$  of the links of the diagram  $\mathcal{D}_{\gamma_{\text{dipole}}} \# \gamma_{\text{int}}$  with unitary irreducible representations of the SU(2) group such that

$$\forall \ell \in \mathcal{G}^{\text{out}} \quad \rho_{k_\ell} = \rho_{k_{\varphi(\ell)}}, \quad (7.7)$$

- a coloring of the nodes of the graphs with the identity operators

$$P_n = \text{id} \in \mathcal{H}_n \otimes \mathcal{H}_n^*, \quad n \in \mathcal{G}^{(0)},$$

- a coloring of the graphs  $\tilde{\theta}_n$  with the natural contractors (6.12),
- a coloring of each connected component of the interaction graph  $\gamma_{\text{int}}$  with the EPRL contractor (6.20).

Let us note that the induced coloring of the corresponding foam is not exactly that of the SU(2) operator spin-foam model with the EPRL vertex but rather that of the symmetric but not natural model from section 5.3.3. However, the resulting operator spin foam is equivalent to an SU(2) operator spin foam with the EPRL vertex amplitude.

## 7. Dipole Cosmology

5. Consider all the possible: orientations of the links of  $\gamma_{\text{dipole}}$ , interaction graphs  $\gamma_{\text{int}}$ , node relations between the nodes of the interaction graph and corresponding nodes of static diagram, glueing maps, colorings of the links with unitary irreducible representations of the SU(2) group.

The algorithm is a special case of a general algorithm for finding all spin foams with a given boundary graph, number of internal vertices and number of internal edges that was introduced in [130]. Let us note that strictly speaking the foam corresponding to  $\mathcal{D}_{\gamma_{\text{dipole}}} \# \gamma_{\text{int}}$  has more than one internal vertex. The first reason is that there are internal vertices corresponding to the graphs  $\tilde{\theta}_n$ . The second reason is that there is one internal vertex corresponding to each connected component of  $\gamma_{\text{int}}$  and if the graph  $\gamma_{\text{int}}$  is not connected, each connected component contributes one internal vertex. However, the resulting operator spin foam can be obtained from an operator spin foam with 1 internal vertex by a sequence of moves of splitting edges and faces from section 5.1.2 supplemented by a move of pulling the internal vertices apart from [28]. As a result, thanks to the chosen coloring, the operator spin foam is equivalent to an SU(2) operator spin foam with 1 internal (EPRL) vertex.

### 7.3. All the possible interaction graphs

In this subsection we construct all the possible graphs  $|\gamma_{\text{int}}|$ . We depicted the resulting graphs in figure 7.10. In order to obtain an interaction graph  $\gamma_{\text{int}}$ , we assign to each link of a graph  $|\gamma_{\text{int}}|$  an orientation consistent with the orientation of the boundary. Let us note that such assignment is not always possible. For example, take graph 1 from figure 7.10 as a graph  $|\gamma_{\text{int}}|$ . It is not possible to choose orientations of the links of this graph compatible with orientation of the links of the boundary graph from figure 7.3a, because the boundary graph in figure 7.3a has a node with three outgoing and one incoming link and such structure of incoming/outgoing links is not possible for any node of the graph 1 from figure 7.10 (since each link of this graph forms a loop, the number of incoming links and outgoing links needs to be equal at every node). Note, that there is a distinguished graph  $|\gamma_{\text{int}}|$  – the graph 19 from figure 7.10 used in [49]. This graph may be oriented in a way compatible with any boundary graph  $\gamma_{\text{dipole}}$ . There arises a question if each interaction graph from figure 7.10 can be oriented in a such way that its orientation is compatible with some orientation of the boundary graph. The answer is affirmative: for each graph  $|\gamma_{\text{int}}|$  the orientations of its links may be chosen to be compatible with a boundary graph oriented in a such way that at every node the number of incoming links equals to the number of outgoing links.

We now present in detail the construction of unoriented graphs with exactly 4 nodes, all of which are four-valent, i.e. all possible graphs  $|\gamma_{\text{int}}|$ . It is well known that each unoriented graph may be encoded in adjacency matrix. It is a symmetric matrix  $A \in \text{Sym}(N)$  with the number of columns/rows equal to the number of the vertices of this graph. The entries  $A_{IJ}$  are equal to the numbers of links connecting node I with node J, with a specification that links forming closed loops (corresponding to diagonal entries) are counted twice. An example of such matrix and the corresponding graph is given on figure 7.5.

However, to a given graph there are many corresponding matrices, because for each

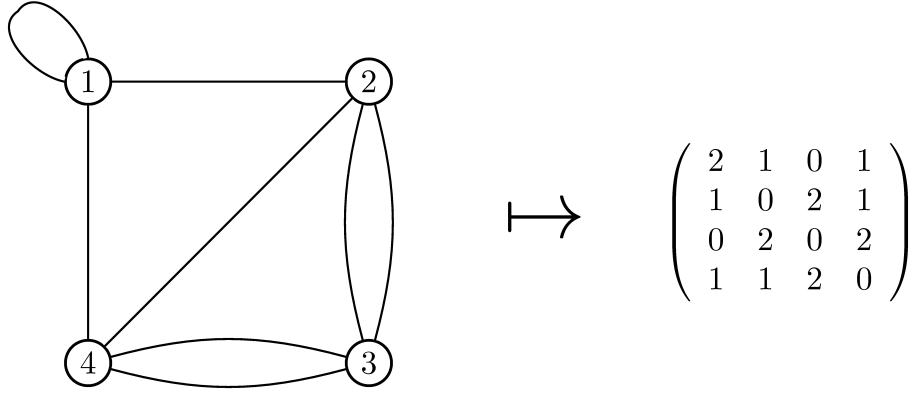


Figure 7.5.: A graph and the corresponding adjacency matrix.

permutation  $\pi \in S_N$  the matrices

$$(\pi \circ A)_{IJ} := A_{\pi(I)\pi(J)} \quad (7.8)$$

and  $A_{IJ}$  define the same graph. There is a natural bijective correspondence between the graphs with  $N$  vertices and the orbits of the action (7.8) of the permutation group on the set of symmetric matrices, i.e. elements of  $\text{Sym}(N)/S_N$ .

In our case the graphs have four nodes. We are therefore interested in  $4 \times 4$  symmetric matrices. The condition that each node is 4-valent corresponds to an assumption that the sum of numbers in each row/column is equal to 4:

$$\forall I \quad \sum_{J=1}^4 A_{IJ} = 4. \quad (7.9)$$

The set of the possible interaction graphs is therefore characterized by the moduli space:

$$\left\{ A \in \text{Sym}(4) : \forall I \quad \sum_{J=1}^4 A_{IJ} = 4 \right\} / S_4. \quad (7.10)$$

First, we introduce a parametrization of the space of symmetric matrices with natural number entries satisfying (7.9) and then we find the moduli space (7.10) using Wolfram's Mathematica 8.0.

To define our parametrization in a transparent way we introduce a triple  $(K_4, d, m)$  (see figure 7.6):

- the complete graph  $K_4$  on four nodes, i.e. an unoriented graph with four nodes,  $K_4^{(0)} = \{n_1, n_2, n_3, n_4\}$ , and six links,  $K_4^{(1)} = \{\ell_{12}, \ell_{13}, \ell_{14}, \ell_{23}, \ell_{24}, \ell_{34}\}$ , each link  $\ell_{IJ}$  connecting a node  $n_I$  with a node  $n_J$ ;
- a labelling of its nodes  $d : K_4^{(0)} \rightarrow \{0, 2, 4\}$ ,

$$n \mapsto d_n, \quad (7.11)$$

such that the numbers  $d_{n_1}, d_{n_2}, d_{n_3}, d_{n_4}$  satisfy the generalized triangle inequalities:

$$\forall I \quad d_{n_I} \leq \sum_{J \neq I} d_{n_J}. \quad (7.12)$$

## 7. Dipole Cosmology

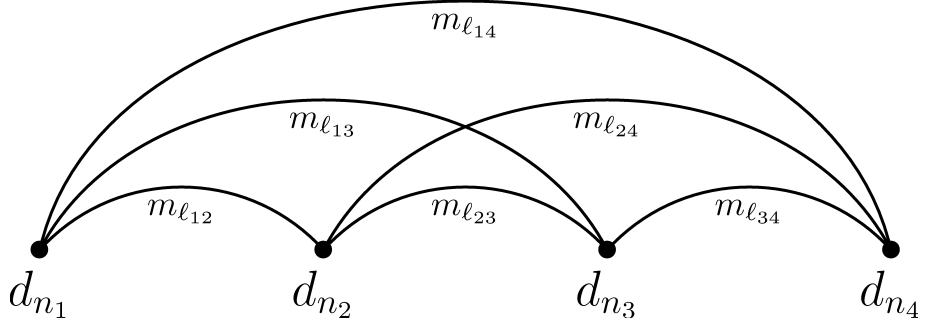


Figure 7.6.: A graphical representation of  $(K_4, d, m)$ .

- a labeling of its links  $m : K_4^{(1)} \rightarrow \{0, 1, 2, 3, 4\}$ ,

$$\ell \mapsto m_\ell, \quad (7.13)$$

such that

$$\forall_{n \in K_4^{(0)}} \sum_{\{\ell \in K_4^{(1)} : \ell \cap n \neq \emptyset\}} m_\ell = d_n \quad (7.14)$$

The condition that  $d_n, n \in K_4^{(0)}$  satisfy the generalized triangle inequalities (7.12) ensures the existence of at least one labeling  $m^1$ .

To each triple  $(K_4, d, m)$  there corresponds an unoriented graph  $|\gamma_{(K_4, d, m)}|$ , defined in the following way (see also an example on figure 7.7):

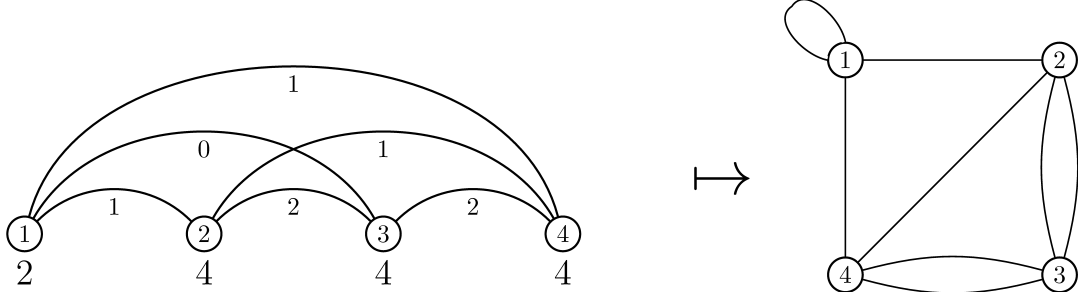


Figure 7.7.: An example of the correspondence between  $(K_4, d, m)$  and  $|\gamma_{(K_4, d, m)}|$ . The numbering of the nodes is redundant here. However, we add it to make the exposition clearer.

- it has the same set of nodes,  $\gamma_{(K_4, d, m)}^{(0)} = K_4^{(0)}$ ,
- two different nodes  $n_I$  and  $n_J$  of  $|\gamma_{(K_4, d, m)}|$  are connected with precisely  $m_{\ell_{IJ}}$  links,
- for each node  $n$  there are precisely  $(4 - d_n)/2$  links connecting  $n$  with itself (figure 7.8).

Alternatively we may read from  $(K_4, d, m)$  the corresponding adjacency matrix:

---

<sup>1</sup>This well known fact is used for example in the representation theory of SU(2) to construct the invariant tensors in the tensor product  $\mathcal{H}_{d_{n_1}/2} \otimes \mathcal{H}_{d_{n_2}/2} \otimes \mathcal{H}_{d_{n_3}/2} \otimes \mathcal{H}_{d_{n_4}/2}$ , where  $\dim \mathcal{H}_j = 2j + 1$ , and  $d_{n_1} + \dots + d_{n_4} \in 2\mathbb{N}$  by the construction.

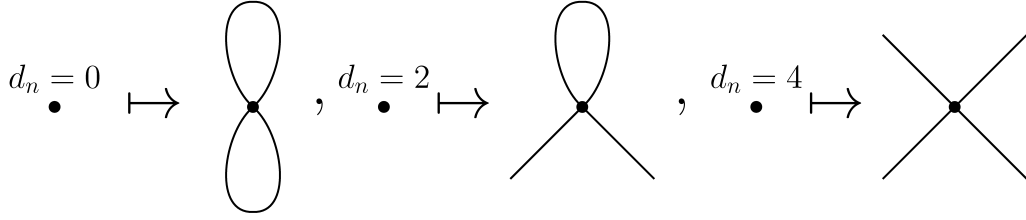


Figure 7.8.: The correspondence between the number  $d_n$  and the structure of the links at the node  $n \in \gamma_{(K_4, d, m)}^{(0)}$ .

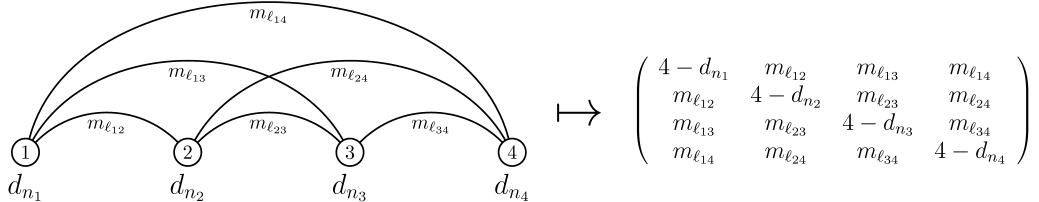


Figure 7.9.: The adjacency matrix corresponding to  $(K_4, d, m)$ .

- the diagonal entries of the adjacency matrix are equal to  $4 - d_{n_l}$ , i.e.  $A_{ll} := 4 - d_{n_l}$ ,
- the off-diagonal entries of the adjacency matrix are equal to  $m_{\ell_{lj}}$ , i.e.

$$A_{lj} := \begin{cases} m_{\ell_{lj}} & \text{if } l < j, \\ m_{\ell_{jl}} & \text{if } j < l. \end{cases}$$

This correspondence is depicted in figure 7.9. Let us note that being given the numbers  $d_n$ , the total number of links going from nodes  $n_1, n_2$  to nodes  $n_3, n_4$  (we denote the number by  $k$ ) and the number  $m_{\ell_{23}}$ , we can reconstruct the remaining coloring of  $(K_4, d, m)$ . As a result those numbers give the parametrization of the adjacency matrix. Explicitly, we parametrize the solutions to equations (7.9) with

- four numbers  $d_1, d_2, d_3, d_4 \in \{0, 2, 4\}$  satisfying triangle inequalities (7.12),
- a natural number  $k \in [|d_1 - d_2|, d_1 + d_2] \cap [|d_3 - d_4|, d_3 + d_4]$ , such that  $k + d_1 + d_2 \in 2\mathbb{N}$ ,
- an even natural number  $m \in [d_3 - d_4 + d_2 - d_1, \min\{d_3 - d_4 + k, d_2 - d_1 + k\}]$ .

The corresponding parametrization is:

$$A = \begin{pmatrix} 4 - d_1 & \frac{d_1 + d_2 - k}{2} & \frac{d_2 - d_1 + k - m}{2} & \frac{d_4 - d_3 + d_1 - d_2 + m}{2} \\ \frac{d_1 + d_2 - k}{2} & 4 - d_2 & \frac{m}{2} & \frac{d_3 - d_4 + k - m}{2} \\ \frac{d_2 - d_1 + k - m}{2} & \frac{m}{2} & 4 - d_3 & \frac{d_3 + d_4 - k}{2} \\ \frac{d_4 - d_3 + d_1 - d_2 + m}{2} & \frac{d_3 - d_4 + k - m}{2} & \frac{d_3 + d_4 - k}{2} & 4 - d_4 \end{pmatrix}. \quad (7.15)$$

Next, using Mathematica 8.0 we find the orbits of the action of the permutation group  $S_4$  on the set of the matrices of the form (7.15). The resulting graphs are depicted in figure 7.10.

## 7. Dipole Cosmology

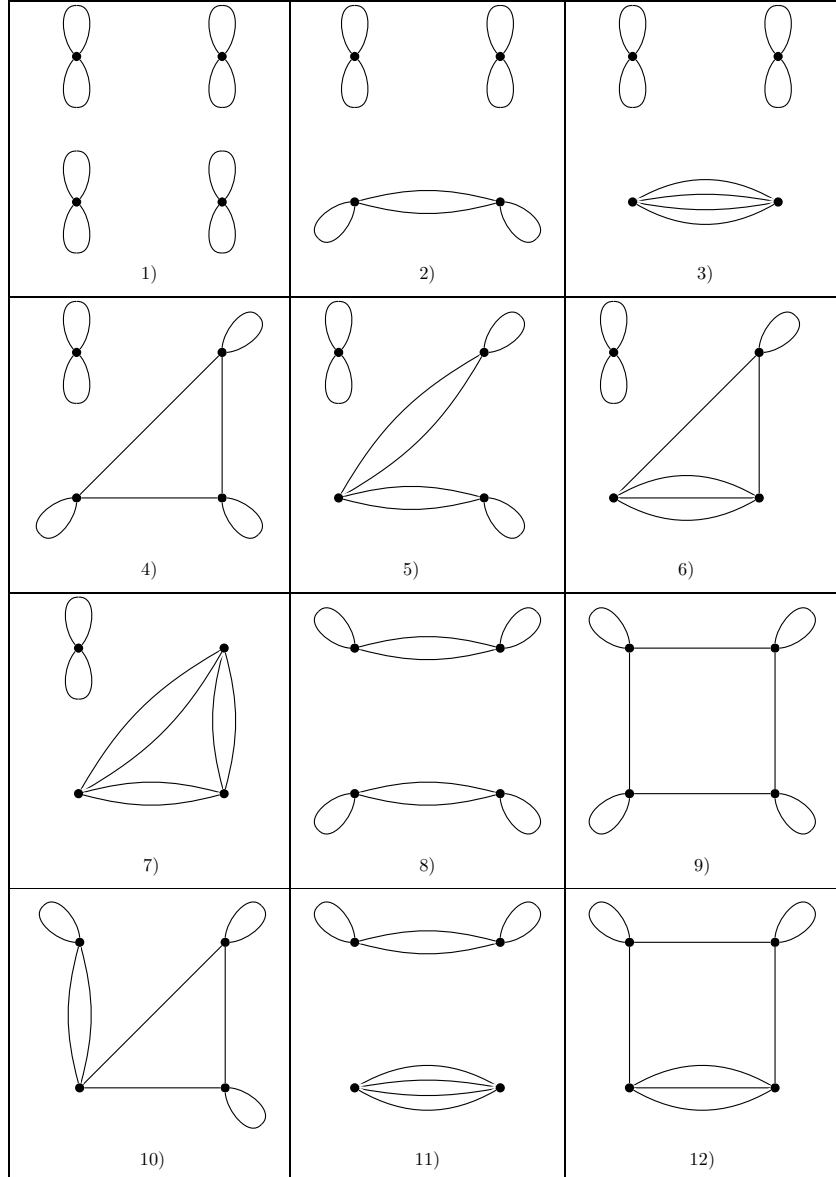


Figure 7.10.: The list of all the possible interaction graphs in the first order of the vertex expansion (modulo orientations).

Note that the spin foams considered in [115] have the interaction graphs of type 17, 18 or 19.

Let us note that one could further restrict the number of matrices considered by requiring that the sequence  $(d_1, d_2, d_3, d_4)$  is monotonous and considering only orbits under the action of  $S_4/H$ , where  $H$  is the subgroup, which does not change the sequence  $(d_1, d_2, d_3, d_4)$ . This remark enables one to do the calculation without using a computer. On the other hand, one could write a program which does not use the parametrization we introduced – e.g. one could generate matrices with entries taking values in the set  $\{0, 1, 2, 3, 4\}$  (with even numbers on diagonal) and choose only those which satisfy equa-

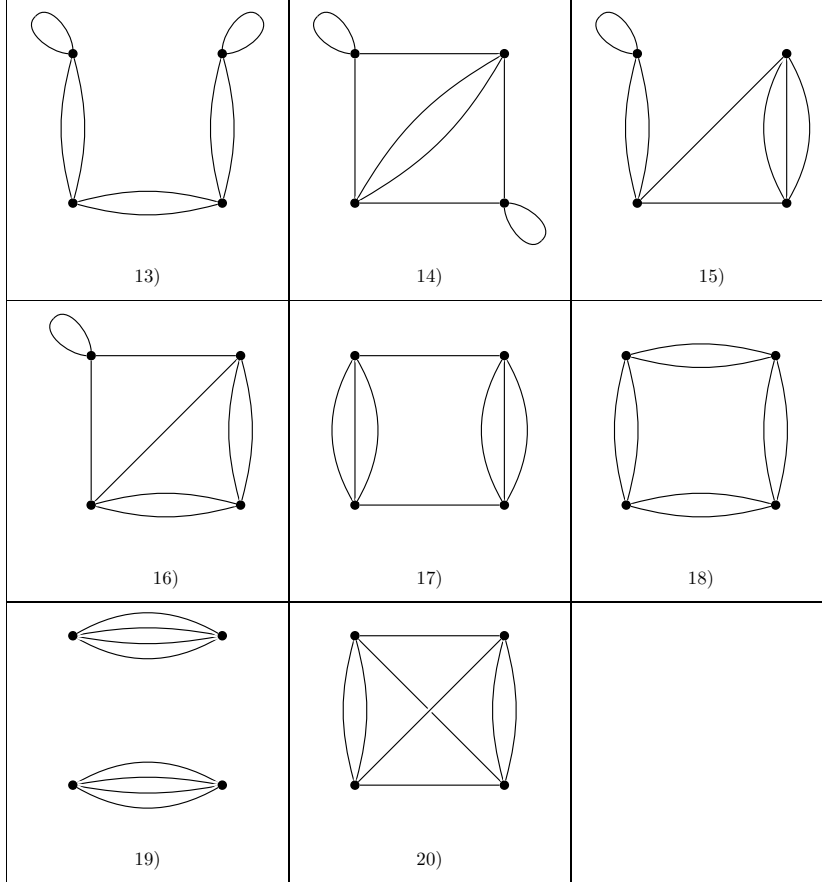


Figure 7.10.: (Continued.)

tion (7.9) (a direct method). We have chosen the method we present here, because it gives better understanding of the structure of the graphs considered, it is less laborious than calculation without using computer and it is easily applicable to a more general case studied in [181, 56] where the four nodes are not necessarily four-valent. When  $d_1, d_2, d_3, d_4$  are becoming larger, this method becomes considerably faster than the direct method.

## 7.4. Possible operator spin-network diagrams

As we have explained in the previous subsection, there are exactly 20 interaction graphs. In this subsection we discuss in more detail the diversity of the operator spin-network diagrams resulting from the procedure from section 7.2.

### 7.4.1. Possible graph diagrams

For a given oriented interaction graph  $\gamma_{\text{int}}$  and a static diagram  $\mathcal{D}_{\gamma_{\text{dipole}}}$ , there may be more than one graph diagram  $\mathcal{D}_{\gamma_{\text{dipole}}} \# \gamma_{\text{int}}$ . The ambiguity is in the choice of the node relation and the glueing map.

## 7. Dipole Cosmology

- **The ambiguity in the choice of a node relation.** It exists if an oriented interaction graph  $\gamma_{\text{int}}$  has two nodes, say  $n_1$  and  $n_2$ , such that the number of the incoming/outgoing links at  $n_1$  is equal to the number of the incoming/outgoing links at  $n_2$ . Then, for every node relation between the nodes of the interaction graph and the corresponding nodes of the static diagram, there is another, different node relation obtained by switching the nodes  $n_1$  and  $n_2$  – see figure 7.11.

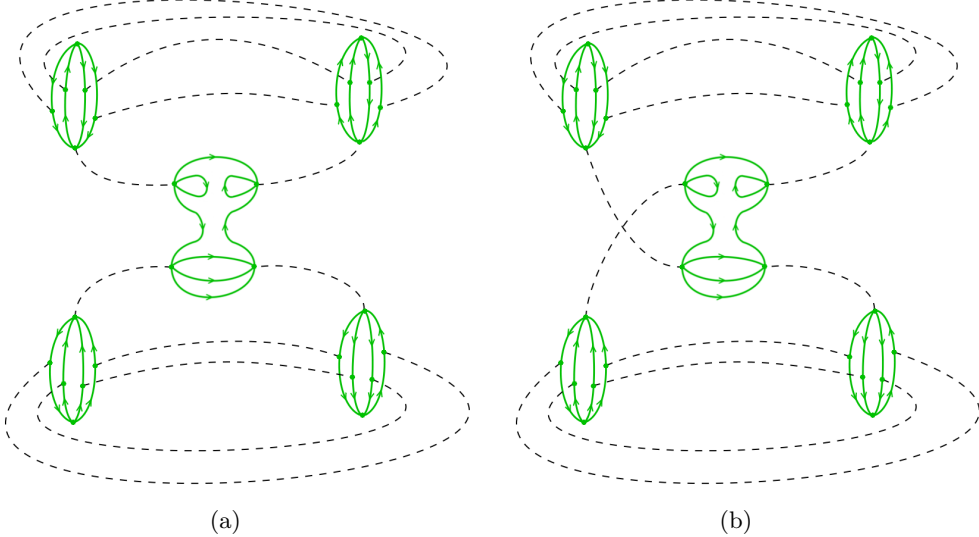


Figure 7.11.: Two nonequivalent graph diagrams  $\mathcal{D}_{\gamma_{\text{dipole}}} \# \gamma_{\text{int}}$  obtained by different choices of a node relation between the nodes of the interaction graph and the nodes of the static diagram. The nodes connected by a dashed line are in node relation.

- **The ambiguity in the choice of a glueing map.** Having settled down the node relation, there are still many possible glueing maps (see figure 7.12).

### 7.4.2. Possible colorings

We say that a coloring of the links of the boundary graph  $\rho_k : \gamma_{\text{dipole}}^{(1)} \rightarrow \text{Irr}(\text{SU}(2))$  is compatible with a graph diagram  $\mathcal{D}_{\gamma_{\text{dipole}}} \# \gamma_{\text{int}}$ , if there exists a coloring  $\tilde{\rho}_k$  of the links of the graph diagram  $\mathcal{D}_{\gamma_{\text{dipole}}} \# \gamma_{\text{int}}$  satisfying (7.7) and such that

$$\tilde{\rho}_{k_{(n,s_\ell)}} = \rho_{k_\ell}, \quad \tilde{\rho}_{k_{(n,t_\ell)}} = \rho_{k_\ell}, \quad (7.16)$$

where  $n \in \{n^d, n^u\} \subset \tilde{\theta}_n^{(0)}$ . If the coloring  $\rho_k$  is compatible with a graph diagram  $\mathcal{D}_{\gamma_{\text{dipole}}} \# \gamma_{\text{int}}$  then the conditions (7.7) and (7.16) uniquely define a coloring  $\tilde{\rho}_k$  of the links of the graph diagram  $\mathcal{D}_{\gamma_{\text{dipole}}} \# \gamma_{\text{int}}$ . For a given coloring  $\tilde{\rho}_k$  the coloring with operators  $P$  and contractors  $\mathcal{A}$  is uniquely defined (see section 7.2). As a result each coloring  $\rho_k$  of the links of the boundary graph  $\gamma_{\text{dipole}}$  compatible with a graph diagram  $\mathcal{D}_{\gamma_{\text{dipole}}} \# \gamma_{\text{int}}$  defines a coloring of this graph diagram. Each coloring of a graph diagram  $\mathcal{D}_{\gamma_{\text{dipole}}} \# \gamma_{\text{int}}$  can be defined this way.

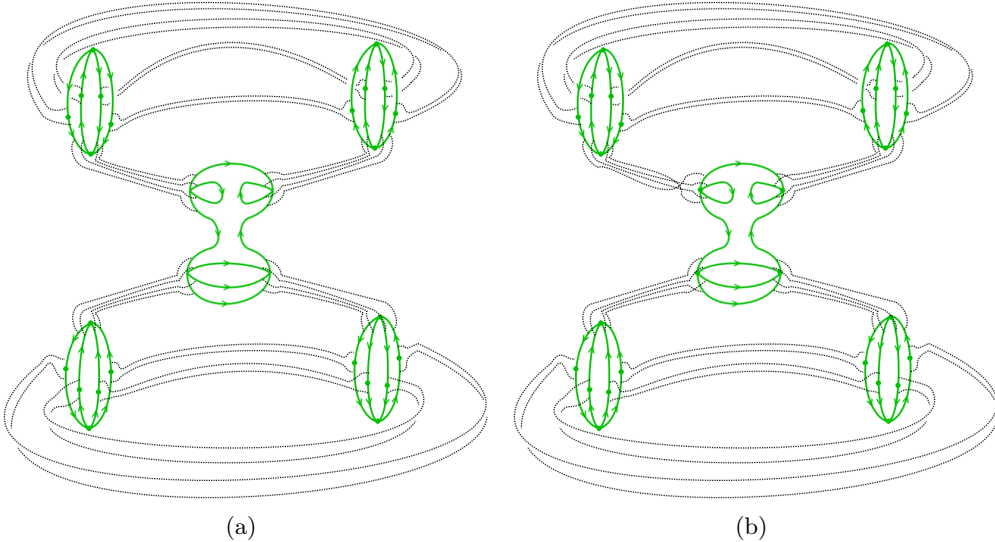


Figure 7.12.: Being given an oriented interaction graph, a static diagram and a node relation one may choose different glueing maps. Diagrams (a) and (b) are different. The node relation is depicted in figure 7.11a, the glueing map is denoted by the dotted lines.

Some colorings of the links of the boundary graph  $\rho_k : \gamma_{\text{dipole}}^{(1)} \rightarrow \text{Irr}(\text{SU}(2))$  are not compatible with a given graph diagram  $\mathcal{D}_{\gamma_{\text{dipole}}} \# \gamma_{\text{int}}$ . For example, let us consider the coloring of the boundary graph depicted in figure 7.13a and the OSD in figure 7.13b (node relations are depicted in figure 7.11a, the coloring with operators and contractors was described in section 7.2). It is straightforward to see that there exists a coloring of the links satisfying the conditions (7.7) and (7.16) if and only if

$$\rho_4 = \rho_5, \quad \rho_6 = \rho_7.$$

There is a distinguished graph diagram, which is not limited by the coloring in the way described above – it is the BRV graph diagram (see figure 7.14), i.e. the graph diagram which corresponding foam is the BRV foam. It is compatible even with a coloring of the links of the boundary graph with pairwise different representations. Moreover, it is the only graph diagram compatible with such generic coloring.

## 7.5. The transition amplitude

We expect that the contribution from the BRV foam is dominating all other contributions in the limit of large volume of the universe. As a result, the total transition amplitude still recovers the vacuum Friedmann dynamics in the classical limit. In this section we present some arguments supporting this scenario. The full proof will appear in [126].

We calculate an amplitude  $W(z_{\text{in}}, z_{\text{out}})$  corresponding to a graph diagram  $\mathcal{D}_{\gamma_{\text{dipole}}} \# \gamma_{\text{int}}$  in the limit of large volume of the universe. First, we use the Peter-Weyl expansion of the

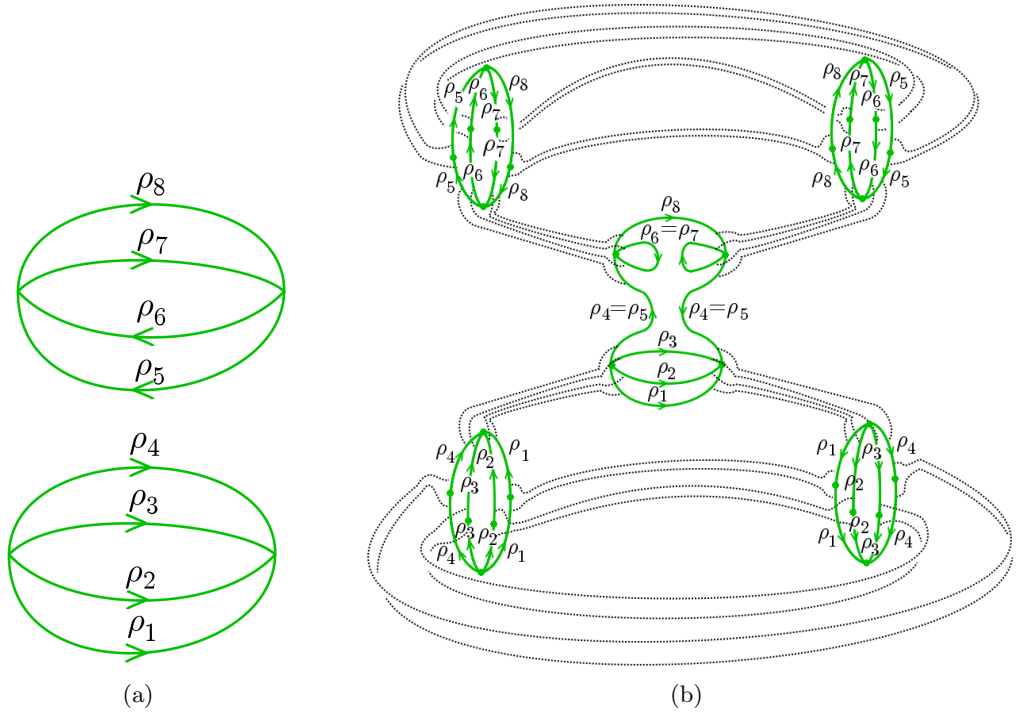


Figure 7.13.: Compatibility of a coloring of the boundary graph with a given graph diagram – an example. (a) A coloring of the links of a boundary graph. (b) A coloring of the links of a graph diagram. The glueing map is denoted by the dotted lines. The node relation if depicted in figure 7.11a and the corresponding coloring with operators and contractors was described in section 7.2. The coloring (a) is compatible with the graph diagram (b) if and only if  $\rho_4 = \rho_5$  and  $\rho_6 = \rho_7$ . If this condition is satisfied the coloring (a) induces the coloring (b).

heat-kernel function:

$$K_t(g_{t(\ell)}^{-1} U_\ell g_{s(\ell)} H_\ell^{-1}) = \sum_{k_\ell} (2k_\ell + 1) e^{-k_\ell(k_\ell+1)t} \text{Tr} \left( \rho_{k_\ell} (g_{t(\ell)}^{-1} U_\ell g_{s(\ell)}) \rho_{k_\ell} (H_\ell^{-1}) \right).$$

Next, we approximate  $\rho_{k_\ell}(H_\ell^{-1})$  in the limit of large volume of the universe [45, 49]:

$$\rho_{k_\ell}(H_\ell^{-1}) \approx e^{-iz_\ell k_\ell} \rho_{k_\ell}(u_\ell) |k_\ell k_\ell\rangle \langle k_\ell k_\ell| \rho_{k_\ell}(u_\ell^{-1}) = e^{-iz_\ell k_\ell} |k_\ell \vec{n}_\ell\rangle \langle k_\ell \vec{n}_\ell|, \quad (7.17)$$

where

$$|k_\ell \vec{n}_\ell\rangle = \rho_{k_\ell}(u_\ell) |k_\ell k_\ell\rangle$$

is the Perelomov coherent state [143]<sup>2</sup>. The transition amplitude becomes:

$$W(z_{\text{in}}, z_{\text{out}}) = \prod_{\ell \in \gamma_{\text{dipole}}^{(1)}} \sum_{k_\ell} \sqrt{2k_\ell + 1} e^{-k_\ell(k_\ell+1)t - iz_\ell k_\ell} \langle s_{\text{out}} | \mathcal{Z}(\mathcal{D}_{\gamma_{\text{dipole}}} \# \gamma_{\text{int}}, \tilde{\rho}_k, P, \mathcal{A}) | s_{\text{in}} \rangle, \quad (7.18)$$

<sup>2</sup>The Perelomov coherent states are defined up to a phase. Obviously the expression (7.17) does not depend on the choice of the phase.

where  $s_{\text{in}} = (\theta_{\text{in}}, \rho_k|_{\theta_{\text{in}}}, \iota^{\text{LS}})$  and  $s_{\text{out}} = (\theta_{\text{out}}^\dagger, \rho_k|_{\theta_{\text{out}}}^\dagger, \iota^{\text{LS}\dagger})$  are spin networks such that: the graphs  $\theta_{\text{in}}, \theta_{\text{out}}$  are the connected components of the boundary graph  $\gamma_{\text{dipole}}$ ;  $\rho_k|_{\theta_{\text{in}}}$  and  $\rho_k|_{\theta_{\text{out}}}$  are the colorings of the links of the graph  $\theta_{\text{in}}$  and respectively  $\theta_{\text{out}}$  obtained by restricting the coloring  $\rho_k$  of the links of the boundary graph  $\gamma_{\text{dipole}}$ ;  $\iota^{\text{LS}}$  is a labelling of the nodes of the graphs  $\theta_{\text{in}}, \theta_{\text{out}}$  with the Livine-Speziale coherent intertwiners [134, 63, 97]:

$$\iota_n^{\text{LS}} = \int d\mu_H(g_n) \bigotimes_{\ell:s(\ell)=n} \rho_{k_\ell}(g_n) |k_\ell \vec{n}_\ell\rangle \otimes \bigotimes_{\ell:t(\ell)=n} \langle k_\ell \vec{n}_\ell | \rho_{k_\ell}(g_n^{-1}). \quad (7.19)$$

The in and out states in (7.18) are:

$$|s_{\text{in}}\rangle = \iota_{n_1}^{\text{LS}} \otimes \iota_{n_2}^{\text{LS}}, \quad |s_{\text{out}}\rangle = (\iota_{n_3}^{\text{LS}})^\dagger \otimes (\iota_{n_4}^{\text{LS}})^\dagger,$$

where  $n_1, n_2$  are the nodes of  $\theta_{\text{in}}$  and  $n_3, n_4$  are the nodes of  $\theta_{\text{out}}$ . The coloring  $\tilde{\rho}_k$  is the coloring of the links of the graph diagram  $\mathcal{D}_{\gamma_{\text{dipole}}} \# \gamma_{\text{int}}$  induced by a coloring  $\rho_k$  of the links of the boundary graph  $\gamma_{\text{dipole}}$  (see section 7.4.2). The amplitude

$$\langle s_{\text{out}} | \mathcal{Z}(\mathcal{D}_{\gamma_{\text{dipole}}} \# \gamma_{\text{int}}, \tilde{\rho}_k, P, \mathcal{A}) | s_{\text{in}} \rangle$$

is zero if the coloring  $\rho_k$  is not compatible with the graph diagram  $\mathcal{D}_{\gamma_{\text{dipole}}} \# \gamma_{\text{int}}$ . We introduce the following notation:

$$\delta_{\text{comp}}(k) = \begin{cases} 1 & \text{if } \rho_k \text{ is compatible with } \mathcal{D}_{\gamma_{\text{dipole}}} \# \gamma_{\text{int}}, \\ 0 & \text{otherwise.} \end{cases}$$

Each compatible coloring of the boundary links defines unambiguously a coloring of all links of the graph diagram. In particular it defines a coloring of the links of the interaction graph. The coloring of the nodes of the graph  $\gamma_{\text{dipole}}$  with the Livine-Speziale coherent intertwiners naturally transfers to a coloring of the nodes of the interaction graph (without loss of generality, it can be assumed that  $n \in \gamma_{\text{int}}^{(0)}$  is in relation with  $n^d \in \tilde{\theta}_n^{(0)}$ ). As a result, the interaction graph is equipped with a spin-network structure:

$$s_{\text{int}} = (\gamma_{\text{int}}, \rho_k, \iota^{\text{LS}}).$$

We will call it an interaction spin network. Using this notation,

$$W(z_{\text{in}}, z_{\text{out}}) = \sum_k \prod_{\ell \in \gamma_{\text{dipole}}^{(1)}} e^{-k_\ell(k_\ell+1)t - iz_\ell k_\ell} \delta_{\text{comp}}(k) \prod_{[\ell] \in \mathfrak{F}_{\text{closed}}} (2k_{[\ell]} + 1) \mathcal{A}_{\text{int}}^{\text{EPRL}}(s_{\text{int}}), \quad (7.20)$$

where  $k_{[\ell]} = k_\ell$  for any  $\ell \in [\ell]$ , the sum is over all possible colorings  $k : \gamma_{\text{dipole}}^{(1)} \rightarrow \frac{1}{2}\mathbb{N}$  of the links of the boundary graph with spins such that  $\frac{1 \pm \beta}{2} k_\ell \in \frac{1}{2}\mathbb{N}$  and the action of  $\mathcal{A}_{\text{int}}^{\text{EPRL}}$  on  $s_{\text{int}}$  is defined in (1.54).

A BRV graph diagram is depicted in figure 7.14. In the following we consider some other graph diagrams contributing to the transition amplitude. We compare an amplitude

$$\delta_{\text{comp}}(k) \prod_{[\ell] \in \mathfrak{F}_{\text{closed}}} (2k_{[\ell]} + 1) \mathcal{A}_{\text{int}}^{\text{EPRL}}(s_{\text{int}}) \quad (7.21)$$

corresponding to an operator spin-network diagram  $(\mathcal{D}_{\gamma_{\text{dipole}}} \# \gamma_{\text{int}}, \tilde{\rho}_k, P, \mathcal{A})$  to an amplitude corresponding to the BRV operator spin-network diagram with the coloring induced

## 7. Dipole Cosmology

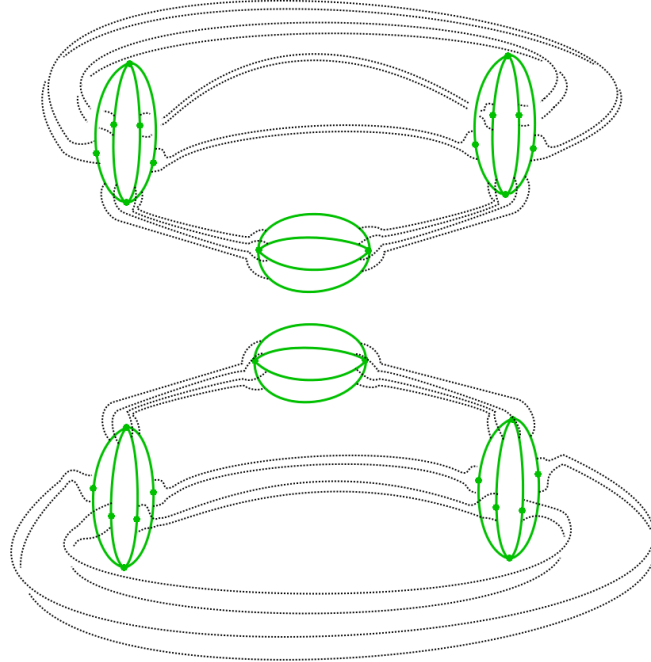


Figure 7.14.: Any choice of orientations of the links makes the diagram depicted on this figure a graph diagram. Any such graph diagram will be called a BRV graph diagram.

by the same coloring  $\rho_k$  of the boundary links. Since the gaussians in (7.20) are peaked at approximately  $\frac{\Im(z_\ell)}{2t}$  [49] which is large, we compare the amplitudes in the limit of large spins. We show that in this limit the amplitudes can be neglected when compared to the amplitude of the corresponding BRV operator spin-network diagram.

Clearly, when the coloring of the boundary is not compatible with the graph diagram, the amplitude is zero (but the BRV amplitude is not zero) and therefore it is enough to consider the amplitude for compatible colorings, i.e. for the colorings such that

$$\delta_{\text{comp}}(k) = 1.$$

### 7.5.1. Face amplitudes

In this section we discuss the factor

$$\prod_{[\ell] \in \mathfrak{F}_{\text{closed}}} (2k_{[\ell]} + 1) \quad (7.22)$$

from (7.21). Let us note, that

$$\begin{aligned} \mathcal{G}^{\text{out}} = & \gamma_{\text{int}}^{(1)} \cup \{(n^d, s_\ell) : \ell \in \gamma_{\text{dipole}}^{(1)}, n \in \gamma_{\text{dipole}}^{(0)}\} \cup \\ & \cup \{(n^d, t_\ell) : \ell \in \gamma_{\text{dipole}}^{(1)}, n \in \gamma_{\text{dipole}}^{(0)}\} \cup \{(n^u, t_\ell) : \ell \in \gamma_{\text{dipole}}^{(1)}, n \in \gamma_{\text{dipole}}^{(0)}\}. \end{aligned}$$

Let us recall that without loss of generality, it can be assumed that  $n \in \gamma_{\text{int}}^{(0)}$  is in relation with  $n^d \in \tilde{\theta}_n^{(0)}$ . It can be also assumed that

$$\gamma_{\text{int}}^{(1)} = \gamma_{\text{dipole}}^{(1)}$$

and

$$\varphi(n^d, t_\ell) = \ell,$$

where  $(n^d, t_\ell) \in \tilde{\theta}_n^{(1)}$ . With this conventions, the glueing map uniquely defines and is uniquely defined by a permutation  $\pi : \gamma_{\text{dipole}}^{(1)} \rightarrow \gamma_{\text{dipole}}^{(1)}$ :

- $\varphi(n^u, t_\ell) = (n'^u, s_\ell)$  if  $n = t(\ell) \in \gamma_{\text{dipole}}^{(0)}$ ,  $n' = s(\ell) \in \gamma_{\text{dipole}}^{(0)}$ ,
- $\varphi(n^d, s_\ell) = (n'^d, t_\ell)$  if  $n = s(\ell) \in \gamma_{\text{dipole}}^{(0)}$ ,  $n' = t(\ell) \in \gamma_{\text{dipole}}^{(0)}$ ,
- $\varphi(n^d, t_\ell) = \ell$  if  $n^d$  is in node relation with  $t(\ell) \in \gamma_{\text{int}}^{(0)}$ ,
- $\varphi(\ell) = (n^d, s_{\pi(\ell)})$  if  $s(\ell) \in \gamma_{\text{int}}^{(0)}$  is in node relation with  $n^d$ .

For a given interaction graph and a node relation not all permutations are allowed, for example the identity permutation is allowed only in a BRV graph diagram.

The closed equivalence classes of the face relation are of the form:

$$\{(n^d, s_\ell), (n'^d, t_\ell), \ell, (n''^d, s_{\pi(\ell)}), \dots\},$$

where  $s(\ell) = n \in \gamma_{\text{dipole}}^{(0)}$ ,  $t(\ell) = n' \in \gamma_{\text{dipole}}^{(0)}$ ,  $n''^d$  is in node relation with  $s(\ell) \in \gamma_{\text{int}}^{(0)}$ . Therefore they are in 1-1 correspondence with the cycles of the permutation  $\pi$  and a compatible coloring of the boundary graph satisfies:

$$k_{\pi(\ell)} = k_\ell.$$

Since the number of cycles is at most 8 and is equal to 8 only for the identity permutation, we conclude that the polynomial

$$\prod_{[\ell] \in \mathfrak{F}_{\text{closed}}} (2k_{[\ell]} + 1)$$

is of degree at most 8 and it is of degree 8 only for a BRV graph diagram.

### 7.5.2. Vertex amplitudes

From the analysis of the factor  $\prod_{[\ell] \in \mathfrak{F}_{\text{closed}}} (2k_{[\ell]} + 1)$  done in the previous subsection it follows that in order to show that an amplitude (7.21) corresponding to an operator spin-network diagram  $(\mathcal{D}_{\gamma_{\text{dipole}}} \# \gamma_{\text{int}}, \tilde{\rho}_k, P, \mathcal{A})$  can be neglected in the limit of large spins when compared to the amplitude corresponding to the BRV operator spin-network diagram with the same coloring  $\rho_k$  of the boundary links, it is enough to show that the modulus of the vertex amplitude is not greater than the corresponding BRV vertex amplitude. We expect that this is indeed the case. We present some examples when this inequality holds. In fact, in the first example the modulus of the vertex amplitude is not only not greater than the BRV vertex amplitude but is negligibly small when compared to the BRV vertex amplitude (in the limit of large spins).

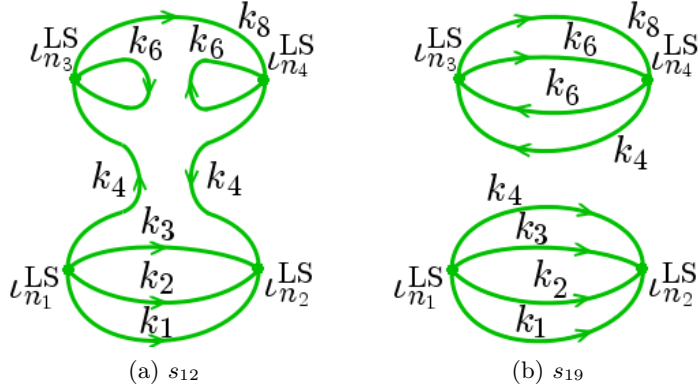


Figure 7.15.: The interaction spin networks  $s_{12}$  and  $s_{19}$ . The nodes are labelled with the Livine-Speziale coherent intertwiners  $\iota_n^{\text{LS}}$  and the links are labelled with unitary irreducible representations  $\rho_k$  of the SU(2) group. To make the picture clearer we indicate only the spin  $k_\ell$  of the representation  $\rho_{k_\ell}$ . The vertex amplitude  $\mathcal{A}_{12}^{\text{EPRL}}(s_{12})$  as a function of the spins  $k_\ell$  is decaying exponentially. Since the corresponding BRV vertex amplitude  $\mathcal{A}_{19}^{\text{EPRL}}(s_{19})$  is decaying as inverse polynomial, the contribution from the graph diagram depicted in figure 7.13b can be neglected.

### Loops (interaction graphs 1-16)

The first example is depicted in figure 7.13b. The interaction graph contains two links starting and ending at the same node (forming loops). The compatible coloring  $k$  satisfies  $k_4 = k_5, k_6 = k_7$ . The interaction spin network  $s_{\text{int}} = s_{12}$  is depicted in figure 7.15a. The amplitude  $\mathcal{A}_{12}^{\text{EPRL}}(s_{12})$  is of the following form:

$$\mathcal{A}_{12}^{\text{EPRL}}(s_{12}) = \delta_{k_4 k_8} \frac{1}{(2j_4^+ + 1)^2 (2j_4^- + 1)^2} |\langle k_4 \vec{n}_4 | k_4 \vec{n}_8 \rangle|^2 |\langle k_6 \vec{n}_6 | k_6 \vec{n}_7 \rangle|^2 \cdot \langle \iota_{\text{EPRL}}(\iota_{n_1}^{\text{LS}}) | \iota_{\text{EPRL}}(\iota_{n_1}^{\text{LS}}) \rangle, \quad (7.23)$$

where  $j_4^\pm = \frac{|1 \pm \beta|}{2} k_4$ . Since the tetrahedra associated to the nodes are regular, it follows that  $\vec{n}_4 \cdot \vec{n}_8 = -\frac{1}{3}$ ,  $\vec{n}_6 \cdot \vec{n}_7 = -\frac{1}{3}$  and [143]

$$|\langle k_4 \vec{n}_4 | k_4 \vec{n}_8 \rangle|^2 |\langle k_6 \vec{n}_6 | k_6 \vec{n}_7 \rangle|^2 = \left( \frac{1 + \vec{n}_4 \cdot \vec{n}_8}{2} \right)^{2k_4} \left( \frac{1 + \vec{n}_6 \cdot \vec{n}_7}{2} \right)^{2k_6} = \left( \frac{1}{3} \right)^{2(k_4 + k_6)}.$$

As a result the amplitude (7.23) as a function of the spins decays exponentially. The amplitude of a BRV operator spin-network diagram with the same coloring  $\rho_k$  is (compare figure 7.15b)

$$\mathcal{A}_{19}(s_{19}) = \langle \iota_{\text{EPRL}}(\iota_{n_3}^{\text{LS}}) | \iota_{\text{EPRL}}(\iota_{n_3}^{\text{LS}}) \rangle \langle \iota_{\text{EPRL}}(\iota_{n_1}^{\text{LS}}) | \iota_{\text{EPRL}}(\iota_{n_1}^{\text{LS}}) \rangle.$$

and decays as inverse polynomial [134]. As a result, for sufficiently large spins the amplitude  $\mathcal{A}_{12}^{\text{EPRL}}(s_{12})$  is negligibly small when compared to the amplitude  $\mathcal{A}_{19}(s_{19})$ . Whenever there is a loop in an interaction graph, there is a factor exponentially decaying [129]. We therefore expect that a contribution from any graph diagram with an interaction graph 1 – 16 can be neglected in the limit of large volume of the universe.

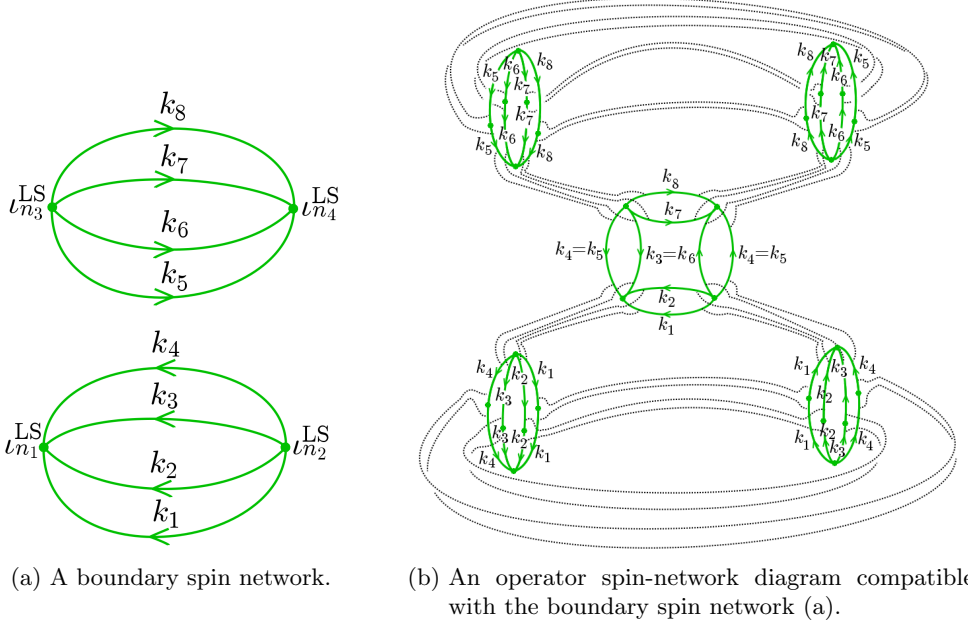
**Interaction graphs 17, 18 and 19**


Figure 7.16.: In this example we limit to graph diagrams with the boundary graph oriented as on figure (a). One possible graph diagram is depicted on figure (b). The coloring of the boundary links compatible with the graph diagram satisfies  $k_4 = k_5$ ,  $k_3 = k_6$ . The permutation corresponding to the graph diagram is  $\pi = \begin{pmatrix} \ell_1 & \ell_2 & \ell_3 & \ell_4 & \ell_5 & \ell_6 & \ell_7 & \ell_8 \\ \ell_1 & \ell_2 & \ell_6 & \ell_5 & \ell_4 & \ell_3 & \ell_7 & \ell_8 \end{pmatrix}$ .

In this section we discuss all contributions from the interaction graphs that are compatible with an orientation of the boundary graph from figure 7.16a. An example of such graph diagram is depicted in figure 7.16b. The interaction graphs compatible with this orientation are graphs 17, 18 and 19.

We use the observation from the section 7.5.1 that to each graph diagram there corresponds a permutation  $\pi : \gamma_{\text{dipole}}^{(1)} \rightarrow \gamma_{\text{dipole}}^{(1)}$ . In the cases studied in this section, the vertex amplitude can be written in the following form:

$$\langle \Psi | \mathcal{A}_\pi | \Psi \rangle,$$

where  $|\Psi\rangle = \iota_{\text{EPRL}}(\iota_{n_2}^{\text{LS}}) \otimes \iota_{\text{EPRL}}(\iota_{n_3}^{\text{LS}})$  and  $\mathcal{A}_\pi : \bigotimes_{\ell \in \gamma_{\text{dipole}}^{(1)}} \mathcal{H}_{j_\ell^+ j_\ell^-} \rightarrow \bigotimes_{\ell \in \gamma_{\text{dipole}}^{(1)}} \mathcal{H}_{j_\ell^+ j_\ell^-}$  is the operator permuting the indices:

$$(\mathcal{A}_\pi)_{B_{\ell_1}^+ \dots B_{\ell_8}^+ B_{\ell_1}^- \dots B_{\ell_8}^-}^{A_{\ell_1}^+ \dots A_{\ell_8}^+ A_{\ell_1}^- \dots A_{\ell_8}^-} = \delta_{B_{\pi(\ell_1)}^+}^{A_{\ell_1}^+} \dots \delta_{B_{\pi(\ell_8)}^+}^{A_{\ell_8}^+} \delta_{B_{\pi(\ell_1)}^-}^{A_{\ell_1}^-} \dots \delta_{B_{\pi(\ell_8)}^-}^{A_{\ell_8}^-}.$$

Since  $\mathcal{A}_\pi$  is unitary:

$$| \langle \Psi | \mathcal{A}_\pi | \Psi \rangle | \leq \langle \Psi | \Psi \rangle = \mathcal{A}_{19'}^{\text{EPRL}}(s_{19'}),$$

where the spin network  $s_{19'}$  is depicted in figure 7.17b and  $\mathcal{A}_{19'}^{\text{EPRL}}(s_{19'})$  is a BRV vertex amplitude. As a result, the modulus of each vertex amplitude considered in this section

## 7. Dipole Cosmology

is not greater than the BRV vertex amplitude. Together with the result about the face amplitudes from section 7.5.1 it shows that in the limit of large spins the amplitude corresponding to a BRV operator spin-network diagram is dominating among the amplitudes corresponding to the operator spin-network diagrams considered in this section.

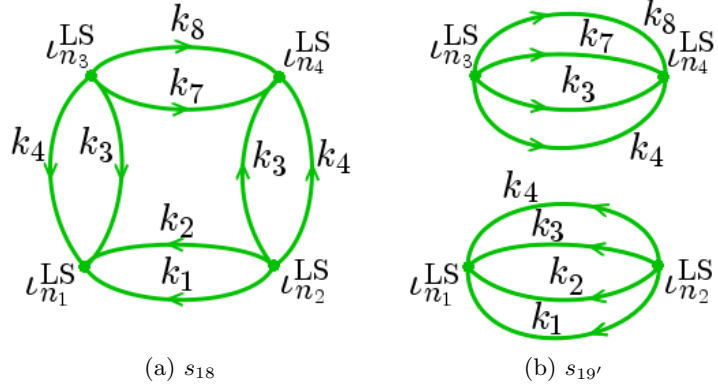


Figure 7.17.: We show that  $|\mathcal{A}_{18}^{\text{EPRL}}(s_{18})| \leq \mathcal{A}_{19'}^{\text{EPRL}}(s_{19'})$ . Such inequality holds for the vertex amplitude of any operator spin-network diagram with the orientation of the boundary graph fixed to be the one depicted in figure 7.16a.

### Interaction graph 20

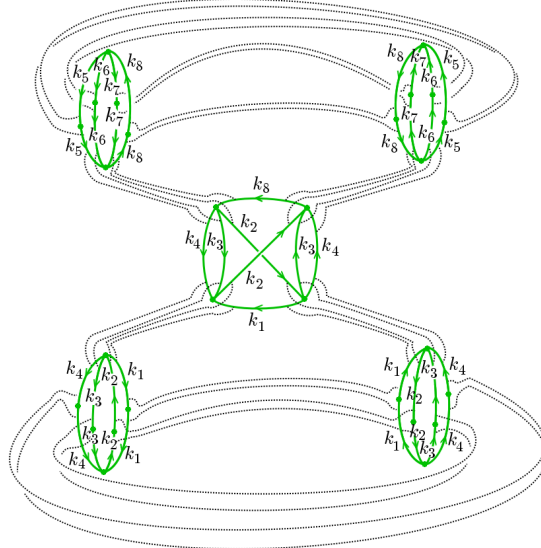


Figure 7.18.: An operator spin-network diagram with interaction graph 20. A coloring of the boundary links compatible with the graph diagram satisfies  $k_2 = k_7$ ,  $k_3 = k_6$ ,  $k_4 = k_5$ .

In this section we discuss a contribution from a graph diagram with interaction graph 20. The graph diagram is depicted in figure 7.18. The compatible coloring of the boundary

links satisfies  $k_2 = k_7, k_3 = k_6, k_4 = k_5$ . The interaction spin network  $s_{20}$  is depicted in figure 7.19a.

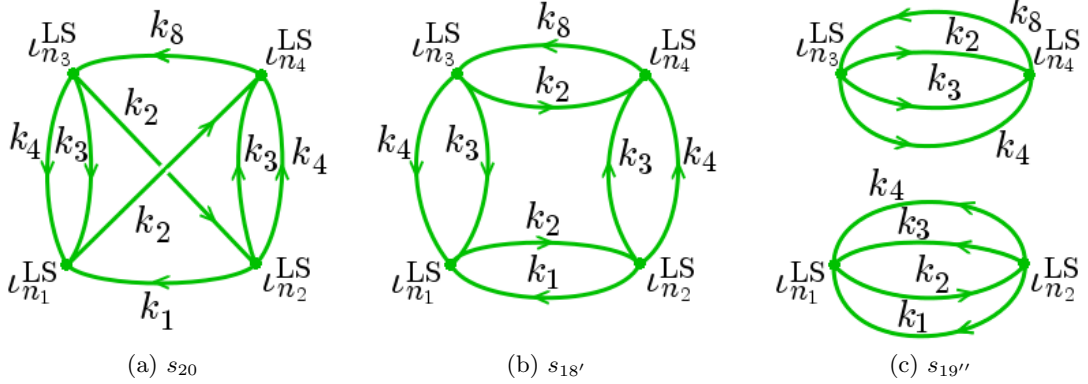


Figure 7.19.: We show that  $|\mathcal{A}_{20}^{\text{EPRL}}(s_{20})| \leq \mathcal{A}_{18'}^{\text{EPRL}}(s_{18'}) \leq \mathcal{A}_{19''}^{\text{EPRL}}(s_{19''})$ .

We define:

$$\begin{aligned} \Psi_1 &= \frac{A_{\ell_1}^+ A_{\ell_1}^-}{A_{\ell_2}^+ A_{\ell_2}^- A_{\ell_7}^+ A_{\ell_7}^-} \frac{A_{\ell_8}^+ A_{\ell_8}^-}{A_{\ell_3}^+ A_{\ell_3}^- A_{\ell_4}^+ A_{\ell_4}^-} = \\ &= \iota_{\text{EPRL}}(\iota_{n_2}^{\text{LS}}) \frac{A_{\ell_1}^+ A_{\ell_1}^-}{A_{\ell_2}^+ A_{\ell_2}^-} \frac{A_{\ell_3}^+ A_{\ell_3}^- A_{\ell_4}^+ A_{\ell_4}^-}{A_{\ell_7}^+ A_{\ell_7}^-} \iota_{\text{EPRL}}(\iota_{n_4}^{\text{LS}}) \frac{A_{\ell_8}^+ A_{\ell_8}^-}{A_{\ell_3}^+ A_{\ell_3}^- A_{\ell_4}^+ A_{\ell_4}^- A_{\ell_7}^+ A_{\ell_7}^-}. \end{aligned}$$

In this notation the vertex amplitude is of the following form:

$$\mathcal{A}_{20}^{\text{EPRL}}(s_{20}) = \langle \Psi_1 | \mathcal{A}_1 | \Psi_1 \rangle,$$

where

$$(\mathcal{A}_1) \frac{B_{\ell_1}^+ B_{\ell_1}^- A_{\ell_2}^+ A_{\ell_2}^- A_{\ell_7}^+ A_{\ell_7}^- B_{\ell_8}^+ B_{\ell_8}^-}{A_{\ell_1}^+ A_{\ell_1}^- B_{\ell_2}^+ B_{\ell_2}^- B_{\ell_7}^+ B_{\ell_7}^- A_{\ell_8}^+ A_{\ell_8}^-} = \delta_{A_{\ell_1}^+ A_{\ell_1}^- B_{\ell_2}^+ B_{\ell_2}^- B_{\ell_7}^+ B_{\ell_7}^-}^{B_{\ell_1}^+ B_{\ell_1}^-} \delta_{A_{\ell_2}^+ A_{\ell_2}^- B_{\ell_7}^+ B_{\ell_7}^-}^{A_{\ell_2}^+ A_{\ell_2}^-} \delta_{B_{\ell_8}^+ B_{\ell_8}^-}^{A_{\ell_8}^+ A_{\ell_8}^-}$$

is a unitary operator

$$\mathcal{A}_1 : \mathcal{H}_{j_{\ell_1}^+ j_{\ell_1}^-} \otimes \mathcal{H}_{j_{\ell_2}^+ j_{\ell_2}^-}^* \otimes \mathcal{H}_{j_{\ell_7}^+ j_{\ell_7}^-}^* \otimes \mathcal{H}_{j_{\ell_8}^+ j_{\ell_8}^-} \rightarrow \mathcal{H}_{j_{\ell_1}^+ j_{\ell_1}^-} \otimes \mathcal{H}_{j_{\ell_2}^+ j_{\ell_2}^-}^* \otimes \mathcal{H}_{j_{\ell_7}^+ j_{\ell_7}^-}^* \otimes \mathcal{H}_{j_{\ell_8}^+ j_{\ell_8}^-}.$$

It follows that

$$|\mathcal{A}_{17}^{\text{EPRL}}(s_{17})| = |\langle \Psi_1 | \mathcal{A}_1 | \Psi_1 \rangle| \leq \langle \Psi_1 | \Psi_1 \rangle = \mathcal{A}_{18'}^{\text{EPRL}}(s_{18'}),$$

where  $s_{18'}$  is the spin network depicted in figure 7.19b. Now, we use an argument similar to the one used in the previous subsection. We define

$$\Psi_2 = \iota_{\text{EPRL}}(\iota_{n_2}^{\text{LS}}) \otimes \iota_{\text{EPRL}}(\iota_{n_3}^{\text{LS}})$$

and note that

$$\mathcal{A}_{18'}^{\text{EPRL}}(s_{18'}) = \langle \Psi_2 | \mathcal{A}_2 | \Psi_2 \rangle,$$

where

$$\begin{aligned} (\mathcal{A}_2) &= \frac{B_{\ell_1}^+ B_{\ell_1}^- A_{\ell_2}^+ A_{\ell_2}^- B_{\ell_3}^+ B_{\ell_3}^- A_{\ell_4}^+ A_{\ell_4}^- B_{\ell_5}^+ B_{\ell_5}^- A_{\ell_6}^+ A_{\ell_6}^- B_{\ell_7}^+ B_{\ell_7}^- A_{\ell_8}^+ A_{\ell_8}^-}{A_{\ell_1}^+ A_{\ell_1}^- B_{\ell_2}^+ B_{\ell_2}^- A_{\ell_3}^+ A_{\ell_3}^- A_{\ell_4}^+ A_{\ell_4}^- A_{\ell_5}^+ A_{\ell_5}^- A_{\ell_6}^+ A_{\ell_6}^- A_{\ell_7}^+ A_{\ell_7}^- B_{\ell_8}^+ B_{\ell_8}^-} = \\ &= \delta_{A_{\ell_1}^+ A_{\ell_1}^- B_{\ell_2}^+ B_{\ell_2}^- A_{\ell_3}^+ A_{\ell_3}^- A_{\ell_4}^+ A_{\ell_4}^- A_{\ell_5}^+ A_{\ell_5}^- A_{\ell_6}^+ A_{\ell_6}^- A_{\ell_7}^+ A_{\ell_7}^- B_{\ell_8}^+ B_{\ell_8}^-}^{B_{\ell_1}^+ B_{\ell_1}^-} \delta_{A_{\ell_2}^+ A_{\ell_2}^- B_{\ell_3}^+ B_{\ell_3}^- A_{\ell_4}^+ A_{\ell_4}^- B_{\ell_5}^+ B_{\ell_5}^- A_{\ell_6}^+ A_{\ell_6}^- B_{\ell_7}^+ B_{\ell_7}^- A_{\ell_8}^+ A_{\ell_8}^-}^{A_{\ell_2}^+ A_{\ell_2}^- B_{\ell_3}^+ B_{\ell_3}^- A_{\ell_4}^+ A_{\ell_4}^- B_{\ell_5}^+ B_{\ell_5}^- A_{\ell_6}^+ A_{\ell_6}^- B_{\ell_7}^+ B_{\ell_7}^- A_{\ell_8}^+ A_{\ell_8}^-} \end{aligned}$$

## 7. Dipole Cosmology

is a unitary operator mapping

$$\mathcal{H}_{j_{\ell_1}^+ j_{\ell_1}^-} \otimes \mathcal{H}_{j_{\ell_2}^+ j_{\ell_2}^-}^* \otimes \mathcal{H}_{j_{\ell_3}^+ j_{\ell_3}^-} \otimes \mathcal{H}_{j_{\ell_4}^+ j_{\ell_4}^-} \otimes \mathcal{H}_{j_{\ell_5}^+ j_{\ell_5}^-} \otimes \mathcal{H}_{j_{\ell_6}^+ j_{\ell_6}^-} \otimes \mathcal{H}_{j_{\ell_7}^+ j_{\ell_7}^-} \otimes \mathcal{H}_{j_{\ell_8}^+ j_{\ell_8}^-}^*$$

to itself. As a result,

$$|\langle \Psi_2 | \mathcal{A}_2 | \Psi_2 \rangle| \leq \langle \Psi_2 | \Psi_2 \rangle = \mathcal{A}_{19''}^{\text{EPRL}}(s_{19''}),$$

where the spin network  $s_{19''}$  is depicted in figure 7.19c. In summary,

$$|\mathcal{A}_{20}^{\text{EPRL}}(s_{20})| \leq \mathcal{A}_{19''}^{\text{EPRL}}(s_{19''}).$$

Together with the result about the face amplitudes from section 7.5.1 this inequality shows that in the limit of large spins an amplitude corresponding to an operator spin-network diagram studied in this section is negligibly small when compared to an amplitude corresponding to the BRV operator spin-network diagram with the same coloring  $\rho_k$ .

## 8. Discussion and outlook

In this thesis we studied the spin-foam dynamics of the LQG states. We presented a generalization of the EPRL vertex amplitude to arbitrary vertex graphs and discussed two models with the generalized vertex amplitude. The models are compatible with the LQG framework and accommodate all the spin-network states.

Each of the generalized models describes a dynamics of the Loop Quantum Gravity states. In order to be a theory of Quantum Gravity, it should define a transition amplitude that reproduces the dynamics of General Relativity in the classical limit. The results concerning the semi-classical limit of a single 4-simplex amplitude are encouraging [40, 41]. However, the studies of a transition amplitude truncated to a finite foam [51, 50, 148, 106, 105, 116] point to a problem with the semi-classical limit that is called a flatness problem. Most Regge geometries are suppressed in the semi-classical limit, and the only non-suppressed geometries are those satisfying certain curvature constraints,  $\beta\Theta_f = 0 \bmod 2\pi$ , limiting the possible values of the deficit angle  $\Theta_f$  of the holonomy around a face  $f$ . In [116] the authors argue that this problem could be solved at a price of loosing the connection to the LQG state space.

The generalized EPRL models provide a link between the LQG formalism and the spin-foam formalism. An open problem is to find a precise correspondence between them. Such correspondence would be a strong argument for a given model of dynamics of the LQG states, could clarify what class of foams should be used and could lead to approximate methods in the spin-foam formalism – it could justify the vertex expansion used, for example, in the Dipole Cosmology [168]. A Feynman-like derivation of the spin-foam transition amplitude from the LQG formulation was first proposed in [158, 161]. The correspondence was studied in some simpler models: in [138] the correspondence between canonical and covariant (spin-foam) quantization of 3D Gravity was presented and in [15, 16, 58] a spin-foam formulation of Loop Quantum Cosmology was proposed. Some research in this direction has been also done in the case of 4D Gravity [85, 109, 108, 76, 7, 179]. However, the picture is still not satisfactory [179, 117]. Some interesting new ideas were presented in [168, 117] in the context of quantum cosmology. A regulator  $\delta$  was introduced and the physical scalar was obtained in the limit of  $\delta \rightarrow 0$ .

Some issues with the derivation of the spin-foam models of 4D Quantum Gravity were raised. The quantum simplicity and closure constraints do not commute (in the EPRL model the constraints are imposed weakly [75, 74]). In [110] the authors argue that an imposition of the closure constraint gives non-trivial restrictions on the measure and propose a new model. Let us recall how the closure constraint is treated in this thesis: we impose (commuting) quantum simplicity and reduced closure constraint and obtain quantum polyhedra in 4D orthogonal to  $n^I$  (see section 3.2.4). Then in section 3.2.4 we construct the Hilbert space of quantum polyhedra in 4D as a space of orbits under the action of the Spin(4) group on the set of embedded quantum polyhedra. As a result the states are Spin(4) invariant. We interpret this property as imposition of the (full) quantum closure constraint. Another issue concerning the imposition of the constraints was discussed in

## 8. Discussion and outlook

[13, 10, 9, 12, 101, 11, 78, 77, 79]. The authors argued that the simplicity constraints should be supplemented by secondary constraints. As a result in [9] a modification of the BC vertex amplitude was proposed and in [11] a modification of general spin-foam quantization procedure of theories of Plebański type was proposed. In [78, 77, 79] the authors argued that the secondary constraints impose certain shape-matching conditions reducing certain more general geometries called twisted geometries [98, 99, 80, 171] to Regge geometries. This scenario is currently under debate [102, 14]. Another issue with the EPRL model was raised in [81]. The author argues that the EPRL model mixes the  $II+$ ,  $II-$  and  $deg$  Plebański sectors and in [83, 82] proposes a modification of the EPRL 4-simplex amplitude selecting only the desired sector  $II+$ . The model is defined only for triangulations and its generalization to more general foams is still an open problem. The issue with mixing the sectors is related to a cosine problem: the semi-classical limit of an EPRL 4-simplex amplitude is of the form  $e^{iS_v} + e^{-iS_v}$ , rather than  $e^{iS_v}$ , where  $S_v$  is a discretization of the Einstein-Hilbert action on the 4-simplex  $v$  (see (1.45)). The model [83, 82] extracts only the exponential term  $e^{iS_v}$  in the semi-classical limit. On the other hand, the existence of the two terms may be related to the fact that the propagation forward and backward in the coordinate time are indistinguishable and the path integral should involve both terms [162, 165]. In [60] the authors proposed another interesting interpretation – they suggested that the existence of the two terms may reflect an existence of regions of space-time where the determinant of the tetrad  $e_\mu^I$  is negative.

We presented a formulation of spin foams called operator spin foams useful for studying symmetries of the spin-foam models. We introduced moves on operator spin foams such as splitting a face, splitting an edge, reorienting an edge, reorienting a face, adding a face. The symmetric models are invariant under these moves. The moves are analogous to the moves on spin networks introduced by Baez [22] allowing to flip the orientation of a link, split a link, add a link or add a node. The Baez's moves can be used to map a spin network into a spin network defined on any finer graph. It would be interesting to look for a complete set of moves that will allow to map an operator spin foam to an operator spin foam defined on any finer foam. This problem could be translated into the language of operator spin-network diagrams and the solution could be looked for in this language.

In this thesis we presented two Euclidean models with the EPRL vertex amplitudes. One of them is a Spin(4) operator spin-foam model and the second one is an SU(2) operator spin-foam model. The Spin(4) model can be interpreted as a restriction of the operator spin-foam model of Spin(4) BF theory to histories satisfying the simplicity constraints. The model is symmetric with respect to the moves discussed in the previous paragraph but it is naturally interpreted in terms of histories of Spin(4) EPRL spin networks rather than the LQG SU(2) spin networks. On the other hand the SU(2) model is not symmetric with respect to the moves but it is naturally interpreted in terms of histories of the LQG SU(2) spin networks. We have constructed an SU(2) spin-foam model equivalent to the Spin(4) model with the EPRL vertex and we compared it with the SU(2) operator spin-foam model with the EPRL vertex – they differ by the face and the edge amplitudes. A Lorentzian version of the SU(2) spin-foam model with the EPRL vertex was proposed in [48, 163, 165]. It uses a generalization of the Lorentzian EPRL 4-simplex amplitude [86]. The definition of the Lorentzian vertex amplitude needs a regularization that amounts to dropping spurious integration over the  $SL(2, \mathbb{C})$  group. After the regularization, the vertex amplitudes corresponding to 3-edge connected graphs are finite [122]. However, this regularization is often not sufficient for vertex graphs that are not 3-edge connected,

for example any Lorentzian EPRL vertex amplitude corresponding to a graph  $\gamma'$  obtained from a 3-edge connected graph  $\gamma$  by splitting one of its links is infinite. One possibility to deal with this problem is to discard all foams that have a vertex such that the corresponding vertex graph is not 3-edge connected. Another possibility is to improve the regularization, in the simple example we presented above we could just define the vertex amplitude corresponding to a vertex spin network  $s' = (\gamma', \iota', \rho')$  obtained from a vertex spin network  $s = (\gamma, \iota, \rho)$  by the move of splitting a link to be equal to the vertex amplitude corresponding to  $s$  (or proportional by some finite proportionality factor). The graphs that are not 3-edge connected appear in the face splitting move. This makes the definition of the symmetric model more complicated. In the Euclidean case the requirement of invariance of a model under the face splitting move fixes the face amplitude. We expect that in the Lorentzian model the face amplitude can be chosen to be the natural  $SU(2)$  face amplitude (as in the model [48, 163, 165]) and the invariance under the face splitting move can be translated into a condition on the (improved) regularization. Imposing further invariance with respect to the edge splitting move will lead to a non-trivial internal edge amplitude.

We showed that an Euclidean EPRL map is injective unless its co-domain is trivial and its domain is non-trivial. The EPRL map can also be defined in the (physical) Lorentzian signature [122]. Since the states annihilated by the map are not given any chance to play a role in the physical Hilbert space, it would be worthy to extend this result to the Lorentzian signature.

We presented operator spin foams as a version of the spin-foam formalism where the sum over intertwiners has been already performed. The sum over the representations is more problematic, because it is often divergent – see [144, 147, 65, 66, 55, 53, 54, 116, 52, 159, 59] for some studies of these divergences. An interesting possibility is to regularize the divergences by replacing classical groups with certain quantum groups. The regularization can be related to an introduction of a (non-zero) cosmological constant. This idea comes from the spin-foam quantization of 3D Gravity with cosmological constant [180]. In [91, 103, 104] generalizations of the EPRL model to a quantum group are proposed and in [72, 104] it is shown that the modified 4-simplex amplitude [104] reproduces the 4D (Regge) Gravity with cosmological constant in the semi-classical limit. However, from the point of view of canonical quantization the question why the quantum group should be introduced is non-trivial. The case of 3D Gravity with cosmological constant sheds some light on the problem – in [151] it is shown that the deformation of the group into a quantum group is caused by the dynamics. The generalizations of the EPRL model to a quantum group are defined for the vertex graph that is the 1-skeleton of a 4-simplex. It would be interesting to extend these models to arbitrary vertex graphs (and boundary graphs) and settle a link between the extended spin-foam model and kinematics of the canonical theory similar to the one we settled in the case of vanishing of the cosmological constant [123].

The transition amplitude involves a sum over the foams or a refinement limit [166]. A proper definition of the transition amplitude needs therefore a proper definition of the class of foams. We defined a class of foams by using graph diagrams. Let us mention that another class of foams defined combinatorially was proposed in [166]. In the literature also other classes of the 2-complexes are used, for example: simplicial [86], cubular [33], piecewise linear [20, 123] or the foams derived as the Feynman diagrams from actions of Group Field Theory models [69, 94, 43, 131, 142]. Our class is certainly bigger than the

## 8. Discussion and outlook

class of simplicial and cubular foams. In this thesis we constructed an (oriented) CW-complex corresponding to a graph diagram. It would be interesting to understand the relation between our class and the class of combinatorially defined foams [166].

We have found all possible graph diagrams such that the corresponding foam has the same boundary graph as the BRV foam, one internal vertex and four internal edges. Similar algorithm could be applied to the graphs of many-node/many-link approaches to spin-foam cosmology [181, 56]. In particular, the computer algorithm for finding all interaction graphs we presented can be easily extended to the many links dipole graph [181] (generalized theta graph with  $N > 4$  links).

We discussed some examples of the first-order contributions to the Dipole Cosmology transition amplitude. We presented some arguments supporting a hypothesis that the contribution from the BRV foam dominates all other contributions. The proof will be presented in [126]. We expect that the arguments we used can be generalized for the case of many link dipole graph [181]. We considered only the Euclidean case. The calculation of Bianchi, Rovelli and Vidotto transfers to the Lorentzian case [153]. An important problem is to investigate also a possible extension of the arguments we presented to the Lorentzian case. Since interaction graphs which are not 3-edge connected are present on the list on figure 7.10 a proper regularization of the Lorentzian model is needed (see discussion of the Lorentzian EPRL model above). In some cases (for example interaction graphs 1, 3 or 18) the standard regularization is sufficient, but in some cases (for example graphs 9 or 17) additional regularization is required. Obviously the argument about the face amplitudes from section 7.5.1 transfers to the Lorentzian model. In those cases where the interaction graph has a loop (and the standard regularization is sufficient) an exponentially decaying term appears [129] and therefore, it seems reasonable to expect that after a proper regularization the contributions from graph diagrams with interaction graphs 1 – 16 can be neglected also in the Lorentzian case. It is more difficult to transfer to the Lorentzian case the arguments concerning the transition amplitudes corresponding to graph diagrams with interaction graphs 17 – 20 and the study of these amplitudes may require different methods.

## A. The condition for non-triviality of $SU(2)$ invariants

This appendix is dedicated to the following theorem and its proof:

**Theorem 9.** *Let us denote by  $\mathcal{H}_k$  the Hilbert space of the irreducible  $2k + 1$  dimensional representation of  $SU(2)$ . The space  $\text{Inv}(\mathcal{H}_{k_1} \otimes \cdots \otimes \mathcal{H}_{k_N})$  of tensors invariant under the action of the  $SU(2)$  group is non-trivial if and only if the following conditions are satisfied:*

$$k_l \leq \sum_{j \neq l} k_j, \quad l = 1, \dots, N, \quad (\text{A.1})$$

$$\sum_l k_l \in \mathbb{N}. \quad (\text{A.2})$$

We give now arguments that conditions (A.1) and (A.2) are necessary and sufficient for non-triviality of the space  $\text{Inv}(\mathcal{H}_{k_1} \otimes \cdots \otimes \mathcal{H}_{k_N})$ . The proof is an inductive proof with respect to  $N$ .

First, let us note that for  $N \in \{1, 2, 3\}$  the theorem is obviously true. Let  $N \geq 4$ . Let us assume that the theorem is satisfied for  $N - 1$ .

- *The conditions (A.1) and (A.2) are sufficient.*

Without loss of generality we may assume that  $k_N$  and  $k_{N-1}$  are the lowest spins among  $k_1, k_2, \dots, k_N$ . It is straightforward to check that  $k'_1 = k_1, k'_2 = k_2, \dots, k'_{N-2} = k_{N-2}, k'_{N-1} = k_N + k_{N-1}$  satisfy

$$k'_l \leq \sum_{j \neq l} k'_j, \quad l = 1, \dots, N - 1,$$

$$\sum_l k'_l \in \mathbb{N}.$$

Therefore the space  $\text{Inv}(\mathcal{H}_{k_1} \otimes \cdots \otimes \mathcal{H}_{k_{N-2}} \otimes \mathcal{H}_{k_N+k_{N-1}})$  is non-trivial. This shows that in the decomposition

$$\text{Inv}(\mathcal{H}_{k_1} \otimes \cdots \otimes \mathcal{H}_{k_N}) = \bigoplus_{k=|k_N-k_{N-1}|}^{k_N+k_{N-1}} \text{Inv}(\mathcal{H}_{k_1} \otimes \cdots \otimes \mathcal{H}_{k_{N-2}} \otimes \mathcal{H}_k)$$

the term corresponding to  $k = k_N + k_{N-1}$  is non-trivial. As a result

$$\text{Inv}(\mathcal{H}_{k_1} \otimes \cdots \otimes \mathcal{H}_{k_N})$$

is non-trivial.

A. The condition for non-triviality of  $SU(2)$  invariants

- The conditions (A.1) and (A.2) are necessary.

Being given  $k_1, \dots, k_N$ , choose any two spins, say  $k_N$  and  $k_{N-1}$  (the problem is insensitive on an ordering in the  $N$ -tuple). Decompose  $\text{Inv}(\mathcal{H}_{k_1} \otimes \dots \otimes \mathcal{H}_{k_N})$  into the direct sum  $\text{Inv}(\mathcal{H}_{k_1} \otimes \dots \otimes \mathcal{H}_{k_N}) = \bigoplus_{k=|k_N-k_{N-1}|}^{k_N+k_{N-1}} \text{Inv}(\mathcal{H}_{k_1} \otimes \dots \otimes \mathcal{H}_{k_{N-2}} \otimes \mathcal{H}_k)$ . From the non-triviality of  $\text{Inv}(\mathcal{H}_{k_1} \otimes \dots \otimes \mathcal{H}_{k_N})$  follows that there is  $k \in \frac{1}{2}\mathbb{N}$  such that  $|k_N - k_{N-1}| \leq k \leq k_N + k_{N-1}$ ,  $k + k_N + k_{N-1} \in \mathbb{N}$ , and the space

$$\text{Inv}(\mathcal{H}_{k_1} \otimes \dots \otimes \mathcal{H}_{k_{N-2}} \otimes \mathcal{H}_k)$$

is non-trivial. It follows that

$$|k_N - k_{N-1}| \leq k \leq k_1 + \dots + k_{N-2}.$$

From those inequalities we have

$$k_N - k_{N-1} \leq k_1 + \dots + k_{N-2},$$

hence

$$k_N \leq k_1 + \dots + k_{N-2} + k_{N-1}.$$

Since  $k_N$  is arbitrarily chosen from among of  $k_1, \dots, k_N$ , this shows that the generalized triangle inequality (A.1) is satisfied. To check that the condition (A.2) is fulfilled, note that

$$k_1 + \dots + k_{N-2} + k + k_N + k_{N-1} + k \in \mathbb{N},$$

since  $k_1 + \dots + k_{N-2} + k \in \mathbb{N}$  and  $k_N + k_{N-1} + k \in \mathbb{N}$ . However,  $2k \in \mathbb{N}$ , therefore

$$k_1 + \dots + k_{N-2} + k_{N-1} + k_N \in \mathbb{N}.$$

In conclusion, both conditions (A.1) and (A.2) are satisfied.

## B. Notation

### Index conventions

$\alpha, \beta, \mu, \nu$  Space-time indices.

$A, B, C, D$  Indices in a representation space. See  $\mathcal{H}_\ell, \mathcal{H}_f, \mathcal{H}_k$ .

$a, b, c, d$  Space indices (i.e. indices in  $\Sigma$ ).

$\mathbf{a}, \mathbf{b}, \mathbf{c}, \mathbf{d}$  Indices in the space  $\text{Inv}(\mathcal{H}_{k_1} \otimes \dots \otimes \mathcal{H}_{k_M} \otimes \mathcal{H}_{k_{M+1}}^* \otimes \dots \otimes \mathcal{H}_{k_N}^*)$ .

$a, b, c, d$  A numbering of tetrahedra in a 4-simplex (the indices take values in  $\{0, 1, 2, 3, 4\}$ ).

$I, J, K, L$  Indices in the internal space  $V$ .

$i, j, k, l$  Indices in the space  $V_\perp$ .

$\mathsf{I}, \mathsf{J}, \mathsf{K}$  Indices taking values in  $\{1, 2, \dots, N\}$  or  $\{1, 2, \dots, M\}$ .

### List of symbols

$\#S$  The number of elements in the set  $S$ .

$Y \prec X$   $Y$  is face of  $X$ . See section 1.3.3.

$\Gamma_a^i$  The connection compatible with the triad  $e_a^i$ . See section 1.1.3.

$\mathcal{I}$  An SU(2) invariant tensor – an element of  $\text{Inv}(\mathcal{H}_{k_1} \otimes \dots \otimes \mathcal{H}_{k_M} \otimes \mathcal{H}_{k_{M+1}}^* \otimes \dots \otimes \mathcal{H}_N^*)$ .

$\Lambda$  An isomorphism of  $\text{Inv}(\mathcal{H} \otimes \mathcal{H}^*)$  and  $\mathbb{C}$ , such that  $\Lambda(\text{id}) = 1$ . See section 5.1.2.

$\Sigma$  A space manifold – oriented, compact 3-dimensional manifold without boundary.

$\Sigma_t$  A constant time slice ( $t = t$  slice). See section 1.1.2.

$\beta$  The Barbero-Immirzi parameter. See section 1.1.1.

$\gamma$  A graph (embedded or abstract). See section 1.2.1 and section 1.2.2.

$\gamma^{(0)}$  The set of nodes of the graph  $\gamma$ . See section 1.2.2.

$\gamma^{(1)}$  The set of links of the graph  $\gamma$ . See section 1.2.2.

$\gamma_{\text{dipole}}$  A dipole boundary graph. See section 7.2.

$\gamma_n^{\text{in}}$  The set of the links of the graph  $\gamma$  incoming to  $n$ ,  $\gamma_n^{\text{in}} = t^{-1}(n)$ . See section 6.1.

*List of symbols*

- $\gamma_{\text{int}}$  An interaction graph. See section 7.2.
- $|\gamma|$  An unoriented abstract graph. See section 1.2.2.
- $\epsilon_{IJKL}$  The alternating tensor on  $V$  such that the orientation of  $\epsilon_{IJKL} e^I \wedge e^J \wedge e^K \wedge e^L$  agrees with the orientation of  $\mathcal{M}$ .
- $\epsilon_{ijk}$  The alternating tensor on  $V_\perp$ :  $\epsilon_{ijk} = \mathfrak{q}_i^I \mathfrak{q}_j^J \mathfrak{q}_k^K n^L \epsilon_{IJKL}$ . See section 1.1.3.
- $\bar{\eta}_{IJ}$  An inner product on  $V = \mathbb{R}^4$ . The signature of  $\bar{\eta}_{IJ}$  is either  $-,+,+,+$  or  $+,+,+,+$ . See section 1.1.1.
- $\eta^{abc}$  The Levi-Civita tensor density on  $\Sigma$  which orientation agrees with the orientation of  $\Sigma$ .
- $\eta^{\alpha\beta\mu\nu}$  The Levi-Civita tensor density on  $\mathcal{M}$  which orientation agrees with the orientation of  $\mathcal{M}$ .
- $\eta_{ij}$  An inner product on  $V_\perp$ . See section 1.1.3.
- $\theta_t$  Embedding  $\theta_t : \Sigma \rightarrow \mathcal{M}$ , such that  $\theta_t(\Sigma) = \Sigma_t$ . See section 1.1.2.
- $\iota$  A labelling of nodes of a graph with intertwiners or a labelling of edges of a 2-complex (foam) with intertwiners. See section 1.2.2 and section 1.3.3.
- $\partial\iota_n$  The invariant tensor induced on the node  $n$  of the boundary of a spin foam. See (1.53).
- $\iota_{\text{EPRL}}$  An EPRL map,  $\mathcal{I} \mapsto \iota_{\text{EPRL}}(\mathcal{I})$ . See section 3.3.2.
- $\iota_{\text{EPRL}}(\mathcal{I})$  An EPRL intertwiner. See (3.28).
- $\iota_{k_1\dots k_N}$  The map analogous to EPRL map defined under modified conditions **Con n**. See (4.22).
- $\iota'_{k_1\dots k_N}$  The map analogous to  $\iota_{k_1\dots k_N}$  defined without the projections onto invariants of  $\text{Spin}(4)$ . See (4.25).
- $\iota_n^{\text{LS}}$  The Livine-Speziale coherent intertwiner assigned to the node  $n$ . See (7.19).
- $\iota_{\text{poly}}(n^I, \mathcal{I})$  The quantum polyhedron in 4D orthogonal to  $n^I$  corresponding to a quantum polyhedron in 3D  $\mathcal{I}$ . See (3.20).
- $\dot{\iota}_{\text{poly}}(\mathcal{I})$  The quantum polyhedron in 4D orthogonal to  $\dot{n}^I$  corresponding to a quantum polyhedron in 3D  $\mathcal{I}$ . See (3.19).
- $\iota_{\text{poly}}^n$  A quantum polyhedron in 4D orthogonal to  $n^I$ . See section 3.2.4.
- $\kappa$  A foam (2-complex). See section 1.3.3.
- $\kappa^{(0)}$  The set of vertices of  $\kappa$ . See section 1.3.3.
- $\kappa_{\text{int}}^{(0)}$  The set of internal vertices of  $\kappa$ . See section 1.3.3.

- $\kappa^{(1)}$  The set of edges of  $\kappa$ . See section 1.3.3.
  - $\kappa_{\text{int}}^{(1)}$  The set of internal edges of  $\kappa$ . See section 1.3.3.
  - $\kappa^{(2)}$  The set of faces of  $\kappa$ . See section 1.3.3.
  - $\partial\kappa$  The boundary graph of a foam  $\kappa$ . See section 1.3.3.
  - $\kappa_{\mathcal{D}}$  The foam corresponding to the graph diagram  $\mathcal{D}$ . See section 6.1.3.
  - $\mu_H$  The Haar measure.
  - $\rho$  A labelling of links of a graph with unitary irreducible representations or a labelling of faces of a 2-complex (foam) with unitary irreducible representations. See section 1.2.2, section 1.3.3, section 5.1.1.
  - $\partial\rho_\ell$  The unitary irreducible representation induced on the link  $\ell$  of the boundary of a spin foam. See (1.52).
  - $\rho_{j^+j^-}$  The Spin(4) representation defined by a pair of SU(2) unitary irreducible representations  $\rho_{j^+}, \rho_{j^-}$ :  $\rho_{j^+j^-}(g^+, g^-) = \rho_{j^+}(g^+) \otimes \rho_{j^-}(g^-)$ ,  $j^+, j^- \in \frac{1}{2}\mathbb{N}$ . See section 3.2.4.
  - $\rho'_{j^+j^-}$  The representation of the  $\text{spin}(4)=\text{so}(4)$  Lie algebra induced by the Spin(4) representation  $\rho_{j^+j^-}$  (the tangent map of  $\rho_{j^+j^-}$ ).
  - $\rho_k$  An SU(2) unitary irreducible representation of spin  $k$ .
  - $\rho'_k$  The representation of the  $\text{su}(2)$  Lie algebra induced by the SU(2) representation  $\rho_k$  (the tangent map of  $\rho_k$ ).
  - $\sigma$  The sign of the determinant of the metric  $\bar{\eta}$ . See section 1.1.1.
  - $\varphi$  A glueing map. See section 6.1.
  - $\omega_\mu{}^I{}_J$  A connection one-form on  $\mathcal{M}$ . In this thesis it is a global one-form on  $\mathcal{M}$  with values in  $\text{so}(\bar{\eta})$ .
- 1** The trivial representation.
- $A_a^i$  A connection one-form on  $\Sigma$ . See section 1.1.3.
  - $\mathcal{A}$  A labelling of internal vertices of a spin-foam with contractors:  $\mathcal{A} : \kappa_{\text{int}}^{(0)} \rightarrow \mathcal{H}_v^*$ . The complex number  $\mathcal{A}_v(s^\dagger)$  is called a vertex amplitude. See sections 1.3.3, 1.3.3, 5.1.1.
  - $\mathcal{A}_v^{\text{EPRL}}$  The EPRL contractor. See section 3.3.4.
  - $A_e$  An (internal) edge amplitude. See section 5.2.6.
  - $A_{\text{face}}$  A function  $A_{\text{face}} : \text{Irr}(G) \rightarrow \mathbb{C}$ , such that  $A_{\text{face}}(\rho_1) = A_{\text{face}}(\rho_2)$  if the representations  $\rho_1$  and  $\rho_2$  are equivalent. The number  $A_{\text{face}}(\rho_f)$  is called a face amplitude. See section 1.3.4.
  - $A_{\text{link}}$  A function  $A_{\text{link}} : \text{Irr}(G) \rightarrow \mathbb{C}$ , such that  $A_{\text{link}}(\rho_1) = A_{\text{link}}(\rho_2)$  if the representations  $\rho_1$  and  $\rho_2$  are equivalent. The number  $A_{\text{link}}(\partial\rho_\ell)$  is called a boundary link amplitude. See section 1.3.4.

*List of symbols*

$\mathfrak{A}(\Sigma)$  The set of the Lie algebra  $\mathfrak{g}$  valued differential one-forms (connections) on  $\Sigma$ .

$B_{ab}^{IJ}$  A discretization of the field  $B_{\mu\nu}^{IJ}$ . See section 3.1.2.

$B_{\mu\nu}^{IJ}$  An  $\text{so}(4)$  (or  $\text{so}(1,3)$ ) valued 2-form on  $\mathcal{M}$ . See section 3.1.1.

$\hat{B}_{\dagger}^{IJ}$  The quantum operator corresponding to  $B_{ab}^{IJ}$ . See section 3.2.4.

$C_{j_1}^{j_2 j_3}, C_{j_2 j_3}^{j_1}, C_{A_1}^{A_2 A_3}, C_{A_2 A_3}^{A_1}$  The Clebsch-Gordan map: Let  $(j_1, j_2, j_3) \in \frac{1}{2}\mathbb{N} \times \frac{1}{2}\mathbb{N} \times \frac{1}{2}\mathbb{N}$  satisfy triangle inequalities and  $j_1 + j_2 + j_3 \in \mathbb{N}$ . We denote by  $C_{j_1}^{j_2 j_3}$  the natural isometric embedding  $\mathcal{H}_{j_1} \rightarrow \mathcal{H}_{j_2} \otimes \mathcal{H}_{j_3}$  and by  $C_{j_2 j_3}^{j_1}$  the adjoint operator. In the index notation we omit  $j_1, j_2, j_3$ , e.g.  $C_{A_2 A_3}^{A_1} := (C_{j_2 j_3}^{j_1})_{A_2 A_3}^{A_1}$ ,  $A_1 \in \{1, \dots, 2j_1 + 1\}$  corresponds to the space  $\mathcal{H}_{j_1}$ ,  $A_2 \in \{1, \dots, 2j_2 + 1\}$  corresponds to the space  $\mathcal{H}_{j_2}^*$  and  $A_3 \in \{1, \dots, 2j_3 + 1\}$  corresponds to the space  $\mathcal{H}_{j_3}^*$ .

$\text{Cyl}(\mathfrak{A}(\Sigma))$  The space of cylindrical functions. See section 1.2.1.

$\mathcal{D}$  A graph diagram  $\mathcal{D} = (\mathcal{G}, \mathcal{R}_{\text{node}}, \varphi)$ . See section 6.1.1.

$\mathcal{D}_\gamma$  The static diagram of the graph  $\gamma$ . See section 6.2.4.

$d_f$  The dimension of the representation  $\rho_f$  ( $d_f = \dim \mathcal{H}_f$ ).

$e_\mu^I$  A tetrad. See section 1.1.1.

$e$  An edge of a foam, i.e. 1-cell of a 2-complex  $\kappa$ . See section 1.3.3.

$\mathfrak{E}$  The set of the equivalence classes of the edge relation. See section 6.1.2.

$e_{[n]}$  The 1-cell of  $\kappa_{\mathcal{D}}$  corresponding to the equivalence of the edge relation  $[n]$ . See section 6.1.3.

$e_a^i$  A triad,  $e_a^i = \mathfrak{q}_I^i(\theta_t^* e^I)_a$ . See section 1.1.3.

$F_{ab}^i$  The curvature two-form of the connection one-form  $A_a^i$ .  $F = dA + A \wedge A$ .

$f$  A face of a foam, i.e. 2-cell of a 2-complex  $\kappa$ . See section 1.3.3.

$\mathcal{F}$  The curvature two-form of  $\omega$ :  $\mathcal{F} = d\omega + \omega \wedge \omega$ .

$\mathfrak{F}$  The set of the equivalence classes of the face relation. See section 6.1.2.

$\mathfrak{F}_{\text{closed}}$  The set of the closed equivalence classes of the face relation. See section 6.1.2.

$\mathfrak{F}_{\text{open}}$  The set of the open equivalence classes of the face relation. See section 6.1.2.

$f_\ell$  The unique face containing the boundary link  $\ell$ .

$f_{[\ell]}$  The 2-cell of  $\kappa_{\mathcal{D}}$  corresponding to the equivalence class of the face relation  $[\ell]$ . See section 6.1.3.

$G$  The Newton's constant.

$G$  A Lie group (we usually assume that  $G$  is compact).

- $\mathcal{G}$  A finite set of oriented, connected, closed graphs. See section 6.1.
- $\mathcal{G}^{(0)}$  The set of nodes of all graphs in  $\mathcal{G}$ ,  $\mathcal{G}^{(0)} = \bigcup_{\mathbf{l}} \gamma_{\mathbf{l}}^{(0)}$ . See section 6.1.1.
- $\mathcal{G}^{(1)}$  The set of links of all graphs in  $\mathcal{G}$ ,  $\mathcal{G}^{(1)} = \bigcup_{\mathbf{l}} \gamma_{\mathbf{l}}^{(1)}$ . See section 6.1.1.
- $\mathcal{G}^{\text{in}} = \bigcup_{(n,n') \in \mathcal{R}_{\text{node}}} \gamma_n^{\text{in}}$ . See section 6.1.
- $\mathcal{G}^{\text{out}} = \bigcup_{(n,n') \in \mathcal{R}_{\text{node}}} \gamma_n^{\text{out}}$ . See section 6.1.
- $[g]^I_J$  The SO(4) matrix corresponding to  $g \in \text{Spin}(4)$ . See section 3.2.4.
- $g_{\mu\nu}$  Space-time metric:  $g_{\mu\nu} = \bar{\eta}_{IJ} e_{\mu}^I e_{\nu}^J$ .
- $\mathfrak{g}$  The Lie algebra of the Lie group  $G$ .
- $h_{ab}$  The first fundamental form of  $\Sigma$ . See section 1.1.2.
- $\mathcal{H}_{\text{comb}}$  The combinatorial Hilbert space. See section 1.2.5.
- $\mathcal{H}_e$  The edge Hilbert space:  $\mathcal{H}_e = \bigotimes_f \text{opposite orientation to } e \mathcal{H}_f^* \otimes \bigotimes_{f'} \text{same orientation as } e \mathcal{H}_{f'}$ . See section 1.3.3.
- $\mathcal{H}_f$  The representation space of the representation  $\rho_f$ . See section 1.3.3.
- $\mathcal{H}_{j+j-}$  The representation space of the  $\rho_{j+j-}$  representation.  $\mathcal{H}_{j+j-} = \mathcal{H}_{j+} \otimes \mathcal{H}_{j-}$ .
- $\mathcal{H}_k$  The representation space of the  $\rho_k$  representation.
- $\mathcal{H}_{\ell}$  The representation space of the representation  $\rho_{\ell}$ . See section 1.2.2.
- $\mathcal{H}_n$  The node Hilbert space:  $\mathcal{H}_n = \text{Inv} \left( \bigotimes_{\ell \text{ incoming to } n} \mathcal{H}_{\ell}^* \otimes \bigotimes_{\ell' \text{ outgoing from } n} \mathcal{H}_{\ell'} \right)$ . See section 1.2.2.
- $\mathcal{H}_{\text{poly}}$  The Hilbert space of quantum polyhedra in 4D,  $\mathcal{H}_{\text{poly}} = \left( \bigcup_n \mathcal{H}_{\text{poly}}^n \right) / \text{Spin}(4)$ . See section 3.2.4.
- $\mathcal{H}_{\text{poly}}^n$  The Hilbert space of quantum polyhedra in 4D orthogonal to  $n^I$ . See section 3.2.4.
- $\mathcal{H}_{\Sigma}$  The Hilbert space of gauge invariant functions in  $L^2(\mathfrak{A}(\Sigma), \mu_0)$ . See section 1.2.3.
- $\mathcal{H}_{\gamma}$  The Hilbert space of gauge invariant functions in  $L^2(G^{\gamma^{(1)}}, \mu_H)$ . See section 1.2.2.
- $\mathcal{H}_v = \bigotimes_{e \text{ incoming at } v} \text{Inv}(\mathcal{H}_e) \otimes \bigotimes_{e \text{ outgoing at } v} \text{Inv}(\mathcal{H}_e)^*$ . The vertex Hilbert space. See section 1.3.3.
- $\text{id}$  The identity operator.
- $\text{Inv}(\mathcal{H}_{\rho_1} \otimes \dots \otimes \mathcal{H}_{\rho_N})$  The subspace of invariant tensors (intertwiners) in  $\mathcal{H}_{\rho_1} \otimes \dots \otimes \mathcal{H}_{\rho_N}$ .
- $\text{InvEPRL} \left( \mathcal{H}_{j_1^+ j_1^-} \otimes \dots \otimes \mathcal{H}_{j_N^+ j_N^-} \right)$  A space of EPRL intertwiners (the image of an EPRL map). See section 3.3.1.
- $\text{Irr}(G)$  The set of unitary irreducible representations of the group  $G$ .

*List of symbols*

$k = 8\pi G$ .

$K_a^i$  The extrinsic curvature of  $\Sigma$ . See section 1.1.3.

$K_{ab}^i$  The "electric" part of  $B_{ab}^i$ :  $K_{ab}^i = (\mathbf{q}_a)_I^i n_{aJ} B_{ab}^{IJ}$ . See section 3.1.2.

$K_l^i$  The "electric" part of an antisymmetric matrix  $E_l^{IJ}$ :  $K_l^i = \mathbf{q}_l^i n_J E_l^{IJ}$ . See section 3.2.2.

$\hat{K}_l^i$  The quantum operator corresponding to  $K_{ab}^i$ :  $\hat{K}_l^i = n_I \mathbf{q}_J^i \hat{B}_l^{IJ}$ . See section 3.2.4.

$L_{ab}^i$  The "magnetic" part of  $B_{ab}^i$ :  $L_{ab}^i = \frac{1}{2} (\mathbf{q}_a)_I^i n_{aJ} \epsilon^{IJ}_{KL} B_{ab}^{KL}$ . See section 3.1.2.

$L_l^i$  The "magnetic" part of an antisymmetric matrix  $E_l^{IJ}$ :  $L_l^i = \frac{1}{2} \mathbf{q}_l^i n_J \epsilon^{IJ}_{KL} E_l^{KL}$ . See section 3.2.2.

$\hat{L}_l^i$  The quantum operator corresponding to  $L_{ab}^i$ :  $\hat{L}_l^i = \frac{1}{2} n_I \mathbf{q}_J^i \epsilon^{IJ}_{KL} \hat{B}_l^{KL}$ . See section 3.2.4.

$\mathcal{L}$  The Lie derivative.

$\ell$  A link of a graph,  $\ell \in \gamma^{(1)}$ . See section 1.2.2.

$[\ell]$  An equivalence class of a face relation. See section 6.1.2.

$\mathcal{M}$  A space-time manifold. It is assumed that  $\mathcal{M} = \Sigma \times \mathbb{R}$ , where  $\Sigma$  is the space manifold.

$N, N^\alpha$  The lapse and the shift:  $t^\alpha = Nn + N^\alpha$ . See section 1.1.2.

$n$  A node of a graph,  $n \in \gamma^{(0)}$ . See section 1.2.2.

$n^\alpha$  The unit time-like vector field normal to the slices  $\Sigma_t$ . See section 1.1.2.

$[n]$  An equivalence class of an edge relation. See section 6.1.2.

$n^I$  Components of the vector  $\mathbf{n}$ .

$\mathbf{n}$  A vector in  $V$  such that  $n^I n_I = \sigma$ .

$\vec{n}$  A unit vector in  $\mathbb{R}^3$ .

$P$  A coloring of internal edges of a foam with operators  $P_e : \text{Inv}(\mathcal{H}_e) \rightarrow \text{Inv}(\mathcal{H}_e)$  or a coloring of the nodes of the graphs in a graph diagram  $P_n : \mathcal{H}_n \rightarrow \mathcal{H}_n$ . See section 5.1.1 and section 6.2.1.

$P_i^a$  The momentum canonically conjugate to  $A_a^i$ . See section 1.1.3.

$\mathbf{q}, \mathbf{q}_i^I, \mathbf{q}_I^i, q^I_J$  Orthogonal projection  $q : V \rightarrow V$  into the space  $V_\perp$ .  $q_i^I$  is an orthonormal basis of  $V_\perp$ ,  $q_I^i$  is the partial isometry from  $V$  to  $V_\perp$  such that  $q_I^i n^I = 0$  and  $q_I^i q_J^I = \delta_j^i$ . See section 1.1.3.

$R$  The scalar curvature of the metric  $g_{\mu\nu}$ .

$\mathcal{R}_{\text{edge}}$  An edge relation. See section 6.1.2.

$\mathcal{R}_{\text{link}}$  A link relation. See section 6.1.

- $\mathcal{R}_{\text{node}}$  A node relation. See section 6.1.
- $s(\ell)$  The source of the link  $\ell$ . See section 1.2.2.
- $\text{SO}(\bar{\eta})$  The group of transformations in  $V$  leaving  $\bar{\eta}$  invariant.
- $\text{so}(\bar{\eta})$  The Lie algebra of the  $\text{SO}(\bar{\eta})$  group.
- $\text{SO}(\eta)$  The group of transformations in  $V_{\perp}$  leaving  $\eta$  invariant.
- $\text{so}(\eta)$  The Lie algebra of the  $\text{SO}(\eta)$  group.
- $\text{SU}_{\mathbf{n}}(2)$  The subgroup of Spin(4) transformations leaving  $\mathbf{n}$  invariant.
- $s_v$  The vertex spin network. See section 1.3.3.
- $t$  Time function, i.e. a smooth function  $t : \mathcal{M} \rightarrow \mathbb{R}$  such that  $dt$  is everywhere non-zero and each manifold  $t = t$ ,  $t \in \mathbb{R}$  is diffeomorphic to  $\Sigma$ . See section 1.1.2.
- $t(\ell)$  The target of the link  $\ell$ . See section 1.2.2.
- $\text{Tr}(\kappa, \rho, P, \mathcal{A})$  Contracted operator spin foam. See section 5.2.1.
- $\text{Tr}_l$  The distinguished contractor corresponding to the graph  $\gamma_l \in \mathcal{G}$ .  $\text{Tr}_l = \bigotimes_{\ell \in \gamma_l^{(1)}} \text{Tr}_\ell$ , where  $\text{Tr}_\ell \in \mathcal{H}_\ell \otimes \mathcal{H}_\ell^*$  is the trace functional.
- $\text{Tr}(D, \rho, P, \mathcal{A})$  Contracted operator spin-network diagram. See section 6.2.3.
- $\text{Tr}_v$  The vertex trace (BF contractor). See section 1.3.2 and section 5.2.3.
- $\mathbf{t}, t^\alpha$  Time vector  $\mathbf{t} = t^\alpha \partial_\alpha$ , i.e. a (future directed) vector field such that  $t^\alpha \partial_\alpha t = 1$ . See section 1.1.2.
- $V$  Internal vector space. In this thesis  $V = \mathbb{R}^4$ . See section 1.1.1.
- $v$  A vertex of a foam, i.e. 0-cell of a 2-complex  $\kappa$ . See section 1.3.3.
- $v_l$  The 0-cell of  $\kappa_D$  corresponding to the graph  $\gamma_l \in \mathcal{G}$ . See section 6.1.3.
- $v_\ell$  The 0-cell of  $\kappa_D$  corresponding to the graph  $\gamma \in \mathcal{G}$  such that  $\ell \in \gamma^{(1)}$ . See section 6.1.3.
- $v_n$  The 0-cell of  $\kappa_D$  corresponding to the graph  $\gamma \in \mathcal{G}$  such that  $n \in \gamma^{(0)}$ . See section 6.1.3.
- $V_{\perp}$  The subspace of  $V$  of vectors orthogonal to  $\mathbf{n}$ . See section 1.1.3.
- $Z(\kappa, \rho, \iota, \mathcal{A})$  The spin-foam amplitude. See section 1.3.4.
- $\mathcal{Z}(\kappa, \rho, P, \mathcal{A})$  The spin-foam operator. See section 5.2.1.
- $\mathcal{Z}(D, \rho, P, \mathcal{A})$  The spin-network diagram operator. See section 6.2.3.
- $\nabla$  The torsion-free derivative operator compatible with  $g_{\alpha\beta}$ .



# Bibliography

- [1] E. Alesci, “Tensorial Structure of the LQG graviton propagator,” *Int.J.Mod.Phys. A* **23** (2008) 1209–1213, [arXiv:0802.1201 \[gr-qc\]](#).
- [2] E. Alesci, E. Bianchi, E. Magliaro, and C. Perini, “Asymptotics of LQG fusion coefficients,” *Class.Quant.Grav.* **27** (2010) 095016, [arXiv:0809.3718 \[gr-qc\]](#).
- [3] E. Alesci, E. Bianchi, and C. Rovelli, “LQG propagator: III. The New vertex,” *Class.Quant.Grav.* **26** (2009) 215001, [arXiv:0812.5018 \[gr-qc\]](#).
- [4] E. Alesci and C. Rovelli, “The Complete LQG propagator. I. Difficulties with the Barrett-Crane vertex,” *Phys.Rev. D* **76** (2007) 104012, [arXiv:0708.0883 \[gr-qc\]](#).
- [5] E. Alesci and C. Rovelli, “The Complete LQG propagator. II. Asymptotic behavior of the vertex,” *Phys.Rev. D* **77** (2008) 044024, [arXiv:0711.1284 \[gr-qc\]](#).
- [6] E. Alesci and C. Rovelli, “A Regularization of the hamiltonian constraint compatible with the spinfoam dynamics,” *Phys.Rev. D* **82** (2010) 044007, [arXiv:1005.0817 \[gr-qc\]](#).
- [7] E. Alesci, T. Thiemann, and A. Zipfel, “Linking covariant and canonical LQG: New solutions to the Euclidean Scalar Constraint,” *Phys.Rev. D* **86** (2012) 024017, [arXiv:1109.1290 \[gr-qc\]](#).
- [8] A. Alexandrov, *Convex Polyhedra*. Springer Berlin Heidelberg New York, 2005.
- [9] S. Alexandrov, “Simplicity and closure constraints in spin foam models of gravity,” *Phys.Rev. D* **78** (2008) 044033, [arXiv:0802.3389 \[gr-qc\]](#).
- [10] S. Alexandrov, “The new vertices and canonical quantization,” *Phys.Rev. D* **82** (2010) 024024, [arXiv:1004.2260 \[gr-qc\]](#).
- [11] S. Alexandrov, “Degenerate Plebanski Sector and Spin Foam Quantization,” *Class.Quant.Grav.* **29** (2012) 145018, [arXiv:1202.5039 \[gr-qc\]](#).
- [12] S. Alexandrov, M. Geiller, and K. Noui, “Spin Foams and Canonical Quantization,” *SIGMA* **8** (2012) 055, [arXiv:1112.1961 \[gr-qc\]](#).
- [13] S. Alexandrov and P. Roche, “Critical Overview of Loops and Foams,” *Phys.Rept.* **506** (2011) 41–86, [arXiv:1009.4475 \[gr-qc\]](#).
- [14] F. Anzà and S. Speziale, “A note on the secondary simplicity constraints in loop quantum gravity,” [arXiv:1409.0836 \[gr-qc\]](#).
- [15] A. Ashtekar, M. Campiglia, and A. Henderson, “Loop Quantum Cosmology and Spin Foams,” *Phys.Lett. B* **681** (2009) 347–352, [arXiv:0909.4221 \[gr-qc\]](#).

## Bibliography

- [16] A. Ashtekar, M. Campiglia, and A. Henderson, “Casting Loop Quantum Cosmology in the Spin Foam Paradigm,” *Class.Quant.Grav.* **27** (2010) 135020, [arXiv:1001.5147 \[gr-qc\]](https://arxiv.org/abs/1001.5147).
- [17] A. Ashtekar and J. Lewandowski, “Background independent quantum gravity: A Status report,” *Class.Quant.Grav.* **21** (2004) R53, [arXiv:gr-qc/0404018 \[gr-qc\]](https://arxiv.org/abs/gr-qc/0404018).
- [18] A. Ashtekar, J. Lewandowski, D. Marolf, J. Mourao, and T. Thiemann, “Coherent state transforms for spaces of connections,” *J.Funct.Anal.* **135** (1996) 519–551, [arXiv:gr-qc/9412014 \[gr-qc\]](https://arxiv.org/abs/gr-qc/9412014).
- [19] A. Ashtekar, M. Reuter, and C. Rovelli, “From General Relativity to Quantum Gravity,” [arXiv:1408.4336 \[gr-qc\]](https://arxiv.org/abs/1408.4336).
- [20] J. C. Baez, “An Introduction to spin foam models of quantum gravity and BF theory,” *Lect.Notes Phys.* **543** (2000) 25–94, [arXiv:gr-qc/9905087 \[gr-qc\]](https://arxiv.org/abs/gr-qc/9905087).
- [21] J. C. Baez, “Strings, loops, knots and gauge fields,” in *Knots and Quantum Gravity*. 1994. [arXiv:hep-th/9309067 \[hep-th\]](https://arxiv.org/abs/hep-th/9309067).
- [22] J. C. Baez, “Spin network states in gauge theory,” *Adv.Math.* **117** (1996) 253–272, [arXiv:gr-qc/9411007 \[gr-qc\]](https://arxiv.org/abs/gr-qc/9411007).
- [23] J. C. Baez, “Spin foam models,” *Class.Quant.Grav.* **15** (1998) 1827–1858, [arXiv:gr-qc/9709052 \[gr-qc\]](https://arxiv.org/abs/gr-qc/9709052).
- [24] J. C. Baez and J. W. Barrett, “The Quantum tetrahedron in three-dimensions and four-dimensions,” *Adv.Theor.Math.Phys.* **3** (1999) 815–850, [arXiv:gr-qc/9903060 \[gr-qc\]](https://arxiv.org/abs/gr-qc/9903060).
- [25] J. C. Baez and J. W. Barrett, “Integrability for relativistic spin networks,” *Class.Quant.Grav.* **18** (2001) 4683–4700, [arXiv:gr-qc/0101107 \[gr-qc\]](https://arxiv.org/abs/gr-qc/0101107).
- [26] J. C. Baez, J. D. Christensen, T. R. Halford, and D. C. Tsang, “Spin foam models of Riemannian quantum gravity,” *Class.Quant.Grav.* **19** (2002) 4627–4648, [arXiv:gr-qc/0202017 \[gr-qc\]](https://arxiv.org/abs/gr-qc/0202017).
- [27] J. C. Baez and S. Savin, “Diffeomorphism-Invariant Spin Network States,” *J.Fun.An.* **158** (1998) 253–266, [arXiv:9708005 \[q-alg\]](https://arxiv.org/abs/9708005).
- [28] B. Bahr, “On knottings in the physical Hilbert space of LQG as given by the EPRL model,” *Class.Quant.Grav.* **28** (2011) 045002, [arXiv:1006.0700 \[gr-qc\]](https://arxiv.org/abs/1006.0700).
- [29] B. Bahr, F. Hellmann, W. Kaminski, M. Kisielowski, and J. Lewandowski, “Operator Spin Foam Models,” *Class.Quant.Grav.* **28** (2011) 105003, [arXiv:1010.4787 \[gr-qc\]](https://arxiv.org/abs/1010.4787).
- [30] B. Bahr and T. Thiemann, “Gauge-invariant coherent states for Loop Quantum Gravity. I. Abelian gauge groups,” *Class.Quant.Grav.* **26** (2009) 045011, [arXiv:0709.4619 \[gr-qc\]](https://arxiv.org/abs/0709.4619).

- [31] B. Bahr and T. Thiemann, “Gauge-invariant coherent states for loop quantum gravity. II. Non-Abelian gauge groups,” *Class.Quant.Grav.* **26** (2009) 045012, [arXiv:0709.4636 \[gr-qc\]](#).
- [32] A. Baratin, B. Dittrich, D. Oriti, and J. Tambornino, “Non-commutative flux representation for loop quantum gravity,” *Class.Quant.Grav.* **28** (2011) 175011, [arXiv:1004.3450 \[hep-th\]](#).
- [33] A. Baratin, C. Flori, and T. Thiemann, “The Holst Spin Foam Model via Cubulations,” *New J.Phys.* **14** (2012) 103054, [arXiv:0812.4055 \[gr-qc\]](#).
- [34] J. F. Barbero G., “Real Ashtekar variables for Lorentzian signature space times,” *Phys.Rev.* **D51** (1995) 5507–5510, [arXiv:gr-qc/9410014 \[gr-qc\]](#).
- [35] A. Barbieri, “Space of the vertices of relativistic spin networks,” [arXiv:gr-qc/9709076 \[gr-qc\]](#).
- [36] A. Barbieri, “Quantum tetrahedra and simplicial spin networks,” *Nucl.Phys.* **B518** (1998) 714–728, [arXiv:gr-qc/9707010 \[gr-qc\]](#).
- [37] J. W. Barrett, “The Classical evaluation of relativistic spin networks,” *Adv.Theor.Math.Phys.* **2** (1998) 593–600, [arXiv:math/9803063 \[math\]](#).
- [38] J. W. Barrett and L. Crane, “Relativistic spin networks and quantum gravity,” *J.Math.Phys.* **39** (1998) 3296–3302, [arXiv:gr-qc/9709028 \[gr-qc\]](#).
- [39] J. W. Barrett and L. Crane, “A Lorentzian signature model for quantum general relativity,” *Class.Quant.Grav.* **17** (2000) 3101–3118, [arXiv:gr-qc/9904025 \[gr-qc\]](#).
- [40] J. W. Barrett, R. Dowdall, W. J. Fairbairn, H. Gomes, and F. Hellmann, “Asymptotic analysis of the EPRL four-simplex amplitude,” *J.Math.Phys.* **50** (2009) 112504, [arXiv:0902.1170 \[gr-qc\]](#).
- [41] J. W. Barrett, R. Dowdall, W. J. Fairbairn, F. Hellmann, and R. Pereira, “Lorentzian spin foam amplitudes: Graphical calculus and asymptotics,” *Class.Quant.Grav.* **27** (2010) 165009, [arXiv:0907.2440 \[gr-qc\]](#).
- [42] J. W. Barrett and I. Naish-Guzman, “The Ponzano-Regge model,” *Class.Quant.Grav.* **26** (2009) 155014, [arXiv:0803.3319 \[gr-qc\]](#).
- [43] J. Ben Geloun, R. Gurau, and V. Rivasseau, “EPRL/FK Group Field Theory,” *Europhys.Lett.* **92** (2010) 60008, [arXiv:1008.0354 \[hep-th\]](#).
- [44] E. Bianchi, H. M. Haggard, and C. Rovelli, “The boundary is mixed,” [arXiv:1306.5206 \[gr-qc\]](#).
- [45] E. Bianchi, E. Magliaro, and C. Perini, “Coherent spin-networks,” *Phys.Rev.* **D82** (2010) 024012, [arXiv:0912.4054 \[gr-qc\]](#).
- [46] E. Bianchi, E. Magliaro, and C. Perini, “Spinfoams in the holomorphic representation,” *Phys.Rev.* **D82** (2010) 124031, [arXiv:1004.4550 \[gr-qc\]](#).

## Bibliography

- [47] E. Bianchi, L. Modesto, C. Rovelli, and S. Speziale, “Graviton propagator in loop quantum gravity,” *Class.Quant.Grav.* **23** (2006) 6989–7028, [arXiv:gr-qc/0604044 \[gr-qc\]](#).
- [48] E. Bianchi, D. Regoli, and C. Rovelli, “Face amplitude of spinfoam quantum gravity,” *Class.Quant.Grav.* **27** (2010) 185009, [arXiv:1005.0764 \[gr-qc\]](#).
- [49] E. Bianchi, C. Rovelli, and F. Vidotto, “Towards Spinfoam Cosmology,” *Phys.Rev.* **D82** (2010) 084035, [arXiv:1003.3483 \[gr-qc\]](#).
- [50] V. Bonzom, “From lattice BF gauge theory to area-angle Regge calculus,” *Class.Quant.Grav.* **26** (2009) 155020, [arXiv:0903.0267 \[gr-qc\]](#).
- [51] V. Bonzom, “Spin foam models for quantum gravity from lattice path integrals,” *Phys.Rev.* **D80** (2009) 064028, [arXiv:0905.1501 \[gr-qc\]](#).
- [52] V. Bonzom and B. Dittrich, “Bubble divergences and gauge symmetries in spin foams,” *Phys.Rev.* **D88** (2013) 124021, [arXiv:1304.6632 \[gr-qc\]](#).
- [53] V. Bonzom and M. Smerlak, “Bubble divergences from cellular cohomology,” *Lett.Math.Phys.* **93** (2010) 295–305, [arXiv:1004.5196 \[gr-qc\]](#).
- [54] V. Bonzom and M. Smerlak, “Bubble divergences from twisted cohomology,” *Commun.Math.Phys.* **312** (2012) 399–426, [arXiv:1008.1476 \[math-ph\]](#).
- [55] V. Bonzom and M. Smerlak, “Bubble divergences: sorting out topology from cell structure,” *Annales Henri Poincare* **13** (2012) 185–208, [arXiv:1103.3961 \[gr-qc\]](#).
- [56] E. F. Borja, I. Garay, and F. Vidotto, “Learning about quantum gravity with a couple of nodes,” *SIGMA* **8** (2012) 015, [arXiv:1110.3020 \[gr-qc\]](#).
- [57] E. Buffenoir, M. Henneaux, K. Noui, and P. Roche, “Hamiltonian analysis of Plebanski theory,” *Class.Quant.Grav.* **21** (2004) 5203–5220, [arXiv:gr-qc/0404041 \[gr-qc\]](#).
- [58] M. Campiglia, A. Henderson, and W. Nelson, “Vertex Expansion for the Bianchi I model,” *Phys.Rev.* **D82** (2010) 064036, [arXiv:1007.3723 \[gr-qc\]](#).
- [59] M. Christodoulou, M. Langvik, A. Riello, C. Roken, and C. Rovelli, “Divergences and Orientation in Spinfoams,” [arXiv:1207.5156 \[gr-qc\]](#).
- [60] M. Christodoulou, A. Riello, and C. Rovelli, “How to detect an anti-spacetime,” *Int.J.Mod.Phys.* **D21** (2012) 1242014, [arXiv:1206.3903 \[gr-qc\]](#).
- [61] P. Collins and R. Williams, “Dynamics of the Friedmann universe using regge calculus,” *Phys.Rev.* **D7** (1973) 965–971.
- [62] F. Conrady, “Spin foams with timelike surfaces,” *Class.Quant.Grav.* **27** (2010) 155014, [arXiv:1003.5652 \[gr-qc\]](#).
- [63] F. Conrady and L. Freidel, “Quantum geometry from phase space reduction,” *J.Math.Phys.* **50** (2009) 123510, [arXiv:0902.0351 \[gr-qc\]](#).

- [64] F. Conrady and J. Hnybida, “A spin foam model for general Lorentzian 4-geometries,” *Class.Quant.Grav.* **27** (2010) 185011, [arXiv:1002.1959 \[gr-qc\]](#).
- [65] L. Crane, A. Perez, and C. Rovelli, “Perturbative finiteness in spin-foam quantum gravity,” *Phys.Rev.Lett.* **87** (2001) 181301.
- [66] L. Crane, A. Perez, and C. Rovelli, “A Finiteness proof for the Lorentzian state sum spin foam model for quantum general relativity,” [arXiv:gr-qc/0104057 \[gr-qc\]](#).
- [67] R. De Pietri and L. Freidel, “so(4) Plebanski action and relativistic spin foam model,” *Class.Quant.Grav.* **16** (1999) 2187–2196, [arXiv:gr-qc/9804071 \[gr-qc\]](#).
- [68] R. De Pietri, L. Freidel, K. Krasnov, and C. Rovelli, “Barrett-Crane model from a Boulatov-Ooguri field theory over a homogeneous space,” *Nucl.Phys.* **B574** (2000) 785–806, [arXiv:hep-th/9907154 \[hep-th\]](#).
- [69] R. De Pietri and C. Petronio, “Feynman diagrams of generalized matrix models and the associated manifolds in dimension 4,” *J.Math.Phys.* **41** (2000) 6671–6688, [arXiv:gr-qc/0004045 \[gr-qc\]](#).
- [70] C. Di Bartolo, R. Gambini, J. Griego, and J. Pullin, “Canonical quantum gravity in the Vassilev invariants arena. 2. Constraints, habitats and consistency of the constraint algebra,” *Class.Quant.Grav.* **17** (2000) 3239–3264, [arXiv:gr-qc/9911010 \[gr-qc\]](#).
- [71] C. Di Bartolo, R. Gambini, J. Griego, and J. Pullin, “Consistent canonical quantization of general relativity in the space of Vassilev knot invariants,” *Phys.Rev.Lett.* **84** (2000) 2314–2317, [arXiv:gr-qc/9909063 \[gr-qc\]](#).
- [72] Y. Ding and M. Han, “On the Asymptotics of Quantum Group Spinfoam Model,” [arXiv:1103.1597 \[gr-qc\]](#).
- [73] Y. Ding, M. Han, and C. Rovelli, “Generalized Spinfoams,” *Phys.Rev.* **D83** (2011) 124020, [arXiv:1011.2149 \[gr-qc\]](#).
- [74] Y. Ding and C. Rovelli, “Physical boundary Hilbert space and volume operator in the Lorentzian new spin-foam theory,” *Class.Quant.Grav.* **27** (2010) 205003, [arXiv:1006.1294 \[gr-qc\]](#).
- [75] Y. Ding and C. Rovelli, “The Volume operator in covariant quantum gravity,” *Class.Quant.Grav.* **27** (2010) 165003, [arXiv:0911.0543 \[gr-qc\]](#).
- [76] B. Dittrich and P. A. Hohn, “From covariant to canonical formulations of discrete gravity,” *Class.Quant.Grav.* **27** (2010) 155001, [arXiv:0912.1817 \[gr-qc\]](#).
- [77] B. Dittrich and J. P. Ryan, “Simplicity in simplicial phase space,” *Phys.Rev.* **D82** (2010) 064026, [arXiv:1006.4295 \[gr-qc\]](#).
- [78] B. Dittrich and J. P. Ryan, “Phase space descriptions for simplicial 4d geometries,” *Class.Quant.Grav.* **28** (2011) 065006, [arXiv:0807.2806 \[gr-qc\]](#).

## Bibliography

- [79] B. Dittrich and J. P. Ryan, “On the role of the Barbero-Immirzi parameter in discrete quantum gravity,” *Class.Quant.Grav.* **30** (2013) 095015, [arXiv:1209.4892 \[gr-qc\]](#).
- [80] M. Dupuis, J. P. Ryan, and S. Speziale, “Discrete gravity models and Loop Quantum Gravity: a short review,” *SIGMA* **8** (2012) 052, [arXiv:1204.5394 \[gr-qc\]](#).
- [81] J. Engle, “The Plebanski sectors of the EPRL vertex,” *Class.Quant.Grav.* **28** (2011) 225003, Corrigendum-ibid. 30 (2013) 049501, [arXiv:1107.0709 \[gr-qc\]](#).
- [82] J. Engle, “A spin-foam vertex amplitude with the correct semiclassical limit,” *Phys.Lett.* **B724** (2013) 333–337, [arXiv:1201.2187 \[gr-qc\]](#).
- [83] J. Engle, “Proposed proper Engle-Pereira-Rovelli-Livine vertex amplitude,” *Phys.Rev.* **D87** no. 8, (2013) 084048, [arXiv:1111.2865 \[gr-qc\]](#).
- [84] J. Engle, *Springer Handbook of Spacetime*, ch. Spin foams. Springer-Verlag, 2014. [arXiv:1303.4636 \[gr-qc\]](#).
- [85] J. Engle, M. Han, and T. Thiemann, “Canonical path integral measures for Holst and Plebanski gravity. I. Reduced Phase Space Derivation,” *Class.Quant.Grav.* **27** (2010) 245014, [arXiv:0911.3433 \[gr-qc\]](#).
- [86] J. Engle, E. Livine, R. Pereira, and C. Rovelli, “LQG vertex with finite Immirzi parameter,” *Nucl.Phys.* **B799** (2008) 136–149, [arXiv:0711.0146 \[gr-qc\]](#).
- [87] J. Engle and R. Pereira, “Regularization and finiteness of the Lorentzian LQG vertices,” *Phys.Rev.* **D79** (2009) 084034, [arXiv:0805.4696 \[gr-qc\]](#).
- [88] J. Engle, R. Pereira, and C. Rovelli, “The Loop-quantum-gravity vertex-amplitude,” *Phys.Rev.Lett.* **99** (2007) 161301, [arXiv:0705.2388 \[gr-qc\]](#).
- [89] J. Engle, R. Pereira, and C. Rovelli, “Flipped spinfoam vertex and loop gravity,” *Nucl.Phys.* **B798** (2008) 251–290, [arXiv:0708.1236 \[gr-qc\]](#).
- [90] W. Fairbairn and C. Rovelli, “Separable Hilbert space in loop quantum gravity,” *J.Math.Phys.* **45** (2004) 2802–2814, [arXiv:gr-qc/0403047 \[gr-qc\]](#).
- [91] W. J. Fairbairn and C. Meusburger, “Quantum deformation of two four-dimensional spin foam models,” *J.Math.Phys.* **53** (2012) 022501, [arXiv:1012.4784 \[gr-qc\]](#).
- [92] C. Flori and T. Thiemann, “Semiclassical analysis of the Loop Quantum Gravity volume operator. I. Flux Coherent States,” [arXiv:0812.1537 \[gr-qc\]](#).
- [93] C. Flori, “Semiclassical analysis of the Loop Quantum Gravity volume operator: Area Coherent States,” [arXiv:0904.1303 \[gr-qc\]](#).
- [94] L. Freidel, “Group field theory: An Overview,” *Int.J.Theor.Phys.* **44** (2005) 1769–1783, [arXiv:hep-th/0505016 \[hep-th\]](#).

- [95] L. Freidel and K. Krasnov, “Spin foam models and the classical action principle,” *Adv.Theor.Math.Phys.* **2** (1999) 1183–1247, [arXiv:hep-th/9807092 \[hep-th\]](#).
- [96] L. Freidel and K. Krasnov, “A New Spin Foam Model for 4d Gravity,” *Class.Quant.Grav.* **25** (2008) 125018, [arXiv:0708.1595 \[gr-qc\]](#).
- [97] L. Freidel, K. Krasnov, and E. R. Livine, “Holomorphic Factorization for a Quantum Tetrahedron,” *Commun.Math.Phys.* **297** (2010) 45–93, [arXiv:0905.3627 \[hep-th\]](#).
- [98] L. Freidel and S. Speziale, “From twistors to twisted geometries,” *Phys.Rev.* **D82** (2010) 084041, [arXiv:1006.0199 \[gr-qc\]](#).
- [99] L. Freidel and S. Speziale, “Twisted geometries: A geometric parametrisation of SU(2) phase space,” *Phys.Rev.* **D82** (2010) 084040, [arXiv:1001.2748 \[gr-qc\]](#).
- [100] M. Gaul and C. Rovelli, “A Generalized Hamiltonian constraint operator in loop quantum gravity and its simplest Euclidean matrix elements,” *Class.Quant.Grav.* **18** (2001) 1593–1624, [arXiv:gr-qc/0011106 \[gr-qc\]](#).
- [101] M. Geiller and K. Noui, “Testing the imposition of the Spin Foam Simplicity Constraints,” *Class.Quant.Grav.* **29** (2012) 135008, [arXiv:1112.1965 \[gr-qc\]](#).
- [102] H. M. Haggard, C. Rovelli, W. Wieland, and F. Vidotto, “The spin connection of twisted geometry,” *Phys.Rev.* **D87** (2013) 024038, [arXiv:1211.2166 \[gr-qc\]](#).
- [103] M. Han, “4-dimensional Spin-foam Model with Quantum Lorentz Group,” *J.Math.Phys.* **52** (2011) 072501, [arXiv:1012.4216 \[gr-qc\]](#).
- [104] M. Han, “Cosmological Constant in LQG Vertex Amplitude,” *Phys.Rev.* **D84** (2011) 064010, [arXiv:1105.2212 \[gr-qc\]](#).
- [105] M. Han, “Semiclassical Analysis of Spinfoam Model with a Small Barbero-Immirzi Parameter,” *Phys.Rev.* **D88** (2013) 044051, [arXiv:1304.5628 \[gr-qc\]](#).
- [106] M. Han, “On Spinfoam Models in Large Spin Regime,” *Class.Quant.Grav.* **31** (2014) 015004, [arXiv:1304.5627 \[gr-qc\]](#).
- [107] M. Han, W. Huang, and Y. Ma, “Fundamental structure of loop quantum gravity,” *Int.J.Mod.Phys.* **D16** (2007) 1397–1474, [arXiv:gr-qc/0509064 \[gr-qc\]](#).
- [108] M. Han and T. Thiemann, “On the Relation between Operator Constraint –, Master Constraint –, Reduced Phase Space –, and Path Integral Quantisation,” *Class.Quant.Grav.* **27** (2010) 225019, [arXiv:0911.3428 \[gr-qc\]](#).
- [109] M. Han and T. Thiemann, “On the Relation between Rigging Inner Product and Master Constraint Direct Integral Decomposition,” *J.Math.Phys.* **51** (2010) 092501, [arXiv:0911.3431 \[gr-qc\]](#).
- [110] M. Han and T. Thiemann, “Commuting Simplicity and Closure Constraints for 4D Spin Foam Models,” *Class.Quant.Grav.* **30** (2013) 235024, [arXiv:1010.5444 \[gr-qc\]](#).

## Bibliography

- [111] J. Hartle and S. Hawking, “Wave Function of the Universe,” *Phys.Rev.* **D28** (1983) 2960–2975.
- [112] A. Hatcher, *Algebraic topology*. Cambridge University Press, 2001.  
<http://www.math.cornell.edu/~hatcher/AT/AT.pdf>.
- [113] S. Hawking and G. Ellis, *The large scale structure of space-time*. Cambridge University Press, 1973.
- [114] F. Hellmann, *State Sums and Geometry*. PhD thesis, School of Mathematics, University of Nottingham, October, 2010. [arXiv:1102.1688 \[gr-qc\]](https://arxiv.org/abs/1102.1688).
- [115] F. Hellmann, “On the Expansions in Spin Foam Cosmology,” *Phys.Rev.* **D84** (2011) 103516, [arXiv:1105.1334 \[gr-qc\]](https://arxiv.org/abs/1105.1334).
- [116] F. Hellmann and W. Kaminski, “Holonomy spin foam models: Asymptotic geometry of the partition function,” *JHEP* **1310** (2013) 165, [arXiv:1307.1679 \[gr-qc\]](https://arxiv.org/abs/1307.1679).
- [117] A. Henderson, C. Rovelli, F. Vidotto, and E. Wilson-Ewing, “Local spinfoam expansion in loop quantum cosmology,” *Class.Quant.Grav.* **28** (2011) 025003, [arXiv:1010.0502 \[gr-qc\]](https://arxiv.org/abs/1010.0502).
- [118] S. Holst, “Barbero’s Hamiltonian derived from a generalized Hilbert-Palatini action,” *Phys.Rev.* **D53** (1996) 5966–5969, [arXiv:gr-qc/9511026 \[gr-qc\]](https://arxiv.org/abs/gr-qc/9511026).
- [119] J. Hudson, *Piecewise linear topology*. W.A. Benjamin Inc., 1969.
- [120] G. Immirzi, “Quantum gravity and Regge calculus,” *Nucl.Phys.Proc.Suppl.* **57** (1997) 65–72, [arXiv:gr-qc/9701052 \[gr-qc\]](https://arxiv.org/abs/gr-qc/9701052).
- [121] J. Iwasaki, “A Definition of the Ponzano-Regge quantum gravity model in terms of surfaces,” *J.Math.Phys.* **36** (1995) 6288–6298, [arXiv:gr-qc/9505043 \[gr-qc\]](https://arxiv.org/abs/gr-qc/9505043).
- [122] W. Kaminski, “All 3-edge-connected relativistic BC and EPRL spin-networks are integrable,” [arXiv:1010.5384 \[gr-qc\]](https://arxiv.org/abs/1010.5384).
- [123] W. Kaminski, M. Kisielowski, and J. Lewandowski, “Spin-Foams for All Loop Quantum Gravity,” *Class.Quant.Grav.* **27** (2010) 095006, Corrigendum-ibid. **29** (2012) 049502, [arXiv:0909.0939 \[gr-qc\]](https://arxiv.org/abs/0909.0939).
- [124] W. Kaminski, M. Kisielowski, and J. Lewandowski, “The EPRL intertwiners and corrected partition function,” *Class.Quant.Grav.* **27** (2010) 165020, Corrigendum-ibid. **29** (2012) 049501, [arXiv:0912.0540 \[gr-qc\]](https://arxiv.org/abs/0912.0540).
- [125] W. Kaminski, M. Kisielowski, and J. Lewandowski, “The Kernel and the injectivity of the EPRL map,” *Class.Quant.Grav.* **29** (2012) 085001, [arXiv:1109.5023 \[gr-qc\]](https://arxiv.org/abs/1109.5023).
- [126] M. Kisielowski, “First-order contributions to the Dipole Cosmology transition amplitude.” to appear.

- [127] M. Kisielowski, “Dynamics of loop quantum gravity encoded in graphs,” *J.Phys.Conf.Ser.* **360** (2012) 012048.
- [128] M. Kisielowski, *Spinfoams contributing in first order of vertex expansion to the Dipole Cosmology transition amplitude*, ch. 48, pp. 359–364. World Scientific, 2013.
- [129] M. Kisielowski, J. Lewandowski, and J. Puchta, “Feynman diagrammatic approach to spin foams,” *Class.Quant.Grav.* **29** (2012) 015009, [arXiv:1107.5185 \[gr-qc\]](https://arxiv.org/abs/1107.5185).
- [130] M. Kisielowski, J. Lewandowski, and J. Puchta, “One vertex spin-foams with the Dipole Cosmology boundary,” *Class.Quant.Grav.* **30** (2013) 025007, [arXiv:1203.1530 \[gr-qc\]](https://arxiv.org/abs/1203.1530).
- [131] T. Krajewski, J. Magnen, V. Rivasseau, A. Tanasa, and P. Vitale, “Quantum Corrections in the Group Field Theory Formulation of the EPRL/FK Models,” *Phys.Rev.* **D82** (2010) 124069, [arXiv:1007.3150 \[gr-qc\]](https://arxiv.org/abs/1007.3150).
- [132] J. Lewandowski, A. Okolow, H. Sahlmann, and T. Thiemann, “Uniqueness of diffeomorphism invariant states on holonomy-flux algebras,” *Commun.Math.Phys.* **267** (2006) 703–733, [arXiv:gr-qc/0504147 \[gr-qc\]](https://arxiv.org/abs/gr-qc/0504147).
- [133] J. Lewandowski and H. Sahlmann, “A symmetric scalar constraint for loop quantum gravity,” [arXiv:1410.5276 \[gr-qc\]](https://arxiv.org/abs/1410.5276).
- [134] E. R. Livine and S. Speziale, “A New spinfoam vertex for quantum gravity,” *Phys.Rev.* **D76** (2007) 084028, [arXiv:0705.0674 \[gr-qc\]](https://arxiv.org/abs/0705.0674).
- [135] E. R. Livine and S. Speziale, “Consistently Solving the Simplicity Constraints for Spinfoam Quantum Gravity,” *Europhys.Lett.* **81** (2008) 50004, [arXiv:0708.1915 \[gr-qc\]](https://arxiv.org/abs/0708.1915).
- [136] F. Markopoulou, “Dual formulation of spin network evolution,” [arXiv:gr-qc/9704013 \[gr-qc\]](https://arxiv.org/abs/gr-qc/9704013).
- [137] H. Minkowski, “Allgemeine Lehrsätze über die convexen Polyeder,” *Nachrichten von der Gesellschaft der Wissenschaften zu Göttingen, Mathematisch-Physikalische Klasse* **1897** (1897) 198–220. <http://eudml.org/doc/58391>.
- [138] K. Noui and A. Perez, “Three-dimensional loop quantum gravity: Physical scalar product and spin foam models,” *Class.Quant.Grav.* **22** (2005) 1739–1762, [arXiv:gr-qc/0402110 \[gr-qc\]](https://arxiv.org/abs/gr-qc/0402110).
- [139] R. Oeckl, “A ‘General boundary’ formulation for quantum mechanics and quantum gravity,” *Phys.Lett.* **B575** (2003) 318–324, [arXiv:hep-th/0306025 \[hep-th\]](https://arxiv.org/abs/hep-th/0306025).
- [140] R. Oeckl, “Renormalization of discrete models without background,” *Nucl.Phys.* **B657** (2003) 107–138, [arXiv:gr-qc/0212047 \[gr-qc\]](https://arxiv.org/abs/gr-qc/0212047).
- [141] R. Oeckl, “General boundary quantum field theory: Foundations and probability interpretation,” *Adv.Theor.Math.Phys.* **12** (2008) 319–352, [arXiv:hep-th/0509122 \[hep-th\]](https://arxiv.org/abs/hep-th/0509122).

## Bibliography

- [142] D. Oriti, J. P. Ryan, and J. Thürigen, “Group field theories for all loop quantum gravity,” [arXiv:1409.3150 \[gr-qc\]](https://arxiv.org/abs/1409.3150).
- [143] A. Perelomov, “Coherent states for arbitrary lie groups,” *Commun.Math.Phys.* **26** (1972) 222–236.
- [144] A. Perez, “Finiteness of a spinfoam model for Euclidean quantum general relativity,” *Nucl.Phys.* **B599** (2001) 427–434, [arXiv:gr-qc/0011058 \[gr-qc\]](https://arxiv.org/abs/gr-qc/0011058).
- [145] A. Perez, “Spin foam models for quantum gravity,” *Class.Quant.Grav.* **20** (2003) R43, [arXiv:gr-qc/0301113 \[gr-qc\]](https://arxiv.org/abs/gr-qc/0301113).
- [146] A. Perez, “The Spin Foam Approach to Quantum Gravity,” *Living Rev.Rel.* **16** (2013) 3, [arXiv:1205.2019 \[gr-qc\]](https://arxiv.org/abs/1205.2019).
- [147] A. Perez and C. Rovelli, “A Spin foam model without bubble divergences,” *Nucl.Phys.* **B599** (2001) 255–282, [arXiv:gr-qc/0006107 \[gr-qc\]](https://arxiv.org/abs/gr-qc/0006107).
- [148] C. Perini, “Holonomy-flux spinfoam amplitude,” [arXiv:1211.4807 \[gr-qc\]](https://arxiv.org/abs/1211.4807).
- [149] J. F. Plebanski, “On the separation of Einsteinian substructures,” *J.Math.Phys.* **18** (1977) 2511–2520.
- [150] G. Ponzano and T. Regge, “Semiclassical limit of Racah coefficients,” in *Spectroscopic and Group Theoretical Methods in Physics: Racah Memorial Volume*, F. Bloch, S. Cohen, A. De-Shalit, S. Sambursky, and I. Talmi, eds. Amsterdam: North-Holland Publishing Co., 1968.
- [151] D. Pranzetti, “Turaev-Viro amplitudes from 2+1 Loop Quantum Gravity,” *Phys.Rev.* **D89** (2014) 084058, [arXiv:1402.2384 \[gr-qc\]](https://arxiv.org/abs/1402.2384).
- [152] J. Puchta, “Shape of spinfoams encoded in graphs,” *J.Phys.Conf.Ser.* **360** (2012) 012051.
- [153] J. Puchta, “Asymptotic of Lorentzian Polyhedra Propagator,” [arXiv:1307.4747 \[gr-qc\]](https://arxiv.org/abs/1307.4747).
- [154] T. Regge, “General Relativity without Coordinates,” *Nuovo Cim.* **19** (1961) 558–571.
- [155] M. P. Reisenberger, “World sheet formulations of gauge theories and gravity,” [arXiv:gr-qc/9412035 \[gr-qc\]](https://arxiv.org/abs/gr-qc/9412035).
- [156] M. P. Reisenberger, “Classical Euclidean general relativity from ‘left-handed area = right-handed area’,” *Class.Quant.Grav.* **16** (1999) 1357, [arXiv:gr-qc/9804061 \[gr-qc\]](https://arxiv.org/abs/gr-qc/9804061).
- [157] M. P. Reisenberger, “On relativistic spin network vertices,” *J.Math.Phys.* **40** (1999) 2046–2054, [arXiv:gr-qc/9809067 \[gr-qc\]](https://arxiv.org/abs/gr-qc/9809067).
- [158] M. P. Reisenberger and C. Rovelli, “‘Sum over surfaces’ form of loop quantum gravity,” *Phys.Rev.* **D56** (1997) 3490–3508, [arXiv:gr-qc/9612035 \[gr-qc\]](https://arxiv.org/abs/gr-qc/9612035).

- [159] A. Riello, “Self-energy of the Lorentzian Engle-Pereira-Rovelli-Livine and Freidel-Krasnov model of quantum gravity,” *Phys.Rev.* **D88** no. 2, (2013) 024011, [arXiv:1302.1781 \[gr-qc\]](#).
- [160] C. Rourke and B. Sanderson, *Introduction to Piecewise-Linear Topology*. Springer-Verlag Berlin Heidelberg, 1982.
- [161] C. Rovelli, “The Projector on physical states in loop quantum gravity,” *Phys.Rev.* **D59** (1999) 104015, [arXiv:gr-qc/9806121 \[gr-qc\]](#).
- [162] C. Rovelli, *Quantum Gravity*. Cambridge University Press, 2004.
- [163] C. Rovelli, “A new look at loop quantum gravity,” *Class.Quant.Grav.* **28** (2011) 114005, [arXiv:1004.1780 \[gr-qc\]](#).
- [164] C. Rovelli, “Loop quantum gravity: the first twenty five years,” *Class.Quant.Grav.* **28** (2011) 153002, [arXiv:1012.4707 \[gr-qc\]](#).
- [165] C. Rovelli, “Zakopane lectures on loop gravity,” *PoS QGQGS2011* (2011) 003, [arXiv:1102.3660 \[gr-qc\]](#).
- [166] C. Rovelli and M. Smerlak, “In quantum gravity, summing is refining,” *Class.Quant.Grav.* **29** (2012) 055004, [arXiv:1010.5437 \[gr-qc\]](#).
- [167] C. Rovelli and F. Vidotto, “Stepping out of Homogeneity in Loop Quantum Cosmology,” *Class.Quant.Grav.* **25** (2008) 225024, [arXiv:0805.4585 \[gr-qc\]](#).
- [168] C. Rovelli and F. Vidotto, “On the spinfoam expansion in cosmology,” *Class.Quant.Grav.* **27** (2010) 145005, [arXiv:0911.3097 \[gr-qc\]](#).
- [169] C. Rovelli and F. Vidotto, *Covariant Loop Quantum Gravity: An Elementary Introduction to Quantum Gravity and Spinfoam Theory*. Cambridge University Press, 2014.
- [170] H. Sahlmann, T. Thiemann, and O. Winkler, “Coherent states for canonical quantum general relativity and the infinite tensor product extension,” *Nucl.Phys.* **B606** (2001) 401–440, [arXiv:gr-qc/0102038 \[gr-qc\]](#).
- [171] S. Speziale and W. M. Wieland, “The twistorial structure of loop-gravity transition amplitudes,” *Phys.Rev.* **D86** (2012) 124023, [arXiv:1207.6348 \[gr-qc\]](#).
- [172] T. Thiemann, “Anomaly - free formulation of nonperturbative, four-dimensional Lorentzian quantum gravity,” *Phys.Lett.* **B380** (1996) 257–264, [arXiv:gr-qc/9606088 \[gr-qc\]](#).
- [173] T. Thiemann and O. Winkler, “Gauge field theory coherent states (GCS). 2. Peakedness properties,” *Class.Quant.Grav.* **18** (2001) 2561–2636, [arXiv:hep-th/0005237 \[hep-th\]](#).
- [174] T. Thiemann and O. Winkler, “Gauge field theory coherent states (GCS): 3. Ehrenfest theorems,” *Class.Quant.Grav.* **18** (2001) 4629–4682, [arXiv:hep-th/0005234 \[hep-th\]](#).

## Bibliography

- [175] T. Thiemann and O. Winkler, “Gauge field theory coherent states (GCS) 4: Infinite tensor product and thermodynamical limit,” *Class.Quant.Grav.* **18** (2001) 4997–5054, [arXiv:hep-th/0005235 \[hep-th\]](https://arxiv.org/abs/hep-th/0005235).
- [176] T. Thiemann, “Gauge field theory coherent states (GCS): 1. General properties,” *Class.Quant.Grav.* **18** (2001) 2025–2064, [arXiv:hep-th/0005233 \[hep-th\]](https://arxiv.org/abs/hep-th/0005233).
- [177] T. Thiemann, “Complexifier coherent states for quantum general relativity,” *Class.Quant.Grav.* **23** (2006) 2063–2118, [arXiv:gr-qc/0206037 \[gr-qc\]](https://arxiv.org/abs/gr-qc/0206037).
- [178] T. Thiemann, *Modern Canonical Quantum General Relativity*. Cambridge University Press, 2007.
- [179] T. Thiemann and A. Zipfel, “Linking covariant and canonical LQG II: Spin foam projector,” *Class.Quant.Grav.* **31** (2014) 125008, [arXiv:1307.5885 \[gr-qc\]](https://arxiv.org/abs/1307.5885).
- [180] V. Turaev and O. Viro, “State sum invariants of 3 manifolds and quantum 6j symbols,” *Topology* **31** (1992) 865–902.
- [181] F. Vidotto, “Many-nodes/many-links spinfoam: the homogeneous and isotropic case,” *Class.Quant.Grav.* **28** (2011) 245005, [arXiv:1107.2633 \[gr-qc\]](https://arxiv.org/abs/1107.2633).
- [182] R. M. Wald, *General Relativity*. The University of Chicago Press, 1984.
- [183] D. N. Yetter, “Generalized Barrett–Crane Vertices and Invariants of Embedded Graphs,” *Journal of Knot Theory and Its Ramifications* **08** no. 06, (1999) 815–829.